Universitat Autònoma de Barcelona

INc Institut de Neurociències

Institut de Neurociències
Edifici M. UAB
Telèfon 935813861
http://inc.uab.cat

STUDY OF NEW PROPARGYLAMINE AND DONEPEZIL-DERIVED COMPOUNDS AS MULTITARGET AGENTS FOR THE TREATMENT OF ALZHEIMER'S DISEASE

Irene Bolea Tomás

PhD Thesis

Bellaterra, Juny 2011

Universitat Autònoma de Barcelona

Departament de Bioquímica i Biología Molecular
Unitat de Bioquímica de Medicina

Dra. Mercedes Unzeta López, Catedràtica de la Universitat Autònoma de Barcelona,

CERTIFICA:

Que la següent Tesi Doctoral titulada "STUDY OF NEW PROPARGYLAMINE- AND DONEPEZIL-DERIVED COMPOUNDS AS MULTITARGET AGENTS FOR THE TREATMENT OF ALZHEIMER'S DISEASE", presentada per Irene Bolea Tomás, Llicenciada en Bioquímica per la Universitat Autònoma de Barcelona, ha estat realitzada sota la seva direcció al Departament de Bioquímica i Biología Molecular de la Universitat Autònoma de Barcelona i reuneix tots els requisits necessaris per ser llegida i defensada davant el tribunal corresponent, autoritzant la seva presentació per optar al grau de Doctor per la Universitat Autònoma de Barcelona.

Doctoranda	Directora de tesi
Irene Bolea Tomás	Dra. Mercedes Unzeta López

Bellaterra, Juny 2011

Aquesta tesi ha estat realitzada gràcies al finançament dels projectes següents:

- Ministerio de Educación y Ciencia (MEC). Ref. SAF 2006-08764-C02-02 y SAF 2009-07279 (Subproyecto NEF).
- Ministerio de Industria, programa INGENIO 2010, proyecto CENIT, ref. MET-DEV-FUN 2006.
- COST Action D34/0003/05 (2005-2010).

Agraïments

A la Dra. Mercedes Unzeta. Mercedes, te estoy muy agradecida por haberme dado la oportunidad de hacer esta tesis, por confiar en mí para desarrollar el proyecto y darme total libertad para llevarlo a cabo. También por permitirme ampliar mi formación asistiendo a numerosos congresos, cursos, COST meetings y estancias. De forma especial, quiero agradecerte tu comprensión y consejos en aspectos no relacionados con la ciencia.

A la Mar, la Eli, el Tony, la Montse, la Patricia i la Laura. Coincidir en el grup Uz's és molt més que ser companys de grup. Moltes gràcies per haver-me ensenyat a treballar al laboratori, per la vostra paciència, ajuda i disponibilitat. Si aquesta tesis és una realitat és també gràcies a vosaltres. Gerard, el penúltim Uz, mil gràcies per l'ajuda d'aquestes últimes setmanes i ànims amb la tesis!!

Vorrei anche di cuore ringraziare la Prof.ssa Della Corte per avermi permesso di collaborare all'interno del suo laboratorio non una sola, bensì tre. Per avermi accolta sempre a braccia aperte. Non posso dimenticare Alessandra, Manuela, Chiara e anche Andrea. Grazie per il vostro aiuto incondizionato, per mostrarmi tutto sulla microdialisi e l'HPLC e anche per le correzioni dei compiti di lingua italiana. Grazie anche a te, Sabry, la mia sorellina italiana, che hai arricchito la mia vita a Firenze con i numerosi viaggi, chiachere e passeggiate insieme.

A Cris, muchas gracias por esas clases en mis inicios en cultivos, por todos los consejos y ayudas posteriores y por tu disponibilidad a echarme una mano siempre en cualquier momento.

A la Susana, gràcies per ajudar-me a entendre l'HPLC i per fer més agradables els dies bipolars quan vam començar a posar-lo a punt.

A la Dra. Pepi Sabrià, per guiar-nos i donar-nos tants cops de mà amb l'HPLC.

Al Dr. Josep Cladera, per les recomanacions i consells quan vam començar a treballar amb el pèptid β-amiloide.

A la resta de companys de "Bioquim_Medicin" que vau fer tan divertits els inicis amb nombroses activitats extra-tesi, com els caps de setmana a les Cases Rurals, els sopars, les cervesetes i la visita a Florència. Gràcies per tots aquells moments i moltes gràcies també per ajudar-me amb algunes tècniques quan ho he necessitat.

A Jordi Juárez, por las fantásticas figuras de las enzimas y al Dr. F. Javier Luque por enseñarme a trabajar con rigor y valorar mi trabajo.

Als amics, que heu suportat repetidament la meva impuntualitat durant tots aquests anys amb l'excusa de tenir experiments i heu escoltat les meves penes i alegries al lab, gràcies per continuar aguantant-me!!

A Álex. Por donde empiezo? Gracias, por hacerme ver las cosas con perspectiva (no sólo con la tesis), por estar siempre dispuesto a ayudarme, por tu amor, por aguantarme y por compartir tu vida conmigo. Hacer esta tesis hizo posible que nos conociéramos así que ya ha valido la pena.

Als meus pares i a les meves germanes pel vostre amor incondicional, per animar-me, escoltar-me, ajudar-me i donar-me suport sempre.

Als meus pares

I a Álex

Index

Abbreviations

Aβ	Amyloid-beta-peptide
ACh	Acetylcholine
AChE	Acetylcholinesterase
AChEI	Acetylcholinesterase inhibitor
AD	Alzheimer's disease
fAD	familiar Alzheimer's disease
sAD	sporadic Alzheimer's disease
AGEs	Advanced glycation end products
AICD	APP intracellular domain
ALS	Amyotrophic Lateral Sclerosis
AMPA	α-amino-3-hydroxy-5-methyl-4-isoxazole propionic acid
ApoE	Apolipoprotein E
APP	Amyloid precursor protein
ATP	Adenosine triphosphate
BACE-1	β-site APP cleaving enzyme 1
BuChE	Butyrylcholinesterase
CAMKII	Calcium-calmodulin protein kinase 2
CAS	Catalitic anionic site
CAT	Catalase
ChAT	Choline acetyltransferase
ChEIs	Cholinesterase inhibitors
CNS	Central nervous system
CDK-5	cyclin-dependent kinase-5
CSF	Cerebrospinal fluid
CTFα	C-terminal fragment α
CTFβ	C-terminal fragment β
DA	Dopamine
DMSO	Dimethyl sulfoxide
DNA	Desoxiribonucleic acid
ER	Endoplasmic reticulum
FDA	Food and Drug Administration
GPx	Glutatione peroxidase

GR	Glutathione reductase
GSH	Glutathione
GSK-3β	Glycogen syntase kinase 3β
GSSG	Glutathione disulfide
HD	Huntington's disease
HFIP	Hexafluoroisopropanol
HMG-CoA	Hydroxymethyl glutaryl CoA
HMW	High molecular weight
5-HT	5-hydroxytryptamine
HupA	Huperzine A
IL-1	Interleukin-1
IL-6	Interleukin-6
KA	Kainate
LMW	Low molecular weight
mAChR	Muscarinic acetylcholine receptors
MAO	Monoamine oxidase
MAOIs	Monoamine oxidase inhibitors
MAPK	Mitogen-activated protein kinase
MCI	Mild cognitive impairment
MTDL	Multi-target directed ligand
NA	Noradrenalin
nAChR	Nicotinic acetylcholine receptors
NFT	Neurofibrillary tangles
NMDA	N-methyl-D-aspartate
NSAIDs	Non-steroidal anti-inflammatory drugs
OS	Oxidative stress
PAS	Peripheral anionic site
PD	Parkinson's disease
PHF	Paired helical filaments
PKA	Protein kinase A
PriMA	Prolin-rich membrane protein anchor
PS	Presenilin
PUFAs	Polyunsaturated fatty acids
RAGE	Receptor of advanced glycation end products

RCT	Randomised clinical trial
ROS	Reactive oxygen species
RNS	Reactive nitrogen species
SN	*substantia nigra*
SNpc	*substantia nigra pars compacta*
SNpr	*substantia nigra pars reticulata*
SOD	Superoxide dismutase
SP	Senile plaques
Str	*striatum*
TFA	Trifluoroacetic
TFE	Trifluoroethanol
ThT	Thioflavin T
TNF-α	Tumour necrosis factor α
TUNEL	*TdT-mediated X-dUTP nick end labelling*
Tyr	Tyrosine
WM	White matter

Molecular formula

$^{\cdot}O_2^-$	Superoxyde radical
H_2O_2	Hydrogen peroxide
$OH^{\cdot}$	Hydroxyl radical
O_2	Oxygen
NO	Nitric oxyde
$ONOO^-$	Peroxynitrite
NH_4OH	Ammonium hydroxide
NaOH	Sodium hydorxide
NH_3	Ammonia

Preface

PF9601N is a propargylamine-containing irreversible monoamine oxidase B inhibitor (MAOBI) previously identified by our group in an extensive screen of potential MAOIs. Besides its potent inhibitory capacity, it possesses several neuroprotective properties demonstrated in different animal and cellular models of Parkinson's disease (PD). The beneficial effects of PF9601N, which have been related to the propargylamine group present in the molecule, are mediated through actions in pathways that are commonly involved in the neurodegeneration observed in other neurodegenerative disorders such as Alzheimer's disease (AD), thus making this molecule a promising agent in the therapy of this disease as well. Thus, to study the beneficial properties of PF9601N in depth, we investigated its effects against an *in vivo* model of excitotoxicity, an important mechanism involved in the neuronal damage observed in neurodegenerative diseases. The finding that PF9601N was able to prevent the induced excitotoxic damage by decreasing the evoked release of excitatory neurotransmitters and decreasing the output of the inhibitory and neuroprotective taurine as well as preventing the induced glial activation and apoptosis gave more value to this compound to be considered in the therapy.

The current treatment for AD is the use of cholinesterase inhibitors (ChEIs) although there is also a NMDA receptor antagonist. However, far from stopping the disease's progression, these drugs only produce a temporary symptomatic benefit, thus highlighting an urgent need to provide real disease-modifying drugs. At present, the most accepted notion is that AD is a multifactorial disease caused by many different factors and thus drug therapy with multifunctional compounds, the so-called multi-target-directed ligand (MTDL) approach, embracing diverse biological properties will have noticeable advantages over individual-target drugs or cocktails of drugs. In this context, this thesis focuses on the structure-activity relationship (SAR) study and the biological evaluation of different hybrid compounds specifically designed and synthesised to target multiple factors involved in AD. The hybrid molecules combine the benzyl piperidine moiety of Donepezil, a commonly used anticholinesterasic for the treatment of AD, with the propargylamine or the indolyl propargylamine substructure of PF9601N, with the aim of retaining the MAO inhibitory capacity as well as the neuroprotective and antiapoptotic properties observed for this compound. The work presented in this thesis demonstrates that some hybrid compounds are potent MAOIs (nM range) and moderately potent ChEIs (submicroM range). Among them, ASS234 has also been shown to reduce Aβ fibrillogenesis, and to protect neuronal

cells from Aβ and H_2O_2 toxicity. Thus, this compound has proved to be able to block the Aβ-induced cell death in two ways: by preventing caspase cleavage and activation and blocking LDH release.

Overall, the present data suggest ASS234 as a promising MTDL that may have a potential disease-modifying role in the treatment of AD since it is able to interact with diverse targets involved in the pathogenesis underlying AD.

I. INTRODUCTION

1. NEURODEGENERATIVE DISEASES: a challenge of the 21st century

The incidence of neurodegenerative diseases has increased in the global population and is likely to be the result of extended life expectancy brought about by better health care. Despite this increase in the incidence, there has been little improvement in the introduction of new disease-modifying therapies to prevent or delay the onset of these disorders, or reverse the degenerative processes in the brain. Neurodegenerative diseases include those that are of a chronic nature, e.g. Alzheimer's disease (AD), Parkinson's disease (PD), Huntington's disease (HD) and Amyotrophic Lateral Sclerosis (ALS) as well as those originating from an acute initial insult such us traumatic brain injury and stroke. The major basic processes involved in neurodegenerative diseases of a chronic nature are that they are multifactorial and caused by genetic, environmental and endogenous factors. Pathologically, these disorders share a common feature: the selective loss of a particular subset of neurons for as yet unknown reasons. Although each disease has its own molecular mechanisms and clinical manifestations, some general pathways might be recognised in different pathogenic cascades. They include protein misfolding and aggregation, oxidative stress and free radical formation, metal dyshomeostasis, mitochondrial dysfunction and phosphorylation impairment (Jellinger, 2003) (Figure 1).

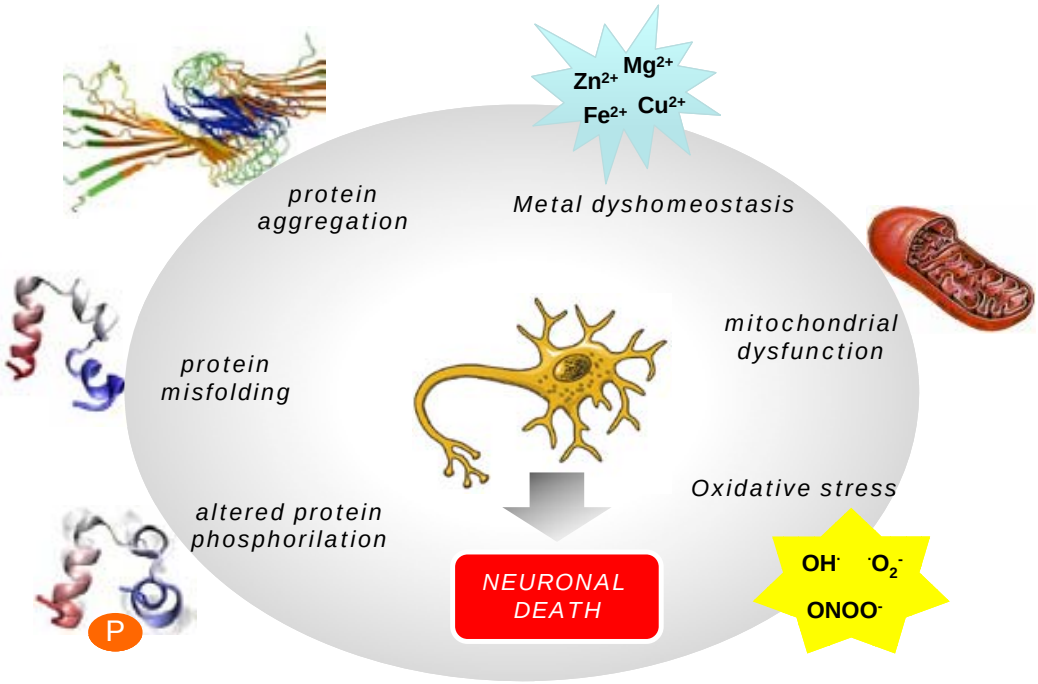

Figure 1. Schematic pathways of the multifactorial events leading to neuronal death in neurodegenerative diseases. Modified from Cavalli et al, 2008.

These events are probably responsible for calcium dysregulation and membrane depolarisation which have also been identified as further common features of most neurodegenerative disorders (Lin & Beal, 2006). The most striking evidence pointing out the complexity of these neurodegenerative diseases is that to date any drug can either prevent the neurodegenerative process or restore the neurons that have died. Pharmaceutical research has only been able to develop drugs that, at best, slightly modulate the symptoms in patients suffering from these disorders. There is therefore an urgent need to provide real disease-modifying drugs for such neurodegenerative disorders.

2. ALZHEIMER'S DISEASE

Among neurodegenerative diseases Alzheimer's disease (AD) appears as the fourth leading cause of death in Western countries and the most common cause of dementia in the elderly population. Data from the Alzheimer's Association (2009) are convincing:

- 10% of people aged over 65 years and almost 50% of people aged 85 years or over suffer from some type of dementia.
- More than 37 million people worldwide present some type of dementia, nearly 7 million in Europe, of which 600,000 are found in Spain.
- In four decades time 35% of the population worldwide will be over 60 years.

According to Wimo et al, 2010, 7.3 million people presented AD in 2008 and in correlation with the increasing average in life expectancy, the number of affected persons is expected to double or even triple by 2050. In this context, the total cost of dementia in the EU27 in 2008 was estimated to be €160 billion (€22.000 per demented person per year). The costs corresponding for the whole of Europe was €177 billion. As the geriatric population significantly increases, the number of AD patients might increase to epidemic numbers by the middle of the 21st century and thus become a serious public health problem (Mount & Downton, 2006). AD and related dementias are therefore a major public health challenge.

2.1 Historical perspective

The history of Alzheimer's disease began with Dr. Alois Alzheimer's first description in 1906 (Alzheimer et al, 1995). After the death of a patient with dementia, he examined her brain and found it to contain "miliary foci, distinguishable by the deposit of a peculiar

substance" and "densely twisted bundles of neurofibrils" which were visible under microscopic observation through a newly developed silver-staining technique. Dr. Alzheimer provided a thorough, unified description of the pathological features that are still recognised today: the neurofribillary tangles (NFT) and the senile plaques (SP). It was later in 1910 that Alzheimer's mentor, Emil Kraepelin, named the condition Alzheimer's disease (Maurer et al., 2000).

2.2 Main features

The predominant clinical manifestation of AD is progressive memory deterioration and changes in brain function, including disordered behaviour and impairment in language, comprehension and visual-spatial skills (Tsolaki et al., 2001). The symptoms progressively worsen over 5 to 10 years (Bayer & Reban, 2004).

In terms of anatomopathology, significant neuronal and synaptic losses are found in brains of AD patients which are further evidenced by atrophy in the hippocampus and the frontal and tempoparietal cortex. These features are accompanied by the two characteristic hallmarks: the NFT, intracellular fibrillar deposits mainly composed by the microtubule-associated protein called tau (Goedert et al., 1988), and the SP, formed by deposition of aggregated amyloid-beta peptide (Aβ) (Glenner & Murphy, 1989) (Figure 2). Besides cognitive deficits, patients frequently exhibit a number of neuropsychiatric symptoms such us depression, psychosis and agitation (Ballard et al., 2008).

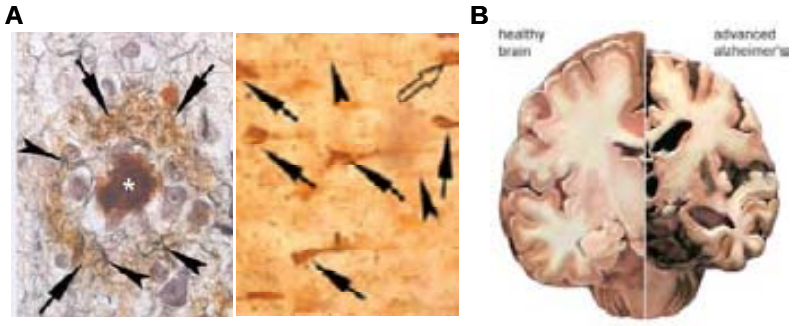

Figure 2. (A) A senile plaque (SP) and neurofibrillary tangles (NFT) in the temporal cortex of an AD sufferer's brain. Taken from Thal et al., 2008. (B) Image showing the loss of brain volume in Alzheimer's disease compared to a healthy brain. Taken from Alzheimer's Association.

AD can be classified into two different types, depending on the onset time of the symptoms: Familiar AD (fAD) and sporadic AD (sAD). fAD is an early-onset form of the disease occurring between the ages of 30 and 60 (Vetrivel et al., 2006), it accounts for less of

3% of all AD cases and is autosomal dominantly inherited. Causative genetic mutations in the genes of the amyloid precursor protein (APP) or presenilins (PS) are detected in fAD (Levy-Lahad et al., 1995; Rogaev et al., 1995; Bayer et al., 1999). In contrast, sAD, which is a late-onset form, is the most common cause of the disease accounting for more than 97% of all AD cases. The causes of sAD still remains unclear, although there are various genes, rather than determining mutations, that cause susceptibility to the disease, mainly the ε4 allele of ApoE gene that codes apolipoprotein E (ApoE) (Sando et al., 2008; Bird, 2008). Nevertheless, other genetic polymorphisms may be involved in susceptibility to the disease.

2.3 Risk factors

Several risk factors for the occurrence of AD have been suggested including cerebrovascular disease, hypertension, arteriosclerosis, diabetes, hypercholesterolemia, depression, stroke, head trauma, environmental toxins, seizures, stress, and a presence of ApoE ε4 allele (Cummings et al., 2007; Craig et al., 2011). However, the main risk factor is aging. As recently reported (Craig et al., 2011), each of these factors on their own are not predictive of whether an individual will develop cognitive impairments. For example, despite the fact that the presence of ε4 allele of ApoE constitutes the best known genetic risk factor for AD (Corder et al., 1993), not all ε4 carriers develop the disease. This suggests that there are additional factors that contribute to the development of the disorder which must be present to exhibit the clinical symptoms associated with AD.

3. ETIOLOGY OF SPORADIC AD

Although the pathogenesis of AD is not yet fully understood, the scientific consensus is quite firm in describing it as a multifactorial disease caused by genetic, environmental and endogenous factors. These factors include excessive protein misfolding and aggregation (Terry et al., 1964; Grundke-Iqbal et al., 1986) oxidative stress and free radical formation (Coyle & Puttfarcken, 1993; Perry, 2000), mitochondrial dysfunction (Swerdlow & Khan, 2009), metal dyshomeostasis (Huang et al, 2004) and excitotoxic and neuroinflammatory processes (Mishizen-Eberz et al., 2004). In this context, several hypotheses have been suggested to be involved in the pathogenesis of AD, such as, the tau protein aggregation and the amyloid cascade hypotheses, the oxidative stress (OS) and metal dyshomeostasis hypotheses, the cholinergic hypothesis, the vascular hypothesis, or the inflammation hypothesis. It seems that these hypotheses are not mutually exclusive but

rather that they complement each other, intersecting at a high level of complexity (Cavalli et al., 2008). Nevertheless, at present it is believed that amyloid protein aggregation plays a central role in the pathogenesis of the disease (Butterfield et al, 2002). Other aspects of these hypotheses are not yet elucidated as cause or effect of AD pathogenesis.

3.1 Oxidative stress and metal dyshomeostasis hypotheses

The oxidative stress (OS) hypothesis was first postulated by Dr. Denham Harman in 1956 regarding the aging process. This theory proposed that brain aging is associated to a progressive imbalance between the anti-oxidant defences and the pro-oxidant species that can occur as a result of either an increase in free radical production or a decrease in antioxidant defence. Later on, Dr Harman proposed that life span is determined by the rate of reactive oxygen species (ROS) damage to the mitochondria (Harman, 1972) giving for the first time an important role to this organelle in the ageing process and establishing the basis for the "mitochondrial theory of ageing". The central nervous system (CNS) is especially vulnerable to oxidative damage as a result of the high oxygen consumption rate (20% of the total oxygen consumption), the abundant content of easily peroxidisable fatty acids, and the relative paucity of antioxidant enzymes compared to other tissues (Reiter, 1995). In aerobic organisms, mitochondria produce semireduced oxygen species during respiration. The initial step of the respiratory chain reaction yields the superoxyde radical ($^{\bullet}O_2^-$), which produces hydrogen peroxide (H_2O_2) by addition of an electron. The reduction of H_2O_2 through the Fenton reaction produces the highly reactive hydroxyl radical ($OH^{\bullet}$), which is the chief instigator of oxidative stress damage and reacts indiscriminately with all biomacromolecules (Figure 3). Under normal conditions, damage by ROS is prevented by an efficient antioxidant cascade, including both enzymatic (copper-zinc superoxide dismutase, manganese superoxide dismutase) and non-enzymatic entities (vitamin C, thiols and perhaps vitamin E). Moreover, monoamine oxidases (MAOs) and L-amino acid oxidase can also produce H_2O_2 during its metabolism which is effectively removed by catalase (CAT) and peroxidases.

In a pro-oxidant environment, like in the case of AD, $^{\bullet}O_2^-$ can also harmfully react with nictric oxide (NO) quickly enough to avoid the action of the antioxidant systems forming peroxynitrite anion ($ONOO^-$) (Beckman et al., 1990). $ONOO^-$ reacts with tyrosine residues (Tyr) of proteins in a non-enzymatic reaction called nitrotyrosination. Moreover, $ONOO^-$ and reactive nitrogen species (RNS) can induce significant OS.

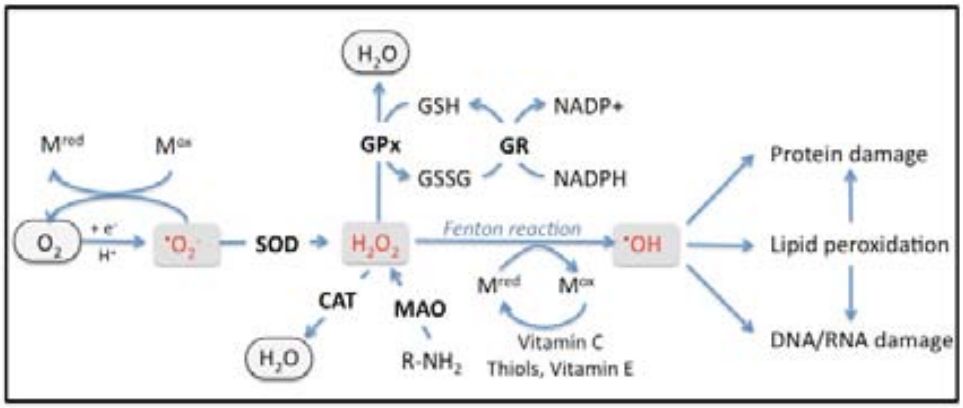

Figure 3. Schematic illustration of the mechanism involved in reactive oxygen species (ROS) formation and elimination. Glutathione peroxidase (GPx), glutathione reductase (GR), superoxide dismutase (SOD), catalase (CAT), monoamine oxidase (MAO), glutathione (GSH), glutathione disulfide (GSSG).

It has been reported that the neurotoxic properties of Aβ are mainly due to the production ROS (Behl et al., 1994) which suggests that OS is the major damaging mechanism in AD (Miranda et al., 2000). The fact that age is the main risk factor for AD development provides considerable support to the OS hypothesis since the effects produced by reactive oxygen species (ROS) can accumulate over the years (Nunomura et al., 2001). The link between AD and OS is additionally supported by the finding of decreased levels of antioxidant enzymes, increased protein, lipid and DNA oxidation and advanced glycation end products (AGEs) and ROS formation in neurons of AD patients (Perry et al., 2000; Barnham et al., 2004). Antioxidant treatment such vitamin E has demonstrated neuroprotective effects against Aβ cytotoxicity (Munoz et al., 2002). Unfortunately, a Cochrane study showed that vitamin E is not effective in a prevention trial in mild cognitive impairment (MCI) to reduce progression to AD nor clearly effective in AD patients (Tabet et al, 2000). It has been reported that the accumulation of the oligomeric form of Aβ, the most toxic form of the peptide, induces OS in neurons (Butterfield et al., 2002), supporting the hypothesis and suggesting a causative role of OS in AD development.

This situation is further exacerbated by the fact that redox active transition metals are aberrantly accumulated in the cytoplasm of neurons in AD. Thus, cerebral concentrations of zinc (Zn), copper (Cu) and iron (Fe) ions are significantly elevated in AD (Adlard & Bush, 2006; Lovell et al., 1998; Bush, 2003). Moreover, there is increasing evidence suggesting that there may be an interaction between metals, APP, Aβ peptide and tau protein that may influence their aggregation and toxicity. These observations have led to "the metal theory of AD" (Bush & Tanzi, 2008) which proposes that age-related endogenous metal

dyshomeostasis in the brain allows binding of redox-active metal ions (Cu^{2+} and Fe^{3+}) to Aβ peptide, stabilising neurotoxic species which ultimately lead to cell death (Garai et al., 2007; Yoshiike et al., 2001).

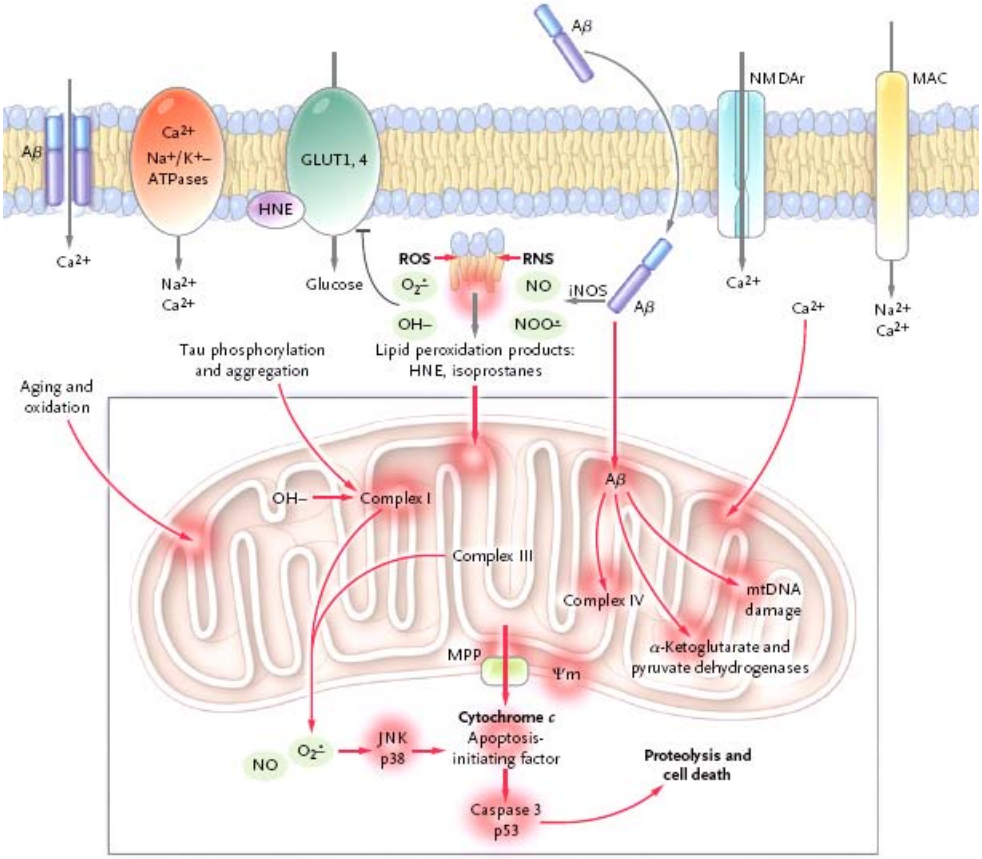

Figure 4. Oxidative stress and mitochondrial impairment leading to apoptosis in AD. Taken from Querfurth & LaFerla, 2010.

Thus, it seems that Aβ, a potent generator of ROS (Combs et al, 2001) and RNS (Yan et al, 1996), is a prime initiator of the oxidative damage by binding to mitochondria where it inhibits key mitochondrial enzymes (Hauptmann et al., 2006; Reddy & Beal, 2008). Therefore, electron transport, ATP production and mitochondrial membrane potential become impaired. The final consequence is the release of cytocrome c which leads to apoptosis (Figure 4). Intracellular calcium accumulation, decreased membrane fluidity and inflammatory processes also counteract the increased sensitivity to apoptotic as well as necrotic cell death (Drouet et al., 2000; Vajda, 2002).

3.2 Inflammatory hypothesis

The inflammatory hypothesis of AD started with the finding of reactive microglia in the AD brain (McGeer et al., 1987; Rogers et al., 1999) and the observation that people suffering from rheumatoid arthritis had a reduced risk of AD (Mc Geer et al., 1990), provoked by the chronic use of non-steroidal anti-inflammatory drugs (NSAIDs) (McGeer & Rogers, 1992). Initially, microglia phagocytes and degrade Aβ. However, in AD, ROS and RNS can bind to microglia via the receptor of advanced glycation end products (RAGE) activating them and producing a release of a variety of potentially neurotoxic compounds, including superoxides, glutamate and NO. Besides, activated microglia release chemokines and a cascade of damaging cytokines, mainly interleukin-1 (IL-1), interleukin-6 (IL-6) and tumour necrosis factor α (TNF-α) (Akiyama et al., 2000). In addition, RAGE can also bind Aβ amplifying the generation of cytokines, glutamate, and NO (Yan et al., 1996; Li et al., 2003). The inflammatory (and the oxidative) events have been reported to be also implicated in the breakdown of the vascular blood-brain barrier (Querfuth & LaFerla, 2010).

3.3 The amyloid cascade hypothesis

Accumulation of extracellular β-amyloid (Aβ) plaques, toghether with the intracellular NFT, is a neuropathological hallmark of AD. β-amyloid protein, the main component of plaques, was purified and sequenced in the early 80's (Glenner & Wong, 1984) and originated the "amyloid hypotheses" of AD (Hardy & Higgins, 1992) which proposes that Aβ, toghether with NFT and cell death, is the culprit of the neurodegenerative process in this disorder.

3.3.1 The amyloid precursor protein

Senile plaques are formed by extracellular accumulation of amyloid-peptide (Aβ) (Glenner & Murphy, 1989) which is formed from amyloid precursor protein (APP) processing. APP is a type I transmembrane glycoprotein that is constitutively expressed in the majority of mammalian cells. Its function has been related with adhesion to the matrix (Mattson, 1997), cell-to cell interactions (Del Toro et al, 2005) and dendritic growth (Dawson et al, 1999; Sabo et al, 2003) as well as to vesicular trafficking trough the axon (Kamal et al, 2000).

APP can be processed by the non-amyloidogenic pathway (Figure 5), in which a α-secretase activity firstly cut APP within the Aβ domain and prevents the formation of full Aβ. Then, the C-terminal fragment (CTFα) is cleaved by the action of a γ-secretase activity

which is formed by a multiprotein complex containing presenilin-1 (PS-1) or presenilin-2 (PS-2) as catalytic units (Edbauer et al, 2003). The result of the non-amyloidogenic pathway is the release of a non-pathological p3 peptide (~3 KDa) and the APP intracellular domain (AICD).

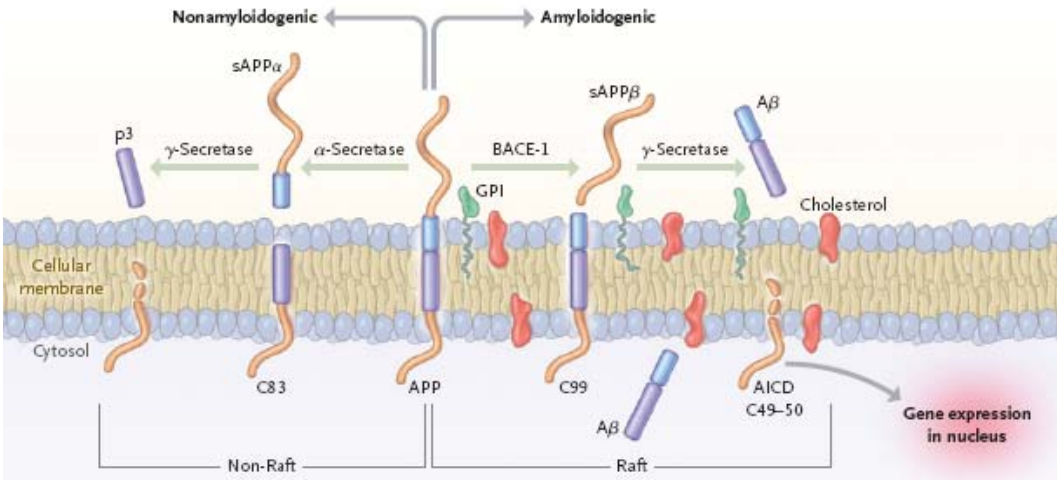

Figure 5. Schematic representation of APP processing. In the non-amyloidogenic pathway cleavage occurs by α-secretase within the Aβ domain and generates sAPPα and C83. The latter is further cut by γ-secretase to render the non-pathological p3 peptide and APP intracellular domain (AICD). The amyloidogenic pathway is produced by β–secretase (BACE-1), rendering a sAPPβ and C99 fragments. Following cleavage of C99 by γ-secretase gives the pathological Aβ peptide. Taken from Querfurth & LaFerla, 2010.

In the pathological amyloidogenic pathway of APP processing, a first cut by β-secretase (BACE-1, *β-site APP cleaving enzyme*) (Vassar et al, 1999) followed by the action of γ-secretase render the Aβ peptide. Depending on the cleavage in the C-terminal fragment (CTFβ), Aβ peptide species can be found from 38 (Aβ38) to 43 (Aβ43) amino acids (Teplow, 1998). Nevertheless, the most common forms found in mature plaques are Aβ40 and Aβ42, the latter less abundant but more pathogenic. Shorter and larger forms, although produced, do not practically contribute to senile plaques (Tabaton & Gambetti, 2006). The proportion of APP cleaved by the amyloidogenic pathway increases with age and in AD (Basha et al, 2005; Wu et al, 2008). Genetic studies of AD have shown that mutations in the gene that codes APP (Chartier-Harlin et al, 1991; Goate et al, 1991; Mullan et al, 1992) or in genes that regulate the proteolytic processing of APP (Levy-Lahad et al, 1995a, 1995b; Sherrington R et al, 1995) cause AD. The phenotypic effects of these mutations result in excessive production of Aβ or in an increase in Aβ42/Aβ40 ratio, facilitating Aβ deposition (Selkoe, 2001; Hardy,

1997a; Corder et al, 1993). Aβ accumulates in the cellular compartments and impairs cellular functions, including mitochondrial dysfunction, synaptic dysfunction and hyperphosphorilation of tau.

3.3.2 Aggregation of Aβ peptide

Aβ40 and Aβ42 peptides (40 and 42 residue long species, respectively) are the major peptides found in plaques. They are released to the extracellular space in a monomeric, disordered form where, through a polymerisation process, they form the typical fibrillar structure found in SP, which is mainly composed of β-sheet structure (Makin & Serpell, 2005). The aminoacid sequences of Aβ40 and Aβ42, the two peptides used in this work, are shown below:

Aβ40 NH_2 – DAEFRHDSGYEVHHQKLVFFAEDVGSNKGAIIGLMVGGVV - COOH

Aβ42 NH_2 – DAEFRHDSGYEVHHQKLVFFAEDVGSNKGAIIGLMVGGVVIA - COOH

The residues with high propensity to form β-sheet structure, the predominant structure found in mature fibrils, are shown in grey (Serpell, 2000).

The kinetics of the aggregation process seems to follow a sigmoidal curve which can be reproduced *in vitro* thanks to the binding of certain dye molecules such as Congo Red and Thioflavin T (ThT). This property is attributed to the existence of regularly spaced arrays of β-sheets (LeVine, 1993). Thus, if there is no β-sheet on the structure, there is no dye binding and therefore no fluorescence is observed. Two consecutive phases are clearly differentiated during the aggregation process (Figure 6):

a) **Lag phase**: The lag phase is also known as the nucleation phase which is mainly formed by soluble monomeric and dimeric random-coil structures (Walsh et al, 1999). Once the aggregation process begins due to the formation of a critical nucleus, the aggregation proceeds rapidly to the formation of fibrils. Before this, the end of the lag phase involves the formation of soluble oligomeric species whose structures are disordered and called small oligomers or low molecular weight (LMW) oligomers. They are spherical, globular, generally resembling small bead-like structures (Figure 6) and often described as micelles or

amorphous aggregates (Dobson, 2004; Walsh et al, 1999). Small Aβ oligomers are approximately 5 nm in diameter with molar masses of 25-50 KDa (Lambert et al, 1998).

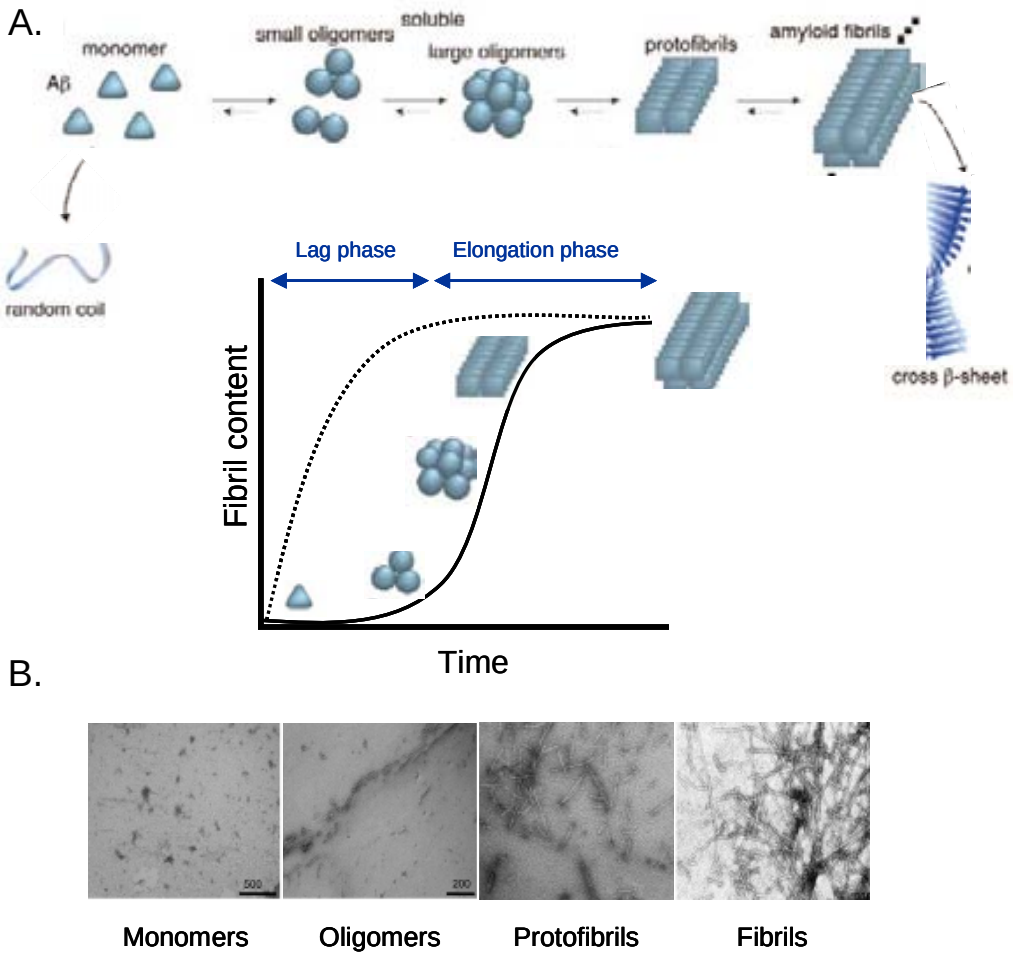

Figure 6. (A) Schematic representation of Aβ monomer aggregation from a random coil structure to amyloid fibrils composed of cross β-sheet structure via several metastable oligomers (small and large) and protofibrils. The details of the events occurring during fibril growth are not yet elucidated. Modified from Tsuyoshi & Mihara, 2008. (B) Electron micrographs of Aβ species in different stages of the aggregation process. Modified from Benseny-Cases et al., 2009.

b) **Elongation phase**: Oligomeric species elongate by linking together to form high molecular weight (HMW) oligomers or large oligomers which are approximately 15 nm in diameter and molar masses approaching 1 million Da (Huang et al, 2000). They are prefibrillar species that transform into species with more distinctive morphologies, known as protofilaments or protofibrils. These structures are short, flexible, often curly, fibrillar species which have been

reported to have a diameter of 4-10 nm and to be up to 200 nm in length (Walsh et al, 1999). Protofilaments are thought to be the precursors of full-length fibrils (Serpell, 2000) by simple lateral association and a degree of structural reorganisation. By this stage, the structures are highly organised, more rigid and longer than protofibrils. Mature fibrils are straight and unbranched, often twisted and tipically about 10 nm diameter which can even reach 10 μm in length (Dobson, 2004).

The aggregation process, then, needs to be nucleated and the rate at which this process takes place can be highly dependent on many different factors (e.g. pH, ionic strength of solvent, iron-pairing agent used in the peptide-purification process, peptide concentration and temperature) some of them not always easily controllable such as sample preparation. Nevertheless, the lag phase can be by-passed in the presence of a pre-formed aggregate producing a more rapid aggregation process known as "seeding" (Figure 6, dotted line) (Harper & Lansbury, 1997). Peptide samples are not pure of monomeric forms and several authors have explained the variability from batch to batch and poor reproducibility of experiments, reported both within and among laboratories, to the presence of seeds in their preparations (Bartolini et al., 2007). To try to address this issue, laboratories have used different methods to remove pre-formed aggregates from their peptide preparations such us filtration or centrifugation and the use of organic solvents (dimethyl sulfoxide –DMSO-, trifluoroethanol –TFE-, or hexafluoroisopropanol –HFIP-, strong acids (trifluoroacetic –TFA-), and concentrated bases (ammonium hydroxide-NH_4OH-, and sodium hydroxide -NaOH-).

It has been reported that Aβ40 and Aβ42 display distinct clinical, biological and biophysical behaviour which could explain the enhanced neurotoxicity relative to Aβ42. In this context, distinct oligomerisation and assembly processes of Aβ40 and Aβ42 have been found (Bitan et al, 2003). The authors show a formation of hexamers, heptamers and even octamers (which they called paranuclei species) in Aβ42 oligomerisation whereas in Aβ40 equilibrium of monomers to tetramers exist. It seems that these differences in the oligomerisation process are related to the Ile-41-Ala-42 dipeptide at the C-terminus of Aβ since studies with Aβ41, Aβ42 and Aβ43 show that the proportion of tetramer to octamer species increases as the peptide length increases.

It is important to characterise the intermediary species of A□ fibril formation since it seems that peptide toxicity is related to the presence of some of these species. It was first

the fibrillar Aβ deposits which were thought to be responsible for the neurodegenerative process of AD (Hardy & Higgins, 1992; Selkoe, 1994; Hardy, 1997b). However, this view was weakened by the observation that the amyloid plaque load did not correlate with the severity of AD (Dickson et al., 1995). Later on, findings showing that soluble aggregates can disrupt synaptic function (Lambert et al., 1998; Walsh and Selkoe, 2004) led to the belief that oligomeric species were the primary pathogenic species (Klein et al, 2001; Hardy and Selkoe, 2002). However, recent data even point to soluble dimeric species as highly neurotoxic (Jin et al., 2011). Numerous efforts have then been directed to identify the most neurotoxic Aβ species in order to find an effective therapeutic strategy. The mechanisms to induce cell damage by oligomers have been reported to be the same as those used by fibrils: ROS production (Schubert et al, 1995), altered signalling pathways (Mattson, 1997) and mitochondrial dysfunction (Shoffner, 1997). It is not still clear whether there is a specific species of Aβ peptide that is the most pathogenic or whether all of them play a role in the neurodegenerative process. In fact, some authors suggest that mature fibrils accumulate around damaged blood vessels accounting for the toxicity while others suggest that, rather that being neurotoxic, they might be a defence mechanism to eliminate the presence of the potentially toxic non-fibrillar species. More recent data have show that amyloid fibrils are a potential reservoir of oligomeric Aβ species (Koffie et al., 2009)

3.4 Tau-protein hypothesis

The tau-protein hypothesis of AD is centred on one of its main hallmarks, the NFT which are primarily composed by a protein called tau. Tau is a cytoplasmatic protein that binds to tubulin during its polymerisation stabilising microtubules (Eliezer et al, 2005). It is expressed in the nervous system and localised in the axons of neurons (Drubin & Kirschner, 1986). Tau contains four tau/MAP repeat sequences, which bind to microtubules (Eliezer et al, 2005). Depending on the number of repeats in the tau/MAP domain we can classify tau isoforms into type I which has 3 repeats and type II, containing 4 repeats (Goedert et al, 1989a). The difference between type I and type II is the presence or absence of exon 10 (Goedert, 1989b). In AD, tau is abnormally phosphorylated (Figure 5), resulting from an imbalance between kinases and phosphatase activities. It has been reported that tau is phosphorilated at serine and threonine by proline-directed protein kinases, cyclin-dependent kinase-5 (CDK5), glycogen syntase kinase 3 (GSK-3β) and mitogen-activated protein kinase (MAPK). Nonproline-directed kinases include Akt, Fyn, protein kinase A (PKA), calcium-calmodulin protein kinase 2 (CaMKII) and microtubule affinity-regulating

kinase (MARK). The hyperphosphorilation of tau finally lead to destabilisation of microtubules (Alonso et al., 1994), loss of neuronal cytoskeletal architecture and/or plasticity (Mandelkow & Mandelkow, 1998), impaired neuronal transport which ultimately induces cell death (Trojanowski et al., 1993). Although with some controversy, it is at present thought that tau aggregation, and therefore the formation of NFT, occurs after amyloid aggregation.

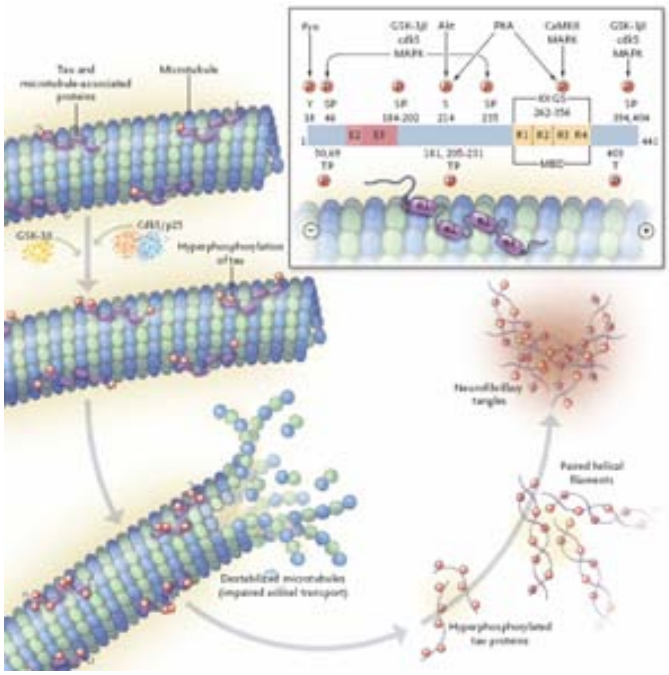

Figure 7. Tau hyperphosphorilation by protein kinases GSK-3□ and CdK-5 leads to impaired axonal transport by destabilisation of microtubules. Hyperphosphorilated tau aggregates forming the paired helical filaments (PHF) and finally the NFT. Modified from Querfurth & LaFerla, 2010.

4. CHOLINERGIC NEUROTRANSMISSION

One of the several features of the neuropathology of AD is the progressive loss of basal forebrain cholinergic neurons, leading to a decrease in cholinergic neurotransmission (Perry et al., 1977; Geula & Mesulam, 1999). The basal forebrain cholinergic complex, comprising medial septum, diagonal band of Broca, and nucleus basalis of Meynert provides the mayor cholinergic projections to the cerebral cortex and hippocampus, while the pontine cholinergic system acts mainly through thalamic intralaminar nuclei and provides only a minor innervation of the cortex (Martinez-Murillo & Rodrigo, 1995) (Figure 8).

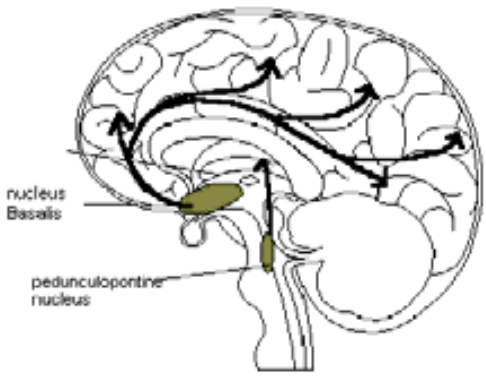

Figure 8. Schematic representation of the major cholinergic projections in the human brain. Nucleus basalis projects to the neocortex and pedunculopontine nucleus (PPN) projects to the thalamus.

Physiologically, the cholinergic system plays a role in controlling cerebral blood flow (Biesold et al, 1989), cortical activity (Detari et al, 1999) and the sleep-wake cycle (Lee et al, 2005) as well as in modulating cognitive function and cortical plasticity (Arendt & Bigl, 1986). The involvement of central cholinergic functions in learning and memory was first postulated by Deutsch in 1971 and later corroborated by a wide number of experimental studies in both animal models and humans (Fibiger, 1991; Christensen et al, 1992; Schliebs, 2005).

Decreased cholinergic neurotransmission was evidenced for the first time by findings in reduced presynaptic cholinergic markers such as acetylcholine (ACh) levels, and the expression of choline acetyltransferase (ChAT), the enzyme responsible for the synthesis of ACh. Muscarinic and nicotinic acetylcholine receptor binding (Davies and Malloney, 1976; Perry et al, 1977a, 1977b) and cell atrophy were also found. These findings were correlated to the rate of the progressing memory deficits with the aging process (Bigl et al, 1990; Arendt et al, 1987) and, later, to the rate of clinical dementia (Nordberg, 1992; Bierer et al, 1995; DeKosky et al, 2002). Thus, these findings suggested an association of cholinergic hypofunction with cognitive deficits and constituted the premises for the so-called "Cholinergic Hypothesis" of AD (Davies & Maloney, 1976) which has survived with little change for decades and proposes cholinergic enhancement as an approach for improving cognitive function in AD (Bartus et al, 1982).

4.1 Cholinesterase enzymes

Acetylcholinesterase (AChE, E.C.3.1.1.7) and butyrylcholinesterase (BuChE, E.C.3.1.1.8) are serine hydrolase glycoproteins that belong to the α/β-fold family, as they

contain a central β-sheet surrounded by α-helices (Figure 9) (Silver, 1974). This structure is also found in other proteins, such us cell adhesion molecules and precursors of hormones (Tsigelny et al, 2000).

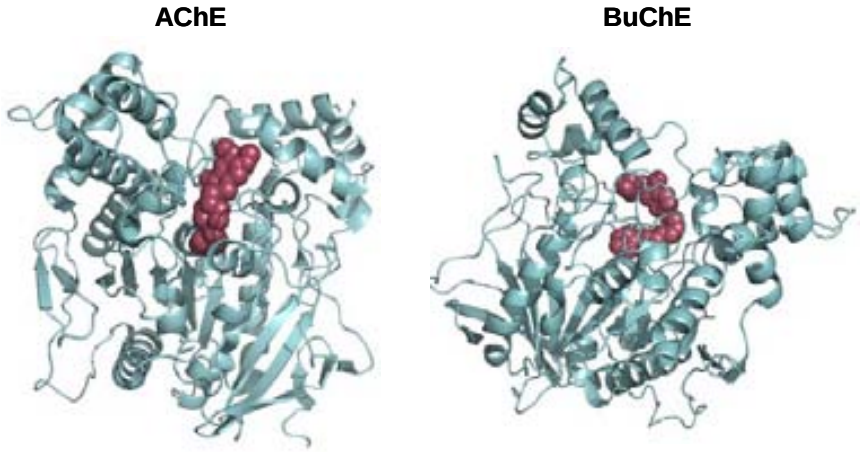

Figure 9. Structures of acetylcholinesterase (AChE) and butyrylcholinesterase (BuChE) enzymes. The magenta spheres represent the catalytic gorge.

They are primarily differentiated by their substrate specificity. Thus, AChE specifically catalyses the hydrolysis of ACh whereas BuChE, also known as pseudocholinesterase or non-specific cholinestrase, catalyses the hydrolysis of different esters of choline, including ACh (Silver, 1974). It has been hypothesised that AChE and BuChE are co-regulators of the duration of action of ACh in cholinergic neurotransmission (Darvesh et al, 1998; Mesulam et al, 2002a,b) which is further supported by the different kinetic properties of both AChE and BuChE. Thus, BuChE is less efficient in hydrolysing ACh at low concentrations but highly effective at high AChE levels at which AChE becomes substrate inhibited (Kamal et al, 2006; Giacobini, 2003). These data indicate a supportive role of BuChE in hydrolysing ACh under conditions of high brain activity. BuChE is structurally and functionally related to AChE but its role in the brain still remains to be elucidated. The finding that mice deficient in AChE but with normal levels of BuChE were viable (Li et al, 2000; Mesulam et al,2002a) suggested an essential function of BuChE in the brain in taking over some actions of AChE and maybe compensating for its loss, a hypothesis that is further supported by its wide distribution. At present, although they are not yet elucidated, both AChE and BuChE appear to exert broader functions in the central nervous system than previously thought (Ballard et al, 2005; Lane et al, 2006).

In a normal brain, AChE predominates, while BuChE activity levels are low in the brain. However, in AD the relative enzymatic activity is altered so that BuChE increases while AChE decreases (Greig 2005). Thus, a striking decrease in the AChE/BuChE ratio occurs in the cerebrospinal fluid (CSF) of AD patients (Arendt et al., 1984).

4.1.1 Neuroanatomical distribution

Although the main cholinesterase in the human brain is AChE, BuChE is more widely distributed (Mesulam et al., 2002b). In a normal brain, BuChE is mainly found in endothelial cells and in glial cells, whereas AChE is primarily found in the somata and axons of neurons (Darvesh et al 1998; Darvesh & Hopkins, 2003). Nevertheless, there are three brain regions with high BuChE-positive neurons: the hippocampus, the thalamus and the amygdale. Particularly in the thalamus, 90% of neurons show high immune-staining for BuChE (Darvesh & Hopkins, 2003). The non-synaptic expression of BuChE and AChE has also suggested another function of these enzymes involving adhesion and the stimulation of neurite outgrowth (Small et al., 1995; Layer et al., 1993). BuChE, but not AChE, can also be found outside the nervous system as in the blood (Silver, 1974). By contrast, AChE appears localized mainly in neurons, although it is also expressed in glial cells. In many brain areas, AChE and BuChE-expressing neurons are intermingled (Darvesh et al., 2003).

In a normal brain, BuChE activity has been located in all regions that receive cholinergic innervation. Thus, it has been reported that AChE-positive neurons in thalamic nuclei project diffusely to the cortex, modulating cortical processing and responses to new and relevant stimuli, while BuChE-positive neurons found in thalamic nuclei project specifically to the frontal cortex, and may have roles in attention (Darvesh & Hopkins, 2003).

4.1.2 Structure and function

AChE and BuChE share a 65% amino acid sequence homology (Soreq & Zakut, 1993). The active site is found at the bottom of a 20Å hydrophobic gorge which comprises the catalytic triad (Ser, His, Glu) (Silver, 1974; Lockridge et al, 1987). In addition, the active site gorge also contains what is termed an "anionic" site, which can bind to the cationic quaternary nitrogen of choline (Vellom et al, 1993), and an acyl pocket, where the acyl group of choline esters is held in place during catalysis (Figure 10a). Once ACh diffuses into this active site, it is hydrolyzed to choline and acetate, thereby terminating its neurotransmitter function (Figure 10b). The residues that line this pocket in AChE are

larger than in BuChE, allowing the accommodation of larger substrates in BuChE. At the entrance to the active site gorge of AChE, about 14 Å away, the peripheral anionic site (PAS) is located, formed by three aromatic amino acids (Figure 10a). This subsite mediates substrate inhibition of AChE (Ordentlich, et al. 1995; Radic et al., 1993). However, the PAS of BuChE is different from that of AChE; it displays weaker affinity for typical PAS ligands and mediates substrate activation. Three aromatic residues of AChE PAS are missing in the PAS of BuChE, which is formed by two amino acid residues (Asp70 and Tyr332). Both cholinesterases have also additional enzymatic activity in the form of an aryl acylamidase that catalyses the hydrolysis of acyl amides of aromatic amines (George & Balasubramaniann, 1981).

The differences in the enzyme kinetic properties and locations of brain AChE and BuChE, have led to the suggestion that, in the normal brain, AChE is the main enzyme responsible for the hydrolysis of ACh while BuChE plays a supportive role (Lane et al., 2006).

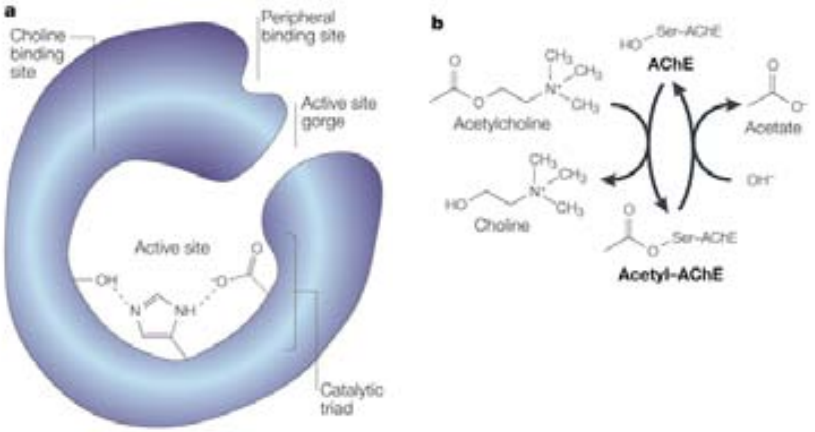

Figure 10. a) Structural features of AChE. The active site formed by the catalytic triad is situated at the bottom of a narrow gorge. A peripheral binding site has also been identified which is the responsible for Aβ-aggregation. b) The AChE reaction. Taken from Soreq & Seidman, 2001.

4.1.3 Genetic polymorphisms

The gene that codes for AChE (*ACH*) is located on chromosome 7, spans 7kb and has 6 exons (Getman et al., 1992) whereas BuChE is coded by a gene located on chromosome 3q26 (*BCHE*) (Allderdice et al., 1991), spans about 70 kb and has four exons and three large introns (Arpagaus et al., 1990). Over 40 mutations of *BCHE* have been identified, although not fully studied, producing different levels of catalytic activity. Genetic polymorphisms

have been implicated in AD but with contradictory results. Some authors have found a correlation of the "K variant" with a greater risk for developing AD (Lehman et al., 1997, 2000) whereas other studies have failed to show an association (Ki et al., 1999; Singleton et al. 2002). Indeed, it has even been suggested that the "K variant" might be a protective factor (Alvarez-Arcaya et al., 2000), due its reduced enzymatic activity.

4.1.4 Molecular forms

There are different molecular forms of AChE and BuChE that consist of similar catalytic properties but different cellular and extracellular distributions (Massoulié et al, 1993; Massoulié & Bond, 1982; Soreq & Seidman, 2001; Chatonnet & Lockridge, 1989) (Figure 11).

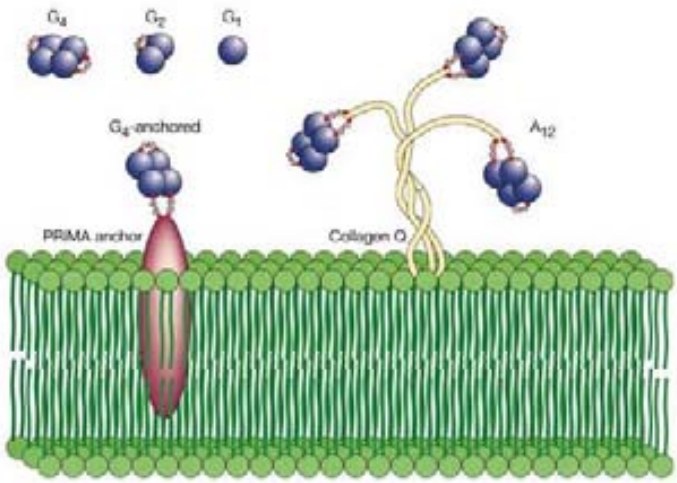

Figure 11. Molecular forms of acetylcholinesterase and butyrylcholinesterase. G1, G2 and G4 are the monomeric, dimeric and tetrameric soluble globular form, respectively. The G4-anchored form is membrane-bound through its proline-rich membrane anchor (PRiMA). A12 is an asymmetric form in which three tetrameric forms are anchored to the membrane by a collagen tail (collagen Q). Taken from Darvesh et al., 2003.

G_1, G2 and G4 forms are symmetrical, hydrophilic and globular and are found mainly in soluble form, but AChE and BuChE also occurs in membrane-bound forms that are amphiphilic and consist of tetramers which are anchored to membranes by a prolin-rich membrane protein anchor (PRiMA) or a non-catalytic, collagen-anchor. The asymmetric forms are called A4, A8 and A12 (Massoulié et al, 1993). In healthy human brains, G4 is the predominant form and AChE predominates over BuChE (Giacobini, 2003). In contrast, in the brains of patients with AD, AChE-G4 levels are lost early and, whereas levels of AChE-G1 remain unchanged (Siek, et al 1990), BuChE-G1 levels show a 30-60% increase (Arendt

et al, 1992). It has been suggested that these changes in molecular forms are direct consequences of Aβ peptide (Saez-Valero et al 2002).

4.2 Cholinesterases and Amyloid-β

Most of the cortical AChE activity in AD is found associated with SP (Geula & Mesulam, 1989), rather than NFT, in which it co-localises with amyloid-β deposits. AChE has shown to accelerate the assembly of Aβ by forming a stable AChE-Aβ complex and thus enhancing the neurotoxic effects of Aβ fibrils (Alvarez et al., 1998; Inestrosa et al., 1996). AChE also facilitates AD plaque formation *in vivo* (Rees et al., 2005). Thus, it has been widely described that AChE plays an important role in amyloid deposition and that this function, independent of the active site, is exerted by its PAS (Selkoe, 1994; Inestrosa, 1996). Thus, it has been reported that inhibitors of the PAS of AChE, may possess notable anti-Aβ aggregating properties (Giacobini, 2003; Castro & Martinez, 2006; Belluti et al., 2005). In this context, as will be explained in more detail in chapter 6, the use of dual AChE inhibitors of both the CAS and the PAS of the enzyme might possess additional benefits for the treatment of AD.

BuChE is found in plaques, tangles, and amyloid-containing vessels (Geula et al., 1994) and the levels of BuChE have been reported to correlate positively with the development of SP and NFT in AD brains (Geula et al 1994; Geula and Mesulam, 1995). Nevertheless, several authors suggest that BuChE cannot promote amyloid formation, presumably because its PAS lacks 3 key hydrophobic amino acids involved in this action in AChE (Inestrosa et al., 1996). By contrast, other authors have suggested that BuChE, rather than promoting Aβ fibrillisation, participates in the maturing of plaques from the diffuse form (benign) to the compact form (pathological) (Mesulam & Geula, 1994; Guillozet et al, 1997) which is consistent with the results obtained by other authors who reported that BuChE has an important role in AD progression (Holmes et al., 2005).

4.3 Cholinesterases and glial cells

In normal human brain, glial cells such astrocytes, microglia and oligodendrocytes release AChE and BuChE into the extracellular space when activated. However, in patients with AD, high levels of BuChE and also AChE are found in glial cells, which are recruited and activated around plaques and tangles, suggesting that this cell type might be a source of the enzyme (Wright et al., 1994). Moreover, in AD, glial BuChE/AChE ratios are

increased in the inferotemporal and enthorrinal cortex (two regions with a high susceptibility to AD pathology) but not in other brain regions (Wright et al., 1993). Despite the increasing evidence of the active participation of glial cholinesterases in AD, their role in the development of this disorder still remains unclear.

AChE and BuChE possess numerous enzymatic and non-enzymatic roles which are modified depending on their cell or subcellular localization, tissue type and health or disease status (Darvesh & Hopkins, 2003; Giacobini, 2003). Particularly BuChE is mainly found in glial cells, myelin and endothelial cells. Extracellular ACh (found outside the synapse) is the main component of brain white matter and a key structural element in functional neural networks (Bartzokis, 2007). Thus, it has been suggested that extracellular ACh may have a role in the maintenance of myelin which suggested the hypothesis that BuChE may have its particular role in myelination and inflammation (Nizri et al., 2006). This suggests an argument that inhibition of the enzymes that break down extracellular ACh might potentially give disease-modifying effects. BuChE rather than AChE may have a predominant role in breaking down extracellular ACh (Greig et al., 2005; Lane et al., 2006), thus, while AChE inhibition (synaptic ACh) might be responsible for the symptomatic impact of cholinesterase inhibitors due to increased neurotransmission, BuChE inhibition (extracellular ACh) might contribute for the disease-modifying effect due to reduced inflammation and the consequent pathological changes. There are, then, several lines of evidence indicating that it might be important to inhibit BuChE in the treatment of AD (Darvesh et al., 2003). Therefore, therapeutic agents that serve as inhibitors of both AChE and BuChE could provide additional benefits in AD when compared with agents that only inhibit AChE (Giacobini, 2000; Greig et al, 2001). Consistent with this suggestion, it has been shown that inhibition of BuChE in AD is correlated with cognitive improvement assessed using neuropsychological test batteries (Giacobini et al, 2002). Consistent with this findings, recent imaging studies have provided empirical evidence that dual inhibition of both AChE and BuChE may be neuroprotective (Venneri et al., 2005).

5. NON-CHOLINERGIC NEUROTRANSMISSION

In addition to generalised cortical cholinergic deficits, several reports have found structural and functional disturbances of other neurotransmitter systems accounting for the symptoms in AD. These are serotoninergic and noradrenergic (Perry et al., 1999, Dringerberg, 2000), as well as glutamatergic (Francis et al., 1993). Nevertheless, the study of

these neurotransmitter systems abnormalities in AD has received less attention relative to ACh. Among them, not only the loss of synapses or degeneration of particular neurons is found, but also a dysfunction in the biosynthesis and degradation of these neurotransmitters. Both muscarinic and nicotinic receptors are present not only on cholinergic nerve terminals but also on monoaminergic nerve terminals. Thus, many recent data indicate that cholinergic dysfunction by itself may not be sufficient to produce learning and memory abnormalities in AD. Rather, a considerable interplay between neurotransmitter systems such as cholinergic-monoaminergic or glutamatergic-cholinergic, would be necessary to produce the loss of cognition found in AD (Dringerberg, 2000, Hydn et al., 2004, Liu et al., 2008).

5.1 Monoaminergic system

The involvement of serotoninergic (5-hydroxytryptamine, 5-HT) atrophy in AD has been widely documented and seems to affect the majority of patients (Baker & Reynolds, 1989; Cross, 1990). NFT and SP, as well as a significant cell loss, are found in the dorsal raphe nucleus of the midbrain of AD patients, providing the serotoninergic afferens to the cortex (Yamamoto & Girano, 1985). Thus, markers of serotoninergic activity in cortical regions are found to be reduced (Cross, 1990; Palmer et al., 1987). A significant reduction is also observed in a number of several types of 5-HT receptors in cortical and limbic regions of AD patients (e.g. 5-HT_1, 5-HT_2 and 5-HT_4) (Reynolds et al., 1995) although these reductions are not specific to AD but a common finding in brains of aged, non-demented humans and other animals (McEntee & Crook, 1991; Meltzer et al., 1996). It has been reported that a decrease in cortical 5-HT occurs early during the disease course (Cross, 1990).

The noradrenergic projection pathway from the locus coeruleus to the forebrain also seems to be affected in AD (Baker & Reynolds, 1989; Rossor & Iversen, 1986). Reduced levels of noradrenalin (NA) or the NA-marker enzyme dopamine-□-hydroxylase in forebrain regions are found as signs of NA degeneration (Bondareff et al., 1982; Cross et al 1981). However, only a subset of AD patients has shown a considerable degree of NA neurodegeneration, while others show very small changes (Haroutunian et al, 1990). It seems that patients dying at younger ages show more robust decreases in NA than those dying later in the course of the disease (Bondareff et al., 1982), thus suggesting that the NA system is differentially affected by different forms of AD.

Although it has been reported that the dopaminergic system shows reductions in AD pathogenesis (Rossor & Iversen, 1986, Baker & Reinolds, 1989), the evidence of a dysfunction has been less conclusive than that found for serotoninergic and noradrenergic systems (Regland, 1993; Dringerberg, 2000). However, the involvement of monoaminergic neurotransmitter systems, particularly dopaminergic, has been strongly related with the high incidence of depression found in AD patients (Ballard et al., 2008, Gualtiery & Morgan, 2008). Indeed, many authors have recently suggested a strong relationship between depression and dementia, concluding that depression can be considered as a risk factor for AD (Geerlings et al, 2000; Ownby et al., 2006; for review see Caraci et al., 2010). Interestingly, SP and NFT are more pronounced in the hippocampus of AD patients with depression than those without depression (Rapp et al, 2008). All these data suggest a beneficial role of monoamine neurotransmission potentiation as target for the treatment of AD, which, in addition, might be useful for the treatment of the depressive symptoms observed in the majority of AD patients. Thus, inhibition of monoamine oxidase (MAO, E.C.1.4.3.4), the enzyme responsible of monoamine metabolism, as will be described in more detail in Chapter 6, might be a useful strategy for achieving this purpose.

5.2 Glutamatergic system

Glutamate is considered the main excitatory amino acid in the central nervous system (CNS), being used in approximately two thirds of synapses, and it is the most abundant in cortical and hippocampal pyramidal neurons, playing important roles in cognition and memory (Fonnum, 1984; Francis et al., 1993). A range of glutamate receptors have been identified falling into two main classes: ionotropic, including N-methyl-D-aspartate (NMDA) receptor, α-amino-3-hydroxy-5-methyl-4-isoxazole propionic acid (AMPA) receptor, and kainate (KA) receptor, and the metabotropic receptor (Ozawa et al., 1998). The ionotropic subtypes display different permeability to Na^+ and Ca^{2+} ions while the metabotropic subtype couple to adenylyl cyclase, phospholipase C or ion channels (Conn & Pin, 1997). Glutamate receptors are very important as they show depolarization of the membrane potential. Once the glutamate receptors are active, a process known as excitotoxicity occurs (Greenamyre et al., 1989) (Figure 12), which is characterised by the opening of the calcium-release channels in the endoplasmic reticulum, resulting in an increase of free calcium into the cytoplasm. This leads to the activation of a cascade of enzymes that degrade proteins and nucleic acids (Berliocchi et al., 2005) ultimately result in cell death by necrosis or apoptosis (Meldrum & Garthwaite, 1990; Lipton, 1999).

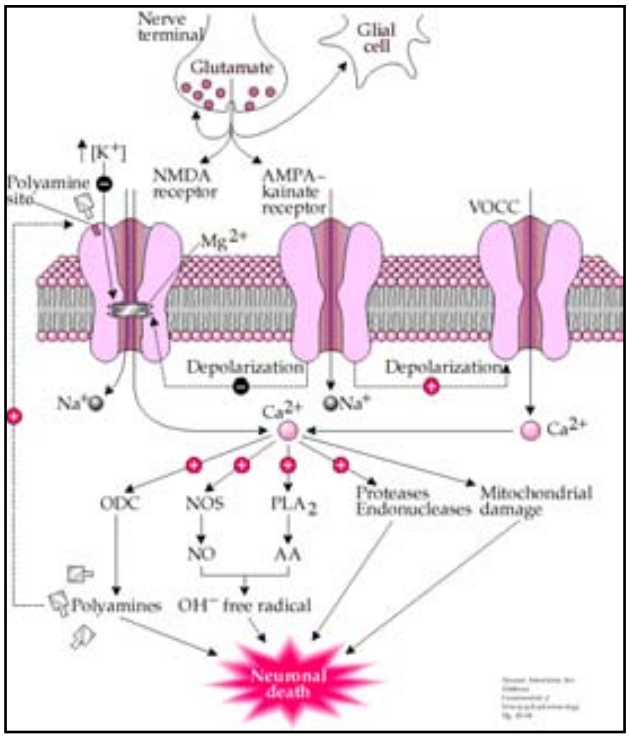

Figure 12. Schematic representation of the excitotoxicity mediated by glutamate receptors.

Excitotoxicity has been reported as an important mechanism in the neuronal damage observed in several neurodegenerative disorders, including AD (Greenamyre & Young, 1989). Thus, high concentrations of cytosolic calcium stimulate Aβ aggregation and amyloidogenesis (Isaacs et al., 2006; Pierrot et al., 2005) which, in turns, reduce glutamatergic transmission (Kamenetz et al., 2003). There is evidence that, in addition to the major cortical afferent systems, glutamergic neurotransmitters also show significant atrophy in AD, particularly in cortical and hippocampal regions (Maragos et al., 1987; Myhrer, 1998). Lesions of certain glutamatergic pathways impair learning and memory. Moreover, the activation of NMDA receptors has been implicated in Aβ-mediated excitatory neurodegeneration (Snyder et al., 2005). The decrease in cortical glutamate transporters and receptors observed in AD brains has led some authors to propose a "glutamatergic hypothesis" of AD. Nonetheless, the only non-cholinergic therapy approved for AD is the use of a NMDA-receptor blocker, memantine.

6. THERAPEUTIC STRATEGIES

At present, the only treatment approved by the Food and Drug Administration (FDA) for AD is the use of the ChE inhibitors (ChEI), donepezil, galantamine and rivastigmine and the N-methyl-D-aspartate (NMDA) receptor antagonist, memantine (Figure 13) (Birks et al., 2000; Birks & Harvey, 2006; Loy & Schneider, 2004; Areosa et al., 2005). This approach is mainly based on the "cholinergic hypothesis" (Davies & Maloney, 1976) and so attempts the improvement of the cholinergic and glutamatergic neurotransmissions.

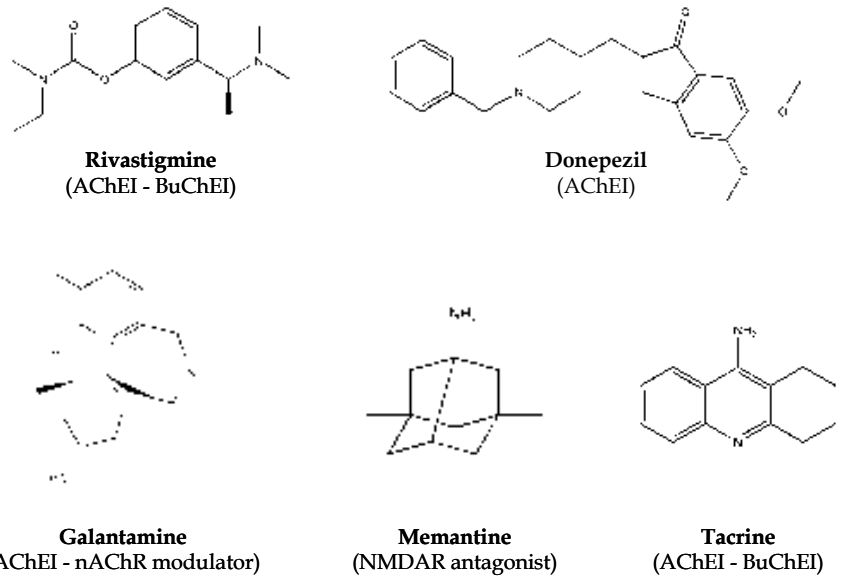

Figure 13. Chemical structures of the current available drugs for the treatment of AD. Action mechanisms are indicated in parenthesis.

Tacrine (Cognex®) is an acridine and was the first anticholinesterase approved by the FDA in 1993 (Waldholz, 1993), which, nevertheless is now rarely used because of its hepatotoxicty. Donepezil *(Aricept®)* is a piperidine that selectively inhibits AChE. At present, it is widely prescribed for the treatment of all stages of AD (Birks & Harvey, 2006). Galantamine (*Reminyl*®) is a tertiary alkaloid that, in addition to inhibit AChE, it can modulate nAChR. It is used for the treatment of mild to moderate AD (Loy & Schneider, 2004). Rivastigmine *(Exelon®)* is a carbamate and currently the only approved non-selective ChEI, so as it inhibits both AChE and BuChE (Birks et al, 2000). As galantamine, rivastigmine is used for the treatment of mild to moderate AD. Memantine (Namenda®) is the unique non-cholinergic drug approved for AD treatment (Areosa et al, 2005). In contrast, it antagonizes NMDA receptors and thus improves glutamatergic neurotransmission. It is important to mention the alkaloid Huperzine A (HupA). This is a

potent and reversible AChEI initially isolated from a Chinese herb that is very commonly used in traditional herbal medicine. HupA has been approved in China for AD treatment of mild to moderate stages (Wang et al., 2009) because of its beneficial actions in cognitive improvement without noticeable side effects. Therefore, some countries currently use HupA as dietary supplement. A clinical trial in phase 2-3 to study the safety and efficacy of HupA in patients with mild to moderate AD is underway (http://clinicaltrials.gov/NCT01282619).

Current pharmacological treatment for AD, however, has to date been shown to produce only temporary relief of the symptoms in some patients (e.g. increased ability to perform daily life activities) but not to stop or slow the progression of the disease. For this reason much effort is nowadays directed towards identifying disease-modifying therapies. A vast quantity of different therapeutic strategies in different phases of development are therefore currently being investigated, including cholinergic and glutamatergic drugs, anti-amyloid and anti-tau therapies, drugs targeting mitochondrial dysfunction, anti-inflammatory drugs, metal chelators, neurotrophins, statins and also other approaches, such us omega-3 polyunsaturated fatty acids (PUFAs), antioxidant vitamins and even metabolic or nutritional drinks (for review see Mangialasche et al., 2010) (Figure 14).

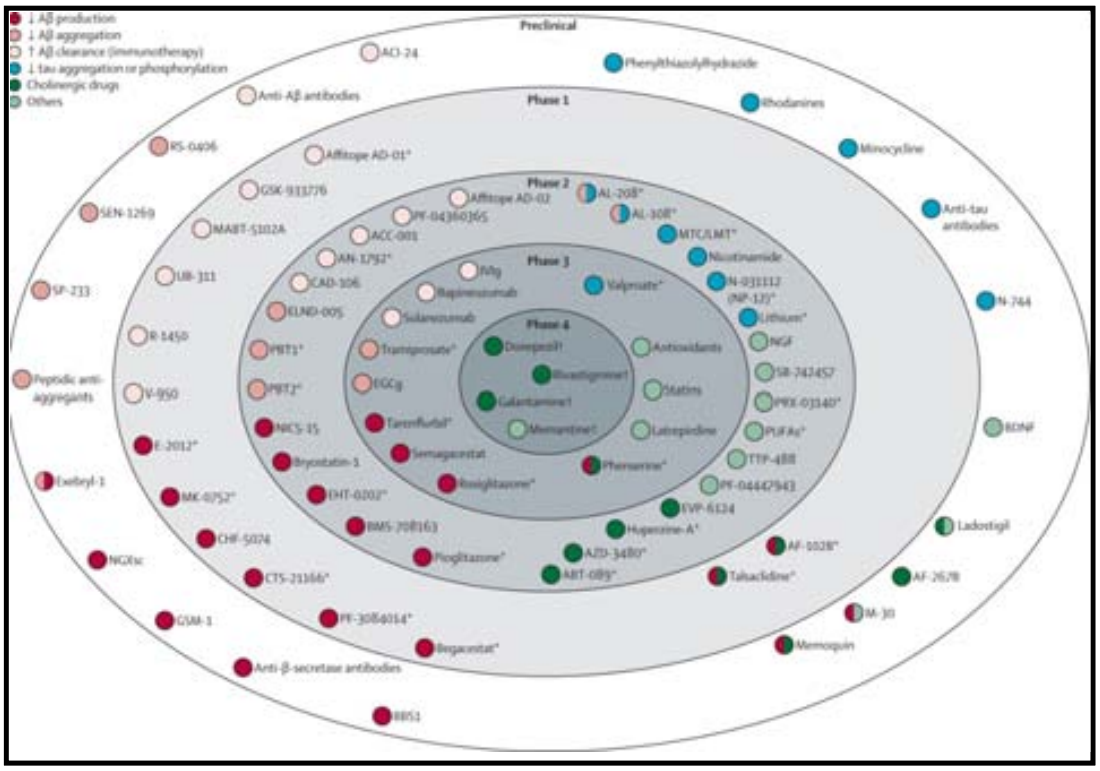

Figure 14. Schematic diagram of drugs being currently investigated for Alzheimer's disease therapy reported according to the phase of the study. Taken from Mangialasche et al., 2010.

6.1 Drugs targeting neurotransmission

6.1.1 Cholinergic drugs

The rationale for the use of cholinergic drugs in the treatment of AD is that the selective loss of basal forebrain cholinergic neurons depletes cortical acetylcholine in this disorder. The actions of the ChEI and the modulators of muscarinic and nicotinic ACh receptors are therefore believed to increase and prolong the availability of acetylcholine in the synapse, thereby improving cognitive processes such us memory and attention. The use of cholinergic receptor agonists (nicotinic, nAChR, and muscarinic, mAChR) has been attempted and several clinical trials have been undertaken. Among the beneficial properties, it has been reported that they can affect Aβ production and improve cognition (Fisher, 2008; Hilt et al., 2009) but their clinical effectiveness is not yet clear and, worse, there have been substantial side effects, so these drugs have not yet achieved general clinical use in AD (Messer, 2002).

The already approved acetylcholinesterase inhibitors (AChEIs) have shown to possess important symptomatic effects making cholinergic improvement an important goal in the development of useful drugs for AD therapy. Nevertheless, to date, little improvement has been made with these drugs, showing an important need for better cholinergic agents. AChEIs exert their effect by preventing the enzymatic degradation of the neurotransmitter ACh, resulting in increased ACh concentrations in the synaptic cleft and the consequent enhanced cholinergic neurotransmission (Lleo et al, 2006) (Figure 15).

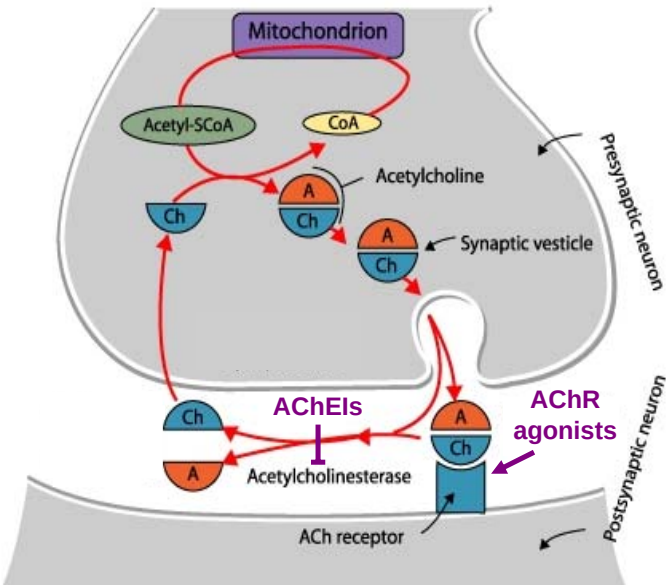

Figure 15. Schematic illustration of the mechanism of action of ACh at a cholinergic synapse. The site of action of AChEIs and AChR agonist is also shown

In addition to enhanced neurotransmission in cholinergic neurons, it seems that the benefits of AChEI in AD as symptomatic drugs are likely to be more complex than simply replacement of lost ACh (Francis et al., 1999; Lopez et al., 2002; Giacobini, 2002; Racchi et al., 2004). In this context, it has been suggested that the significant improvements in cognitive performance and in daily life activities of AChEI may be also due to an improvement in the blood supply (Ebmeier, 1992; Harkins, 1997) and glucose metabolism (Potkin, 2001) of affected areas. In addition, as recently reviewed, AChEIs may block some of the fundamental neurodegenerative processes involved in AD (Francis et al., 2005). Thus, there is evidence that several AChEIs also affect various neuropathological AD markers and modulate the cleavage of the non-amyloidogenic APP processing, reducing A□ secretion (Lahiri et al 1994, 1998; Yang et al 2009; Racchi et al., 2004). It has therefore been suggested that AChEIs possessing neuroprotection and/or APP processing properties might be more beneficial in preventing the pathogenesis of AD than those that only inhibit AChE.

The modulation of the amyloid cascade is also thought to be of prime interest in efforts to modify the course of AD. As reported in Chapter 3, it is known that AChE promotes Aβ aggregation through its PAS (Terry, 1994; Selkoe 1994; Alvarez et al., 1995). It is also now known that dual cholinesterase inhibition of both CAS and PAS of the enzyme have an additional beneficial action (Giacobini et al., 2003). On the other hand, if the therapeutic goal is to increase ACh levels in the brain, it then seems reasonable that inhibition of BuChE, in addition to AChE, should provide a greater response. Thus, it has been suggested that the non-selective cholinesterase inhibition by rivastigmine may produce enhanced benefits over AChE inhibition alone (Touchon et al., 2006; Bullock & Lane, 2007). Moreover, cymserine analogs that are selective BuChE inhibitors (BuChEIs) have shown to increase cerebrocortical ACh levels and improve cognitive function in aged rats, bolstering the case for BuChE as an important drug target in AD and perhaps other forms of dementia (Greig 2005). A recent study about the effects of ChEI in brain white matter volume showed that dual AChE and BuChE inhibition by rivastigmine over a period of 20 weeks in patients with mild to moderate AD reduced WM damage, compared with AChE-specific inhibition (Venneri & Lane, 2009).

It has been reported that ChEIs induce adverse events resulting from activation of peripheral cholinergic systems (Green et al., 2005) which include nausea, vomiting and diarrhea. However, tolerance to these side effects often develops and can usually be managed. A vast quantity of clinical trials testing different cholinesterase inhibitors are currently ongoing (see http://clinicaltrials.gov).

6.1.2 Glutamatergic drugs

As excitotoxicity is known to take place in AD pathogenesis, efforts have also been made to develop drugs that limit glutamate excitotoxicity. In this context, it has been reported that memantine, the only non-cholinergic drug approved for AD treatment, reduces glutamate excitotoxicity and, additionally, decreases Aβ toxicity and prevents hyperphosphorilation of tau (Wenk et al., 2006; Pei et al., 2008; Wu et al., 2009). The use of a combination of cholinergic and glutamatergic drugs has also been attempted. It has therefore been reported that a therapeutic combination of donepezil and memantine have significant beneficial effects on cognitive function, daily life activities and behaviour (Tariot et al., 2004). However, a more recent investigation of this approach in rats resulted in higher neurotoxicity (Creeley, 2008). Another study also suggests a therapeutic combination of galantamine and memantine (Grossberg et al., 2006).

6.2 Anti-amyloid therapies

The huge quantity of current research into potential AD therapies is based on the notion of the "amyloid cascade hypothesis" (Hardy & Higgins, 1992) which, as reported before, claims that the metabolism of Aβ is the main initiator of AD, together with the downstream formation of τ-protein aggregates. This strategy includes several different approaches targeting various events in the metabolism of Aβ. The challenge is to obtain compounds with high blood-brain barrier penetration and low immunogenicity.

Reducing Aβ production

This approach involves the search for β- and γ-secretase inhibitors, the two enzymes responsible for the amyloidogenic pathway of APP processing. It has been reported that secretase inhibitors decrease brain Aβ40 and Aβ42 as well as increase cognition in animal models (Rakover et al., 2007; Solomon, 2010). Nevertheless, to date, the search has been rather disappointing, as these enzymes have many other substrates, such as that involved in myelination, neuregulin-1, whose pathways are severely affected by its blockage. Much effort has been directed towards developing γ–secretase inhibitors but with considerable difficulties due to its large number of substrates. One of them is the Notch receptor, whose signalling pathway inhibition has produced severe collateral effects, such as skin reactions and haematological and gastrointestinal toxicity (Tomita, 2009). Several clinical trials with secretase inhibitors are currently ongoing at different phases of study

and haematological and gastrointestinal toxicity (Tomita, 2009). Several clinical trials with secretase inhibitors are currently ongoing at different phases of study (http://clinicaltrials.gov/NCT00762411, NCT00594508). Stimulation of α-secretase activity, involved in the non-amyloidogenic processing of APP, is also contemplated, as it has been demonstrated that its upregulation can decrease Aβ formation and increase the production of sAPPα, which is potentially neuroprotective (van Marum, 2008). However, no evidence currently supports the use of α-secretase activators in AD treatment (Griffiths et al., 2005). In a recent work, authors have reviewed this issue (Vincent & Govitrapong, 2011). Future trials will help to clarify the potential of α-secretase inhibition in AD therapy.

Preventing Aβ aggregation

It has been reported that Aβ plaques are formed by a vast array of different Aβ aggregates morphologies (Walsh & Selkoe, 2004) whose pathological role is still controversial due to the poor understanding of the *in vivo* polymerization process of Aβ. In this context, numerous peptidic and non-peptidic inhibitors of Aβ aggregation have been reported (Grillo-Bosch et al., 2009; Talaga, 2001; Belluti et al., 2011; Viayna et al., 2010; Camps et al., 2009). However, as noted by Bartolini et al., 2011, the majority of published compounds with an anti-aggregating action were studied for their overall effect on the aggregation process (Durairajan et al., 2008; Byun et al., 2008; Byeon et al., 2007). Nevertheless, as the accepted hypothesis is that toxicity is related to intermediate species, the challenge is to identify them for their detailed interaction with specific species.

The first generation of non-peptidic anti-aggregants, did not meet this challenge. Tramiprosate, which binds to soluble Aβ and maintains it in a non-prefibrillar form, did not prove effective in a phase 3 clinical trial in patients with mild to moderate AD (Aisen et al., 2009). Scyllo-inositol is a stereosisomer of inositol thought to bind Aβ, inhibiting its aggregation, and which is also able to promote the dissociation of preformed aggregates (McLaurin et al., 2006). Moreover, in animal studies, it was shown to reduce brain concentrations of Aβ40 and Aβ42, plaque burden, synaptic loss and glial inflammatory response and to improve spatial memory function (McLaurin et al., 2006). These functions made them promising molecules to be developed for the AD therapy. However, in phase 2 RCT in patients with mild to moderate AD (NCT00568776), the groups with the highest doses have been cancelled due to serious side effects, including nine deaths. The study continues with the group assigned the lower dose.

Epigallocatechin-3-gallate (EGCg) and Myricetin, two well-known natural polyphenols, have also been studied as inhibitors of Aβ aggregation, with very promising results (Mandel et al., 2008; Ono et al., 2003; Hamaguchi et al., 2009; Shimmio et al., 2008).

Promoting Aβ clearance

Active and passive immunotherapies have been developed to remove soluble and aggregated Aβ. Active vaccination is based on the stimulation of the host immune response, whereas the passive vaccination provides exogenous antibodies. Nevertheless, severe autoimmune reactions and hemorrhage frequency have been shown in clinical trials (Gilman et al., 2005). To avoid this toxicity, new vaccines selectively targeting B-cell epitopes without stimulating T-cells have also been developed (Winblad et al., 2009). The most innovative approach in immunization therapy is the development of conformational antibodies that target a specific specie of Aβ, such the specific anti-protofibril antibody BAN2401(AD/PD International Conference, Barcelona 2011). Despite encouraging expectation regarding the use of immunization in the treatment of AD, a post-mortem study of a clinical trial in which patients have received immunisation found that, although patients had no amyloid plaques, the dementia symptoms were present until death (Holmes et al., 2008). This finding showed that clearance of Aβ plaques alone cannot prevent disease progression or repair already damaged neurons. The benefits of vaccination in AD therapy still need therefore to be determined. Passive and active immunisations are at present being tested in human trials (http://clinicaltrials.gov/NCT01284387, NCT00960531).

6.3 Anti-tau therapies

As reported in Chapter 3, NFT are one of the pathological features found in AD patients. NFT are insoluble, intra-neuronal inclusions formed from hyperphosphorylated tau protein aggregates which are produced as a result of an imbalance between phosphatase and kinase activities. Based on this premises, therapies targeting tau protein are focused on two different approaches: 1) the development of compounds able to inhibit tau-phosphorilating kinases, whose protein levels and activities are reported to be up-regulated in AD, and 2) the development of compounds that block tau aggregation. Among the kinases inhibitors, glycogen synthase kinase 3 (GSK3), CDK-5, PKA or PKC (Ferrer et al., 2005; Savage et al., 2002) are contemplated as targets, with GSK-3β being the most studied (Rapoport & Ferreira, 2000; Sarno et al., 2005; Knockaert et al., 2002; Le Corre et al.,

2006). Thus, recent reports have highlighted the importance of GSK-3β in the development of both tau and Aβ pathologies in AD and thus suggesting this kinase as a vital drug target for treatment (Bhat et al., 2004; Martinez et al., 2002; Meijer et al., 2004). However, to date, only one compound has reached phase 3 RCT, but with negative results, as no effect on functional status and cognition was observed (Tariot & Aisen, 2009; Tariot et al., 2009). Moreover, this approach is hindered by the ubiquitous expression of these kinases and the low selectivity of inhibitors for specific kinases, isoforms, and cellular compartments (Churcher, 2006; Iqbal & Grundke-Iqbal, 2008; Stoothoff & Johnson 2005).

6.4 Neuroprotective drugs: Monoamine oxidase inhibitors

Neuroprotection is defined as an intervention able to influence the etiology or the pathogenesis underlying neurodegenerative diseases, thus preventing or delaying the onset or the progression of the disease (Shoulson, 1998). Therefore, neuroprotective compounds must display long–term benefits that are not related to symptomatic effects.

Monoamine oxidase (MAO, E.C.1.4.3.4) is a FAD-containing enzyme located in the outer mitochondrial membrane (Schnaitman et al., 1967) which catalyses the oxidative deamination of a variety of biogenic and xenobiotic amines (Youdim et al., 1988) in a reaction shown below:

$$RCH_2NH_2 + H_2O + O_2 \rightarrow RCHO + NH_3 + H_2O_2$$

The final products of the reaction are the corresponding aldehyde, hydrogen peroxide and ammonia (in case of primary amines) or a substituted amine (in case of secondary and tertiary amines) (Tipton et al., 2004). MAO is present in most mammalian tissues and exists as two distinct enzymatic isoforms, MAO-A and MAO-B, based on their substrate and inhibitor specificities (Johnston, 1968). MAO-A preferentially deaminates serotonin and is selectively and irreversibly inhibited by clorgyline. In contrast, MAO-B preferentially deaminates β-phenylethylamine and benzylamine and is irreversibly inhibited by R-(-)-deprenyl (Grimsby et al., 1990). Dopamine, adrenaline, noradrenaline, tryptamine and tyramine are oxidized by both forms of the enzyme in most species. Nevertheless, there is some evidence that substrate specificity depends also on the specie (Youdim et al., 2006). Thus, whereas only MAO-A is the responsible for dopamine metabolism in rat brain, mainly MAO-B but also MAO-A contribute to dopamine metabolism in human brain.

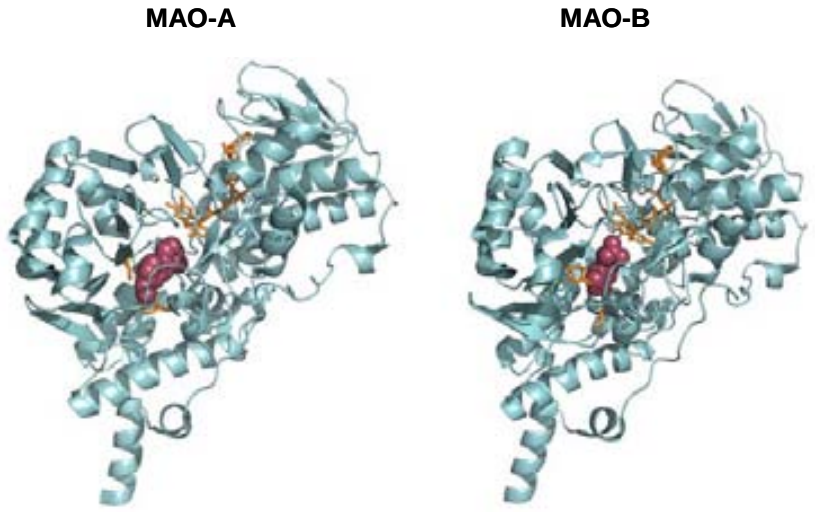

Figure 16. Structures of monoamine oxidases A (MAO-A) and B (MAO-B). The flavin-adenine nucleoside (FAD) cofactor and the residues present in the catalytic gate are shown in orange. The magenta spheres represent the position of ligands in the catalytic site.

Selective inhibitors for MAO-A (MAOAIs) have shown to be effective antidepressants, as they significantly increase amine neurotransmission. They have also been reported to be particularly effective in the treatment of phobic anxiety, hypersomnia, tiredness and bulimia (Zisook, 1985). In contrast, MAO-B inhibitors (MAOBIs), although apparently devoid of antidepressant action, are useful and commonly used in the treatment of Parkinson's disease (PD) due to their ability to extend the effects of endogenous dopamine as well as levodopa, an exogenous source of dopamine (Riederer & Youdim, 1986; The Parkinson Study Group, 1993, 2005). These actions have been reported to be able to delay the onset of disability in early PD (The Parkinson Study Group, 1993, 1996, 2004). The beneficial properties of MAOIs in these disorders have been related not only to the increased amine neurotransmission but also to the reduction of the formation of the neurotoxic products, such us hydrogen peroxide and aldehydes, which promote ROS formation and may ultimately contribute to increased neuronal damage (Pizzinat et al., 1999; Lamensdorf et al., 2000; Kristal et al., 2001; Burke et al., 2004; Marchitti et al., 2007).

Several pre-clinical studies have reported that some MAOBIs, especially those containing a propargylamine moiety, have been particularly promising for the treatment of PD and maybe other neurodegenerative diseases since they have shown also to possess neuroprotective and antiapoptotic properties (Jenner, 2004). In this context, several studies have assessed the mechanisms by which propargylamines confer this beneficial effects,

which have been related to the propargyl group present in these molecules (see Figure 17) (Tatton et al., 2003; Weinreb et al., 2006; Naoi et al., 2007). Hence, it has been reported that proparylamines are potent antioxidants (Wu et al., 1993; Sanz et al., 2004) as they increase the expression of the antioxidant enzymes catalase and superoxide dismutase (Carrillo et al, 1991, 2000). They also increase the expression of trophic factors and the anti-apoptotic proteins Bcl-2 and Bcl-xl (Bar-Am et al., 2005; Akao et al, 2002), prevent cytochrome c release and preserve mitochondrial membrane potential (Jenner, 2004; Mayurama et al., 2002). These findings, led to the suggestion that propargylamines are able to interfere at several different stages of the mechanism pathway that ends in neuronal death in PD (Schapira & Olanow, 2004). Among them, l-deprenyl (selegiline), rasagiline and PF9601N (Figure 17) were shown in different reports to confer neuroprotection by mechanisms independently of their MAO-B inhibition capacity.

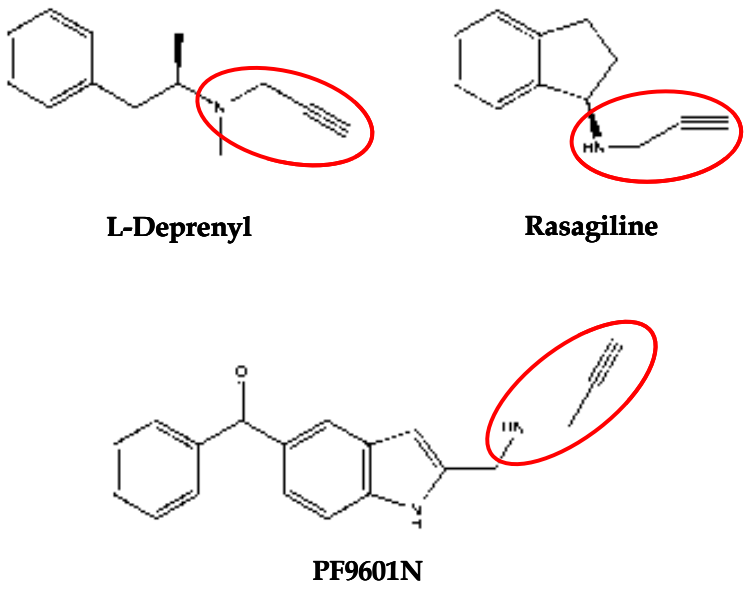

Figure 17. Chemical structures of some propargylamine-related MAOBIs with neuroprotective properties. The propargylamine moiety is highlighted in red.

L-deprenyl

L-deprenyl is an irreversible MAO-B inhibitor commonly used for the treatment of PD and one of the most studied. Its metabolism produces amphetamine-derived compounds (Heinonen et al., 1994) which have been reported to be potentially damaging and to possibly hamper its neuroprotective properties (Bar Am et al., 2004; Ricaurte et al., 1984;

Moszczynska et al., 2004). The neuroprotective properties of l-deprenyl have been extensively reported. These include the prevention of the selective destruction of dopaminergic neurons exposed to MPTP toxin (Cohen et al., 1984) and the reduction of hydroxyl radical formation which demonstrated an antioxidant capacity (Wu et al., 1993) apart from the common properties shown by propargylamine-related compounds.

Rasagiline

Rasagiline is a potent, selective and irreversible MAOBI that belongs to a second generation of MAOBIs that, unlike l-deprenyl, does not produce amphetamine derivatives as it is metabolised to (R)-aminoindan (Finberg et al., 1996). Its neuroprotective properties are similar to that observed for l-deprenyl and the other propargylamine-derived compounds. Rasagiline appeared as a promising molecule for the treatment of PD due to the results obtained from the ADAGIO study (Olanow et al, 2009), a delayed-start clinical trial that found a potential disease-modifying effects (Sampaio & Ferreira, 2010). Nevertheless, some concerns have been raised about the interpretation of this study (Ahlskog & Uitti, 2010; Schwarzschild, 2010). These concerns and the relatively small benefit provided by Rasagiline in this study emphasize the need for new compounds that not only provide symptomatic benefits but that also significantly modify the neurodegenerative process.

PF9601N (FA-73)

PF9601N, [N-(2-propynyl)-2-(5-benzyloxy-indolyl) methylamine], is a propargylamine-containing irreversible MAOBI that was identified by our group in an extensive screen of a series of acetylenic and alenic tryptamine derivatives as potential MAOIs (Balsa et al., 1991, 1994; Avila et al., 1993; Perez et al., 1996). This compound is more potent and selective than the prototypical l-deprenyl (Perez et al, 1999) and its metabolism does not produce amphetamine-like products that may potentially harm cells (Valoti, 2007). PF9601N has shown to increase the duration of L-Dopa-induced actions in an animal model of hemiparkinsonism (Prat et al., 2000) and to inhibit dopamine reuptake in human and rat striatal synaptosomes, with similar potency to that of l-deprenyl (Perez et al., 1999). In addition to the symptomatic effects, PF9601N is also an effective neuroprotective agent, demonstrated in several models of PD. Thus, it attenuates the MPTP-induced striatal dopamine depletion in young-adult and old-adult C57BL/6 mice (Perez & Unzeta, 2003) and reduces the loss of tyrosine hydroxylase (TH)-positive neurons after nigrostriatal injection of 6-hydroxydopamine in rats. Furthermore, PF9601N is able to prevent the

apoptosis evoked by MPP+ toxin which has been reported to be mediated through the prevention of the stabilisation of the pro-apoptotic transcription factor p53 and its subsequent transcriptional activity (Sanz et al., 2008). Finally, PF9601N is the only propargylamine that has been reported to block the responses elicited by endoplasmic reticulum (ER) stress (Sanz et al, 2009), one of the factors recently suggested as underlying the pathogenesis of several neurodegenerative disorders, including AD (Nakagawa et al., 2000; Hoozemans et al., 2005). Taking into account that ER stress and finally an apoptotic process have been suggested as being involved not only in PD but also in other neurodegenerative diseases such as AD, these data suggest a possible therapeutic role of PF9601N in this pathology that remains to be investigated.

It has been extensively reported that, besides increasing with age, MAO-B activity (Saura et al., 1997) is found in high levels in AD patients, probably due to the increased gliosis found in this disorder (Ekblom et al., 1994; Riederer et al., 2004). In this context, the therapeutic potential of MAOIs for the treatment of AD has been widely reported (Thomas, 2000; Riederer et al., 2004; Youdim et al., 2005, 2006). In particular, propargylamine-derived MAOIs possess a promising profile as, besides the neuroprotective properties already highlighted, they have been shown to act on very diverse types of target, including metal chelation, reduction of Aβ aggregation and toxicity (Bar-Am et al., 2009; Youdim et al., 2005) and modulation of the APP processing by promoting the non-amyloidogenic pathway (Yang et al., 2007). In fact, some clinical trials have indicated that l-deprenyl can activate some motor symptoms in AD patients (Filip & Kolibas, 1999; Birks & Flicker, 2003). Furthermore, it has been shown that selegiline has potential cognition-improving efficacy in subjects treated with donepezil (Tsunekawa et al., 2008). It therefore seems that co-administration of selegiline with donepezil had a synergistic cognition-improving effect, presumably mediated through both the dopaminergic and cholinergic systems (Tsunekawa et al, 2008). Rasagiline has also been assessed in clinical trials in combination with donepezil. The study ended in 2009 but the results are not yet available.

A great quantity of beneficial properties has therefore been found for propargylamine-containing compounds. Their beneficial effects are mediated through actions in pathways that are commonly involved in the neurodegeneration observed in several neurodegenerative disorders, including AD. Thus, these findings suggest that propargylamine-derived agents are promising molecules to be used as disease-modifying

agents in AD therapy due to their neuroprotective and antiapoptotic properties, as well as their capacity to inhibit MAO.

6.5 Other approaches

The complex nature of AD has led to the investigation of other non-traditional and very different approaches. Among them, statins (HMG-CoA reductase inhibitors), lithium salts, polyunsaturated fatty acid (PUFAs), estrogens, neurosteroids, vitamins, trophic factors, calcium channel antagonists and metal chelators are found. Interestingly, nutritional drinks and specific diets are also being attempted (for review see Mangialasche et al 2010). Furthermore, combinations of several agents targeting different types of targets are also being investigated.

7. MULTIFUNCTIONAL DRUGS FOR AD THERAPY

Despite the recent advances in the knowledge of the several factors involved in the etiology of AD, slowing or halting the neurodegenerative process has not yet been accomplished and neuroprotection is thus still considered an unmet need. In addition, pharmacological strategies based on AChEIs have shown limited effectiveness, producing moderately useful symptomatic drugs but not being successful as disease-modifying agents. There is therefore an urgent need for real disease-modifying therapies in AD. Several authors have pointed out that the ineffectiveness of current therapies may be related to the multifactorial and extremely complex nature of AD, which makes one single drug hitting a single pathway or target inadequate as treatment (Buccafusco & Terry, 2000; Youdim & Buccafusco, 2005; Sterling et al., 2002). In this context, as first suggested by these authors, it is now widely accepted that an effective therapy for AD would come through the use of compounds able to target the multiple mechanisms underlying the etiology of the disorder (Figure 18).

This new paradigm, called the multi-target-directed-ligand (MTDL) approach, describes compounds whose multiple biological profile is rationally designed to combat a particular disease (Cavalli et al., 2008). MTDLs approach has gained increasing acceptance, as it seems it can address the etiological complexity of the disorder. It has therefore been the subject of increasing attention from many research groups (Zimmermann et al., 2007; Cavalli et al., 2008; Bolognesi et al., 2008; van der Schyf et al., 2006), which have developed a wide variety of compounds acting on very diverse type of targets, including ChEs, MAOs,

Aβ peptide, calcium channels and/or metals (Rodriguez-Franco et al., 2005; Rosini et al., 2003; Elsingorst et al., 2003; Fang et al., 2008; Zheng et al., 2009).

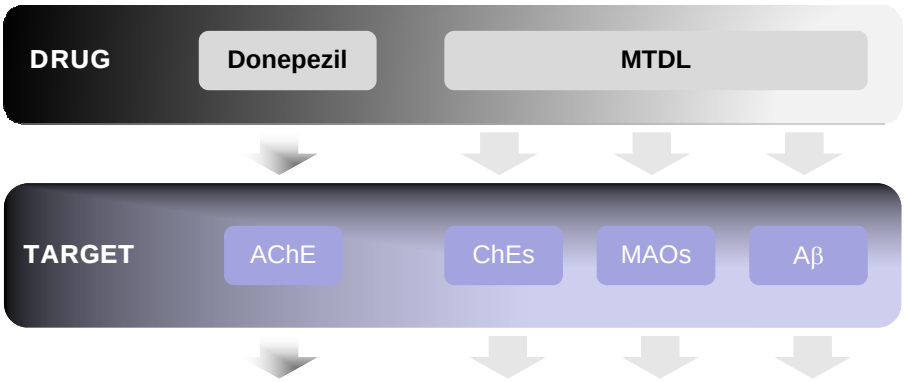

Figure 18. Pathways leading to the discovery of new drugs: On the left, the one target-one molecule paradigm and on the right, the multi-target-directed ligand approach. Modified from Cavalli et al, 2008.

To obtain MTDLs, the design strategy involves the incorporation of distinct pharmacophores of different drugs in the same structure to obtain hybrid molecules. Principally, each pharmacophore of the hybrid drug should retain the ability to interact with its specific site(s) on the target producing the consequent pharmacological response. In the context of AD, the most widely adopted approach is to combine the structure of an AChEI with another drug whose biological properties would be useful for the treatment. Thus, the indanone and the benzylpiperidine moieties of donepezil, the 1,2,3,4-tetrahydroacridine of tacrine and the carbamate of rivastigmine (Figure 19) have been combined with different molecules giving a huge amount of multitarget compounds that have been reported in literature (Rosini et al., 2008, Zheng et al., 2005; Rodriguez-Franco et al., 2005; Rosini et al., 2003; Elsingorst et al., 2003; Fang et al., 2008; Zheng et al., 2009).
The importance of the dual binding site AChE inhibition, due to the blockade of both the CAS and the PAS of the enzyme has been reported in Chapter 6. This could result in a reduction of Aβ aggregation, as well as the increased cholinergic neurotransmission. These suggestions seem to be widely accepted since the majority of the multifunctional compounds found in literature possess this biological profile (Belluti et al, 2005; Bolognesi et al., 2005; Munoz-Ruiz et al, 2005; Camps et al., 2008). Nevertheless, although it has been

extensively reported that non-selective ChE inhibitors, targeting both AChE and BuChE, may possess enhanced benefits over AChE inhibition alone (Giacobini et al., 2003), only a few compounds achieve this goal (Marco et al., 2004).

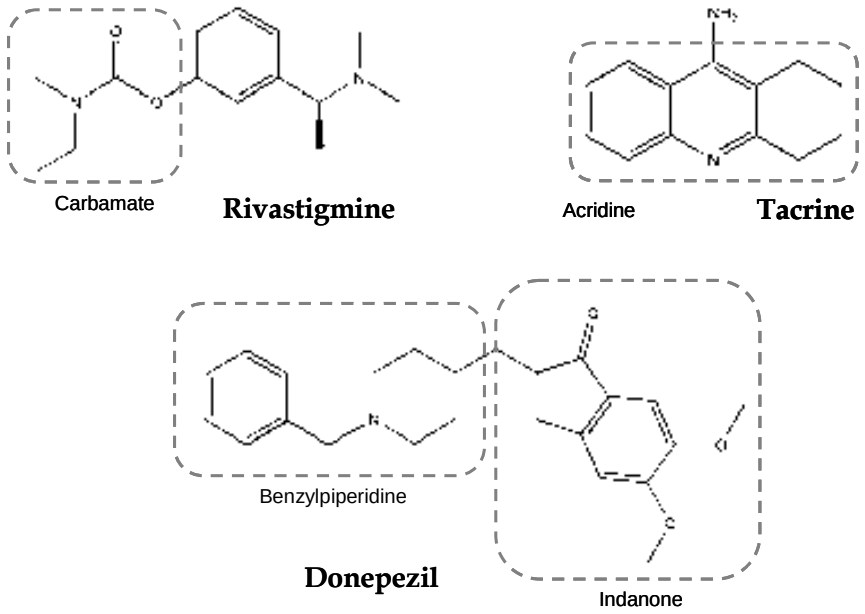

Figure 19. Chemical structures of the ChEIs used in the treatment of AD. Dashed lines show the moieties of each compound used for the development of MTDLs.

In the search for antioxidant compounds able to target the early sources of ROS produced in AD pathogenesis, the combination of lipoic acid or melatonin, two well-known natural antioxidants, with the pharmacophore of tacrine, to improve cholinergic neurotransmission, has been attempted (Bolognesi et al., 2006; Cheng et al., 2006). The results obtained have been quite encouraging as the compounds possess high bioavailability and good blood brain barrier penetration. Moreover, they are powerful inhibitors of AChE, reduce Aβ aggregation through the interaction with PAS, and reduce ROS formation to a greater extent than the parent compounds. Hybrid molecules with the reported radical scavenging properties with and additional metal chelation activity have also been investigated (Dedeoglu et al., 2004; Zheng et al., 2005; Avramovich-Tirosh et al., 2007). Among them, M30 (Figure 20) is a derivative of rasagiline with antioxidant and iron-chelating properties (Weinreb et al., 2009) as well as a good anticholinesterase activity (Zheng et al., 2010).

It has been reported that calcium dyshomeostasis is involved in the pathogenesis of AD. For this reason, calcium channel blockers possessing anticholinesterase activity have

been investigated (Marco-Contelles et al., 2006a, 2006b, 2006c; de los Ríos et al., 2002; Leon et al., 2005). The hybrid compounds found in the literature are mainly tacrine-derived, the so-called "tacripirynes", since tacrine was shown to inhibit voltage-dependent calcium channels (Kelly et al., 1991). Tacripyrines are formed by the conjugation of the tetrahydroaminoquinoline scaffold of tacrine with the dihydropirydine moiety of nimodipine, a well-known calcium channel blocker. These compounds have shown to possess an anti-cholinesterase activity and a calcium blocker profile more potent than the parent compounds (Marco-Contelles et al., 2006c).

The suggestion that other neurotransmitter systems, rather than only cholinergic neurotransmission, may be involved in the behavioural changes, cognitive decline and neuropsychiatric abnormalities observed in AD patients, have focused therapeutic interventions on the improvement of amine neurotransmission. The initial strategy was performed by combining MAO/AChE inhibitors, resulting from the conjugation of the propargylamine pharmacophore present in selegiline with physostigmine, a well known AChEI (Fink et al., 1996). The compounds obtained were good MAOIs/ChEIs but with low bioavailability and brain penetration. Supporting the usefulness of this approach, recent human trials have combined the administration of the MAOBI, selegiline, with either tacrine or physostigmine, reporting possible synergistic effects (Schneider et al., 1993; Marin et al., 1995). Therefore, as reported by Cavalli et al., 2008, MAO appears as an interesting target to be considered when designing MTDLs against AD, not only due to the increased amine neurotransmission, but also because of the reduction of the neurotoxic products of its catalytic activity, which would counteract for the beneficial effect of MAO inhibition in this disorder. Very different structures have been evaluated as MAOIs/ChEIs, including coumarinic (Gnerre et al., 2000) and xantone (Bruhlman et al., 2004) derivatives. A successful approach comes from the combination of the carbamate moiety in rivastigmine, which is currently used for the treatment of AD, with either the indolamine moiety of rasagiline or the phenethylamine substructure of selegiline (Sterling et al., 2002).

Among the derivatives obtained with this strategy, besides inhibiting both ChEs and the two isoforms of MAO, ladostigil (TV3326, Figure 20) has been shown to retain the neuroprotective and antiapoptotic properties observed for propargylamine-derived compounds (Weinstock et al., 2003; Yogev-Falach et al., 2002; Sagi et al., 2003). Hence, through the regulation of the Bcl-2 family proteins, it prevents the cleavage of caspase-3, one of the main executioner caspases that leads to apoptotic death. It also stimulates the

release of the non-amyloidegenic soluble APP, thus reducing Aβ levels (Yogev-Falach et al., 2006; Weinreb et al, 2009). Ladostigil has even reached a phase 2 clinical trial with promising results (Youdim et al., 2006), and another clinical trial started this year to investigate its safety and efficacy in mild to moderate AD (http://clinicaltrials.gov/NCT001354691). Besides MAO inhibition, other approaches have been conducted in order to promote biogenic amine activity, which would be useful to treat the depressive symptoms and neuropsychiatric abnormalities observed in AD patients. Thus, combinations with inhibitors of the serotonin transporter (SERT), which are well-known antidepressants, and ChEIs have been attempted (Kogen et al., 2002; Toda et al., 2003). 5-HT_3 receptor ligands conjugated with ChE inhibitors have also been reported (Petroianu et al., 2006).

Memoquin (Figure 20) also appears as a good product of an MTDL design strategy (Cavalli et al. 2007; Bolognesi et al., 2009). Authors have combined the polyamineamide caproctamine, a well-known AChEI and muscarinic M2 autoreceptor antagonist (Melchiorre et al., 1998) with the 1,4-benzoquinone radical scavenger moiety of idebenone, a synthetic CoQ derivative, which has been shown to improve cognition and behavioural deficits in a clinical trial of AD (Bragin et al., 2005). Authors have reported that memoquin is able to modulate several mechanisms relevant to AD (Bolognesi et al., 2009), including dual AChEI, β-secretase inhibitor, anti-Aβ aggregation, antioxidant, and reduction of tau hyperphosphorylation (Bolognesi et al., 2009).

Huprines are heterocyclic derivatives of Huperzine A (HupA), an alkaloid initially extracted from a Chinese herb and usually used in Chinese traditional medicine, and tacrine (Badia et al., 1998; Camps et al., 1999; Camps et al., 2000b; Camps et al., 2001). Among the synthesised tacrine-HupA hybrids, huprine X (Figure 20) showed the best pharmacological profile (Camps & Munoz-Torrero, 2001). Authors have found that it inhibits AChE even more potently than the currently available AChEIs (Camps et al., 2000a). Moreover, Huprine X has an agonistic action on muscarinic M1 and nicotinic receptors (Romñán et al., 2002, 2004). More recently, an in vivo study has shown that huprine X improves memory and learning activities in aged mice trough the regulation of PKCα and MAPK pathways (Ratia et al., 2010).

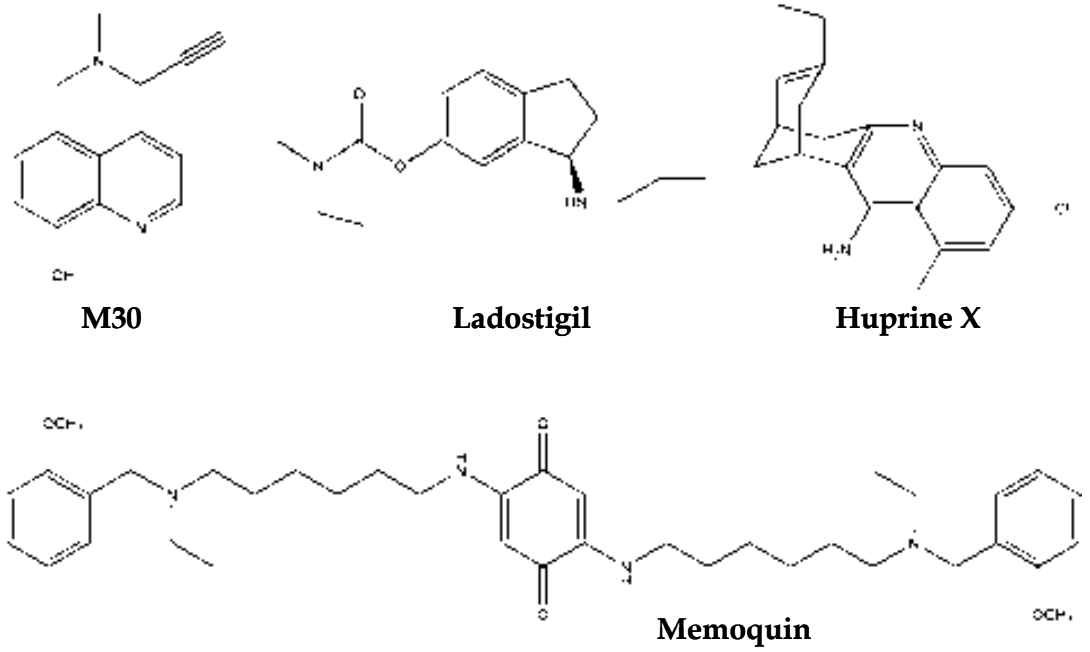

Figure 20. Chemical structures of some multi-target-directed ligands (MTDLs) developed for the treatment of AD. M30 is an iron chelator and MAOI, Ladostigil is a MAOI/ChEI, Huprine X is an AChEI and mACh and nACh receptors antagonist and memoquin is an AChEI/BACEI and a radical scavenger.

Interesting compounds have therefore been developed for the treatment of the multifactorial nature of AD following the most innovative approach, the MTDLs (Buccafusco et al., 2000). These agents appear very useful for a better understanding of the responses of the different features of AD pathogenesis to the pharmacology. Thus, they seem to be good lead compounds for the development of new and better combinations, which are warranted in order to fully address the complexity of AD. However, it is important to mention that better formulations might come through the development of non-tacrine-derived structures, as those based on tacrine could retain the hepatotoxicity observed for this substance, which in the past led to the development of new compounds. It therefore seems reasonable that in order to achieve safer cholinesterase inhibition, it may be better if future hybrid molecules contain moieties present in donepezil or rivastigmine, which, despite some easily controllable adverse effects, they do not produce hepatotoxicity.

II. AIMS

As previously reported, excitotoxicity is involved in the pathology of Alzheimer's disease (AD). Thus, the first aim of the present work was to investigate the effects of PF9601N, a selective monoamine oxidase B inhibitor (MAOBI) with several neuroprotective properties previously demonstrated by our group, in an *in vivo* model of excitotoxicity performed by microdialysis in freely-moving rats.

In the context of the new developed paradigm to combat neurodegenerative diseases, called the multi-target-directed ligands (MTDLs) approach, new hybrid molecules based on two different conjunctive approaches were designed and synthesised (in collaboration with Dr Marco, CSIC, Madrid and Dr Luque, UB, Barcelona) (Figure 1):

1) The combination of the benzyl piperidine moiety of the cholinesterase inhibitor donepezil with the indolyl propargylamino moiety of PF9601N.

2) The conjugation of the benzyl piperidine moiety of donepezil with the propargylamine of PF9601N connected to a central pyridine heterocyclic ring system.

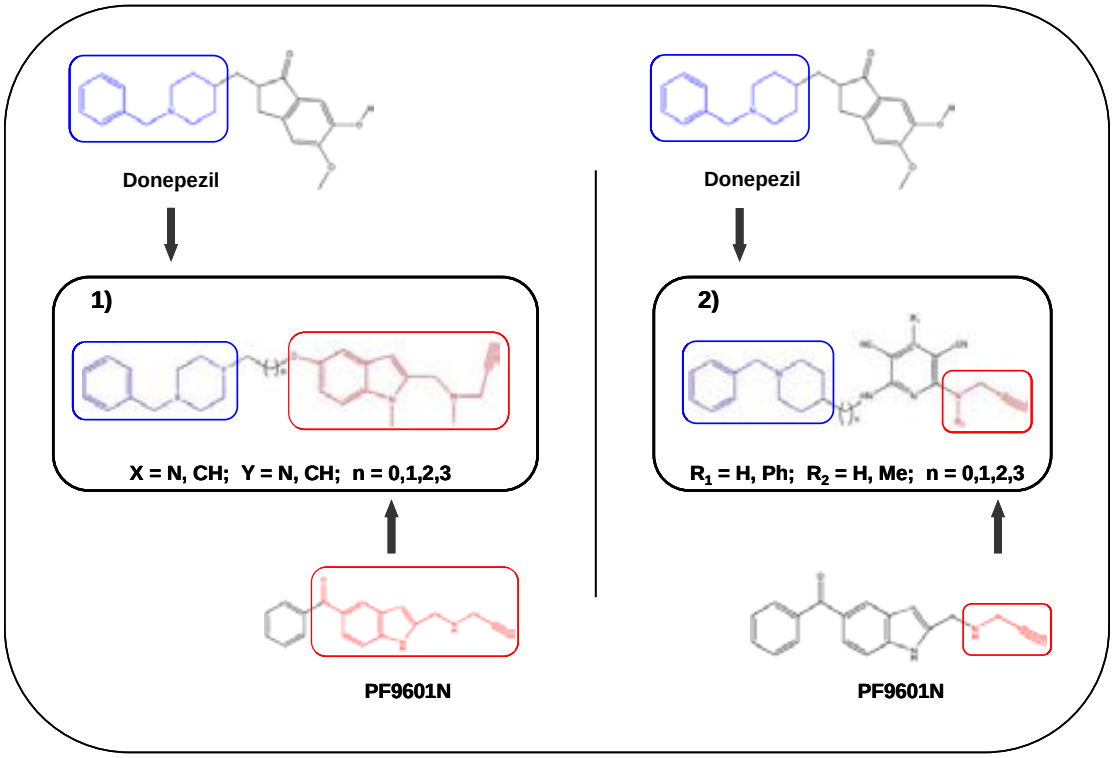

Figure 1. General structures of donepezil, PF9601N and the target molecules. The moieties of the parent compounds present in the target molecules are highlighted in blue and red.

The purpose of this strategy was to preserve the neuroprotective and MAOI activity of PF9601N and also to inhibit acetylcholinesterase (AChE) and butyrylcholinesterase (BuChE), thus obtaining MTDLs. Hence, the second aim of this work was to tackle the study of the structure-activity relationship of the synthesised compound towards the inhibition of MAOs (A and B) and ChEs (AChE and BuChE) as well as to carry out a further investigation about the kinetic profile of these compounds.

Finally, once the best compound in terms of inhibitory potency was found, the third objective of this work was to investigate its inhibitory capacity against Aβ aggregation *in vitro* as well as its potential neuroprotective properties in different cellular models. This was performed by studying the effects of the hybrid compound against different insults involved in AD pathogenesis such as inflammation, oxidative stress and Aβ toxicity.

III. RESULTS & METHODS

CHAPTER I

Neuroprotective effect of the MAO-B inhibitor, PF9601N, in an *in vivo* model of excitotoxicity.

Irene Bolea, Maria Alessandra Colivicchi, Chiara Ballini, José Luis Marco, Keith F. Tipton, Mercedes Unzeta and Laura Della Corte.

Manuscript in preparation

Neuroprotective effect of the MAO-B inhibitor, PF9601N, in an *in vivo* model of excitotoxicity.

Irene Bolea[1,2], Maria Alessandra Colivicchi[2], Chiara Ballini[2], José Luis Marco[3], Keith F. Tipton[4], Mercedes Unzeta[1], Laura Della Corte[2]

[1] *Departament de Bioquimica i Biologia Molecular. Institut de Neurociències, Facultat de Medicina, Universitat Autònoma de Barcelona, 08193 Bellaterra, Barcelona, Spain. Tel: +34935811624. Fax: +34935811573*

[2] *Dipartimento di Farmacologia Preclinica e Clinica M. Aiazzi Mancini. Università degli Studi di Firenze, Viale G. Pieraccini, 6, 50139 Firenze, Italy. Tel: +390554271226. Fax: +39055410778*

[3] *Laboratorio de Radicales Libres y Química Computacional (IQOG, CSIC), C/ Juan de la Cierva 3, 28006-Madrid, Spain. Tel:+34915622900 . Fax: +34915644853*

[4]*Department of Biochemistry, Trinity College Dublin, Dublin 2, Ireland. Tel. +35318961802. Fax: +35316772400*

Correspondence: should be addressed to Irene Bolea. Departament de Bioquímica i Biologia Molecular. Institut de Neurociències, Facultat de Medicina, Universitat Autònoma de Barcelona, 08193 Bellaterra, Barcelona, Spain. Tel: +34 581 1624 Fax: +34 93 581 3861. e-mail: irene.bolea@campus.uab.es

***Abbreviations*:** ABC, avidin-biotin-phosphatase alkaline complex; BCIP, 5-Bromo-4-Chloro-3'-Indolyphosphate p-Toluidine Salt; NBTC, Nitro-Blue Tetrazolium Chloride; DAB, 3,3'-diaminobenzidine; HCl, hydrogen chloride; ACSF, artificial CSF; DOPAC, 3,4-dihydroxyphenylacetic acid; HVA, homovanillic acid; 5HIAA, 5-hydroxyindoleacetic acid; 6-OHDA, 6-hydroxydopamine; MAO, monoamine oxidase; OPA, *o*-phthalaldehyde; PBS, phosphate buffered saline; STR, striatum.

Abstract

Parkinson's disease (PD) is characterised by a progressive loss of the nigrostriatal dopaminergic neurons, leading to a severe depletion of dopamine in the striatum. PF9601N [N-(2-propynyl)-2-(5-benzyloxy-indolyl) methylamine] is an inhibitor of monoamine oxidase B (MAO-B), which has shown to possess neuroprotective properties in several *in vitro* and *in vivo* models of PD. Since excitotoxicity is involved in the pathophysiology of this neurodegenerative disease, the aim of the present work was to investigate the effects of PF9601N in an *in vivo* model of excitotoxicity induced by the local administration of kainic acid during striatal microdialysis in adult rats. The basal and evoked release of neurotransmitters was monitored by HPLC analysis of microdialysate samples and tissue damage was evaluated histologically "*ex vivo*". PF9601N (40 mg/kg, single i.p. administration) was able to reduce the kainate-evoked release of glutamate and aspartate and to increase taurine release, but it had no effect on the release of dopamine, DOPAC, HVA and 5HIAA. PF9601N pre-treatment also resulted in a significant reduction of the kainate-induced astrocytosis, microgliosis and apoptosis. The present results suggest PF9601N as a good candidate for the treatment of PD and other neurodegenerative diseases mediated by excitotoxicity.

Running Title: PF9601N reduces kainate-induced damage in rats striatum

Keywords: Monoamine oxidases, excitotoxicity, kainate, amino acids, amines, glia.

Introduction

Idiopathic Parkinson's disease (PD) is characterised by a dysfunction of the nigro-striatal system as a consequence of the degeneration of pigmented dopaminergic neurons of the pars compacta zone of the substantia nigra (SNc) (Hirsch et al., 1998). However, the causes of this degeneration still remain unclear. Different hypotheses include an accumulation of endogenous and/or exogenous toxins (Stoessl, 1999; Di Montse et al, 2002), mitochondrial dysfunction (Winklhofer and Haass, 2010), iron accumulation (Dexter et al., 1989; Sofic et al., 1991), oxidative stress (Jenner, 2003; Götz et al, 1990), free radical formation (Olanow, 1992) and genetic predisposing factors (Lim and Ng, 2009; Simón-Sánchez et al., 2009). There is also some evidence that excitotoxicity, which has been implicated in a number of other neurodegenerative diseases (for reviews, see Lau and Tymianski, 2010; Mattson, 2003), may also be involved (Nicotera et al, 1999; Caudle and Zhang, 2009; Blandini, 2010).

Although most studies on the role of excitotoxicity in PD have concentrated on the NMDA receptors (Turski et al., 1991; Koutsilieri and Riederer, 2007), non-NMDA receptors also appear to be involved in this process (Michaels and Rothman, 1990; Leist and Nicotera, 1999; Johnson et al., 2009; Lau and, Tymianski, 2010). It has been suggested that kainate receptors might be a target for the development of new pharmacotherapeutic approaches in Parkinson's disease (Jin and Smith, 2007). Kainate is a glutamate cyclic analog commonly used to study the mechanisms, by which excitotoxicity induces cell death (McGeer and McGeer, 1996, Portera-Cailliau 1997, Canals, 2001). It provokes neuronal death by both apoptotic and necrotic processes (Bonfocco et al, 1995; Nakai, 2000) also increases astrogliosis and activates microglia (Matyja, 1986; McBean et al., 1995), and both these processes also appear to be involved in the pathogenesis of PD.

One approach for ameliorating PD has involved inhibitors of the enzyme monoamine oxidase (MAO, E.C.1.4.3.4). MAO catalyzes the oxidative deamination of primary, secondary and some tertiary amines (Youdim et al., 1988). There are two isoforms of MAO, MAO-A, which deaminates serotonin and is sensitive to inhibition by clorgyline (nM range) and MAO-B, which preferentially deaminates, 2-phenylethylamine and is selectively inhibited by *l*-deprenyl (nM range). Both isoforms of MAO are active towards dopamine and tyramine (Johnston, 1968; Grimsby et al., 1990).

l-Deprenyl (Selegiline), which was introduced as an adjunct to levodopa therapy in PD, has been shown to possess neuroprotective properties in several PD models and to slow the rate of the disease progression (for reviews see Ebadi et al, 2002; Youdim et al., 2006). Concerns that *l*-amphetamine was a metabolite of selegiline (Reynolds et al., 1978) led to the development and assessment of other MAO-B inhibitors. Several studies showed that the neuroprotective properties were independent of MAO inhibition (Ansari et al., 1993; Kragten et al., 1998; Speiser et al., 1999). Cruces et al. (1991) described a new series of propargylamine derivatives, among which, PF9601N [N-(2-propynyl)-2-(5-benzyloxy-indolyl) methylamine], an acetylenic tryptamine derivative, was shown to be a more potent and selective MAO-B inhibitor than *l*-deprenyl (Perez et al., 1999). PF9601N (see figure 1) showed neuroprotective properties *in vivo*, against the toxicity induced by MPTP (Perez & Unzeta, 2003) and against the intrastriatal injection of 6-hydroxydopamine (6-OHDA) (Cutillas, et al., 2002). Moreover, it showed an inhibitory capacity towards dopamine reuptake in the human caudate, similar to that of *l*-deprenyl (Perez et al., 1999). *In vitro* studies showed PF9601N to prevent the cell death induced by mitochondrial complex I inhibition and to maintain the mitochondrial membrane potential (Battaglia et al., 2006). It was also protective against endoplasmic

reticulum stress (Sanz et al., 2008, Sanz et al., 2009) and able to prevent the dopamine-induced damage to SH-SY5Y cells (Sanz et al., 2004) as well as to interact with reactive oxygen species (Bellik et al., 2010). The antiapoptotic effects of PF9601N appear to involve through prevention of transcription factor p53 stabilization and its subsequent transcriptional activity (Sanz et al., 2008).

In this study, we investigated the possible beneficial effect of PF9601N against an *in vivo* model of excitotoxicity induced by the intrastriatal perfusion of kainic acid during striatal microdialysis in adult rats. Changes in amino acids and monoamine content in the striatal extracellular fluid were studied by HPLC analysis of microdialysis samples. At the end of the microdialysis experiment, cerebral tissue was evaluated by immunohistochemistry in terms of the ability of PF9601N to reduce the kainate-induced astrogliosis and microglial reactivity and to exert an antiapoptotic effect.

MATERIALS AND METHODS

Materials

The following commercial products were used: 17 amino acids stock solution (Pierce, Rockford, Illinois, USA). GABA, 2-aminoethanesulfonic acid (taurine), kainate, *o*-phthaldialdehyde (OPA), 2-mercaptoethanol, paraffin, *p*-nitrotetrazolium blue chloride (NTBT), 5-bromo-4-chloro-3-indolyl phosphate dipotassium salt (BCIP), eosin, 3,3'-diaminobenzidine tetrahydrochloride hydrate (DAB), Hoechst 33258, N,N-dimethylformamide (DMFM), Hematoxylin, Eosin (Sigma-Aldrich, Milan, Italy). Glacial acetic acid, chloral hydrate and formaldehyde (Merck, Darmstadt, Germany). Methanol (BDH, England). Xylene, ethanol, hydrogen chloride, hydrogen peroxide, gelatin from bovine skin (Panreac, Barcelona, Spain), Triton X100 (Probus, Geneve), Glycine, Tris-HCl (USB), (-)–tetramisole hydrochloride (levamisole), magnesium

chloride solution (Fluka, Milan, Italy), glutamine, fetal bovine serum (Gibco), Vectastain ABC-alcaline phosphatase kit, Vectastain ABC-peroxidase kit, HRP-Streptavidine, anti-rabbit tyrosine hydroxylase (TH), antibody anti-NeuN, Goat Anti-Rabbit Biotinilated IgG, horse Anti-mouse Biotinilated IgG (Vector Laboratories, USA). Anti rabbit-Glial Fibrilar Acidic Protein (GFAP) (Dako, Denmark), Mouse anti-ssDNA (Apostain) (Bender Med Systems, USA), Alexa Fluor 488 Goat Anti-mouse IgG (Molecular Probes). All salts were from Merck (Darmstadt, Germany) and [N-(2-propynyl)-2-(5-benzyloxy-indolyl) methylamine] (PF9601N) was synthesised by the procedure of Cruces et al (1991).

Methods

Animal housing

All the experiments involving laboratory animals were performed according to the Italian Guidelines for Animal Care (D.L. 116/92), which were also in accordance with the European Communities Council Directives (86/609/ECC), with all efforts to minimize animal sufferings and the number of animals necessary to collect reliable scientific data. Formal approval to conduct the experiments described has been obtained from the animal subjects review board of the University of Florence. No alternatives to *in vivo* techniques are available for this type of experiments.

Male Wistar rats weighing 200-220 g (Harlan, Milan, Italy) were housed in transparent cages under controlled conditions of temperature (23±1°C) and humidity, with free access to food and water and with a light/dark cycle consisting on 12h light and 12h dark.

In vivo experiments

Surgery and microdialysis procedure. As previously described (Freinbichler et al, 2008), the rats were anaesthetized with chloral hydrate (400 mg/kg, i.p.) and placed in a stereotaxic apparatus. A microdialysis guide cannula (concentric design, CMA/Microdialysis AB, Stockholm, Sweden) was implanted vertically in the right neostriatum and fixed to the skull with self-curing acrylic (Kerr Italia, Salerno, Italy) and the skin was sutured. Stereotaxic coordinates for the neostriatum, relative to the Bregma, were AP 0.7, L 3.2, DV 5.5 mm (Paxinos and Watson 1986).

The microdialysis experiments were performed on freely-moving rats about 24 h later, always starting at 9.00 AM. The artificial cerebrospinal fluid (aCSF) comprised: 140 mM NaCl, 3 mM KCl, 1.2 mM $CaCl_2$, 1.0 mM $MgCl_2$, 1.2 mM Na_2HPO_4, 0.27 mM NaH_2PO_4 and 7.2 mM glucose (pH 7.4). The dialysis probe (4 mm probe tip, CMA/Microdialysis AB, Stockholm, Sweden) was inserted into the guide cannula, perfused with aCSF at the rate of 3 μL/min, via polyethylene tubing (i.d. 0.38 mm) connected to a 1 mL syringe mounted on a micro-infusion pump (CMA/100, CMA/Microdialysis AB, Stockholm, Sweden). After a 90 min stabilization period, the dialysate samples were collected every 20 min. Three samples were collected to measure the basal extracellular concentrations of neurotransmitters under resting conditions, before the local application of 50 mM KCl for one fraction (20 min). After collecting three more fractions, the rats were anesthetized (chloral hydrate 400 mg/kg i.p.) just before an excitotoxic concentration (1 mM) of the non-NMDA glutamate receptor agonist, kainate, was applied to the neostriatum for 20 min (fraction collected at 100 min) through the dialysis probe. Further dialysate samples were then collected every 20 min, up to 180 min. PF9601N pretreatment consisted in a single i.p. administration of 40 mg/kg disolved in dimethylformamide, 3 h before the intrastriatal kainate perfusion; the untreated group received, 3 h before the application of kainate, an

i.p. administration of the vehicle, dimethylformamide, alone. The dialysate samples were either analyzed immediately or frozen before analysis. At analysis, the dialysate sample was split, 10 µl were used for amino acid determination and 50 µl for amines and metabolites.

The following number of rats underwent microdialysis in each treatment group: K+/kainate (n = 13), K+/kainate + PF9601N (n = 6) and PF9601N alone (n = 5).

Rats were then killed by decapitation 48 hours after kainate stimulation. Then, the striatum was isolated, fixed in 4% formaldehyde solution in PBS for 72h and included onto paraffin. Finally, 5 µm-thick sections were cut using a microtome (Polaron, U.K) and examined by light microscopy (Nikon Eclipse 80i, Nikon, Instrument SpA, Florence, Italy) to verify the correct placement of the probe. Only data obtained from rats with correctly implanted probes were included in the results. The striatum area covering the correct placement of the probes is shown in figure 2.

Amino acid determination. The concentration of the excitatory amino acids, glutamate and aspartate and the inhibitory amino acids taurine and GABA were measured by HPLC with fluorimetric detection as previously described by Bianchi et al. (1999) with little modifications. Briefly, one 10 µl aliquot of each microdyalisate sample was treated to derivatize the amino acids with mercaptoethanol and *o*-phthalaldehyde (OPA). The OPA derivatives were then separated on a 5 µm reverse-phase Nucleosil C18 column (EC 250x4.6mm; Macherey-Nagel, Duren Germany) kept at room temperature, using a mobile phase consisting of methanol and potassium acetate (0.1 M, pH adjusted to 5.48 with glacial acetic acid) at a flow rate of 1.0 ml/min in a three linear steps gradient (from 25% to 90% methanol). The HPLC analysis of the dialysates was carried out using a reverse-phase Shimadzu (Shimadzu Italia S.r.l., Milan, Italy) HPLC system, consisting of LC-10A$_{VP}$ pumps, SIL-10AD$_{VP}$ refrigerated autoinjector, RF-551

fluorescence detector (λ_{ex} = 340 nm and λ_{em} = 455 nm, for the amino acid OPA-derivatives). The manufacturer's software (Class-VP™ 7.2.1 SP1 Client/Server Chromatography Data System) was used for controlling the system and for chromatographic peak recording and integration.

Determination of monoamines and metabolites. The concentration of dopamine and its metabolites, HVA and DOPAC, as well as 5HIAA, in microdialysate samples were analysed by a method developed in our laboratory, using HPLC with coulometric detection. Aliquots (50 µl) of the collected microdialysate fractions were injected into an HPLC apparatus consisting of a LC-10AD Shimadzu Pump and a SIL-10ADvp Shimadzu Auto injector (Shimadzu Italia, Milan, Italy), equipped with a Macherey-Nagel (Duren, Germany), 125/3 nucleosil 100-5 C18 AB column and a µBondapak 10 µm 125A C18 Pre-column (Waters, Milan, Italy). The mobile phase was 75mM sodium dihydrogen phosphate monohydrate, 3 mM 1-octanesulfonic acid sodium salt, 1.2 mM EDTA, 8% acetonitrile, adjusted to pH 3.4 with phosphoric acid. The mobile phase was isocratically run at 0.8 ml/min flow rate. The coulometric detector consisted in 3 ESA cells (Model 6210, Alfatech SpA, Genoa, Italy) (12 electrodes set at the following potentials: E1 -250 mV, E2 -200 mV, E3 -200 mV, E4 -80 mV, E5 -80 mV, E6 0 mV, E7 100 mV, E8 200 mV, E9 300 mV, E10 350 mV, E11 400 mV, E12 400 mV) and an ESA 5600A CoulArray Detector (Alfatech SpA, Genova, Italy). Chromatograms were processed using the CoulArrayWin MFC Application software. The detection limit was 0.200 nM for dopamine and 0.500 nM for its metabolites and 5HIAA.

***Ex vivo* experiments**

For all histological studies, sections were first deparaffinized, gradually hydrated and finally washed twice in 0.1 M PBS (pH 7.4) containing 0.3 % Triton X-100 (PBS-0.3Tx).

Immunohistochemistry

For the immunohistochemical staining of astrocytes, the tissue was treated with 0.5 M HCl for 30 min, blocked with 10% foetal bovine serum for 1h and incubated overnight at 4ºC with antibody anti-GFAP (1:1000). The sections were washed twice with PBS-0.3Tx containing 0.48 g/L levamisole to block endogenous alkaline phosphatase activity and then they were incubated for 1h with anti-rabbit antibody (1:400) in 0.1 M PBS containing also 0.48 g/L levamisole. The antigen-antibody complex was visualized by the ABC kit (1:200). Phosphatase alkaline was developed with BCIP and NBTC substrate solution until obtained a specific blue colour stained.

Tunel assay

Tunel assay was used to analyse the extent of DNA fragmentation. Terminal deoxynucleotidyl Transferase Biotin-dUTP Nick End Labeling immunohistochemistry, using the Klenow fragELMT DNA Fragmentation Detection Kit (Inalco, Milano, Italia) was applied to identify apoptotic nuclei as previously described (Freinbichler et al, 2008). Apoptotic and non-apoptotic nuclei were identified by a brown and a light-blue color, respectively; they were then expressed as percentage of the total number of nuclei. Six to seven fields were counted in each case, corresponding to approximately 2000–3000 nuclei. Quantitative image analysis was performed using the public domain software Scion Image (Scion Corporation, Frederick, MD, USA).

Histochemistry

For the histochemical staining of microglia, sections were incubated in 2% H_2O_2 and 70% methanol in 0.1 M PBS for 10 min to block endogenous peroxidase activity. After

two further washes in PBS-1Tx, sections were incubated in 6 µg/ml of Lectin *Lycopersicon Esculentum* biotinylated in the previous solution for 2 h at 37 ºC. Sections were washed again and incubated with HRP-Streptavidine-Peroxidase (1:200) in 0.1 M PBS for 1h at room temperature. Finally, sections were washed and developed using 0.05% DAB and 0.01% H_2O_2 in 0.1M PB.

Immunohistofluorescence

Apostain, a specific ss-DNA antibody, was used to evidenciate the apoptotic nuclei. After the deparaffination and rehydration process, DNA was denaturalised with 50% formamide in PBS for 30 min at 60 ºC. Sections were washed with PBS-0.3Tx, treated with 0.5 M hydrogen chloride for 30 min at 37 ºC, blocked with 10 % foetal bovine serum for 1 h and incubated overnight at 4 ºC with mouse anti-ssDNA (Apostain, 1:100). After several washes in PBS-0.3Tx, sections were incubated for 1 h at room temperature with goat anti-mouse Alexa Fluor 488 (1:1000). Sections were counterstained with Hoechst 33258 (data not shown) and finally mounted with mowiol medium.

The sections that were not mounted with the aqueous mowiol medium were dehydrated in increasing concentrations of ethanol, cleared with xylene and coverslips were mounted with DPX. All sections were analysed and photographed in a NIKON Eclipse TE 2000-E fluorescence microscope containing a Hamamatsu C-4742-80-12AG digital sight camera and using a 10× and 20× objective lenses. The software used was Metamorph® Imaging System.

Statistical analysis

The statistical analysis of amino acid and amine concentrations in microdialysate fractions was performed on the original values (nM), whereas, for graphical purposes

only, concentrations were expressed as percentage of their respective basal values. The parameter used for statistical analysis was the area under the concentration-time curve (AUC), normalized to the time unit corresponding to one 20 min fraction. Mean basal values obtained either from the AUC between –60 and -20 min, normalised to the 20 min time unit, were not significantly different from those obtained using the concentration of the -20 min fraction collected immediately before the application of the first K^+ stimulation. Thus mean values for the stimulated K^+- and kainate-induced output were obtained from the stimulated AUC values (nM / 20 min) minus their respective basal value, i.e. the concentration in the -20 min and 80 min fraction, respectively. Confidence intervals (95% CI) of means and the one sample test were used for statistical significance of the evoked output. When appropriate, data was analysed by ANOVA, followed by the Bonferroni's test for *post hoc* multiple comparisons, setting the probability level for statistical significance at $p < 0.05$ and using the program Prism 5.0 for Mac OS X (GraphPad Software Inc., La Jolla, USA).

RESULTS

In vivo experiments

Extracellular levels of amino acids in the striatum

In preliminary microdialysis experiments, basal levels of the amino acids, aspartate, glutamate, taurine and GABA, in the absence of any stimulation or treatment were found to be stable over the entire experimental time period, i.e. up to 260 min, during the collection of 20 min microdialysis fractions. In order to study the effect of PF9601N on the basal and K^+ or kainate-evoked release, 3 groups of rats underwent striatal microdialysis. Basal and K^+- or kainate- evoked release of the amino acids, aspartate, glutamate, taurine and GABA, were monitored in one group in the absence and in one

in the presence of PF9601N pre-treatment, while in a third group of rats, PF9601N pre-treatment was administered in the absence of K^+ and kainate stimulation to verify any possible effect on basal levels and their stability over time. The time course of the extracellular concentrations of aspartate, glutamate taurine and GABA, expressed as percentage of their respective basal levels, are shown in Fig. 3. The basal extracellular concentrations observed in the three groups, K+/kainate, K+/kainate + PF9601N and PF9601N alone, respectively, were (mean $\pm$ s.e.m., nM): 218 ± 36, 292 ± 70 and 243 ± 53 for aspartate, 858 ± 142, 835 ± 88 and 857 ± 66 for glutamate, 1,459 ± 94, 1,052 ± 126 and 1,027 ± 180 for taurine and 41 ± 5, 48 ± 10 and 45 ± 7 for GABA. None of these amino acids showed a statistically significant difference in the basal levels of the three treatment groups. The intra-striatal administration of both, K^+ (50 mM) and kainate (1 mM), induced a statistically significant increase in the output of aspartate, glutamate and taurine. The peak increase induced by K^+ was 179, 154 and 187 % of basal values, for aspartate, glutamate and taurine, respectively; that induced by kainate was 201%, 168% and 207% of basal value, for aspartate, glutamate and taurine, respectively. Mean AUC values (nM, 20 min) $\pm$ s.e.m., together with their 95% CL are shown in table 1 A and 1 B. The pre-treatment with PF9601N, while did not affect the K^+-evoked release of aspartate, induced a significant reduction of the kainate-evoked release of aspartate and of both, K^+- and kainate-evoked release of glutamate, as shown by the non statistically significant output (Table 1 A). PF9601N induced, rather than a decrease, an increase of the kainate-evoked release of taurine, from 207 to 342 % of basal values, shown to be statistically significant by analysis of variance followed by the *post hoc* Bonferroni multiple comparison test. Under the present experimental conditions, where kainate stimulation was performed under anaesthesia, no kainate-induced GABA release could be observed. In the absence of K^+ and kainate stimulation,

PF9601N alone did not affect the basal output of the 4 amino acids.

Extracellular levels of monoamines and their metabolites

In the preliminary microdialysis experiments, together with basal levels of amino acids also basal levels of dopamine, and its metabolites, homovanilic acid (HVA) and 3,4-dihydroxyphenylacetic acid (DOPAC) as well as those of the main 5-HT metabolite, 5-hydroxyindoleacetic acid (5-HIAA), in the absence of any stimulation or treatment, were monitored and found to be stable over more than the entire experimental time period, i.e. up to 260 min, collecting 20 min microdialysis fractions. Under the present experimental conditions, the concentration of serotonin (5-hydroxytryptamine, 5-HT) in microdialysate samples could not be detected quantitatively. The extracellular concentrations of dopamine and metabolites were analysed, taking an aliquot from the microdialysate samples obtained from the three treatment groups, i.e. K^+ /kainate, K^+ /kainate plus PF9601N, PF601N alone. The time course of the extracellular concentrations of dopamine, HVA, DOPAC, as well as those of 5-HIAA, represented as % of basal levels, are shown in Fig. 4. The basal extracellular concentrations observed in the three groups, K+/kainate, K+/kainate + PF9601N and PF9601N alone, were (mean $\pm$ s.e.m., nM): 2.024±0.429, 1.926±0.320 and 1.527±0.113 for dopamine, 631±49, 716±66 and 792±164 for DOPAC, 328±78, 371±49 and 391±42 for HVA and 117±13, 135±14 and 121±13 for 5HIAA. Basal values observed in the three treatment groups were not significantly different. The intrastriatal administration of 1 mM kainate induced a statistically significant increase of dopamine release together with a decrease of that of the metabolites, HVA and DOPAC as well as 5-HIAA. None of the kainate-evoked changes were affected by PF9601N pre-treatment. PF9601N alone did not produce any effect on the basal output of dopamine, HVA, DOPAC and 5-HIAA.

Ex vivo experiments

Striatal immunohistochemistry of glial population

Representative microphotographs of microglia (Lectin *Lycopersicon Esculentum* histochemistry) and astrocytes (GFAP immunostaining) are shown in figure 5. A significant increase in microglial reactivity was observed in the striatum of kainate perfused rats (Fig 5 B, G). This was evidenced not only by the number of lectin-positive cells, but also by their degree of reactivity, showing enlarged somas and thickned processes, characteristic of activated microglia. The striatal tissue of animals perfused with kainate, showed also a significant astrocytosis, as evidenced by a statistically significant increase in the number of GFAP-immunopositive cells (Fig. 5 E, H). PF9601N pre-treatment was able to significantly prevent microglial activation (Fig. 5 C, G) as well as astrogliosis (Fig. 5 F, H). Animals pre-treated with PF9601N in the absence of the local administration of kainate did not show a significant microglial activation or astrogliosis.

Striatal immunohistochemistry of apoptotic nuclei

Representative microphotographs of apoptotic nuclei evidenced by Tunel assay are shown in Fig 6. These technique evidences non-apoptotic cells in green and apoptotic cells in brown. The intrastriatal administration of kainate into the striatum induced a significant number of apoptotic nuclei, 70 $\pm$ 13 %, as compared to 3 $\pm$ 1 % in the control group (Fig. 6 A-B, D) (**$p<0.01$). In contrast, pre-treatment with PF9601N was able to reduce the number of apoptotic nuclei down to those observed in control rats, which received PF9601N alone (Fig. 6 B-C, D).

DISCUSSION

Current, treatments for PD are essentially symptomatic, based on agents that are capable of improving some of the characteristic symptoms of the disease, but they are unable to prevent its progression (Factor, 2008). However, l-deprenyl (Selegiline) and some other MAO-B inhibitors have been reported to delay the progression of the disease to some extent (The Parkinson study group, 2002, 2004; Macleod et al., 2005) and also to improve the motor complications in PD patients treated with l-DOPA (Rascol et al., 2005; Marconi et al., 1992).

The propargylamine derivative PF9601N has previously shown to possess neuroprotective properties in several *in vitro* and *in vivo* models of PD and also to prolong the effects of exogenously administered levodopa in different experimental models of PD (Perez et al., 2003; Cutillas et al., 2002; Prat et al., 2000). Thus, the protective effects of PF9601N appear to extend beyond Parkinson's disease. In the present study we have demonstrated that PF9601N is also able to prevent the excitotoxic damage induced by kainic acid, in a process that involves decreasing the evoked release of the excitatory amino acids and increasing the output of the inhibitory and neuroprotective amino acid taurine. The excitotoxicity induced by an hyperactivation of ionotropic glutamatergic receptors has been reported to be involved in a number of neurodegenerative disorders, including those following stroke and head trauma as well as Huntington's disease, PD and Alzheimer's disease (Beal, 1992). The significant decrease observed in the kainate-evoked release of the excitatory amino acids, aspartate and glutamate, when animals were pre-treated with PF9601N suggests a protective effect against excitotoxicity. However, the effects of PF9601N may not be confined to the neuron, since both aspartate and glutamate are also present in some glial populations (Tanaka et al., 2007) and the present work has shown that the glial activation induced by kainate is prevented by PF9601N pre-treatment. The kainate-

evoked release of taurine is considered to be a protective response that balances excessive stimulation and the corresponding osmotic disequilibria. Much of this taurine release in the striatum appears to be from a non-neuronal source, possibly glial (Bianchi et al., 1998). The physiological functions of taurine include osmoregulation and modulation of calcium transport. It has also been claimed to act as a neuromodulator, neurotransmitter and neuroprotective molecule against glutamatergic toxicity (Foos and Woo, 2002). This would be consistent with the increase in taurine release observed after PF9601N pre-treatment having a protective function. Although GABA is released from terminals after kainate administration (100μM) (Bianchi et al., 1998), the failure to detect it in the present experiments can be attributed to anaesthesia (chloral hydrate), necessitated by the high concentration of kainate used.

PF9601N did not have any significant effect on the release of dopamine and its metabolites HVA and DOPAC or 5HIAA. The isoform of MAO responsible for dopamine metabolism depends on the species and cellular location (Youdim et al., 1988). In the rat nerve terminal it appears that only MAO-A is involved in dopamine degradation (Garrick and Murphy, 1980). This would explain the lack of effect of PF9601N, a selective MAO-B inhibitor, in this *in vivo* model.

It has been previously reported that kainate can stimulate glial cells, and this may contribute to the neuronal damage induced by the toxin (Matyja et al., 1986). The present results show that the excitotoxic damage provokes notable astroglial reactivity, evidenced by a significant increase in GFAP immunoreactivity. Animals pre-treated with PF9601N showed less astrogliosis. Yu et al. (1995) have also shown that some aliphatic propargylamine inhibit GFAP mRNA expression. Microglial cells have been reported to be the first population to react against CNS lesions. Their reactions, which appear quite homogeneous and independent from the type of lesion, include changes in

their morphology, proliferation and an increase in surface molecules (Stoll et al., 1998; Stoll & Jander, 1999). The present results showed intrastriatal administration of kainate to induce both an increase in the number of lectin-positive cells and a change in their morphology, characteristic of their activation process. It is difficult to distinguish p53 induction between microglia and macrophages, since they share intracellular and membrane markers (Flaris et al., 1993), such as lectin domains and CR3 (Stoll & Jander, 1999). However, these results suggest a possible immunomodulator effect of PF9601N, since it is able to prevent the microglial reactivity induced by kainate.

The excitotoxicity caused by kainate is still not fully understood, as both necrotic and apoptotic cell deaths are provoked (Portera-Cailliau et al., 1997). Its toxic effects are associated with p53 induction and collapse of the mitochondrial membrane potential (Liu et al., 2001). Since PF9601N has been reported to oppose these effects, it could prove useful in the treatment of excitotoxic origin. Its high selectivity as an inhibitor of MAO-B also confers an additional benefit, as an adjunct to the levodopa treatment of Parkinson's disease. Thus, the protective properties of PF9601N observed in this model, as well as the properties previously observed in several models of Parkinson's disease, suggest that PF9601N could be a good candidate to be used for the treatment of PD and other neurodegenerative disorders that also involve excitotoxicity.

ACKNOWLEDGMENTS

This work was realized in the framework of COST working group: D34/0003/05.

References

Ansari KS, Yu PH, Kruck TP et al (1993) Rescue of axotomized immature rat facial motoneurons by R(-)-deprenyl:stereospecificity and independence from monoamine oxidase inhibition. J Neurosci 13(9):4042-4053

Battaglia V, Sanz E, Salvi M et al (2006). Protective effect of N-(2-propynyl)-2-(5-benzyloxy-indolyl)methylamine (PF9601N) on mitochondrial permeability transition. Cell Mol Life Sci 63:1440-48

Beal MF (1992). Does impairment of energy metabolism result in excitotoxic neuronal death in neurodegenerative illnesses? Ann Neurol. Feb;31(2):119-30

Bellik L, Dragoni S, Pessina F, et al. (2010) Antioxidant properties of PF9601N, a novel MAO-B inhibitor: assessment of its ability to interact with reactive nitrogen species. *Acta Biochim Pol*. Jun 9.

Bianchi L., Della Corte L. and Tipton K. F. (1999) Simultaneous determination of basal and evoked output levels of aspartate, glutamate, taurine and 4-aminobutyric acid during microdialysis and from superfused brain slices. *J. Chromatogr. B* 723, 47–59.

Blandini F (2010). An update on the potential role of excitotoxicity in the pathogenesis of PD. Funct Neurol. Apr-Jun;25(2):65-71

Bonfocco E, Krainc D, Ankarcrona M, et al (1995) Apoptosis and necrosis: two distinct events induced, respectively, by mild and intense insults with N-methyl-D-aspartate or nitric oxide/superoxide in cortical cell cultures. *Proc Natl Acad Sci*, Aug 1; 92(16):7162-6.

Canals JM, Checa N, Marco S, et al (2001). Expression of brain-derived neurotrophic factor in cortical neurons is regulated by striatal target area. *J. Neurosci*., 21, 1, 117-24.

Claude WM and Zhang J (2003) Glutamate. Excitotoxicity and programmed cell death in Parkinson's disease. Exp Neurol 220(2):230-233

Cruces MA, Elorriaga C, Fernandez-Alvarez E, (1991) Acetylenic and allenic derivatives of 2-(5-hydroxyindolil) methylamines: syntesis and in vitro evaluation as monoamine oxidase inhibitors. *Eur. Med. Chem*. 26, 33-41

Cutillas B, Ambrosio S, Unzeta M (2002) Neuroprotective effect of the monoamine oxidase inhibitor PF 9601N [N-(2-propynyl)-2-(5-benzyloxy-indolyl) methylamine] on rat nigral neurons after 6-hydroxydopamine-striatal lesion. *Neurosci Lett.* Aug 30; 329(2):165-8.

Dexter DT, Wells FR, Lees AJ et al (1989) Increased nigral iron content and alteraions in other metal ions occurring in brain in Parkinson's disease. J Neurochem 52(6):1830-1836

Di Monte DA, Lavasani M, Manning-Bog AB (2002). Neurotoxicol Oct 23 (4-5: 487-502 Rev

Ebadi M, Sharma S, Shavali S, et al (2002). Neuroprotective actions of Selegiline. J Neurosci Res. Feb1;67(3):285-9

Flaris NA, Densmore TL, Molleston MC, Hickey WF. (1993) Characterization of microglia and macrophages in the central nervous system of rats: definition of the differential expression of molecules using standard and novel monoclonal antibodies in normal CNS and in four models of parenchymal reaction. *Glia* Jan;7(1):34-40.

Foos TM & Wu JY (2002). The model of taurine in the CNS and the modulation of intracellular calcium homeostasis. *Neurochem. Res*., 27, 21-26.

Freinbichler W, Colivicchi MA, Fattori M et al (2008) Validation of a robust and sensitive method for detecting hydroxyl radical formation together with evoked neurotransmitter release in brain microdialysis. J Neurochem 105(3):738-749

Garrick NA and Murphy DL (1980). Species differences in the deamination of dopamine and other substrates for monoamine oxidase in brain. Psycopharmacology 72, 27-33

Götz ME, Freyberger A, Riederer P (1990). Oxidative stress: A role in the pathogenesis of Parkinson's disease. J Neural Transm Suppl 29:241-9 Rev

Grimsby, J; Lan, N.C; Neve, R; et al (1990). Tissue distribution of human monoamine oxidase A and B mRNA. *J Neurochem*, 55(4), 1166-1169

Hirsch E, Graybiel AM and Agid YA (1988) Melanized dopaminergic neurons are differentially susceptible to degeneration in Parkinson's disease. Nature 334, 345-348

Jenner P (2003) Oxidative stress in Parkinson's disease. Ann Neurol 53 Suppl 3; S26-36

Johnston, J.P.(1968) Some observations upon a new inhibitor of monoamine oxidasein brain tissue. *Biochem Pharmacol*, 17(7), 1285-1297

Johnson KA, Conn PF and Niswender CM (2009) Glutamate receptors as therapeutic targets for Parkinson's disease. CNS Neurol Disord Drug Targets 8(6):475-491. Review

Koutisilieri E and Riederer P (2007) Excitotoxicity and new antiglutamatergic strategies in Parkinson's disease and Alzheimer's disease. Parkinsonism Relat Disord 13 Suppl 3:S329-331. Review

Kragten E, Ladande I, Zimmermann K et al (1998) Glyceraldehide-3-phosphate dehydrogenase, the putative target of the antiapoptotic compounds CGP 3466 and R-(-)-deprenyl. J Biol Chem 273(10):5821-5828

Lau A and Tymianski M (2010) Glutamate receptors, neurotoxicity and neurodegeneration. Pflugers Arch 460(2):525-542

Leist M & Nicotera P. (1998) Apoptosis versus necrosis: the shape of neuronal cell death. *Results Probl Cell Differ*. 24:105-35. Review.

Lim KL and Ng CH (2009) Genetic models of Parkinson's disease. Biochim Biophys Acta 1792(7):604-615. Review

Macleod AD, Counsell CE, Ives N, Stowe R (2005). Monoamine oxidase B inhibitors for early Parkinson's disease. Cechrane Database Syst Rev:CD004898

Marconi R, Bonnet AM, Vidailhet M, Agid Y (1992). The IMAO-B MDL 72.974ª in Parkison's disease. J Neurol Neurosurg Psychiatry; 55:1096-7

Mattson MP (2003) Excitotoxic and excitoprotective mechanisms: abundant targets for the prevention and treatment of neurodegenerative disorders. Neuromolecular Med 3(2):65-94. Review

Matyja E. (1986) Morphologic evidence of a primary response of gila to kainic acid administration into the rat neostriatum; studied in vivo and in vitro. *Exp Neurol*. Jun; 92(3):609-23.

McBean GJ, Doorty KB, Tipton KF, Kollegger H. (1995) Alteration in the glial cell metabolism of glutamate by kainate and N-methyl-D-aspartate. *Toxicon*. Apr; 33(4):569-76.

McGeer PL & McGeer EG. (1996). Anti-inflammatory drugs in the fight against Alzheimer's disease. *Ann. N. Y. Acad. Sci*., 777, 213-20.

Michaels RL, Rothman SM. (1990) Glutamate neurotoxicity in vitro: antagonist pharmacology and intracellular calcium concentrations. *J Neurosci*. Jan; 10(1):283-92.

Nakai M, Qin ZH, Chen JF, Wang Y, Chase TN (2000). Kainic acid-induced apoptosis in rat striatum is associated with nuclear factor-kappaB activation. J Neurochem., 74, 647-658.

Nicotera P, Leist M, Ferrando-May E. (1999) Apoptosis and necrosis: different execution of the same death. *Biochem Soc Symp*. 66:69-73. Review

Olanow C.F. (1992) An introduction to the free radical hypothesis. *Ann Neurol* 32; S2-S9

Paxinos G. and Watson C. (1982) The rat brain in stereotaxic coordinates. *Academic Press*, San Diego

Perez V, Romera M, Lizcano JM, et al. (2003) Protective effect of N-(2-propynyl)-2-(5-benzyloxyindolyl) methylamine (PF 9601N), a novel MAO-B inhibitor, on dopamine-lesioned PC12 cultured cells. *J Pharm Pharmacol*. May 55; (5):713-6.

Perez V, Marco JL, Fernandez-Alvarez E, et al. (1999) Relevance of bencyloxy group in 2-indolyl methylamines in the selective MAO-B inhibition. *Br. J. Pharmacol*. 127: 869-876

Portera-Cailliau C, Price DL, Martin LJ. (1997). Non-NMDA and NMDA receptor-mediated excitotoxic neuronal deaths in adult brain are morphologically distinct: further evidence for an apoptosis-necrosis continuum. *J. Comp. Neurol*., 378, 1, 88-104.

Prat G, Perez V, Rubi A, et al (2000). The novel type B MAO inhibitor PF9601N enhances the duration of L-DOPA-induced contralateral turning in 6-hydroxydopamine lesioned rats. J Neural Transm;107:409-17

Rascol O, Brooks DJ, Melamed E et al (2005). Rasagiline as an adjunct to levodopa in patients with Parkinson's disease and motor fluctuations (LARGO, lasting effect in Adjunct therapy with Rasagiline given Once daily, study): a randomised, double-bind, parallel-group trial. Lancet;356:947-54.

Reynolds GP, Elsworth JD, Blau K, Sandler M, Lees AJ & Stern GM. (1978). Deprenyl is metabolized to methamphetamine and amphetamine in man. Br J Clin Pharmacol. Dec;6(6):542-4

Sanz E, Quintana A, Hidalgo J, et al. (2009) PF9601N [N-(2-propynyl)-2-(5-benzyloxy-indolyl) methylamine] confers MAO-B independent neuroprotection in ER stress-induced cell death. *Mol Cell Neurosci*. May; 41(1):19-31.

Sanz E, Quintana A, Battaglia V, et al. (2008) Anti-apoptotic effect of Mao-B inhibitor PF9601N [N-(2-propynyl)-2-(5-benzyloxy-indolyl) methylamine] is mediated by p53 pathway inhibition in MPP(+)-treated SH-SY5Y human dopaminergic cells. J *Neurochem.* Apr 9.

Sanz E, Romera M, Bellik L, et al. (2004) Indolalkylamines derivatives as antioxidant and neuroprotective agents in an experimental model of Parkinson's disease. *Med Sci Monit.* Dec; 10(12):BR477-84.

Simon-Sanchez J, Schulte C, Bras JM et al (2009) Genome-wide association study reveals genetic risk underlying Parkinson's disease. Nat Genet 41(12):1308-1312

Sofic E, PAulus W, Jellinger K et al (1991) Selective increase of iron in substantia nigra zona compacta of parkinsonian brains. J Neurochem 56(3):978-982

Speiser Z, Mayk A, Eliash S, Cohen S. (1999) Studies with rasagiline, a MAO-B inhibitor in experimental focal ischemia in the rat. *J. Neural Transm.* 106 (7/8): 593-606.)

Stoessl AJ. (1999) Etiology of Parkinon's disease. Can J Neurol Sci Ang 26 Suppl 2: S5-12 Rev

Stoll G, Jander S, Schroeter M. (1998) Inflammation and glial responses in ischemic brain lesions. *Prog Neurobiol.* Oct;56(2):149-71. Review.

Stoll G, Jander S. (1999) The role of microglia and macrophages in the pathophysiology of the CNS. Prog Neurobiol. Jun; 58(3):233-47. Review.

Tanaka K. (2007) Roles of glutamate transporters in astrocytes. *Brain Nerve.* Jul;59(7):677-88.

The Parkinson Study group (2002). A controlled trial of rasagiline in early Parkinson's disease: the TEMPO study. Arch Neurol 59:1937-43

The Parkinson Study group (2004). A controlled, randomized, delayed-start study of rasagiline in early Parkinson's disease. Arch Neurol 61:561-66

Turski L, Bressler K, Rettig KJ, et al. (1991) Protection of substantia nigra from MPP+ neurotoxicity by N-methyl-D-aspartate antagonists. Nature. Jan 31; 349(6308):414-8.

Wilkhofer KF and Haass C (2010) Mitochondrial dysfunction in Parkinson's disease. Biochim Biophys Acta 1802(1):29-44. Review

Youdim, M. B. H.; Finberg, J. P. M.; Tipton, K. F. (1988) Monoamine oxidase. In U. Tredelenburg, N. Weiner, Springer-Verlag, Berlin, 119-192.

Yu PH, Davis BA, Zhang X, Zuo DM, Fang J, Lai CT, Li XM, Paterson IA, Boulton AA. (1995) Neurochemical, neuroprotective and neurorescue effects of aliphatic N-methylpropargylamines; new MAO-B inhibitors without amphetamine-like properties. *Prog Brain* Res. 106:113-21. Review.

Figure Legends

Figure 1. Chemical structure of PF9601N

Figure 2. Localisation of the microdialysis probe. Positions of the probes were identified by the histological analysis and drawn onto diagrams taken from the atlas of Paxinos and Watson (Compact third edition, 1997). The shaded area defines the area within which the probes of all used rats were localised.

Figure 3. Time course of the release of glutamate, aspartate, taurine and GABA evoked by local administration of K^+ and kainate (KA). The extracellular concentrations were expressed as percentage of their respective basal levels only for graphic reasons. Original concentration values were fmol/µl of perfusate (nM), the mean net stimulated output ± s.e.m., obtained from the area under the K^+ or kainate-evoked concentration-time curve (AUC), normalised to one time interval of 20 min, subtracted of basal output are shown in Table 1, together with their statistical analysis parameters. The concentrations peaks of aspartate, glutamate and taurine evoked by K^+ and KA were statistically significant. The peak was not statistically significant, either in the absence of stimulation or when the stimulation was applied to PF9601N pre-treated animals. However, in the case of GABA the KA did not evoke a statistically significant output. PF9601N pre-treatment, in the absence of k^+ and KA, did not affect the basal release of the four amino acids.

Table 1A. Effect of local application of K^+ (50 mM) and kainate (1 mM) on the output of aspartate and glutamate from the striatum in vehicle and PF9601N pre-treated rats.

Table 1B. The effect of local application of K^+ (50 mM) and kainate (1 mM) on the output of taurine and GABA from the striatum in vehicle and PF9601N pre-treated rats.

Figure 4. Time course of the release of dopamine and metabolites evoked by local administration of K^+ and kainate (KA).

The extracellular concentrations were expressed as percentage of their respective basal levels only for graphic reasons. Original concentration values were fmol/µl of perfusate (nM), the mean net stimulated output ± s.e.m., obtained from the area under the K^+ or kainate-evoked concentration-time curve (AUC), normalised to one time interval of 20 min, subtracted of basal output are shown in Table 2, together with their statistical analysis parameters. The concentration increases of dopamine evoked by K^+ and KA were statistically significant and they were not affected by PF9601N pre-treatment. The concentration of the metabolites of dopamine, DOPAC and HVA, and the metabolite of 5HT, 5IHAA, were significantly reduced by K^+ and KA, and were not affected by PF9601N pre-treatment. PF9601N pre-treatment, in the absence of K^+ and KA, did not affect the basal release of dopamine and metabolites.

Table 2. Effect of the local application of K^+ (50 mM) and kainate (1 mM) on the output of dopamine, DOPAC, HVA and 5HIAA, from the striatum in vehicle and PFN9601N pre-treated rats.

Figure 5. Glial activation. Representative microphotographs of microglial reactivity (A-C, Lectin histochemistry) and astrocytosis (D-F, GFAP immunostaining) in the striatum of animals after KA administration. A significant increase in microglial activation was also observed in the striatum of KA lesioned rats (A-B) shown by both

the number of positive cells and their reactivity. Moreover, a significant astrogliosis was found when animals were administered with kainate (KA) (D-E). PF9601N pre-treatment was able to prevent the activation of both astroglial (E-F, H) and microglial cells (B-C, G). (*$p<0.05$), (**$p<0.01$).

Figure 6. Apoptosis. Representative microphotographs of Tunel technique immunohistochemistry. The local administration of kainate (KA) in the striatum provoked a significant number of apoptotic nuclei (A-B,D). In contrast, pre-treatment with PF9601N was able to prevent the apoptotic process induced by KA as the number of apoptotic nuclei found was similar to the control group (C, D). (***$p<0.01$).

Figure 1

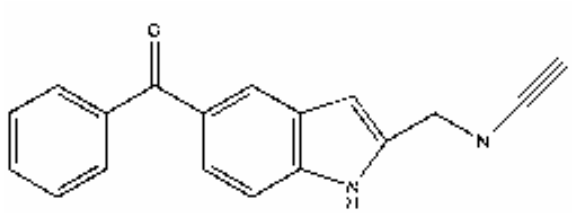

Figure 2

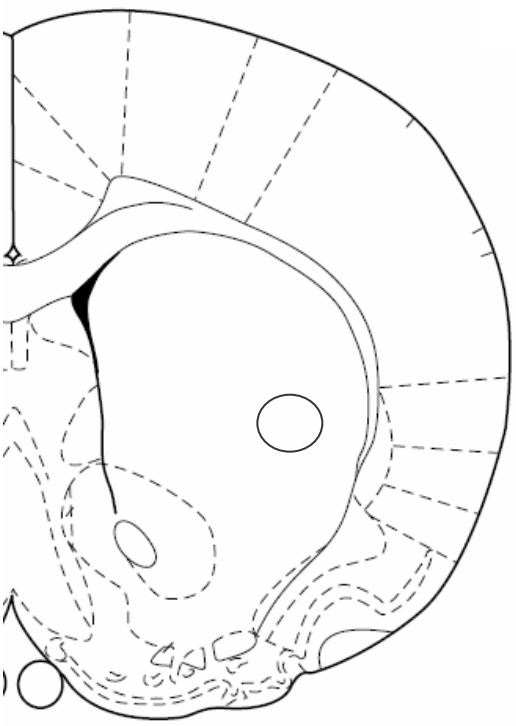

Figure 3

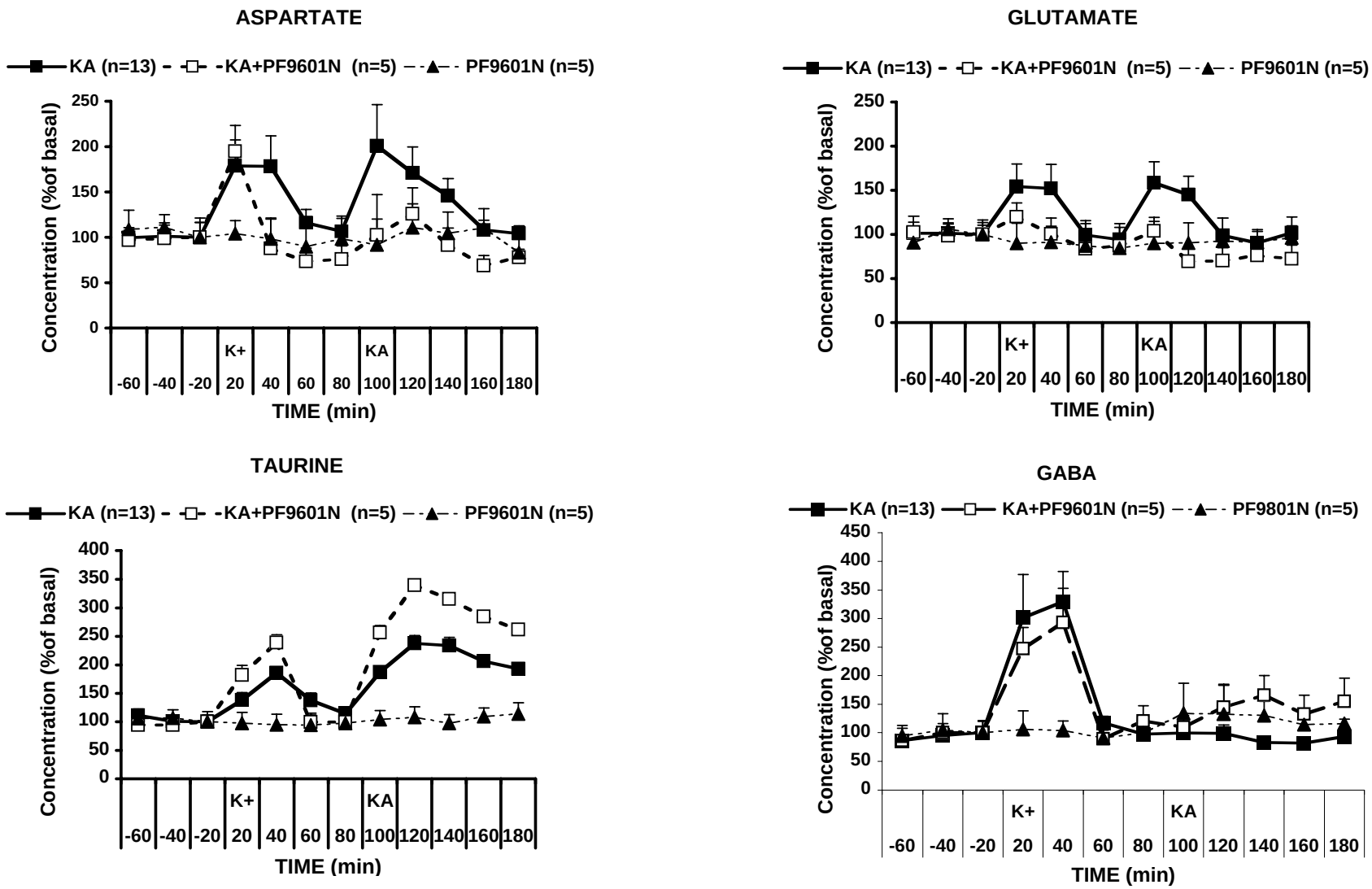
ASPARTATE
KA (n=13)
KA+PF9601N (n=5)
PF9601N (n=5)
Concentration (%of basal)
250
200
150
100
50
0
K+
KA
-60 -40 -20 20 40 60 80 100 120 140 160 180
TIME (min)
GLUTAMATE
KA (n=13)
KA+PF9601N (n=5)
PF9601N (n=5)
Concentration (%of basal)
250
200
150
100
50
0
K+
KA
-60 -40 -20 20 40 60 80 100 120 140 160 180
TIME (min)
TAURINE
KA (n=13)
KA+PF9601N (n=5)
PF9601N (n=5)
Concentration (%of basal)
400
350
300
250
200
150
100
50
0
K+
KA
-60 -40 -20 20 40 60 80 100 120 140 160 180
TIME (min)
GABA
KA (n=13)
KA+PF9601N (n=5)
PF9801N (n=5)
Concentration (%of basal)
450
400
350
300
250
200
150
100
50
0
K+
KA
-60 -40 -20 20 40 60 80 100 120 140 160 180
TIME (min)

Table 1A. The effect of local application of K^+ (50 mM) and kainate (1 mM) on the output of aspartate and glutamate from the striatum in vehicle and PF9601N pre-treated rats.

AMINO ACID AUC (nM, 20 min)	K^+			Kainate (KA)		
	K^+/KA (Vehicle) N=13	K^+/KA (PF9601N) N=5	none (PF9601N) N=5	K^+/KA (Vehicle) N=13	K^+/KA (PF9601N) N=5	none (PF9601N) N=5
ASPARTATE						
Evoked (mean ± SEM)	120 ± 34	129 ± 39	-2 ± 17	138 ± 43	82 ± 42	7 ± 11
95% CI of the mean	(45 - 195)	(20 – 239)	(-50 – 45)	(45 -231)	(-34 -199)	(-23 -37)
One sample test	p<=0.0045	p=0.0304	NS	p=0.0070	NS	NS
GLUTAMATE						
Basal (mean ± SEM)	303 ± 96	38 ± 72	-23 ± 46	354 ± 81	33 ± 34	58 ± 53
95% CI of the mean	(94 -512)	(-162 – 238)	(-151 – 105)	(176 -531)	(-59 – 129)	(-89 -205)
One sample test	p=0.0083	NS	NS	p=0.0010	NS	NS

Figures represent the mean net stimulated output ± s.e.m., obtained from the area under the K^+ or kainate-evoked concentration-time curve (AUC), normalised to one time interval of 20 min, subtracted of basal output. Concentration values were fmol/µl of perfusate (nM). 95% CL not including zero and the probability level of the one sample test were taken as an indication of the statistical significance of the mean evoked output of each treatment group. N, indicates the number of animals of each treatment group, where compounds could be determined. NS, not significant.

Table 1B. The effect of local application of K^+ (50 mM) and kainate (1 mM) on the output of taurine and GABA from the striatum in vehicle and PF9601N pre-treated rats.

AMINO ACID AUC (nM, 20 min)	K^+			Kainate (KA)		
	K^+/KA (Vehicle) N=13	K^+/KA (PF9601N) N=5	none (PF9601N) N=5	K^+/KA (Vehicle) N=13	K^+/KA (PF9601N) N=5	none (PF9601N) N=5
TAURINE						
Evoked (mean ± SEM)	694 ± 111	784 ± 117	-34 ± 14	1,295 ± 138	1,852 ± 118	55 ± 24
95% CI of the mean	(452 - 935)	(459 – 1,108)	(-74 – 6)	(994 -1,597)	(1,525 -2,180)	(-12 - 122)
One sample test	p<0.0001	p<0.0026	NS	p<0.0001	p<0.0001	NS
GABA						
Evoked (mean ± SEM)	68 ± 15	54 ± 15	0.8 ± 5	-2 ± 2	8 ± 3	13 ± 5
95% CI of the mean	(35 -101)	(11 – 96)	(-12 – 14)	(-7 – 4)	(-0.1 – 14)	(-3 – 22)
One sample test	p<0.0010	p=0.0243	NS	NS	NS	NS

Figures represent the mean net stimulated output ± s.e.m., obtained from the area under the K^+ or KA-evoked concentration-time curve (AUC), normalised to one time interval of 20 min, subtracted of basal output. Concentration values were fmol/µl of perfusate (nM). 95% CL not including zero and the probability level of the one sample test were taken as an indication of the statistical significance of the evoked output of each treatment group. N, indicates the number of animals of each treatment group, where compounds could be determined; NS, not significant. Analysis of variance indicated a statistically significant difference of the kainate-evoked output of taurine between the three treatment groups (treatment: $F_{2,22}$=26.66, p<0.0001) and the *post hoc* Bonferroni multiple comparison test indicated that the increase of the kainate-induced release induced by PF9601N pre-treatment was statistically significant (p<0.05).

Figure 4

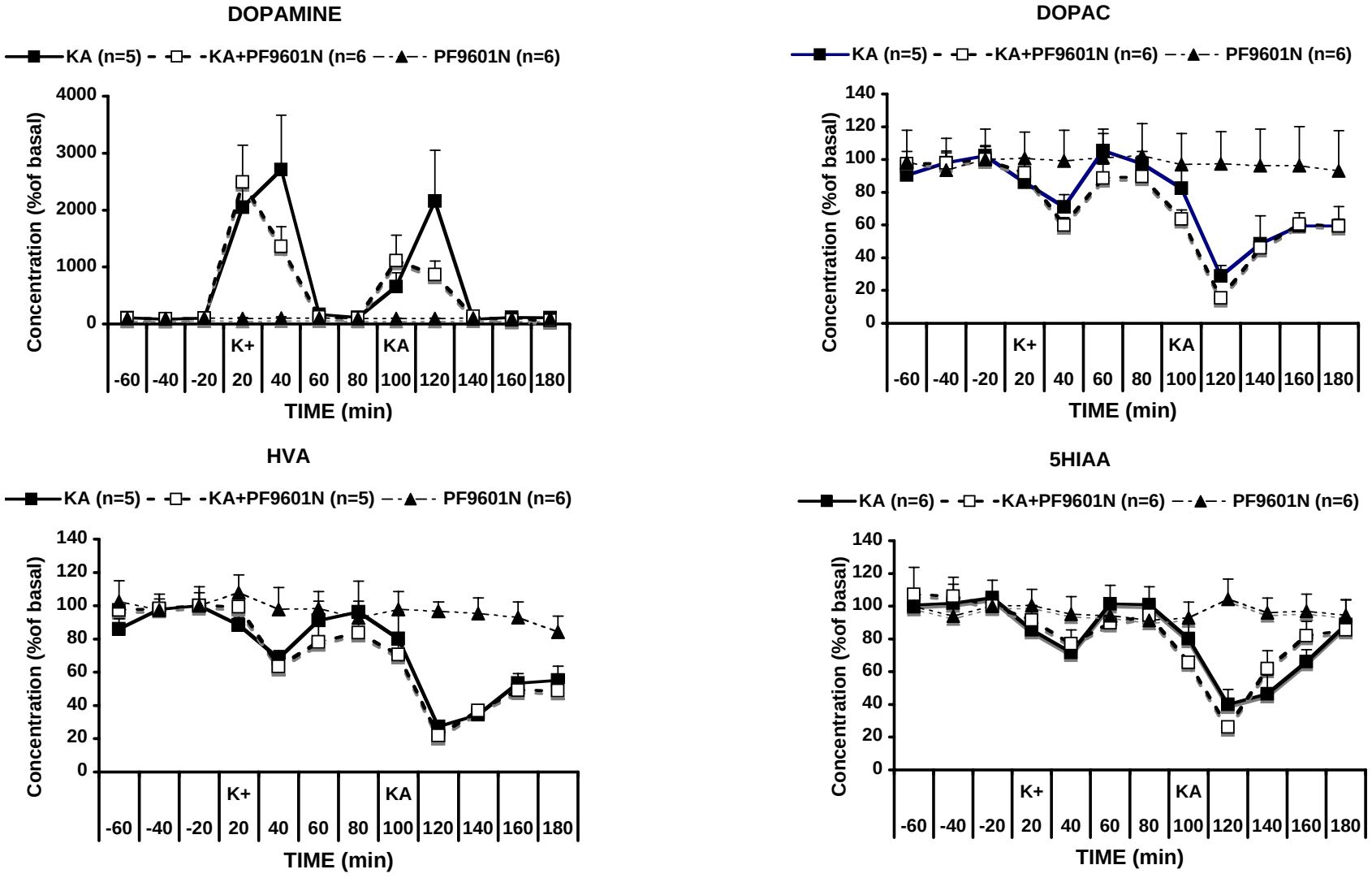
DOPAMINE
KA (n=5)
KA+PF9601N (n=6
PF9601N (n=6)
Concentration (%of basal)
4000
3000
2000
1000
0
K+
KA
-60 -40 -20 20 40 60 80 100 120 140 160 180
TIME (min)
DOPAC
KA (n=5)
KA+PF9601N (n=6)
PF9601N (n=6)
Concentration (%of basal)
140
120
100
80
60
40
20
0
K+
KA
-60 -40 -20 20 40 60 80 100 120 140 160 180
TIME (min)
HVA
KA (n=5)
KA+PF9601N (n=5)
PF9601N (n=6)
Concentration (%of basal)
140
120
100
80
60
40
20
0
K+
KA
-60 -40 -20 20 40 60 80 100 120 140 160 180
TIME (min)
5HIAA
KA (n=6)
KA+PF9601N (n=6)
PF9601N (n=6)
Concentration (%of basal)
140
120
100
80
60
40
20
0
K+
KA
-60 -40 -20 20 40 60 80 100 120 140 160 180
TIME (min)

Table 2. Effect of the local application of K^+ (50 mM) and kainate (1 mM) on the output of dopamine, DOPAC, HVA and 5HIAA, from the striatum in vehicle and PFN9601N pre-treated rats.

AUC (Stim – Bas) nM, 20 min	K^+			Kainate (KA)		
	K^+/KA (Vehicle)	K^+/KA (PF9601N)	none (PF9601N)	K^+/KA (Vehicle)	K^+/KA (PF9601N)	none (PF9601N)
DOPAMINE (nM)	N=5	N=6	N=5	N=5	N=4	N=5
Evoked (mean ± s.e.m.)	26.90 ± 6,77	23.03 ± 6,19	(-)0.007 ± 0,088	15.15 ± 4.38	14.41 ± 4.31	(-)0.001 ± 0,029
95% CI of the mean	(8.09 – 45.71)	(7.11 – 38.94)	(-0.24 – 0.25)	(2.99 – 27.31)	(0.708 – 28.12)	(-0.083 – 0.080)
One sample test	p=0.0165	p=0.0137	NS	p=0.0258	p=0.0442	NS
DOPAC (nM)	N=5	N=6	N=5	N=5	N=6	N=5
Mean ± s.e.m.	(-)98.46 ± 21.38	(-)144.20 ± 29.40	1.33 ± 23.67	(-)286.90 ± 37.72	(-)335.2 ± 43.15	2.47 ± 26.81
95% CI of the mean	(-157.8 – -39.09)	(-219.8 – -68.60)	(-64.37 – 64.04)	(-391.6 – 68.59)	(-446.2 – -224.3)	(-71.98 – 76.92)
One sample test	p=0.0100	p=0.0045	NS	p=0.0016	p=0.0006	NS
HVA (nM)	N=4	N=6	N=5	N=5	N=5	N=5
Mean ± s.e.m.	(-)50.62 ± 8.33	(-)72.70 ± 16.63	6.27 ± 8.96	(-)124.00 ± 35.70	(-)147.1 ± 27.11	(-)8.34 ± 13.03
95% CI of the mean	(-77.13 – -24.10)	(-115.4 – -29.96)	(-18.61 – 31.16)	(-223.31 – -24.84)	(-223.3 – -71.81)	(-44.51 – 27.82)
One sample test	p=0.0090	p=0.0072	NS	p=0.0255	p=0.0056	NS
5HIAA	N=5	N=6	N=5	N=6	N=6	N=5
Mean ± s.e.m.	(-)22.48 ± 6.38	(-)24.67 ± 8.98	(-)3.22 ± 4.28	(-)42.09 ± 8.70	(-)59.17 ± 7.38	7.24 ± 5.07
95% CI of the mean	(-40.18 – -4.77)	(-47.76 – -1.59)	(-15.10 – 8.66)	(-64.45 – -19.74)	(-78.15 – -40.20)	(-6.84 – 21.33)
One sample test	p=0.0243	p=0.0404	NS	p=0.0047	p=0.0005	NS

Figures represent the mean net stimulated output ± s.e.m., obtained from the area under the K^+ or KA-evoked concentration-time curve (AUC), normalised to one time interval of 20 min, subtracted of basal output. N, indicates the number of animals of each treatment group, where compounds could be determined. Concentration values were fmol/µl of perfusate (nM); NS, not significant. 95% CI not including zero were taken as an indication of the statistical significance of the mean basal output of each treatment group. Analysis of variance followed by the *post hoc* Bonferroni multiple comparison test did not give evidence of any significant difference in the basal levels of the three treatment groups.

Figure 5

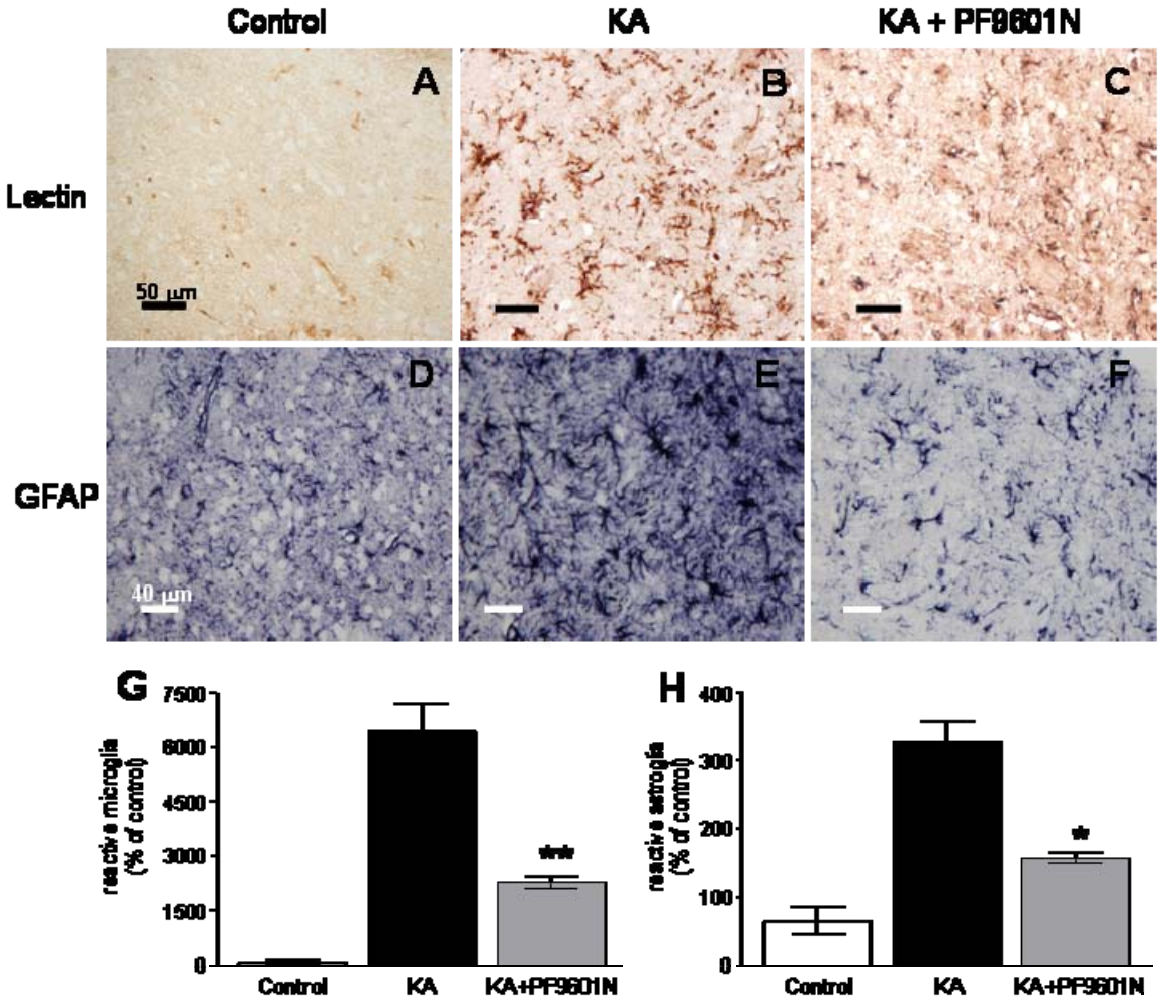
Control
KA
KA + PF9601N
Lectin
GFAP
A
B
C
D
E
F
50 µm
40 µm
G
H
reactive microglia (% of control)
reactive astroglia (% of control)
7500
6000
4500
3000
1500
0
400
300
200
100
Control
KA
KA+PF9601N

Figure 6

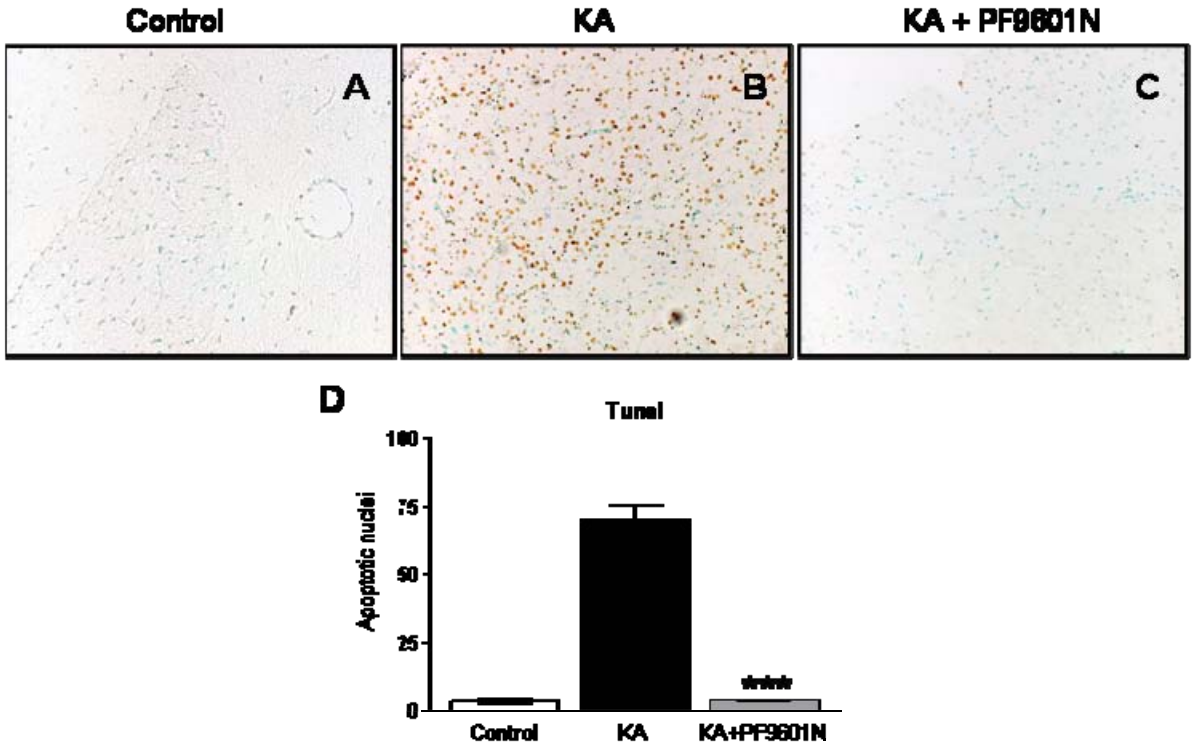
Control
KA
KA + PF9601N
A
B
C
D
Tunel
Apoptotic nuclei
100
75
50
25
0
Control
KA
KA+PF9601N

CHAPTER II

Synthesis, Biological Assessment and Molecular Modeling of New Multipotent MAO and Cholinesterase Inhibitors as Potential Drugs for the Treatment of Alzheimer's Disease.

Abdelouahid Samadi, Mourad Chioua, Irene Bolea, Cristóbal de los Ríos, Isabel Iriepa, Ignacio Moraleda, Agatha Bastida, Gerard Esteban, Mercedes Unzeta, Enrique Gálvez and José Marco-Contelles.

European Journal of Medicinal Chemistry, 2011, 1-4

European Journal of Medicinal Chemistry xxx (2011) 1–4

Contents lists available at ScienceDirect

European Journal of Medicinal Chemistry

journal homepage: http://www.elsevier.com/locate/ejmech

Short communication

Synthesis, biological assessment and molecular modeling of new multipotent MAO and cholinesterase inhibitors as potential drugs for the treatment of Alzheimer's disease

Abdelouahid Samadi [a,*], Mourad Chioua [a], Irene Bolea [b], Cristóbal de los Ríos [c,d], Isabel Iriepa [d], Ignacio Moraleda [d,c], Agatha Bastida [e], Gerard Esteban [b], Mercedes Unzeta [b], Enrique Gálvez [d], José Marco-Contelles [a,*]

[a] Laboratorio de Radicales Libres y Química Computacional (IQOG, CSIC), C/Juan de la Cierva 3, 28006 Madrid, Spain
[b] Departament de Bioquímica i Biología Molecular, Facultat de Medicina, Universitat Autònoma de Barcelona, 08193 Bellaterra, Barcelona, Spain
[c] Instituto Teófilo Hernando, Fundación de Investigación Biomédica, Hospital Universitario de la Princesa, C/Diego de León, 62, 28006-Madrid, Spain
[d] Departamento de Química Orgánica, Universidad de Alcalá, Ctra, Madrid-Barcelona, Km. 33,6, 28871, Alcalá de Henares, Madrid, Spain
[e] Departamento de Química Bioorgánica (IQOG, CSIC), C/Juan de la Cierva 3, 28006-Madrid, Spain

ARTICLE INFO

Article history:
Received 23 March 2011
Received in revised form
16 May 2011
Accepted 19 May 2011
Available online xxx

Keywords:
Pyridines
Naphthyridines
Multipotent molecules
AChE
BuChE
MAO-A
MAO-B
Kinetic analysis
Inhibition mechanism
Molecular modeling
Alzheimer's disease

ABSTRACT

The synthesis, biological evaluation and molecular modeling of new multipotent inhibitors of type **I** and type **II**, able to simultaneously inhibit monoamine oxidases (MAO) as well as acetylcholinesterase (AChE) and butyrylcholinesterase (BuChE), is described. Compounds of type **I** were prepared by sequential reaction of 2,6-dichloro-4-phenylpyridine-3,5-dicarbonitrile (**14**) [or 2,6-dichloropyridine-3,5-dicarbonitrile (**15**)] with prop-2-yn-1-amine (or *N*-methylprop-2-yn-1-amine) and 2-(1-benzylpiperidin-4-yl)alkylamines **22**–**25**. Compounds of type **II** were prepared by Friedländer type reaction of 6-amino-5-formyl-2-(methyl(prop-2-yn-1-yl)amino)nicotinonitriles **32** and **33** with 4-(1-benzylpiperidin-4-yl)butan-2-one (**31**). The biological evaluation of molecules **1**–**11** showed that most of these compounds are potent, in the nanomolar range, and selective AChEI, with moderate and equipotent selectivity for MAO-A and MAO-B inhibition. Kinetic studies of compound **8** proved that this is a *Ee*AChE mixed type inhibitor ($IC_{50} = 16 \pm 2$; $Ki = 12 \pm 3$ nM). Molecular modeling investigation on compound **8** confirmed its dual AChE inhibitory profile, binding simultaneously at the catalytic active site (CAS) and at the peripheric anionic site (PAS). In overall, compound **11**, as a potent and selective dual AChEI, showing a moderate and selective MAO-A inhibitory profile, can be considered as an attractive multipotent drug for further development on two key pharmacological targets playing key roles in the therapy of Alzheimer's disease.

© 2011 Elsevier Masson SAS. All rights reserved.

1. Introduction

Alzheimer's disease (AD) is an age-related neurodegenerative process characterized by a progressive memory loss, decline in language skills and other cognitive impairments [1]. Although the etiology of AD is not known, amyloid-β (Aβ) deposits [2], τ-protein aggregation, oxidative stress [3] and low levels of acetylcholine [4] are thought to play significant roles in the pathophysiology of the disease [5]. The cholinergic theory [6] suggests that the loss of cholinergic neurons in AD results in a deficit of acetylcholine (ACh) in specific brain regions that mediate learning and memory functions [7]. Consequently, a number of acetylcholinesterase inhibitors (AChEI) such as tacrine [8], rivastigmine [9], donepezil [10] and galanthamine [11] have been developed, but with limited therapeutic benefits, mainly due to the multifactorial nature of AD. The multi-target-directed ligand (MTDL) approach, based on the "one molecule, multiple target" paradigm [12], has been the subject of increasing attention by many research groups, which have developed a number of compounds acting simultaneously on different receptors implicated in AD [13]. In this context, alterations in other neurotransmitter systems, especially the serotoninergic and

* Corresponding authors. Tel.: +34 91 5622900.
E-mail addresses: samadi@iqog.csic.es (A. Samadi), mchioua@iqog.csic.es (M. Chioua), Irene.Bolea@campus.uab.cat (I. Bolea), cristobal.delosrios@uam.es (C. de los Ríos), isabel.iriepa@uah.es (I. Iriepa), ignacio.moraleda@uah.es (I. Moraleda), agatha.bastida@iqog.csic.es (A. Bastida), gerardo.esteban@uab.cat (G. Esteban), mercedes.unzeta@uab.cat (M. Unzeta), enrique.galvez@uah.es (E. Gálvez), jlmarco@iqog.csic.es (J. Marco-Contelles).

0223-5234/$ – see front matter © 2011 Elsevier Masson SAS. All rights reserved.
doi:10.1016/j.ejmech.2011.05.048

Please cite this article in press as: A. Samadi, et al., Synthesis, biological assessment and molecular modeling of new multipotent MAO and cholinesterase inhibitors as potential drugs for the treatment of Alzheimer's disease, European Journal of Medicinal Chemistry (2011), doi:10.1016/j.ejmech.2011.05.048

dopaminergic, are also thought to be responsible for the observed behavioral disturbances [14,15]. Monoamine oxidase (MAO; EC 1.4.3.4) is an important target to be considered for the treatment of AD, as catalyzes the oxidative deamination of a variety of biogenic and xenobiotic amines, with the concomitant production of hydrogen peroxide [16]. MAO is a FAD-containing enzyme bound to mitochondrial outer membrane of neuronal, glial and other cells [17]. MAO exists as two isozymes: MAO-A and MAO-B, showing different substrate specificity, sensitivity to inhibitors, and amino-acid sequences. MAO-A preferentially oxidizes norepinephrine and serotonine, and is selectively inhibited by chlorgyline, while MAO-B preferentially deaminates β-phenylethylamine and is irreversibly inhibited by l-deprenyl [18]. X-ray crystal structures of human MAO-A [19] and MAO-B [20] have been reported.

With these ideas in mind, and based on our previous work in the synthesis and biological evaluation of MAO inhibitors (MAOI) [21] and AChE inhibitors (AChEI) [22], we have now designed new multipotent MAO and ChE inhibitors (**I** and **II**, Chart 1) for the potential treatment of AD. This approach has been previously analyzed with success by other laboratories [23–26]. What is new and original in our strategy is that the design of our molecules based on a conjunctive approach that combines for the first time the *N*-benzyl piperidine and the *N*-propargylamine moieties present in the AChE inhibitor donepezil [10], and PF9601N, a well known MAOI [21], respectively, connected through an appropriate linker to a central pyridine (or 1,8-naphthyridine) ring (Chart 1). In this preliminary communication, we report the synthesis and pharmacological evaluation of polyfunctionalized pyridines **1**–**8**, naphthyridines **9**–**11** (Table 1), and the identification of compound **11**, as a potent, in the nanomolar range, and selective dual AChEI, showing a moderate and selective MAO-A inhibitory profile.

2. Results and discussion

2.1. Chemistry

Type **I** compounds (Chart 1) were prepared by sequential reaction of 2,6-dichloro-4-phenylpyridine-3,5-dicarbonitrile (**14**) [27] (or 2,6-dichloropyridine-3,5-dicarbonitrile (**15**) [28]) with commercially available prop-2-yn-1-amine (or *N*-methylprop-2-yn-1-amine) and 2-(1-benzylpiperidin-4-yl)alkylamines **22-25** (Chart 2). Compounds of type **II** were prepared by Friedländer type reaction of 6-amino-5-formyl-2-(methyl(prop-2-yn-1-yl)amino)nicotinonitriles **32** and **33** with 4-(1-benzylpiperidin-4-yl)butan-2-one (**31**) (Supplementary data).

The *in vitro* activity of these new molecules against *Ee*AChE and eqBuChE was determined using Ellman's method [29] (Supplementary data) with tacrine and donepezil as reference compounds (Table 1). From these data some interesting SAR can be obtained. The IC_{50} values suggest that most of these molecules are

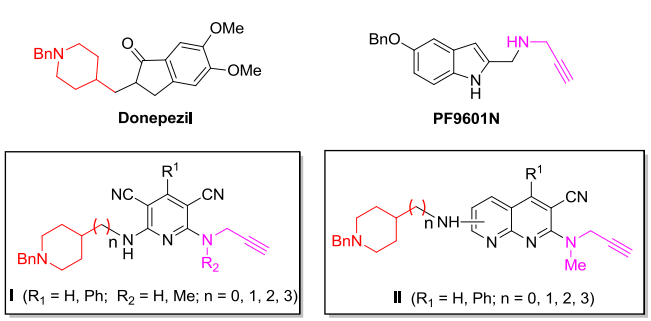

Chart 1. General structure of PF9601N, and the MAO and ChE inhibitors **I** and **II**.

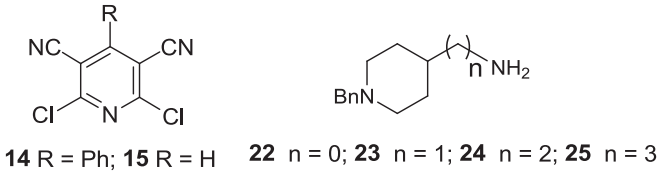

Chart 2. Structure of precursors: Pyridines **14**,**15**, and amines **22**–**25**.

potent, in the nanomolar range, and selective *Ee*AChE inhibitors, the most potent are compounds **3**, **4**, **6**, and **8** [IC_{50} (*Ee*AChE) = 13–16 nM], which are more potent than tacrine, but equipotent with donepezil for the *Ee*AChE inhibition.

All compounds are less potent than the reference compounds for BuChE inhibition, except compound **4**, 4-fold more potent than donepezil. Regarding the effect of the linker, for compounds **1**–**4** bearing a phenyl group at C4 and a methyl group at N(C6), the inhibition of both *Ee*AChE and eqBuChE increases on going from $n = 0$ to $n = 2$ or 3. For the same length in the linker ($n = 0$), changing only the methyl group by hydrogen (compare compound **1** with **5**), the *Ee*AChE inhibitory potency decreases 3.3-fold, while both compounds remain inactive for eqBuChE inhibition. Similarly, for the same length in the linker ($n = 2$), changing only the phenyl at C4 by a hydrogen (compare compound **3** with **6**), the *Ee*AChE inhibitory potency remains similar, affording the most potent AChEI (**6**) in this series [IC_{50} (*Ee*AChE) = 13 nM], while the eqBuChE potency is reduced, becoming around 3-fold less potent. Very interestingly, the substitution of the methyl group in compound **6** by a hydrogen, with the same length ($n = 2$), results in the potent, but completely selective *Ee*AChEI **8**. However, this potency is lost in inhibitor **7** bearing the same type of substituent, the length of the linker being now $n = 0$. Note also that for $n = 2$, compound **3** with the functional couple Ph(C-4)/N(C-6)Me is equipotent with compound **8** bearing the functional couple H(C-4)/N(C-6)H for the inhibition of *Ee*AChE. Definitively, compound **4** with the longest length ($n = 3$), bearing a phenyl group at C4 and a methyl group at N(C6) remains as the most potent eqBuChe inhibitor [IC_{50} (eqBuChE) = 230 nM].

Based on our previous work on the area [30], and in order to evaluate the presumed critical effect of the pyridine ring in compounds **1**–**8** on the biological activity, we prepared naphthyridine derivatives **9**–**11** [31] (Table 1). According to the observed IC_{50} values (Table 1), these three compounds are also potent and selective AChEI, the most potent is compound **11** [IC_{50} = 37 nM], while compound **10** shows the worst inhibitory potency for both enzymes.

To determine the type of the *Ee*AChE inhibition mechanism on these compounds, a kinetic study was carried out with inhibitor **8** [IC_{50} (*Ee*AChE = 16 ± 2 nM); IC_{50} (eqBuChE > 100000 nM)] (Supplementary data). The type of inhibition was established from the analysis of Lineweaver–Burk reciprocal plots (Fig. 1) showing both increasing slopes (lower V_{max}) and intercepts (higher K_m) with higher inhibitory concentration. This suggests a mixed-type inhibition [32]. The graphical analysis of steady-state inhibition data for compound **8** is shown in Fig. 1. A K_i value of 12.2 nM was estimated from the slopes of double reciprocal plots versus compound **8** concentrations.

Based on these results, compound **8** was analyzed in order to investigate the possible interactions between the inhibitor and the amino acid residues on the catalytic active site (CAS), and in the peripheral anionic site (PAS) of AChE. Ligand docking studies were performed with AUTODOCK VINA [33] using a single catalytic subunit of *Ee*AChE (PDB: 1C2B) (Supplementary data). The docking procedure was applied to the whole protein target ("blind docking"). To account for side chain flexibility during docking, flexible

Please cite this article in press as: A. Samadi, et al., Synthesis, biological assessment and molecular modeling of new multipotent MAO and cholinesterase inhibitors as potential drugs for the treatment of Alzheimer's disease, European Journal of Medicinal Chemistry (2011), doi:10.1016/j.ejmech.2011.05.048

Table 1
Inhibition of AChE from Electrophorus electricus (EeAChE), equine serum butyrylcholinesterase (eqBuChE) and monoamineoxidase (MAO-A and MAO-B) by compounds **1**–**11**.[a]

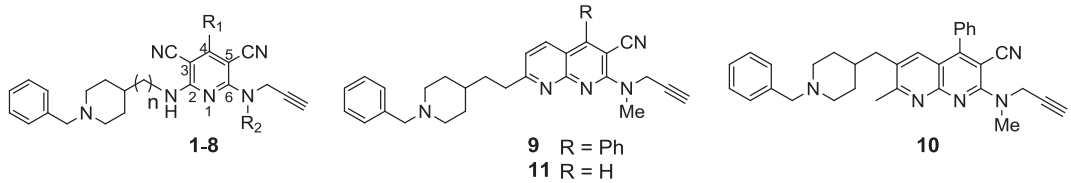

Compound	R_1	R_2	n	IC_{50} (nM)		Selectivity	IC_{50} (μM)		Selectivity
				*Ee*AChE	EqBuChE	BuChE/AChE	MAO-A	MAO-B	MAO-B/MAO-A
1	Ph	Me	0	1200 ± 200	>100 000	>83	>100	>100	>1
2	Ph	Me	1	270 ± 52	5000 ± 700	18.5	>100	>100	>1
3	Ph	Me	2	16 ± 2	1110 ± 30	69.4	>100	>100	>1
4	Ph	Me	3	14 ± 1	230 ± 30	16.4	>100	>100	>1
5	Ph	H	0	4000 ± 100	>100 000	>25	25 ± 1	>100	>4
6	H	Me	2	13 ± 1	3100 ± 300	238.5	>100	>100	>1
7	H	H	0	530 ± 70	>100 000	>188	>100	>100	>1
8	H	H	2	16 ± 2	>100 000	>6250	>100	>100	>1
9				53 ± 3	3500 ± 350	66	>100	32 ± 3	>0.32
10				2300 ± 300	>100 000	>34	>100	97 ± 24	>1
11				37 ± 4	1990 ± 270	54	41 ± 7	>100	>2.4
tacrine				27 ± 2	5.2 ± 0.2	0.19	40 ± 10	>100	>2.5
donepezil				13.4 ± 0.9	840 ± 50	63	>100	15 ± 2	>0.15

[a] Values are expressed as mean ± standard error of the mean of at least three different experiments in quadruplicate.

torsions in the ligand were assigned, and the acyclic dihedral angles were allowed to rotate freely. In the docking simulation, the pose with the lowest docking energy was selected as the best solution. The "blind docking" of the **8**-*Ee*AChE molecules was successful as indicated by the statistically significant scores. Fig. 2 shows the complex of *Ee*AChE with ligand **8**. As can be seen, docking results indicate that the cyano group makes hydrogen bonding with residue Ser203 in the catalytic triad, playing an important role in the molecular recognition as well as in the inhibition process. The pyridine nitrogen of compound **8** is likely to form a hydrogen interaction with the OH Tyr337 side chain, located in the constricted region in the gorge. Additionally, inhibitor **8** seems to stabilize through π–π stacking interactions between the phenyl group and the indole ring of Trp286 in the PAS. Therefore, ligand **8** is a dual *Ee*AChEI, able to simultaneously interact with both, the CAS and PAS of the enzyme, a result that is in good agreement with its mixed-type inhibition profile [34]: the pyridine moiety of this inhibitor binds at the CAS, while the linker spans theactive-sitegorge, and the phenyl ring binds at the PAS [35].

Finally, and in order to test their multipotent profile, compounds **1**–**11** have been evaluated as MAO-A and MAO-B inhibitors (Table 1) (Supplementary data). These results show that pyridines **2**, **3**, **6** and **7** are inactive, and pyridines **1**, **4**, **8**, and naphthyridine **10** are poor MAO inhibitors. Only pyridine **5** (IC_{50} = 25 ± 1 μM) and naphthyridine **11** (IC_{50} = 41 ± 7 μM) were moderate, in the micromolar range, selective MAO-A inhibitors, while pyridine **9** showed selective MAO-B inhibition activity (IC_{50} = 32 ± 3 μM). Thus, the substitution of a phenyl at C4 in compound **9** by a hydrogen in inhibitor **11** drives the MAO selectivity from MAO-B to MAO-A, with the potency remaining similar. In general, the

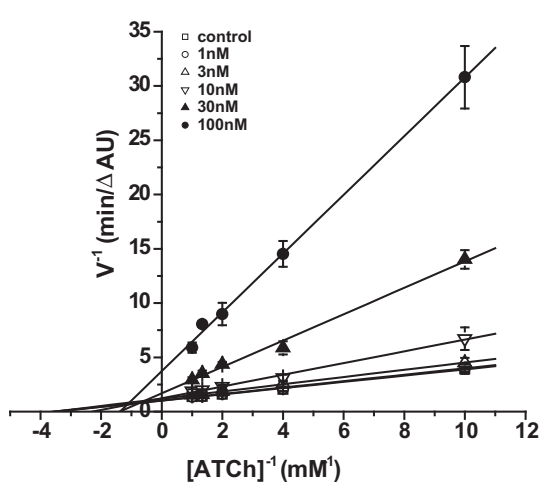

Fig. 1. Steady-state inhibition of AChE hydrolysis of acetylthiocholine (ATCh) by compound **8**. Lineweaver–Burk reciprocal plots of initial velocity and substrate concentrations (0.1–1 mM) are presented. Lines were derived from a weighted least-squares analysis of data.

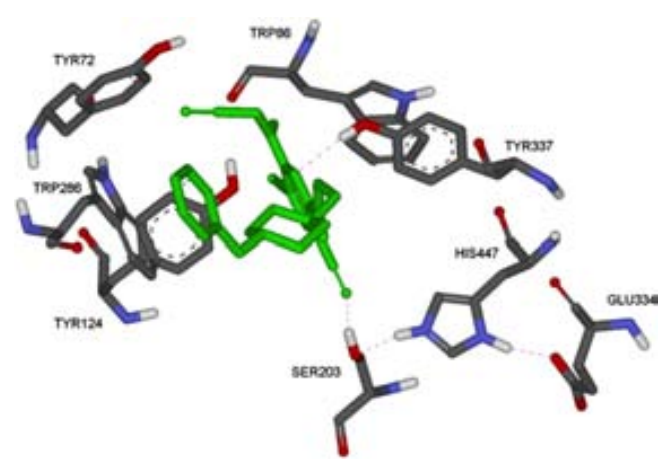

Fig. 2. Binding mode of **8** on *Ee*AChE as the outcome of docking simulations. The compound is rendered as sticks and illustrated in green. The hydrogen bonds are represented in dashed yellow lines. (For interpretation of the references to colour in this figure legend, the reader is referred to the web version of this article.)

Please cite this article in press as: A. Samadi, et al., Synthesis, biological assessment and molecular modeling of new multipotent MAO and cholinesterase inhibitors as potential drugs for the treatment of Alzheimer's disease, European Journal of Medicinal Chemistry (2011), doi:10.1016/j.ejmech.2011.05.048

naphthyridine core seems to be a more promising hit. However, no clear SAR can be deduced from these results, and a careful molecular modeling analysis in progress should possibly afford the keys in order to rationalize the observed inhibition trends.

3. Conclusions

To sum up, compounds **1**–**11**, designed as hybrids from donepezil and PF9601N, bearing *N*-benzyl piperidine and propargylamine moieties attached to a central pyridine or naphthyridine ring, have been synthesized and subjected to pharmacological evaluation. The biochemical results clearly identify compound **8**, and particularly, **11** as multipotent drugs showing strong and selective AChE inhibitory activity [(IC_{50} = 37 ± 4 nM)], and moderate, but selective MAO-A inhibitory profile [(IC_{50} = 41 ± 7 μM)]. We conclude that the most sensitive moiety to modulate AChE inhibition is the length of the spacer, which would control the dual interaction of these molecules with both CAS and PAS sites, improving inhibition when both binding sites are spatially targeted at the same time. Compared to tacrine, compound **11** is equipotent for the AChE and MAO-A inhibition, less potent for the inhibition of BuChE and more potent for the inhibition of MAO-B. Compared to donepezil, compound **11** is less potent for the inhibition of AChE, BuChE, and MAO-B, and more potent for the inhibition of MAO-A. Comparing the two pyridine derivatives **9** and **2**, with the same length in the linker, compound **9** (linker: CH_2CH_2) is 5-fold less potent than inhibitor **2** (linker: CH_2NH) for the inhibition of *Ee*AChE, and 1.4-fold less active for the inhibition of eqBuChE. Conversely, regarding MAO inhibition, while pyridine **2** was inactive, naphthyridine **9** showed a moderate, but selective MAO-B inhibitory profile. The pharmacological profile of compound **11**, as well as the fact that it is a readily available compound in a short synthetic sequence, in good chemical yields, prompts us to select it as a lead-compound for further optimization in our current research programme targeted to the preparation of new molecules for the potential treatment of AD. Work is now in progress and will be reported in due course.

Acknowledgments

A. Samadi thanks CSIC for a I3P-post-doc contract. M. Chioua thanks ISCIII (MICINN) for a “Sara Borrell” post-doctoral contract. J. Marco-Contelles thanks MICINN (SAF2006-08764-C02-01, SAF2009-07271) and CAM (S/SAL-0275-2006) financial support. C. de los Ríos thanks ISCIII for a “Miguel Servet” contract and financial support (Fundación CIEN and “Miguel Servet Program”).

Appendix. Supplementary data

Supplementary data associated with this article can be found, in the online version, at doi:10.1016/j.ejmech.2011.05.048.

References

[1] M. Goedert, M.G. Spillantini, Science 314 (2006) 777–781.
[2] A. Castro, A. Martínez, Curr. Pharm. Des. 12 (2006) 4377–4387.
[3] A. Gella, N. Durany, Cell. Adh. Migr. 3 (2009) 88–93.
[4] L. Cummings, J. Rev, Neurol. Dis. 1 (2004) 60–69.
[5] E. Scarpini, P. Scheltens, H. Feldman, Lancet Neurol. 2 (2003) 539–547.
[6] E.K. Perry, B.E. Tomlinson, G. Blessed, K. Bergmann, P.H. Gibson, R.H. Perry, British Med. J (1978) 1457–1459.
[7] V.N. Talesa, Mech. Ageing Dev. 122 (2001) 1961–1969.
[8] K.L. Davis, P. Powchick, Lancet 345 (1995) 625–630.
[9] C.M. Spencer, S. Noble, Drugs Aging 13 (1998) 391–400.
[10] E.L. Barner, S.L. Gray, Ann. Pharmacother. 32 (1998) 70–77.
[11] J.J. Sramek, E.J. Frackiewicz, N.R. Cutler, Expert Opin. Invest. Drugs 9 (2000) 2393–2402.
[12] D. Muñoz-Torrero, P. Camps, Curr. Med. Chem. 13 (2006) 399–422.
[13] A. Cavalli, M.L. Bolognesi, A. Minarini, M. Rosini, V. Tumiatti, M. Recanatini, C. Melchiorre, J. Med. Chem. 51 (2008) 347–372.
[14] M. García-Alloza, F.J. Gil-Bea, M. Díez-Ariza, C.P. Chen, P.T. Francis, B. Lasheras, M. Ramirez, J. Neuropsychologia 43 (2005) 442–449.
[15] A.V. Terry, J.J. Buccafusco, C. Wilson, Behav. Brain Res. 195 (2008) 30–38.
[16] M.B.H. Youdim, J.P.M. Finberg, K.F. Tipton, in: U. Tredelenburg, N. Weiner (Eds.), Monoamine Oxidase, Springer-Verlag, Berlin, 1988, pp. 119–192.
[17] J. Mitoma, A. Ito, J. Bio. Chem. 111 (1992) 20–24.
[18] T.P. Singer, in: F. Müller (Ed.), Chemistry and Biochemistry of Flavoenzymes, Vol III, CRC Press, Boca Ratón, FL, USA, 1990, pp. 437–470.
[19] S.Y. Son, A. Ma, Y. Kondou, M. Yoshimura, E. Yamashita, T. Tsukihara, Proc. Natl. Acad. Sci. USA 105 (2008) 5739–5744.
[20] C. Binda, P. Newton-Vinson, F. Hubalek, N. Restelli, D.E. Edmondson, A. Mattevi, Nat. Struct. Biol. 2 (2002) 22–26.
[21] V. Pérez, J.L. Marco, E. Fernández-Álvarez, M. Unzeta, Brit. J. Pharmacol. 127 (1999) 869–876.
[22] C. de los Ríos, J. Egea, J. Marco-Contelles, R. León, A. Samadi, I. Iriepa, I. Moraleda, E. Gálvez, A.G. García, M.G. López, M. Villarroya, A. Romero, J. Med. Chem. 53 (2010) 5129–5143.
[23] H. Zheng, M.B.H. Youdim, M. Fridkin, J. Med. Chem. 52 (2009) 4095–4098.
[24] J. Sterling, Y. Herzig, T. Goren, N. Finkelstein, D. Lerner, W. Goldenberg, I. Miskolczi, S. Molnar, F. Rantal, T. Tamas, G. Toth, A. Zagyva, A. Zekany, G. Lavian, A. Gross, R. Friedman, M. Razin, W. Huang, B. Krais, M. Chorev, M.B. Youdim, M. Weinstock, J. Med. Chem. 45 (2002) 5260–5279.
[25] C. Brühlmann, F. Ooms, P.-A. Carrupt, B. Testa, M. Catto, F. Leonetti, C. Altomare, A. Carotti, J. Med. Chem. 44 (2001) 3195–3198.
[26] D.M. Fink, M.G. Palermo, G.M. Bores, F.P. Huger, B.E. Kurys, M.C. Merriman, G.E. Olsen, W. Petko, G.J. O'Malley, Bioorg. Med. Chem. Lett. 6 (1996) 625–630.
[27] (a) C. Peinador, M.C. Veiga, J. Vilar, J.M. Quintela, Heterocycles 38 (1994) 1299–1305;
(b) A.G. E.Merck, DE1182896; 1963, Chem. Abstr. 62 (1965) 4013a Patent.
[28] (a) A. Duindam, V.L. Lishinsky, D.J. Sikkema, Synth. Commun. 23 (1993) 2605–2609;
(b) D.V. Vilarelle, C. Peinador, J.M. Quintela, Tetrahedron 60 (2004) 275–283.
[29] G.L. Ellman, K.D. Courtney, B.J. Andres, R.M. Featherstone, Biochem. Pharmacol. 7 (1961) 88–95.
[30] J. Marco-Contelles, R. León, C. de los Ríos, A. Samadi, M. Bartolini, V. Andrisano, O. Huertas, X. Barril, F.J. Luque, M.I. Rodríguez-Franco, B. López, M.G. López, A.G. García, M.C. Carreiras, M. Villarroya, J. Med. Chem. 52 (2009) 2724–2732.
[31] Compounds 9 and 11 were prepared by Friedländer type reaction of 6-amino-5-formyl-2-(methyl(prop-2-yn-1-yl)amino)-4-phenylnicotinonitrile (32) with 4-(1-benzylpiperidin-4-yl)butan-2-one (31), while compound 10 was obtained as the only product in a similar reaction between 6-amino-5-formyl-2-(methyl(-prop-2-yn-1-yl)amino)nicotinonitrile (33) and ketone 31 (Supplementary data).
[32] A. Rampa, A. Bisi, F. Belluti, S. Gobbi, P. Valenti, V. Andrisano, V. Cavrini, A. Cavalli, M. Recanatini, Bioorg. Med. Chem. 8 (2000) 497–506.
[33] O. Trott, A.J. Olson, J. Comput. Chem. 31 (2010) 455–461.
[34] D. Alonso, I. Dorronsoro, L. Rubio, P. Muñoz, E. García-Palomero, M. Del Monte, A. Bidon-Chanal, M. Orozco, F.J. Luque, A. Castro, M. Medina, A. Martínez, Bioorg. Med. Chem. 13 (2005) 6588–6597.
[35] N.C. Inestrosa, A. Álvarez, C.A. Pérez, R.D. Moreno, M. Vicente, C. Linker, O.I. Casanueva, C. Soto, J. Garrido, J. Neuron 16 (1996) 881–891.

1. Annex Chapter II.

1.1 Supplementary Table 1.

The structure-activity relationship (SAR) of an extensive series of *N*-propargylamine derivatives of tacrine towards MAO (A and B) as well as AChE and BuChE inhibition was investigated (Table S1).

According to literature, tacrine appeared as a potent ChEI (nM range) being 5-fold more selective for BuChE than for AChE. In contrast, it behaved as a poor MAO inhibitor being 10-fold more selective for isoform A. The introduction of the *N*-propargylamine moiety of PF9601N into tacrine to give compound CVC96 provoked a reduction towards MAO-A inhibition of one order of magnitude. Moreover, a dramatic decrease in the potency towards both AChE and BuChE was observed, even finding a striking change in the selectivity. Further changes in the type of substituents on the main structure of tacrine (compounds CVC91 to CVC 93) did not produce any effect on the inhibitory capacity towards MAO. However, some interesting SARs were found regarding ChEs. When a methoxy and a carbonitrile group were introduced in CVC96 to give CVC91, AChE inhibition was improved to the high nanomolar range whereas BuChE inhibition was completely lost. However, the replacement of the methoxy by a chloro to yield CVC99 provoked a decrease in the potency towards AChE. BuChE was not affected. Interestingly, the replacement of the methoxy group by a dimethylamino to yield CVC110 notably improved the inhibitory capacity towards AChE 48-fold. More interestingly, the introduction of voluminous substituents such as a pyrrolidin-1-yl (CVC104) and a piperidin-1-yl (CVC107) or the introduction of the *N*-propargylamine into the position 1 of tacrine ring did not produce a significant effect in the potency towards AChE, which was similar to that found for the parent compound tacrine. By contrast, the inhibition of BuChE was clearly affected as we observed activity near the micromolar range.

We also studied the SAR of the introduction of different substituents into a N-propargylamine-derived molecule containing a single ring of tacrine (compounds ASS87 to ASS114). No compound of the series was able to inhibit AChE and BuChE, or any isoform of MAO.

Table S1. Inhibitory activities towards monoamine oxidases A (MAO-A) and B (MAO-B) and acetylcholinesterase (AChE) and butyrylcholinesterase (BuChE) by a series of *N*-propargylamine derivatives. Activities of the reference compound, tacrine, are also shown. Data are the mean ± SEM of three independent experiments in triplicate.

		IC_{50} (μM)		Selectivity	IC_{50} (μM)		Selectivity
Compound	**Structure**	**MAO-A**	**MAO-B**	**MAO-B/ MAO-A**	**AChE**	**BuChE**	**BuChE/ AChE**
Tacrine	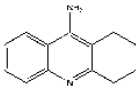	40 ± 10	>100	>2.5	0.027 ± 0.002	0.0052 ± 0.0002	0.19
CVC96		>100	>100	>1	1.5 ± 0.2	6.6 ± 0.5	4.4
CVC91		>100	>100	>1	0.54 ± 0.08	>100	>185
CVC99		>100	>100	>1	1.4 ± 0.22	>100	>71.5
CVC110		>100	>100	>1	0.029 ± 0.009	>100	>3448
CVC104		>100	>100	>1	0.025 ±0.003	27 ± 2	1080
CVC107		>100	>100	>1	0.066 ± 0.009	10 ± 1	151
CVC93		>100	>100	>1	0.030 ± 0.003	2.6 ± 0.3	86.7
ASS87		>100	>100	>1	>100	>100	>1
ASS162		>100	>100	>1	>100	>100	>1
ASS161		>100	>100	>1	>100	>100	>1
ASS114		>100	>100	>1	>100	>100	>1

CHAPTER III

Synthesis, Biological Evaluation and Molecular Modeling of Donepezil and N-[(5-(benzyloxy)-1-methyl-1H-indol-2-yl) methyl]-N-methylprop-2-yn-1-amine Hybrids, as New Multipotent Cholinesterase/Monoamine oxidase Inhibitors for the Treatment of Alzheimer's Disease.

Irene Bolea, Jordi Juárez-Jiménez, Cristóbal de los Ríos, Mourad Chioua, Ramón Pouplana, F. Javier Luque, Mercedes Unzeta, José Marco-Contelles and Abdelouahid Samadi

Revision Submitted to the Journal of Medicinal Chemistry

Synthesis, Biological Evaluation and Molecular Modeling of Donepezil and N-[(5-(Benzyloxy)-1-methyl-1H-indol-2-yl)methyl]-N-methylprop-2-yn-1-amine Hybrids, as New Multipotent Cholinesterase/Monoamine Oxidase Inhibitors for the Treatment of Alzheimer's Disease.

Journal:	*Journal of Medicinal Chemistry*
Manuscript ID:	jm-2011-00853t
Manuscript Type:	Additions and Corrections
Date Submitted by the Author:	30-Jun-2011

Complete List of Authors:	Bolea, Irene; Universitat Autònoma de Barcelona. Institut de Neurociències, Departament de Bioquimica i Biologia Molecular Juárez-Jiménez, Jordi; Universitat de Barcelona, Departament de Fisicoquimica Delosrios, Cristobal; CSIC Chioua, Mourad; IQOG, CSIC, Laboratorio de Radicales Libres y Quimica Computacional Pouplana, Ramon; Universitat de Barcelona, Departament de Fisicoquimica Luque, F. Javier; Universitat de Barcelona, Fisicoquimica; Universitat de Barcelona, Departament de Fisicoquimica Unzeta, Mercedes; University Autonoma Barcelona. Institut de Neurociències, Bioquimica i Biologia Molecular Marco-Contelles, Jose; IQOG, CSIC, Laboratorio de Radicales Libres y Quimica Computacional Samadi, Abdelouahid; IQOG, CSIC, Laboratorio de Radicales Libres y Quimica Computacional

SCHOLARONE™
Manuscripts

Synthesis, Biological Evaluation and Molecular Modeling of Donepezil and *N*-[(5-(Benzyloxy)-1-methyl-1*H*-indol-2-yl)methyl]-*N*-methylprop-2-yn-1-amine Hybrids, as New Multipotent Cholinesterase/Monoamine Oxidase Inhibitors for the Treatment of Alzheimer's Disease.

Irene Bolea,[±,#] Jordi Juárez-Jiménez,[&,#] Cristóbal de los Ríos,[‡] Mourad Chioua,[¶] Ramón Pouplana,[&] F. Javier Luque,[&] Mercedes Unzeta,[±,*] and José Marco-Contelles[¶,*] Abdelouahid Samadi[¶,]

Departament de Bioquímica i Biología Molecular, Facultat de Medicina. Institut de Neurociències. Universitat Autònoma de Barcelona, 08193 Bellaterra, Barcelona, Spain; Departament de Fisicoquímica, Facultat de Farmàcia, and Institut de Biomedicina (IBUB), Universitat de Barcelona, Av. Diagonal 643, E-08028, Barcelona, Spain; Laboratorio de Radicales Libres y Química Computacional (IOG, CSIC), Juan de la Cierva 3, E-28006, Madrid, Spain; Instituto Teófilo Hernando, Fundación de Investigación Biómedica, Hospital Universitario de la Princesa, C/ Diego de León, 62, E-28029, Madrid, Spain

[#] Those authors have contributed equally to this work.

*To whom correspondence should be addressed:

Mercedes Unzeta: Phone: +34-93-5811439; Fax: +34-93-5811573; E-mail: mercedes.unzeta@uab.es

José Marco-Contelles: Phone: +34-91-5621900; Fax: +34-91-5644853; E-mail: iqoc21@iqog.csic.es

[±]Departament de Bioquímica i Biología Molecular, Facultat de Medicina, Universitat Autònoma de Barcelona

[&]Departament de Fisicoquímica, Facultat de Farmàcia, and Institut de Biomedicina (IBUB), Universitat de Barcelona

[¶] Laboratorio de Radicales Libres y Química Computacional (IQOG, CSIC)

[‡] Instituto Teófilo Hernando, Fundación de Investigación Biómedica, Hospital Universitario de la Princesa, C/ Diego de León, 62, E-28029, Madrid, Spain

Abbreviations: AD, Alzheimer's disease; ACh, acetylcholine; AChE, acetylcholinesterase; Aβ, β-amyloid peptide; BuChE, butyrylcholinesterase; AChEI, acetylcholinesterase inhibitors; hAChE, human acetylcholinesterase; Ee, *Electrophorus electricus*; CAS, catalytic active site; PAS, peripheral anionic site; MAO, Monoamine Oxidase-A/B; IMAO, Monoamine oxidase inhibitors.

Abstract

A new family of multi-target molecules able to interact with acetylcholinesterase (AChE) and butyrylcholinesterase (BuChE), as well as with monoamino oxidase (MAO) A and B has been synthesized. Novel compounds (**3**-**9**) have been designed using a conjunctive approach that combines the benzyl piperidine moiety of the AChE inhibitor donepezil (**1**), and the indolyl propargylamino moiety of the MAO inhibitor *N*-[(5-benzyloxy-1-methyl-1*H*-indol-2-yl)methyl]-*N*-methylprop-2-yn-1-amine (**2**), connected through an oligomethylene linker. The most promising hybrid (**5**) is a potent inhibitor of both MAO-A (IC_{50}= 5.2 ± 1.1 nM) and MAO-B (IC_{50}= 43.1 ± 7.9 nM), and a moderately potent inhibitor of AChE (IC_{50}= 0.35 ± 0.01 μM) and BuChE (IC_{50}= 0.46 ± 0.06 μM). Moreover, molecular modeling and kinetic studies support the dual binding site to AChE, which explains the inhibitory effect exerted on Aβ aggregation. Overall, the results suggest that the new compounds are promising multi-target drug candidates with potential impact for Alzheimer's disease therapy.

Introduction

Alzheimer's disease (AD), the most common form of adult onset dementia, is an age-related neurodegenerative disorder characterized by a progressive memory loss, a decline in language skills and other cognitive impairments.[1] Although the etiology of AD is not completely known, several factors such as amyloid-β (Aβ)[2] deposits, τ-protein aggregation[3], oxidative stress[4,5] or low levels of acetylcholine (ACh) are thought to play significant roles in the pathophysiology of the disease.[6] The selective loss of cholinergic neurons in AD results in a deficit of ACh in specific brain regions that mediate learning and memory functions.[7] However, alterations in other neurotransmitter systems, specially serotoninergic and dopaminergic[8,9], are also thought to be responsible for the behavioural disturbances observed in patients with AD.[10] These evidences have led to the suggestion that inhibitors of monoamine oxidase (IMAOs) might be also valuable for the treatment of AD.[11,12] Thus, monoamine oxidase (MAO; EC 1.4.3.4), the enzyme that catalyses the oxidative deamination of a variety of biogenic and xenobiotic amines,[13] is also an important target to be considered for the treatment of specific features of this multifactorial disease. MAO exists as two distinct enzymatic isoforms, MAO-A and MAO-B, based on their substrate and inhibitor specificities.[14] MAO-A preferentially deaminates serotonin, adrenaline and noradrenaline and is selectively and irreversibly inhibited by clorgyline. In contrast, MAO-B preferentially deaminates β-phenylethylamine and benzylamine and is irreversibly inhibited by R-(-)-deprenyl.[15] Selective inhibitors for MAO-A have shown to be effective antidepressants, whereas MAO-B inhibitors, although apparently devoid of antidepressant action, are useful in the treatment of Parkinson's disease.[16] Besides the increased amine neurotransmission, the beneficial properties of IMAOs are also related to the reduction of the formation of the neurotoxic products, such as hydrogen peroxide and aldehydes, which promote the

formation of reactive oxygen species ROS and may ultimately contribute to increased neuronal damage.[17,18] Moreover, AD patients commonly present depressive symptoms which have even been considered as a risk factor for the development of the disease[19]. Increased MAO-B levels due to enhanced astrogliosis in the brain of AD patients has also been reported.[11] Overall, these observations suggest that dual inhibition of MAO-A and MAO-B, rather than MAO-B alone, may be of value for AD therapy.

At present, there are three FDA-approved drugs (donepezil, galanthamine and rivastigmine)[20-22] that improve AD symptoms by inhibiting acetylcholinesterase (AChE; E.C.1.1.1.7), i.e. the enzyme responsible for the hydrolysis of ACh, and, thereby, rising ACh content in the synaptic cleft. Apart from the beneficial palliative properties of AChE inhibitors in AD,[23-25] cholinergic drugs have shown little efficacy to prevent the progression of the disease. In fact, the multifactorial nature of AD supports the most current innovative therapeutic approach based on the "*one molecule, multiple targets*" paradigm.[26,27] Thus, a single drug that acts on a specific target to produce the desired clinical effects might not be suitable for the complex nature of AD. Accordingly, the multi-target-directed ligand (MTDL) approach has been the subject of increasing attention by many research groups, which have developed a variety of compounds acting on very diverse targets.[28-33] A very successful approach came from the combination of the carbamate moiety of rivastigmine with the indolamine moiety present in rasagiline, a well-known MAO-B inhibitor, leading to the compound ladostigil.[34] Besides inhibiting MAO and AChE, it possesses neuroprotective and antiapoptotic activities,[35] which have been attributed to the propargylamine group present in the molecule, thus retaining the beneficial properties observed for rasagiline.[36] The potential therapeutic effect of this compound, which has reached clinical trials,[37] is also supported by recent findings showing the ability of

propargylamine-containing compounds to modulate cleavage of β-amyloid protein precursor.[38] Hybrid compounds targeting cholinesterases and amyloid plaques,[39] as well as site-activated chelators targeting MAO and AChE have also been recently attempted.[40-43]

In the development of IMAOs for the treatment of neurodegenerative diseases, initial works of our group extensively investigated the effect of the introduction of a benzyloxy group in a series of acetylenic and allenic derivatives of tryptamine, which were previously reported to be selective for MAO-A.[44] We observed that the introduction of this moiety changed the selectivity towards the B isoform of the enzyme, and that it was significantly decreased when a hydrogen atom was attached to the nitrogen atom of the indole ring and/or the side-chain was substituted by a CH_3 group.[45,46] Based on these previous works, we have designed a novel family of hybrid compounds of type **I** to act as potential inhibitors of both MAO and AChE (Figure 1). The novel hybrids have been conceived by a conjuctive approach that combines donepezil (**1**), and *N*-[(5-benzyloxy-1-methyl-1*H*-indol-2-yl)methyl]-*N*-methylprop-2-yn-1-amine (**2**), which is one of the most interesting IMAOs previously investigated in our laboratory[46]. The underlying strategy is to retain the 1-benzylpiperidine fragment present in donepezil (**1**), which binds to the catalytic and mid-gorge sites of AChE, with the 1-methyl-1*H*-indol-2-yl)methyl]-*N*-methylprop-2-yn-1-amine moiety shown in compound **2** (Figure 1), which should occupy the substrate binding site in MAO.

By doing this conjunctive approach, the novel hybrids are expected to behave as dual binding site AChE inhibitors, since the 1-methyl-1*H*-indol-2-yl)methyl]-*N*-methylprop-2-yn-1-amine moiety could presumably interact at the peripheral anionic site (PAS) of AChE. The possibility of targeting both catalytic active site (CAS) and PAS of AChE

will largely depend the length of the linker, a crucial structural feature to facilitate the binding of both 1-benzylpiperidine and 1-methyl-1*H*-indol-2-yl)methyl]-*N*-methylprop-2-yn-1-amine moieties to CAS and PAS, respectively, in AChE. This particular mode of action should result in a significant AChE inhibitory potency, of interest for the management of the symptomathology of AD arising from the cholinergic deficit but, more interestingly, it could also recognize the peripheral site, which appears to mediate the Aβ proagreggating action of AChE.[47-50] On the other hand, the correct alignment of the 1-benzylpiperidine and 1-methyl-1*H*-indol-2-yl)methyl]-*N*-methylprop-2-yn-1-amine moieties in MAO will also depend on the tether, as the length and chemical nature of the linker should also affect the accommodation of the hybrid through the residues that define the bottleneck between the entrance and substrate cavities in MAO.

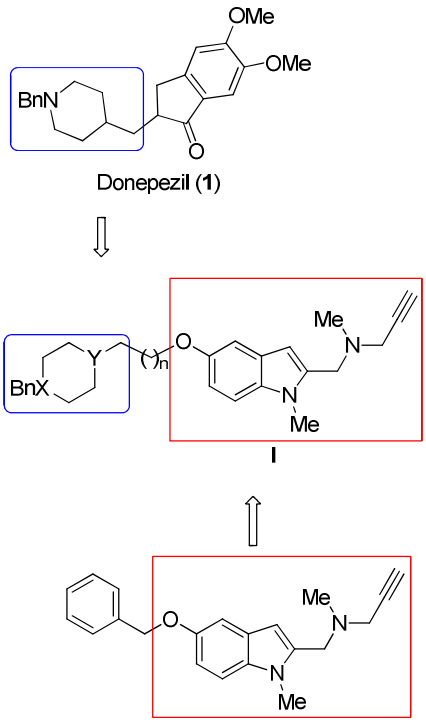

Figure 1. Schematic representation of the conjunctive approach designed to synthesize the novel IMAO/IAChE hybrids.

In this work we describe the synthesis, pharmacological evaluation and molecular modeling of representative molecules of this new family of compounds (**I**; Figure 1). The pharmacological evaluation of these novel compounds includes AChE and butyrylcholinesterase (BuChE) inhibition, the inhibition of MAO–A and MAO–B, the kinetics of enzyme inhibition, as well as the AChE-dependent and self-induced Aβ aggregation. Finally, molecular modeling studies are performed to gain insight into the binding mode and structure-activity relationships of the novel hybrid compounds.

Results and Discussion

Chemistry. To explore the suitability of the conjunctive strategy outline above, compounds **3-9** (Figure 2) were synthesized differing in either the length of the tether and the location and/or the number of nitrogens in the tethered-benzyl substituted cyclohexane ring linked to indolyl moiety.

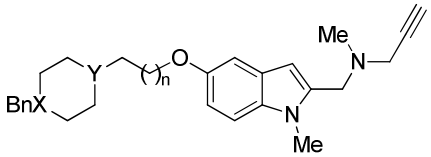

3 X= N, Y= CH, n= 0
4 X= N, Y= CH, n= 1
5 X= N, Y= CH, n= 2
6 X= N, Y= CH, n= 3
7 X= CH, Y= N, n= 1
8 X= CH, Y= N, n= 2
9 X, Y= N, n= 2

Figure 2. General structure for the target molecules (**3-9**).

The 1-benzyl-4-substituted piperidine derivatives **3-6** were synthesized by sodium hydride/DMF promoted reaction of compounds **10-13**, and 1-methyl-2-{[ethyl(prop-2-yn-1-yl)amino]ethyl}-1*H*-indol-5-ol **14**[51] (Scheme 1).

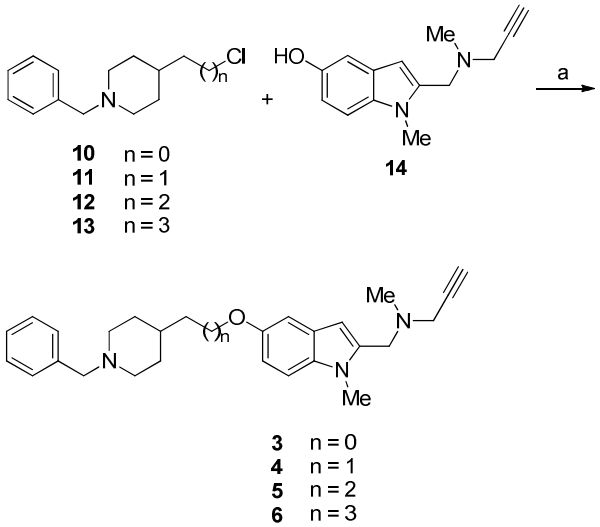

Scheme 1. Reagents and conditions: (a) NaH, DMF, rt.

1-Benzyl-4-(chloromethyl) piperidine **10** and 1-benzyl-4-(chloroethyl) piperidine **11** were synthesized following the methods reported in literature[52]. 1-Benzyl-4-(3-chloropropyl) piperidine **12** was prepared as shown in Scheme 2, starting from commercial 4-pyridinecarboxaldehyde **15**, *via* the known intermediate **16**,[53] whose hydrogenation,[54] under Pd/C and PtO_2, in the presence of hydrochloric acid, and work-up with methanol, afforded methyl ester **17**.[55] Next, *N*-benzylation to give 1-benzylpiperidine **18**, reduction with lithium aluminium hydride (LAH) to provide alcohol **19**,[56] and treatment with thionyl chloride, furnished the chloride derivative **12** in quantitative yield.

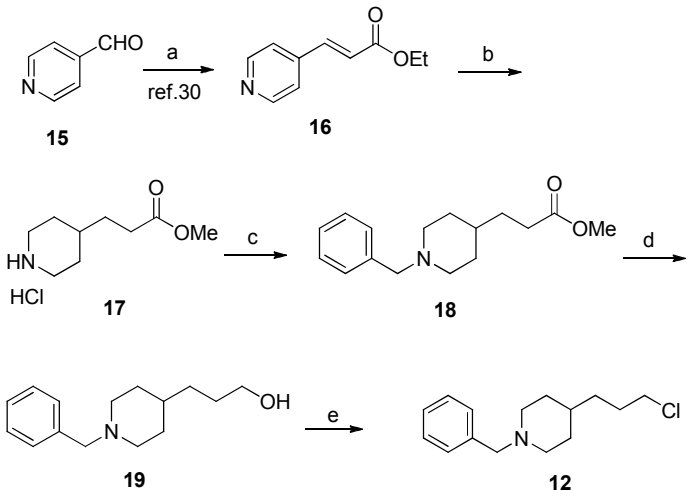

Scheme 2. Reagents and conditions: (a) $(EtO)_2P(O)CH_2CO_2Et$, THF, K_2CO_3, reflux (92%); (b) i. H_2, Pd/C 10%, PtO_2, 4N HCl in dioxane, EtOH, rt; ii. MeOH (90%); (c) BnBr, TEA, CH_2Cl_2 (75%); (d) $LiAlH_4$, THF, reflux (98%); (e) $SOCl_2$, CH_2Cl_2, reflux (99%).

1-Benzyl-4-(4-chlorobutyl)piperidine **13** was prepared as shown in Scheme 3. Treatment of commercial 1-benzyl-4-piperidone **20** with triethyl 4-phosphonocrotonate in the presence of sodium hydride in dry ethanol afforded compound **21** in 78% yield, whose catalytic hydrogenation over Pd/C in ethanol at room temperature gave ester **22** in 99% yield.[57] Next, reaction of **22** with benzyl bromide to give ester **23**, followed by reduction with LAH gave the desired alcohol **24**, which was then treated with thionyl chloride to give the chloro derivative **13** in almost quantitative yield.[57]

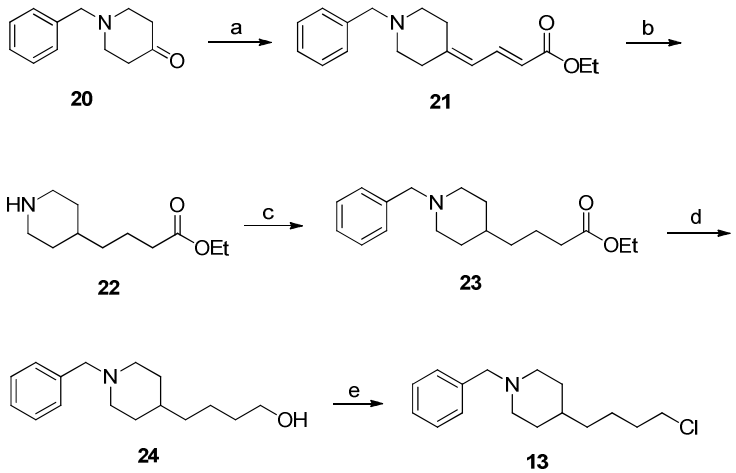

Scheme 3. Reagents and conditions: (a) $(EtO)_2P(O)CH_2CH{=}CHCO_2Et$, EtOH, NaH, reflux (78%); (b) H_2, Pd/C 10%, EtOH, rt (99%); (c) BnBr, TEA, CH_2Cl_2 (70%); (d) $LiAlH_4$, THF, reflux (99%); (e) $SOCl_2$, CH_2Cl_2, reflux (99%).

Compounds **7-9** (Figure 2) were synthesized as shown in Schemes 4 and 5. Reaction of indole **14** with 1,2-dibromoethane gave **25**, which after treatment with 4-benzylpiperidine afforded **7** (Scheme 4).[51] Similarly, the reaction of indole **14** with 1,3-dibropropane gave intermediate **26**, whose reaction with 4-benzylpiperidine or 1-benzylpiperazine afforded **8** and **9**, respectively (Scheme 5).[51]

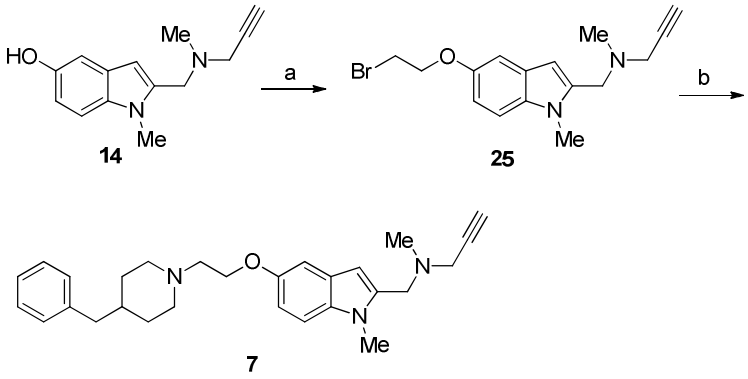

Scheme 4. Reagents and conditions: (a) $Br(CH_2)_2Br$, 2-butanone, K_2CO_3, 85 ºC, 6 h (37%); (b) 4-benzylpiperidine, K_2CO_3, THF, 80 ºC (77%).

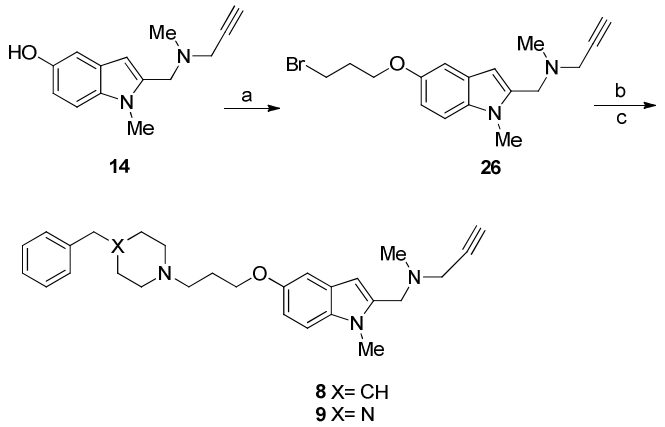

Scheme 5. Reagents and conditions: (a) $Br(CH_2)_3Br$, 2-butanone, K_2CO_3, 85 ºC, 6 h (80%); (b) 4-benzylpiperidine, K_2CO_3, THF, 80 ºC (64%); (c) 1-benzylpiperazine, K_2CO_3, THF, 80 ºC (85%).

All new compounds showed analytical and spectroscopic data in good agreement with their structures (see **Experimental Part**).

AChE and BuChE inhibition. To study the multipotent profile of the hybrid compounds, they were first evaluated as inhibitors of AChE and BuChE. The AChE inhibitory activity was tested against the *Electrophorus electricus* enzyme (*Ee*AChE), and the inhibition of BuChE was carried out using the equine serum enzyme (eqBuChE). The inhibitory activities of the hybrids were compared with those determined for the parent compounds, donepezil (**1**) and *N*-[(5-benzyloxy-1-methyl-1*H*-indol-2-yl)methyl]-*N*-methylprop-2-yn-1-amine (**2**).[46]

Biological evaluation. The 1-benzylpiperidin-4-yl derivatives **3**-**6** were found to be moderately potent regarding to the inhibition of *Ee*AChE. The IC_{50} values were similar in all cases (ranging from 0.26 to 0.42 μM; Table 1). Moreover, they exhibit similar potencies against eqBuChE, as the IC_{50} values range from 0.46 to 2.1 μM, leading to a very slight selectivity for AChE (the ratio IC_{50}(eqBuChE)/IC_{50}(*Ee*AChE) varies from 1.3 to 5). Accordingly, the length of the linker does not seem to be a crucial factor for

the inhibitory potency against AChE and BuChE. The most potent compounds are **5** and **6**, which are characterized by IC_{50} values of 0.35 and 0.26 μM against AChE, and 0.46 and 0.99 μM against BuChE. Compared with donepezil (**1**), they are 39 to 52-fold less potent for the inhibition of AChE, but 7 to 16-fold more potent regarding the BuChE inhibition.

Table 1. AChE and BuChE inhibitory activities of donepezil (**1**), the reference compound **2**, and *N*-[(1-methyl-1*H*-indol-2-yl)methyl]-*N*-methylprop-2-yn-1-amines **3**-**9**.

Compound	**IC_{50} (μM)[a]**		**Selectivity**
	***Ee*AChE**	**eqBuChE**	**eqBuChE/*Ee*AChE**
1 (donepezil)	0.00670 ± 0.00035	7.40 ± 0.10	1100
2	0.25 ± 0.01	>100	>100
3 (n= 0)	0.31 ± 0.04	1.10 ± 0.20	3.5
4 (n= 1)	0.42 ± 0.04	2.10 ± 0.20	5.0
5 (n= 2)	0.35 ± 0.01	0.46 ± 0.06	1.3
6 (n= 3)	0.26 ± 0.07	0.99 ± 0.08	3.8
7 (n= 1)	>100	0.80 ± 0.10	>100
8 (n= 2)	18.10 ± 0.40	2.20 ± 0.40	0.12
9 (n= 2)	>100	7.60 ± 0.40	>100

[a]Values are expressed as mean ± standard error of the mean of at least three different experiments in quadruplicate.

Compared to derivatives **3**-**6**, reversion of the piperidine ring in **7** and **8** has a dramatic effect on the inhibitory potency in *Ee*AChE. A drastic reduction in activity is also found upon replacement of the piperidine unit by a piperazine one (leading to compound **9**). Thus, compounds **7** and **9** are completely inactive against *Ee*AChE,

whereas the inhibitory activity of **8** is decreased 52-fold. Nevertheless, these chemical modifications have less effect on the eqBuChE potency, as compounds **7**-**9** are roughly equipotent (**7**) or slightly less potent (**8** and **9**) compared to **3**-**6**.

Overall, the results point out the relevant role played by the 1-benzylpiperidin-4-yl unit on the AChE inhibitory activity, suggesting that this moiety is the main factor in mediating the binding to AChE. On the other hand, it is worth noting that compounds **3**-**6** are active for the BuChE inhibition. This is particularly important in view of the renewed interest in dual AChE/BuChE cholinergic inhibitors as therapeutic agents for AD, as they have been described to improve cognition.[58] More specifically, compound **5** is presented as a dual ChE inhibitor by having both AChE and BuChE inhibition in the same submicromolar level. For this reason and due to its pharmacological properties, we evaluated its inhibitory activity against human recombinant AChE (hrAChE), the cerebral enzyme expressed in the HEK-293 cell line, and of human serum BuChE (hBuChE). Thus, compound **5** inhibited hrAChE with an IC_{50} of 0.38 ± 0.05 μM (tacrine, used as a standard, inhibited hrAChE with an IC_{50} of 122 ± 2 nM) and hBuChE with an IC_{50} of 1.7 ± 0.2 μM (tacrine inhibited hBuChE with an IC_{50} of 36 ± 4 nM).

Kinetic studies. To gain further insight into the mechanism of action of this family of compounds on AChE, a kinetic study was carried out with the most promising compound of the series, **5**, using *Ee*AChE. Graphical analysis of the reciprocal Lineweaver–Burk plots (Figure 3) showed both increased slopes (decreased V_{max}) and intercepts (higher K_m) at increasing concentration of the inhibitor. This pattern indicates a mixed-type inhibition and, therefore, supports the dual site binding of this compound. Replots of the slope versus concentration of compound **5** gave an estimate of the inhibition constant, K_i, of 149 nM.

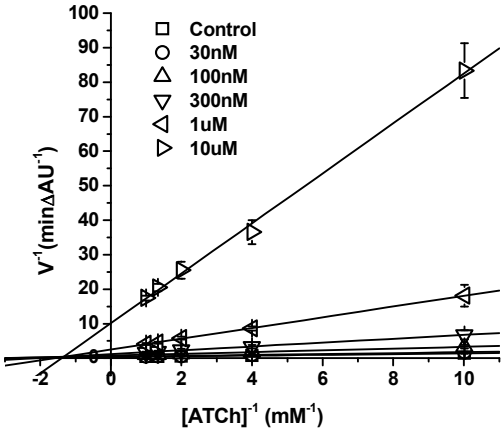

Figure 3. Kinetic study on the mechanism of *Ee*AChE inhibition by compound **5**. Overlaid Lineweaver –Burk reciprocal plots of AChE initial velocity at increasing substrate concentration (0.1-1 mM) in the absence of inhibitor and in the presence of **5** are shown. Lines were derived from a weighted least-squares analysis of the data points.

MAO inhibition. To complete the study of the multipotent biological profile of the hybrid compounds, the inhibitory activity against MAO-A and MAO-B (from rat liver mitochondria) was determined and compared with the inhibition exerted by the parent compounds, donepezil (**1**) and *N*-[(5-benzyloxy-1-methyl-1*H*-indol-2-yl)methyl]-*N*-methylprop-2-yn-1-amine (**2**).

Biological evaluation. The 1-benzylpiperidin-4-yl derivatives **3-6** showed a potent MAO-A inhibition (Table 2), acting in the nanomolar range (IC_{50} ranging from 82.2±3.2 to 5.2±1.1 nM). In contrast, they were less potent against MAO-B, with the exception of **5**, which was found to be the most potent compound towards both isoforms (IC_{50}= 5.2±1.1 and 43.1±7.9 nM for MAO-A and MAO-B, respectively). The most selective inhibitor resulted to be compound **6** (n= 3) towards MAO-A, whereas **5** was much less selective. It is worth noting the large sensitivity of the inhibitory potency on the length of the tether. Thus, removal of a single methylene group in **6** to yield **5**

ACS Paragon Plus Environment

increased the inhibitory potency against MAO-A and MAO-B by a factor of 2 and 64, respectively. Likewise, further reduction of the tether to just one methylene (from **5** to yield **4**) did not affect the MAO-A inhibitory potency, but reduced the potency against MAO-B by 3-fold.

Table 2. MAO-A and MAO-B inhibitory activities of donepezil (**1**), reference compound **2**, and the *N*-[(1-methyl-1*H*-indol-2-yl)methyl]-*N*-methylprop-2-yn-1-amine derivatives (**3-9**).

Compound	IC_{50} (nM)[a]		Selectivity
	MAO-A	MAO-B	MAO-B/MAO-A
1 (donepezil)	854800± 13300	15400± 2200	0.020
2	100 ± 7.0	63 ± 2.0	0.63
3 (n= 0)	82 ± 3.0	745 ± 20	9.1
4 (n= 1)	6.7 ± 1.8	130 ± 41	19
5 (n= 2)	5.2 ± 1.1	43 ± 8.0	8.3
6 (n= 3)	10 ± 4.0	2774 ± 116	264
7 (n= 1)	143 ± 44	1457 ± 499	10.2
8 (n= 2)	65 ± 17	11320 ± 2380	173.1
9 (n= 2)	31 ± 14	1640 ± 707	53.8

[a] Values are expressed as mean ± standard error of the mean of at least three different experiments in quadruplicate.

Compounds **7** and **8**, bearing a 4-benzylpiperidin-1-yl residue, also inhibited MAO-A quite potently, but showed less potency towards MAO-B. Similarly, compound **9**, containing a 4-benzylpiperazin-1-yl residue, also showed a good MAO-A inhibitory potency but a lower activity towards MAO-B. Interestingly, we found that compound **7** was 21-fold and 11-fold less potent for MAO-A and MAO-B, respectively, than the analogous inhibitor **4**. Similarly, compounds **8** and **9** were significantly less potent for both isoforms than the analogous inhibitor **5** (12-fold and 6-fold for MAO-A, and 262-fold and 38-fold for MAO-B, respectively). Altogether, these results show that

compounds bearing the donepezil 1-benzylpiperidin-4-yl motif were the best MAO inhibitors and that, among them, **5** was the most potent inhibitor, even more than the reference compound **2**.

Kinetic studies. To study the type of inhibition towards MAO, we analysed the reversibility/irreversibility of the binding of compound **5**, the most potent inhibitor of the series. We observed that **5** irreversibly inhibited MAO-A, since the inhibition was not reverted after three consecutive centrifugations and washings with buffer (Figure 4A). This hypothesis is also in agreement with the time-dependent inhibition of MAO-A upon incubation with the inhibitor (Figure 4B), and thus reflects the inhibition mechanism found for the parent compound **2.**[46] Strinkingly, whereas the inhibition of MAO-B was also found to depend on the incubation time (Figure 4D), a significant fraction (80.5±3.3%) of the activity was recovered by washing the enzyme three times after incubation for 30 minutes (Figure 4C). These findings point out that the addition of the benzylpiperidine unit to the reference compound **2** in order to yield **5** does not affect the proper alignment of the indolyl propargylamino moitey in the binding cavity of MAO-A, thus leading to the complete inactivation of the enzyme by chemical modification of the cofactor. However, present results suggest that docking of **5** into the binding cavity of MAO-B is more impeded than in MAO-A, which should prevent the proper alignment of the propargyl amino moiety, thus making less efficient the inactivation of the enzyme.

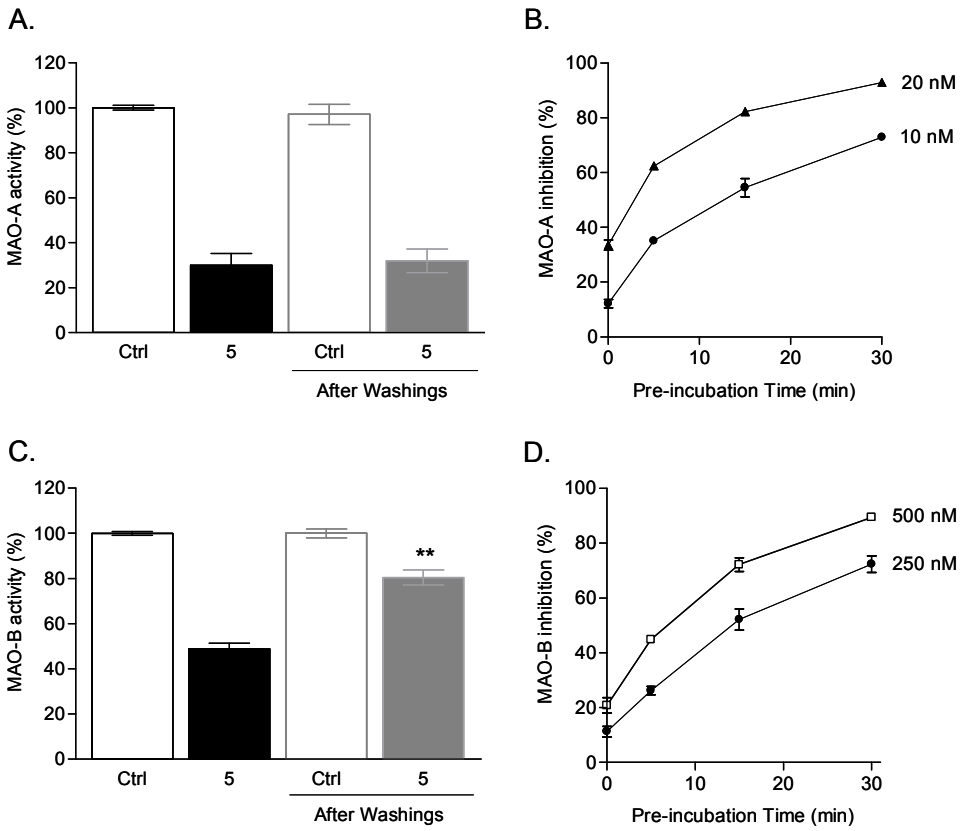

Figure 4. Reversibility studies of MAO-A and MAO-B inhibition by compound **5**. MAO-A (A) and MAO-B (C) were inhibited at 6 nM and 45 nM of **5**, respectively, for 30 minutes. Then, three consecutive washings were performed with buffer. MAO-B inhibition (C) was reverted (recovering 80.5±3.3% of enzyme activity), whereas the inhibition of MAO-A remained unaltered after washings (A). Time-dependence inhibition was studied at several times of pre-incubation (0-30 min) of MAO with compound **5**. Both MAO-A (B) and MAO-B (D) inhibition were found time-dependent. Data are mean±SEM of four independent experiments in triplicate.

To clarify the different behavior of **5** towards MAO-A and MAO-B, we further investigated the progress curves of substrate consumption for a longer period in the presence of the inhibitor. As expected, the final rate became zero in both cases, proving that the inhibition of **5** towards both MAO-A and MAO-B occurs in an irreversible process. Nevertheless, the time needed for the total inactivation of MAO-B was higher than that needed for MAO-A (Figure 5), thus showing that although irreversible, the inactivation of MAO-B by **5** is clearly slower. These findings explain the different

behavior found in the reversibility studies, which were performed pre-incubating the enzymes with **5** for 30 min. Figure 5 shows that at this time the velocity of the reaction for MAO-A was clearly decreased and thus substrate consumption was rapidly approaching to zero. In contrast, the velocity of the reaction for MAO-B shows a little reduction at 30 min pre-incubation time, thus supporting the suggestion that docking of **5** into the cavity of MAO-B is more impeded than in MAO-A, finding a slower substrate consumption, and explaining the recovery of MAO-B activity in the reversibility study.

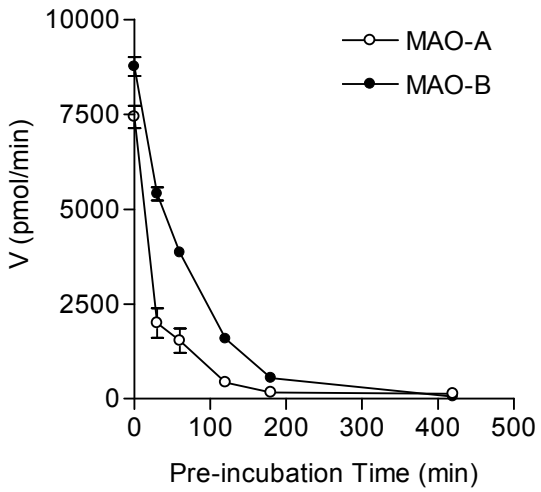

Figure 5. Progress curves of substrate consumption for MAO-A (5-HT, 100μM) and MAO-B (PEA, 20μM) in the presence of **5** (10 nM for MAO-A and 100 nM for MAO-B). MAO-A and MAO-B were pre-incubated with the inhibitor for long period (0 to 420 min) and the catalytic activity was determined. The time needed for the total inactivation of the enzyme was greater for MAO-B than for MAO-A. Data are the mean±SEM of three independent experiments in triplicate.

The kinetic behavior of **5** towards MAO-B determined from the initial rates showed that this compound behaves as a non-competitive inhibitor, as shown in the Lineweaver–Burk plot (Figure 6A). Thus, the V_{max} decreased as the amount of **5** was increased, whereas the K_M value remained constant (Figure 6B). Determination of

Michaelis constants gave a value of K_M = 6.7±0.3 μM and V_{max} = 277.8±6.1 pmol/min for MAO-B substrate, β-phenylethylamine (PEA), and an estimated K_i value of 11.0±0.39 nM.

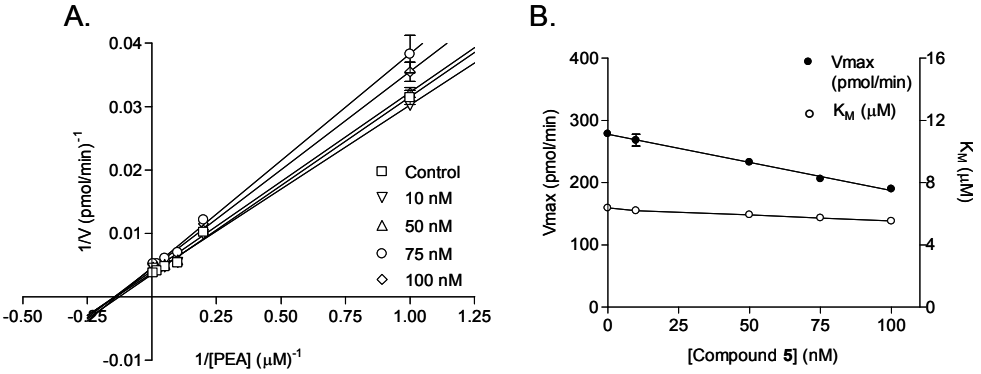

Figure 6. Kinetic study on the mechanism of MAO-B inhibition by **5**. (A) Overlaid Lineweaver–Burk reciprocal plots of MAO-B initial velocity at increasing substrate concentration (PEA, 1-200 μM) in the absence or presence of **5** (10-100 nM) are shown. Lines were derived from a weighted least-squares analysis of the data points. (B) V_{max} decreased as the amount of **5** increased, whereas the K_M value remained constant. Data are mean ± SEM of four independent experiments in triplicate.

Molecular modeling. The preceding studies point out that **5** seems to be a promising multitarget inhibitor. However, they also show up distinctive trends in the pharmacological profile. First, it is unclear why the inhibitory potency against AChE (and BuChE) is slightly affected by the length of the tether, whereas it has a large effect in the inhibition of both MAO-A and MAO-B. Moreover, reversion of the piperidine unit in compounds **5** and **8** notably affects the inhibition of both AChE and MAO. Finally, **5** leads to an irreversible inhibition of MAO-A, whereas inactivation of MAO-B is slower. To shed light into these questions, a series of docking and molecular dynamics (MD) simulations were conducted to identify the binding mode of **5** to AChE, MAO-A and MAO-B.

AChE inhibition. The binding mode of **5** to AChE was investigated by considering three structural models of the enzyme, which were built up taking advantage of the X-ray structure of donepezil bound to *Torpedo californica* AChE (*Tc*AChE; PDB entry 1EVE).[59] These models retain the structural details of the benzylpiperidine moiety bound to the AChE gorge, but differ in the orientation of Trp279 (numbering in *Tc*AChE), as the inspection of the available X-ray structures for complexes of AChE with dual site binding inhibitors reveals that Trp279 adopts three main conformations at the PAS.[60,61] Thus, the side chain of Trp279 can be characterized by dihedral angles χ_1 ($N–C_\alpha–C_\beta–C_\gamma$) and χ_2 ($C_\alpha–C_\beta–C_\gamma–C_{\delta 2}$) close to i) −60 and −80, ii) −120 and +50, and iii) −160 and −120 degrees. Representative structures of these orientations are PDB entries 1EVE, 2CKM, and 1Q83, which correspond to the AChE complexes with donepezil, *bis*(7)-tacrine[62] and *syn*-TZ2PA6,[63] respectively. In the following these models will be denoted AChE(1EVE), AChE(2CKM) and AChE(1Q83).

The binding of **5** to the three AChE models was first explored by docking calculations performed with rDock,[64,65] which yielded reliable predictions for the binding mode of known dual site binding AChE inhibitors.[60] Suitable restraints were introduced to impose the benzylpiperidine moiety to mimic the known binding mode of the same fragment of donepezil in its complex with *Tc*AChE.[59] In turn, this permits to enhance the conformational sampling of the indolyl propargylamino moiety at the PAS. Finally, the structural integrity and energetic stability of the binding mode proposed for each AChE-**5** complex were examined from the snapshots sampled in 20 ns MD simulations. For the sake of comparison, an additional 20 ns MD simulation was run for the complex between AChE and donepezil.

MD simulations yielded stable trajectories in the last 10 ns, as noted by the time evolution of the potential energy and the root-mean square deviation (RMSD) of the

protein backbone, which ranged from 1.4 to 1.6 Å (a RMSD value of 1.3 Å was obtained for the AChE-donepezil complex; see Figures S1 and S2 in Supporting Information). The RMSD of the residues that delineate the binding site in catalytic, midgorge and peripheral sites (defined as those residues with at least one atom placed at a distance less than 4 Å from the ligand) was stable for AChE-donepezil (1.4 Å) and AChE(1EVE)-**5** (1.6 Å) complexes, they being similar to the RMSD values determined for the backbone. Larger RMSD values were found for the binding site residues in AChE(2CKM) (2.0 Å) and AChE(1Q83) (1.7 Å).

No large structural alterations were found in the catalytic site, and the benzylpiperidine moiety adopts a similar arrangement in all cases (Figure 7). Little structural fluctuations were also found in the midgorge and peripheral sites for complexes AChE-donepezil and AChE(1EVE)-**5**. In particular, the indanone unit of donepezil and the indolyl ring of **5** were stacked against Trp279, whose side chain was stable along the trajectory. Thus, the torsional angles χ_1 and χ_2 showed small fluctuations around average values of -70 and -110 degrees (see Figure S3 in Supporting Information; the corresponding angles in 1EVE are -52 and -84 degrees). In contrast, larger rearrangements were found at the PAS, mainly involving Trp279, for AChE(1Q83)-**5** and AChE(2CKM)-**5**. In the former case χ_1, which was initially assigned a value close to 180 degrees (as found in 1Q83), remained stable during the first 11 ns, but then suddenly changed to a value close to -60 degrees (see Figure S3). Thus, the initial binding mode, which was chosen to mimic the orientation of *syn*-TZ2PA6 bound to *Tc*AChE, was lost and Trp279 adopted a new arrangement close to the conformation found in the AChE-donepezil and AChE(1EVE)-**5** complexes (see above and Figure 7). With regard to AChE(2CKM)-**5**, Trp279 was initially oriented as to reproduce the conformation found in the *Tc*AChE-*bis*(7)-tacrine complex

(characterized by χ_1 and χ_2 close to -120 and +50 degrees). After 3 ns, the angle χ_1 changed to 180 degrees and remained stable for 3 ns, but then changed to a new value of +60 degrees, which was stable along the rest of the trajectory (see Figure S3 in Supporting Information). Such change was accompanied by the readjustment of χ_2, which adopted a value close to +90 degrees. At the end of the simulation, a novel structure was obtained were the protonated propargylamino unit remains close to Tyr70, but has lost the interactions with Trp279 (see Figure 7).

The preceding analysis demonstrates the structural integrity of the AChE(1EVE)-**5** model, which mimics the structural features of the binding of donepezil to *Tc*AChE. The reliability of this binding mode is reinforced by the conformational change observed in the PAS of the AChE(1Q83)-**5** complex, which leads to a binding mode close to that found in AChE(1EVE)-**5**, and by the structural change found in AChE(2CKM)-**5**, which leads to a binding mode characterized by a conformation of Trp279 that, to the best of our knowledge, has no counterpart in the available X-ray structures of AChE complexes deposited in the PDB. As a further test, we have determined the relative binding affinity between models AChE(1EVE)-**5** and AChE(2CKM)-**5** by means of MM/PBSA calculations. They were performed for 100 snapshots taken evenly during the last 5 ns of the trajectories using both the standard radii implemented in the AMBER force field and an alternative set of atomic radii that have been explicitly optimized for their use in MM/PBSA calculations with AMBER.[66] The results (see Table S1 in Supporting Information) indicate that binding of **5** to AChE(1EVE) is favored by near 2.3 (standard radii) and 4.0 (optimized radii) kcal/mol relative to AChE(2CKM). Similar trends were observed when MM/PBSA computations were performed by retaining a single water molecule which was hydrogen-bonded to the

protonated nitrogen of the piperidine unit of the ligand along the trajectories (data not shown).

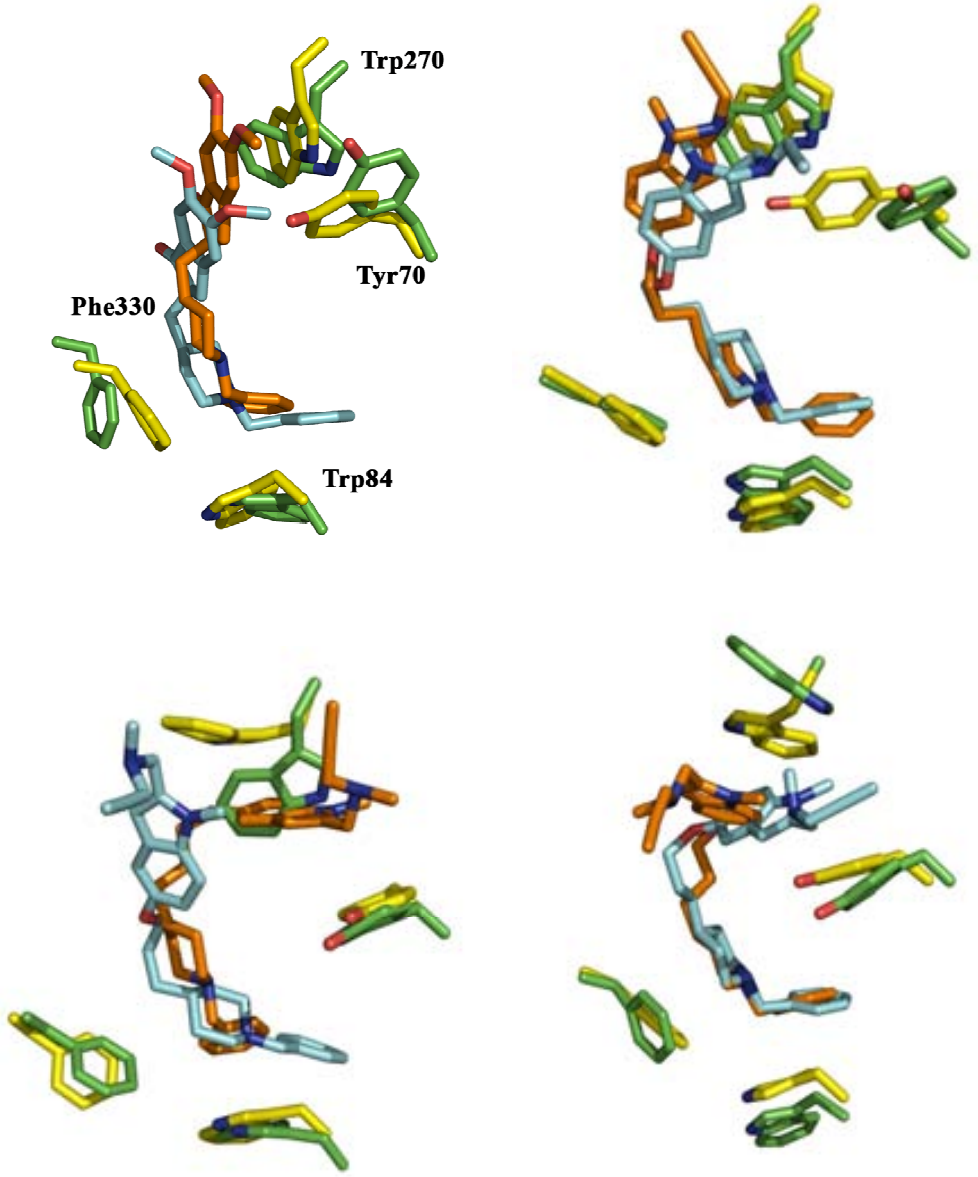

Figure 7. Representation of the binding mode of donepezil and **5** at the beginning and end of the MD simulations: (*top-left*) AChE-donepezil, (*top-right*) AChE(1EVE)-**5**, (*bottom-left*) AChE(1Q83)-**5**, (*bottom-right*) AChE(2CKM)-**5**. Relevant residues at the catalytic (Trp84, Phe330) and peripheral (Trp279, Tyr70) binding sites are also shown. The ligand/residues at the end of the simulations are shown in blue/green, respectively (the representation at the begining of the simulation is made in orange/yellow).

The preceding structural and energetic analysis suggests that compound **5** mimics the binding mode of donepezil (see Figure S4). Thus, the benzylpiperidine

moieties of donepezil and **5** exhibit a similar alignment in the CAS, though there is a weaker overlap between the benzene unit of **5** and the indole ring of Trp84. More importantly, there is a change in the orientation of residues Tyr334 and Asp72, which remain hydrogen-bonded, but are displaced toward the PAS. In turn, this structural change facilitates the stacking of the indole ring of **5** between the aromatic rings of Tyr334 and Trp279. On the other hand, there is a water molecule that bridges the protonated nitrogen of the piperidine unit with the hydroxyl groups of Tyr121 and Ser122 (not shown in Figure 8 for the sake of clarity). Finally, the largest structural flexibility of the inhibitor is localized in the propargylamino unit, which forms transient van der Waals interactions with the benzene ring of Tyr70.

This binding mode allows us to rationalize the low sensitivity of the inhibitory activity on the length of the tether, as i) it is reasonable to expect that the benzylpiperidine moiety will fill the same binding pocket, but ii) shortening or lengthening of the tether will be accompanied by displacements of the indole ring of **5** along the gorge that would increase the stacking against Tyr334 or Trp279 (see Figure S5 in Supporting Information). On the other, the lower inhibitory potency associated with reversion of the piperidine unit (compounds **5** and **8**) can be explained by two factors: i) the lost of the water-assisted hydrogen bonds formed between the protonated nitrogen and Tyr121 and Ser122 (data not shown), and ii) the weakening of the electrostatic stabilization due to cation-pi interactions with the aromatic rings of Phe330 and Trp84, and with the negative charges of Asp72 and Glu198 (see Figure S6).

As a final test, we explored the suitability of an alternative binding mode where the orientation of **5** was reverted, so that the propargylamino group fills the CAS, and the benzylpiperidine moiety occupies the PAS. As in the preceding discussion, compound **5** was docked in the binding site of the enzyme for the three AChE structural

models (1EVE, 1Q83 and 2CKM), but without imposing positional restraints. Inspection of the first ranked poses showed a preference for the placement of the benzylpiperidine moiety in the CAS. Thus, only 1, 7 and 2 poses out of the first 13, 15 and 7 ranked solutions (covering a range of 8 kcal/mol in the score in each case) corresponded to the reverted orientation of **5** upon docking to models AChE_1EVE, AChE_1Q83 and AChE_2CKM, respectively, which reinforces the reliability of the binding mode discussed above. To further explore the suitability of the inverted binding mode, a series of 20 ns MD simulation were run for the three AChE complexes with the reversed orientation of the inhibitor. Inspection of the binding mode sampled along the last 10 ns of the trajectory run for AChE_1EVE (Figure S7) shows that the propargylamino unit remains stacked onto the indole ring of Trp84, filling part of the region occupied by the benzyl moiety of donepezil. However, there are notable structural fluctuations of the methylated indole ring of **5**, which eventually leads to steric clashes with the benzene ring of Phe330. Similarly, the large fluctuations of the benzylpiperidine moiety also argue against a firm stacking with Trp279 at the PAS. The structural instability of the ligand was also found in the simulations run for AChE_1Q83 and AChE_2CKM (see Figure S7), particularly seen in the large mobility of the ligand at the PAS, which affects the stacking between Trp279 and Tyr70. In fact, comparison of the relative free energies determined from MM/PBSA calculations for the different AChE complexes also supports the energetic destabilization of the inverted binding mode (see Table S2). Finally, let us remark that the enhanced flexibility of the piperidine moiety in the PAS, which reflects the lack of strong interactions, does not provide a straightforward explanation to the significant reduction in the inhibitory potency found upon reversion of the ring (compare **5** and **8** in Table 1).

BuChE inhibition. The binding mode of **5** to BuChE was explored by means of docking calculations (see Methods). The results indicate a marked preference for the insertion of the benzylpiperidine moiety in the CAS, as noted in the fact that only 4 out of the first 20 ranked poses (comprising a range of 5 kcal/mol in the score) were found with the inverted arrangement (in fact, the first inverted pose was ranked as the 9th solution). Hence, a new docking calculation was run imposing the benzene unit of **5** to stack against Trp79 (equivalent to Trp84 in the CAS of AChE), thus mimicking the interaction found in the AChE complex with donepezil (PDB entry 1EVE). Even in this case, the results indicate a substantial degree of flexibility to accommodate **5** in the binding site of BuChE, especially regarding the indolylpropargylamine moiety, but also even the piperidine ring (see Figure S8). Nevertheless, this finding is not unexpected due to the wider volume of the binding site in BuChE compared to AChE, which can be ascribed to mutations between specific binding site residues in the two enzymes, such as the replacement of Phe330 in the CAS of AChE by Ala, the substitution of Tyr70 and Phe290 at the midgorge of AChE by Asn and Val, respectively, and the mutation of Trp279 in the PAS of AChE by Ala. Accordingly, it can be expected that the binding of **5** to BuChE will be mainly guided by the interactions due to the benzylpiperidine moiety, thus explaining the lack of large differences in the selectivity between the two enzymes.

MAO inhibition. The binding mode of hybrid **5** in MAO-A and MAO-B was investigated in order to explain the different inhibitory behavior found for the two isoforms. To this end, we first explored the potential binding mode of **5** by means of docking calculations, which showed a clear preference to accommodate the indolyl propargylamino unit in the substrate cavity. In fact, this is not surprising as the reference compound **2** was found to be an irreversible inhibitor of the two MAO

isoforms, which indicates that the binding mode places the propargylamino unit properly oriented to react with the flavin adenine dinucleotide (FAD) present in the substrate cavity of both MAO-A and MAO-B.[43] Then, a representative member of the most populated cluster of the docked poses was chosen as starting structure for MD simulations of the complexes of **5** with MAO-A and MAO-B. In the two cases MD simulations yielded stable trajectories, as noted by inspection of the time evolution of the potential energy, and by the small fluctuations of the RMSD profile along the last 5 ns of the trajectories (see Figures S7 and S8). Thus, the RMSD determined for the protein backbone in the MD simulations run for MAO-A and MAO-B is close to 1.4 Å, whereas the RMSD determined for the residues that define the walls of the binding cavity amounts to 2.0 Å.

Inspection of Figure 8 clearly shows that binding of **5** to MAO-A has little effect on the residues that delineate the binding site, suggesting a suitable fit of the indolyl propargylamino unit in the substrate cavity. In fact, the indole fragment of **5** matches well the corresponding moiety in harmine, as noted upon superposition of the X-ray structure of the human MAO-A-harmine complex[67] and the last snapshot of the MD simulation (see Figure S9). The only exception to the structural integrity of the binding pocket concerns few residues located at the entrance of the gorge leading to the substrate cavity, which reflects the adjustment of the ligand, as expected from the larger flexibility of the solvent-exposed loops that shape the entrance cavity (see Figure S9). It is worth noting how the tether fills the hydrophobic region that defines the bottleneck of the binding pocket, which is mainly due to Phe208 and Ile325. The dependence of the inhibitory potency with the length of the tether can be explained by the steric contrains imposed by the side chains of vicinal apolar residues, such as Leu97, Leu337, Val210 and Cys323, as shortening of the tether would lead to steric clashes with the piperidine

unit of the ligand. On the other hand, simulations also show that the positive charge of the piperidine unit in **5** is stabilized by water-mediated hydrogen bond interactions with the backbone carbonyl groups of Arg109 and Gly110.

Figure 8. Representation of the binding mode of 5 in (top) MAO-A and (bottom) MAO-B. Five snapshots taken every ns along the last 5 ns of the trajectory are superposed. The ligand is shown as orange sticks, FAD as blue sticks, and selected residues in the entrance and substrate cavities as green sticks.

The structural integrity of the binding mode of **5** in MAO-B is also supported by inspection of the snapshots collected at the end of the trajectory (Figure 8). The five-membered ring of the indole moiety of **5** superposes the benzene ring of deprenyl in its complex with human MAO-B (PDB entry 2BYB;[67] see Figure S10). As in MAO-A, the tether occupies the hydrophobic region delineated by residues Ile199, Ile316, Tyr326 and Leu88, which presumably would lead to steric clases with the piperidine ring upon

shortening of the methylenic chain of the inhibitor. Finally, besides water-mediated contacts with the carbonyl groups of Arg100 and Gly101, the positive charge of the piperidine unit in **5** appears to be stabilized by the carboxylate group of Glu84.

As noted above, treatment of MAO-A with **5** leads to a significant inactivation of the enzyme, which remains unaltered after repeated washings. In contrast, a significant recovery of MAO-B activity is found after washings due to a slower inactivation of this isoform. This different behavior suggest that the propargylamino moiety of **5** in MAO-A is better oriented for chemical modification of FAD than in MAO-B. Nevertheless, since both ligand and FAD are treated classically in MD simulations, the electronic effects that promote the chemical inactivation of the enzyme by the propargyl moiety are not properly accounted for. Therefore, we have compared the relative orientation of **5** obtained from MD simulations with the orientation found for deprenyl, rasagiline and its ((ethyl(methyl)amino)carbonyl)oxy derivative (PDB entries 2BYB, 1S2Q and 2C65)[67-69] paying attention to the relative positioning of the carbon atom attached to the protonated amine of **5** relative to the nitrogen atom of FAD involved in chemical modification by the irreversible inhibitors. Inspection of Figure 9 shows that in MAO-A places the carbon atom is slightly closer to the FAD nitrogen atom than in MAO-B. Thus, the distance between those atoms (averaged over the snapshots sampled in the last 5 ns) amounts to 6.8±0.3 Å in MAO-A, and to 7.7±0.4 Å in MAO-B (see Figure S10). The larger separation found in MAO-B agrees with the lower degree of enzyme inactivation found upon incubation with **5**.

To further check this assumption, we have run additional simulations forcing the nitrogen atom of the propargyl amino group to occupy the position and orientation relative to FAD found for the corresponding atom in deprenyl, rasagiline and its ((ethyl(methyl)amino)carbonyl)oxy derivative. To this end, restrained simulations (1ns)

have been run by triplicate for each enzyme, and then we have determined the difference in the interaction energy (from MM/PBSA calculations) between the inhibitor and the enzyme. In order to avoid artefactual results arising from steric clashes of the propargyl amino group with binding site residues while steering the nitrogen atom, the propargyl group has been replaced by a methyl group. The MM/PBSA results indicate that the interaction energy in MAO-A becomes more negative (relative to the initial state) by around 7 kcal/mol, whereas it is destabilized by around 6 kcal/mol in MAO-B. Therefore, from a qualitative point of view, these results reinforce the notion that adoption of a reactive configuration of **5** in MAO-B is more impeded than in MAO-A, which explains the different rate of enzyme inactivation.

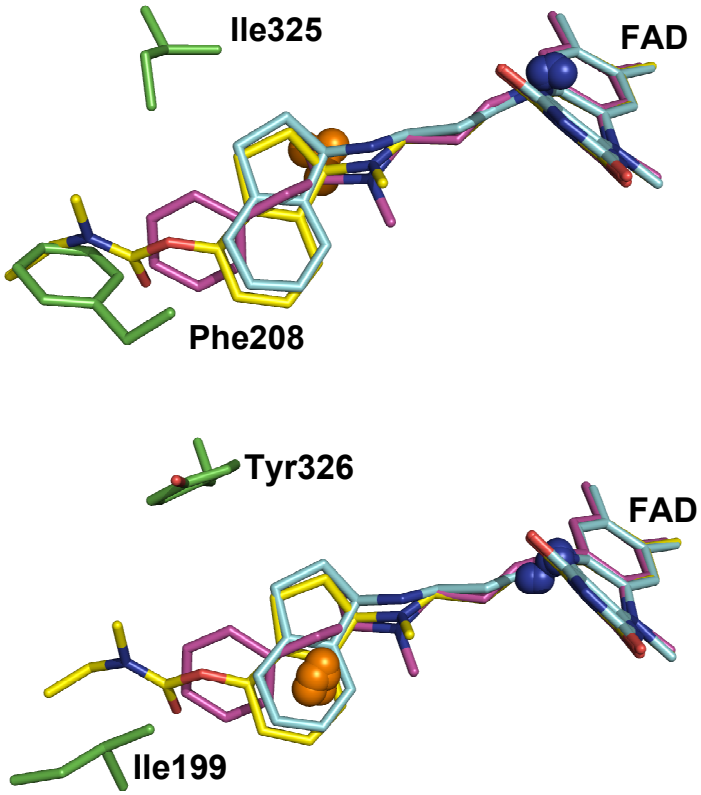

Figure 9. Superposition of the X-ray crystallographic structures of MAO-B complexes with deprenyl, rasagiline and its ((ethyl(methyl)amino)carbonyl)oxy derivative (shown as blue, magenta and yellow sticks, respectively). The spheres show the position of the carbon atom that bears the protonated amine of **5** (orange), and the chemically modified nitrogen atom of FAD (blue). Representation includes the positions of those atoms in

snapshots taken every ns along the last 5 ns of the trajectory run for (*top*) MAO-A and (*bottom*) MAO-B.

Inspection of Figure 9 also reveals that the different inhibitory profile found for **5** can be mainly ascribed to the residues that define the bottleneck in the gorge that leads to the substrate binding site. In particular, the replacement of Ile199 in MAO-B by Phe208 in MAO-A pushes the inhibitor toward the FAD, whereas the replacement of Ile325 in MAO-A by Tyr326 in MAO-B triggers the opposite effect. In this context, though the methylenic (n=2) tether designed for **5** seems well suited to fit the gorge in the two isoforms, the spatial constraints imposed to the orientation of the indole ring upon binding to MAO-B leads to a less effective chemical interaction with the FAD. In turn, these findings suggest that extension of the ((methyl)amino)propargylamino unit in **5** could be a useful strategy to enhance the inactivation of MAO-B, while reducing the inhibition at MAO-A. This strategy could be beneficial to minimize side effects related to the potentiation of the cardiovascular effect of tyramine (the so-called "cheese effect"), a limited side effect of older generation of non-selective MAO inhibitors.

Inhibition of Aβ self-aggregation and AChE-induced aggregation. A number of dual binding site AChE inhibitors have been found to exhibit a significant inhibitory activity on Aβ self-aggregation.[60,70-74] Thus, compound **5** was also tested for its ability to inhibit the self-induced $A\beta_{1-42}$ aggregation and the AChE-induced $A\beta_{1-42}$ aggregation. In the former case a 47.8±2.1% inhibition was found when compound **5** was tested at 10 μM concentration (Table 3) (Aβ/inhibitor=4/1). We used propidium iodide (PI) as reference compound and we obtained a reduction of Aβ self-induced aggregation of 33.3±2.1%, this value being significantly lower than that found for **5**. When PI was tested at equimolar concentrations (Aβ/PI=1/1), similarly to that previously reported by other

groups, we found a reduction of Aβ aggregation of 78.6±3.8%. This effect is significantly higher than that reported for donepezil (<5%) under similar experimental conditions[72] and similar to that found for other IAChE.[60,71,72] Then, **5** can be considered a moderate inhibitor of $A\beta_{1-42}$ self-induced aggregation. Regarding the inhibition of the human AChE-dependent $A\beta_{1-40}$ aggregation, the results indicate that **5** at 100 μM concentration was able to prevent hAChE-induced $A\beta_{1-40}$ aggregation in a 32.4 ± 7.0 % (Table 3). This value is similar to the inhibition elicited by donepezil (22%) and significantly higher than that found for tacrine (7%), two of the first FDA-approved drugs for the treatment of AD. However, it is significantly lower than that of propidium[75] and other IAChE previously described,[70-72] which show potencies in the low micromolar range.

Table 3. Inhibition of AChE-induced $A\beta_{1-40}$ aggregation and $A\beta_{1-42}$ self-induced aggregation by compound **5**.

	% inhibition of Aβ aggregation ± SEM	
Compound	AChE-induced[a]	Self-induced[b]
5	32.4 ± 7.0	47.8 ± 2.1

[a]Inhibition of AChE-induced Aβ (1-40) aggregation. The concentration of **5** and Aβ (1-40) was 100μM and 40μM, respectively. The ratio Aβ/AChE was equal to 100/1. [b]Inhibition of self-induced Aβ (1-42) aggregation (40μM) produced by **5** at 10μM. Data are the mean ± SEM of at least three independent experiments.

Conclusions

A new series of hybrid compounds containing the benzyl piperidine moiety of donepezil and the indolyl propargylamino moiety of *N*-[(5-benzyloxy-1-methyl-1*H*-indol-2-yl)methyl]-*N*-methylprop-2-yn-1-amine have been investigated as novel

multitarget agents against AChE, BuChE and MAO (A/B). These new compounds have been designed to simultaneously interact with the active, peripheral and mid-gorge binding sites of AChE, as well as to occupy the substrate binding site in MAO.

The length of the tether that connects the two main structural fragments of the novel hybrids has a relevant effect on the binding to MAO, whereas it seems to have little impact on the inhibitory activity against AChE and BuChE. Among these hybrid compounds, **5** is the most potent IMAO, even more than the parent compounds. Surprisingly, although donepezil (**1**) is a slight inhibitor of BuChE and **2** is not even active, the ability of **5** to inhibit BuChE is found on the submicromolar range. This is particularly important in view of the renewed interest in dual cholinergic inhibitors as therapeutic agents for AD.[58] Normally, AChE predominates in the brain, while BuChE activity levels are low. However, in AD the relative enzymatic activity is altered such that BuChE increases while AChE decreases.[76,77] Then, if the therapeutic goal is to increase ACh levels in the brain, a compound able to inhibit both AChE and BuChE would be valuable to elicit a larger protective response. In addition, the inhibition of MAO-B by **5** might be beneficial for modulating the cholinergic neurotransmission and for restoring the serotoninergic neurotransmission. Moreover, the potent MAO-A inhibition enables the drug to exert an antidepressant activity like that of amitriptyline and moclobemide, two triciclic antidepressants primarily used to treat depression. Compound **5** also presents a significant inhibitory profile of Aβ-self induced and human AChE-dependent aggregation, being more potent (human AChE-dependent) or similar (self-induced) than the parent compound donepezil (**1**). Overall, the present data indicate that **5** is not only an interesting lead compound for the design of novel MTDL with a good IMAO/IAChE inhibitory potency and a significant activity against amyloid

formation and aggregation, but also that itself may have a potential disease-modifying role in the treatment of AD.

Experimental Part

General Methods. Melting points were determined in a Koffler apparatus, and are uncorrected. ^{1}H NMR and ^{13}C NMR spectra were recorded at room temperature in $CDCl_3$ or DMSO-d_6 at 300, 400 or 500 MHz and at 75.4, 100.6 or 125.6 MHz, respectively, using solvent peaks [$CDCl_3$: 7.27 (*D*), 77.2 (*C*) ppm and DMSO-d_6 2.50 (D) and 39.7 (C) ppm] as internal references. The assignment of chemical shifts is based on standard NMR experiments (^{1}H, ^{13}C, ^{1}H-^{1}H COSY, ^{1}H-^{13}C HSQC, HMBC, DEPT). Mass spectra were recorded on a GC/MS spectrometer with an API-ES ionization source. Tlc analyses were performed on silica F254 and detection by UV light at 254 nm, or by spraying with phosphomolybdic-H_2SO_4 dyeing reagent. Column chromatographies were performed on silica Gel 60 (230 mesh). "Chromatotron" separations were performed on a Harrison Research Model 7924. The circular disks were coated with Kieselgel 60 PF254 (E. Merck). The chlorydrate salts were prepared by solubilising the compound in a minimum of ether and a solution of ether saturated with HCl(*g*) was added dropwise. A white solid was formed immediately. The precipitated hydrochloride was separated by filtration, washer with ether and dried. The purity ($\geq$ 95%) of the samples has been determined by elemental analysis, carried out at the IQOG (CSIC, Spain).

Methyl 4-(piperidin-4-yl)butanoate (17)[55] A solution of (*E*)-ethyl 3-(pyridin-4-yl)acrylate **16**[52] (1.52 g, 8.58 mmol) in EtOH (20 mL) and 4N HCl in 1,4-dioxane (2 mL) was hydrogenated under Pd/C 10% (0.152 g) and PtO_2 (152 mg), overnight at

room temperature. Then, the catalyst was filtered off, washed with MeOH, and the filtrate was concentrated. The residual solid was triturated with Et_2O, filtered, washed with Et_2O, and dried to give known methyl ester **17** (1.60 g, 90%) as a solid: ^{1}H NMR (300MHz, DMSO-d_6) δ 9.29–9.10 (br, 2H), 3.55 (s, 3H, CO_2CH_3), 3.16–3.12 (m, 2H), 2.78–2.67 (m, 2H), 2.31-2.27 (m, 2H), 1.73–1.69 (m, 2H), 1.46–1.21 (m, 5H); MS (ES) m/z 172 $[M+H]^+$.

1-Benzyl-4-piperidinepropanol (19).[56] To a solution of methyl 4-(piperidin-4-yl)butanoate **17**[55] (1.60 g, 7.21 mmol) and benzyl bromide (1.85 g, 10.82 mmol) in 20 mL of CH_2Cl_2 was added triethylamine (3.3 mL, 21.65 mmol), while the internal temperature in the reaction was below 20 ºC by cooling with an ice-water bath. The reaction was stirred at room temperature overnight. After complete reaction (tlc analysis), the reaction was concentrated and purified by column chromatography to give methyl 3-(1-benzylpiperidin-4-yl)propanoate (**18**) [(1.41 g, 75%): oil; ^{1}H NMR (300 MHz, $CDCl_3$) δ 7.35−7.23 (m, 5H), 3.66 (s, 3H, CO_2CH_3), 3.51 (s, 2H, CH_2-Ph), 2.89 (br d, J= 11.5 Hz, 2H), 2.32 (br t, J = 7.5 Hz, 2H, CH_2-CO_2CH_3), 1.94 (t, J= 10.9 Hz, 2H), 1.66−1.54 (m, 4H), 1.34 – 1.21 (m, 3H, CH+CH_2); MS (EI) *m/z* (%): 91 (100) $[PhCH_2]^+$, 188 (66) $[M– CH_2CH_2CO_2Me]^+$, 202 (13) $[M–CO_2Mt]^+$, 230 (19) $[M-OMe]^+$, 246 (9) $[M-CH_3]^+$, 260 (73) $[M-H]^+$, 261 (50) $[M]^+$], which was used in the next reaction without further analysis.

To a suspension of LAH (0.176 g, 4.66 mmol, 2 equiv) in dry THF (10 mL) was added methyl 3-(1-benzylpiperidin-4-yl)propanoate (**18**) (0.61 g, 2.33 mmol, 1 equiv) in dry THF (10 mL), at 0 °C. The mixture was refluxed for 2 h, and after cooling unreacted $LiAlH_4$ was quenched by careful addition of 10% NaOH solution (20 mL). The solution was filtered and washed with H_2O and EtOAc. The filtrate was extracted with EtOAc, and the combined organic layers, dried over Na_2SO_4, were concentrated to give known

compound **19**[56] (0.535 g, 98%): oil; ^{1}H NMR (300 MHz, $CDCl_3$) δ 7.32-7.20 (m, 5H), 3.60 (t, *J*= 6.4 Hz, 2H, CH_2O), 3.48 (s, 2H, CH_2Ph), 2.87 (br d, *J*= 11.5 Hz, 2H), 1.92 (br d, *J*= 11.1 Hz, 2H), 1.68-1.60 (m, 2H), 1.61-1.49 (m, 2H), 1.30-1.15 (m, 5H); MS (EI) *m/z* (%): 91 (100) $[PhCH_2]^+$, 142 (26) $[M–CH_2Ph]^+$, 156 (17) $[M-Ph]^+$, 174 (8) $[M-(CH_2)_3OH]^+$, 188 (18) $[M-(CH_2)_2OH]^+$, 202 (14) $[M-CH_2OH]^+$, 232 (37) $[M- H]^+$, 233 (20) $[M]^+$.

1-Benzyl-4-(3-chloropropyl)piperidine (12). To a solution of 1-benzyl-4-piperidinepropanol (**19**)[56] (0.53 g, 2.27 mmol) in CH_2Cl_2 (5 mL), $SOCl_2$ (0.66 mL, 9.08 mmol, 4 equiv) was added dropwise with ice cooling. The mixture was refluxed for 3 h and then evaporated. The residue was rendered alkaline with 10% K_2CO_3 solution and extracted with CH_2Cl_2. The organic layer, dried over Na_2SO_4, was evaporated under reduce pressure to give compound **12** (0.582 g, 99%): oil; IR 3027, 2923, 2849, 2800, 2756, 1672, 1493, 1452, 1366, 1342, 1263, 738, 698 cm^{-1}; ^{1}H NMR (400 MHz, CDCl3) *δ* 7.22−7.36 (m, 5H), 3.51 (t, *J*= 8.0 Hz, 2H, CH_2Cl), 3.51 (s, 2H, CH_2Ph), 2.89 (br d, *J*= 11.5 Hz, 2H), 1.95 (br t, *J*= 11.0 Hz, 2H), 1.78 (dt, *J* = 11.9 and 6.9 Hz, 2H, CH_2-CH_2Cl), 1.65 (br d, *J*= 11.4 Hz, 2H), 1.32−1.42 (m, 2H), 1.21-1.30 [m, 3H, CH+CH_2-$(CH_2)_2Cl$]; ^{13}C NMR (100 MHz, $CDCl_3$) δ 138.1 (C-Ph), 129.1 (2xCH-Ph), 128.0 (2xCH-Ph), 126.8 (CH-Ph), 63.3 (CH_2-Ph), 53.6 (2CH_2-piperidine), 45.2 (CH_2Cl), 35.1 (CH), 33.6 [CH_2-$(CH_2)_2Cl$], 32.1 (2CH_2-pieridine), 29.9 (CH_2, CH_2-CH_2Cl); MS (EI) *m/z* (%): 91 (100) $[PhCH_2]^+$, 160 (23) $[M-Bn]^+$, 174 (27) $[M-(CH_2)_3Cl]^+$, 188 (17) $[M-(CH_2)_2Cl]^+$, 202 (9) $[M-CH_2 Cl]^+$, 216 (88) $[M-Cl]^+$, 250 (35) $[M-1]^+$. Anal. Calcd for $C_{15}H_{22}ClN$: C, 71.55; H, 8.81; N, 5.56. Found C, 71.84; H, 9.02; N, 5.83.

1-Benzyl-4-(4-chlorobutyl)piperidine (13). To a solution of 1-benzyl-4-(4-hydroxybutyl)piperidine (**24**)[57] (0.508 g, 2.05 mmol) in CH_2Cl_2 (5 mL), $SOCl_2$ (0.6 mL, 8.214 mmol, 4 equiv) was added dropwise, with ice cooling. The mixture was refluxed

for 2 h and then evaporated. The residue was rendered alkaline with 10% K_2CO_3 solution and extracted with CH_2Cl_2. The organic layer, dried over Na_2SO_4, was evaporated under reduce pressure to give compound **13** (0.54 g, 99%) as yellow oil: IR 3062, 3027, 2921, 2847, 2799, 2757, 1493, 1454, 1366, 1341, 1311, 1287, 1126, 1073, 1029, 979, 737, 698 cm^{-1}; ^1H NMR (300 MHz, $CDCl_3$) δ 7.34-7.21 (m, 5H), 3.53 (t, *J*= 6.7 Hz, 2H, CH_2Cl), 3.50 (s, 2H, CH_2Ph), 2.88 (br d, *J*= 11.4 Hz, 2H), 1.93 (br t, *J*= 11.9 Hz, 2H), 1.75 (tt, *J*= 8 Hz, 2H, CH_2-CH_2Cl), 1.70-1.59 (m, 2H), 1.49−1.37 (m, 2H), 130-1.20 (m, 5H); ^{13}C NMR (100 MHz, $CDCl_3$) δ 32.2 (2CH_2), 32.7 (CH_2, CH_2-CH_2Cl), 32.8 (CH_2), 36.2 (CH_2), 45.0 (CH_2Cl), 53.8 (2CH_2), 63.4 (CH_2-Ph), 126.8 (CH-Ph), 128.0 (2xCH-Ph), 129.1 (2xCH-Ph), 138.3 (C-Ph); MS (EI) *m/z* (%): 91 (100) $[PhCH_2]^+$, 174 (42) $[M-(CH_2)_4Cl]^+$, 188 (43) $[M-(CH_2)_3Cl]^+$, 202 (16) $[M-(CH_2)_2Cl]^+$, 216 (8) $[M-CH_2Cl]^+$, 230 (28) $[M-Cl]^+$, 264 (45) $[M]^+$. HRMS (ES+): Exact Mass: calcd for $C_{16}H_{25}ClN$ $(M+H)^+$: 266,1676. Found *m/z* 266.1687.

***N*-((5-((1-Benzylpiperidin-4-yl)methoxy)-1-methyl-1*H*-indol-2-yl)methyl)-*N*-methylprop-2-yn-1-amine (3).** To a solution of 1-methyl-2-{[ethyl(prop-2-yn-1-yl)amino]ethyl}-1*H*-indol-5-ol **4**[52] (0.21 g, 0.94 mmol) and 1-benzyl-4-(chloromethyl)piperidine **10**[27] (0.33 g, 1.51 mmol, 1.5 equiv) in acetonitrile (5 mL), NaH (120 mg, 3 mmol, 3 equiv, 60% mineral oil) was added. The reaction mixture was stirred at 50 ºC for 10 h. After complete reaction (tlc analysis), the reaction was concentrated, diluted with water, and extracted with CH_2Cl_2. The organic phase was washed with brine, dried ($MgSO_4$), and evaporated. The crude product was purified by flash chromatography (CH_2Cl_2/MeOH, 100:1) to give compound **3** (126.3 mg, 32%) as white solid: R*f*= 0.24 (CH_2Cl_2/MeOH, 10/1); mp 123-5 ºC; IR (KBr) ν 3252, 2938, 2913, 1620, 1489, 1466, 1195, 1163, 1029, 1008 cm^{-1}; ^1H NMR (400 MHz, $CDCl_3$) δ 7.35-7.24 (m, 5H), 7.18 (d, *J*= 8.8 Hz, 1H, CH7-indole), 7.04 (d, *J*= 2.3 Hz, 1H, CH4-

indole), 6.86 (dd, *J*= 8.8 and 2.3 Hz, 1H, CH6-indole), 6.34 (s, 1H, CH3-indole), 3.85 (d, *J*= 6.0 Hz, 2H, -CH_2O-), 3.73 (s, 3H, N-CH_3), 3.68 (s, 2H, indole-CH_2-N), 3.53 (s, 2H, CH_2-Ph), 3.31 (d, 2H, *J*= 2.2 Hz, CH_2-C≡CH), 2.95 (d, *J*= 11.4 Hz, 2H), 2.35 (s, 3H, N-CH_3), 2.30 (t, *J*= 2.2 Hz, C≡CH), 2.02 (t, *J*= 16, 2H), 1.91-1.81 (m, 3H), 1.49-1.39 (m, 2H); ^{13}C NMR (100 MHz, $CDCl_3$) δ 153.3 (C5-indole), 138.3 (C1'-Ph), 137.8 (C2-indole), 133.3 (C7a-indole), 129.1 (2xCH-Ph), 128.1 (2xCH-Ph), 127.5 (C3a-indole), 126.8 (CH4'-Ph), 111.9 (CH6-indole), 109.5 (CH7-indole), 103.3 (CH4-indole), 102.0 (CH3-indole), 78.4 (-C≡), 73.6 (CH_2-O), 73.4 (≡CH), 63.4 (CH_2-Ph), 54.0 (2xCH_2), 63.4 (Ph-CH_2), 53.4 (2 x CH_2), 51.7 (Ind-CH_2-N), 44.6 (CH_2-C≡), 41.5 (N-CH_3), 35.9 (CH-piperidine), 29.8 (N-CH_3), 29.1 (2xCH_2); MS (EI) *m/z* (%): 416 (100) $[M+H]^+$, 438 (2) $[M+Na]^+$. 3.2HCl: white powder; mp 230-3 ºC; IR (KBr) ν 3423, 3200, 2933, 2511, 1620, 1486, 1466, 1208 cm^{-1}; ^{1}H NMR (300 MHz, D_2O) δ 7.34-7.25 (m, 6H, CH7-indole + 5H-Ph), 7.05 (d, *J* = 2.2 Hz, 1H, CH4-indole), 6.85 (dd, *J* = 9.0, 2.2 Hz, 1H, CH6-indole), 6.59 (s, 1H, CH3-indole), 4.47 (s, 2H, CH_2), 4.11 (s, 2H, CH_2), 3.86 (d, *J* = 2.4 Hz, 2H, CH_2-C≡CH), 3.79 (t, *J* = 6.0 Hz, 2H, O-CH_2-), 3.59 (s, 3H, indole-CH_3), 3.38 (d, *J* = 12.8 Hz, 2H, CH_2), 2.97 (t, *J* = 2.3 Hz, 1H, C≡CH), 2.85 (t, *J* = 12.7 Hz, 2H, CH_2), 2.76 (s, 3H, N-CH_3), 1.98 (d, *J* = 12.8 Hz, 2H, CH_2), 1.89-1.83 (m, 1H, CH), 1.48-1.34 (m, 2H, CH_2). Anal. Calcd. for $C_{27}H_{35}Cl_2N_3O$: C, 66.39; H, 7.22; Cl, 14.52; N, 8.60. Found: C, 66.21; H, 7.43; Cl, 14.42; N, 8.63.

***N*-{[5-(2-(1-Benzylpiperidin-4-yl)ethoxy)-1-methyl-1*H*-indol-2-yl]methyl}-*N*-methylprop-2-yn-1-amine (4).** To a solution of 1-methyl-2-{[ethyl(prop-2-yn-1-yl)amino]ethyl}-1*H*-indol-5-ol **14**[52] (160 mg, 0.7 mmol) and 1-benzyl-4-(2-chloroethyl)piperidine **11**[53] (0.25 g, 1.05 mmol, 1.5 equiv) in DMF (5 mL), NaH (84 mg, 2.1 mmol, 3 equiv, 60% mineral oil) was added. The reaction mixture was stirred at room temperature for 3 h. After complete reaction, the solvent was removed, and the

crude diluted with water, and extracted with CH_2Cl_2. The organic phase was washed with brine, dried ($MgSO_4$), and evaporated at reduced pressure. The crude product was purified by flash chromatography (CH_2Cl_2/MeOH, 100:1) to give compound **4** (0.216 g, 72%) as a white solid: R*f*= 0.27 (CH_2Cl_2/MeOH, 10/1); mp 86-7 ºC; IR (KBr) ν 3275, 2941, 2921, 2876, 2807, 2782, 2768, 1619, 1488, 1473, 1289, 1250, 1207, 1161, 1030 cm^{-1}; ^1H NMR (400 MHz, $CDCl_3$) δ 7.34-7.23 (m, 5H), 7.18 (d, *J*= 8.8 Hz, 1H, CH7-indole), 7.03 (d, *J*= 2.4 Hz, 1H, CH4-indole), 6.85 (dd, *J*= 8.8 and 2.4 Hz, 1H, CH6-indole), 6.33 (s, 1H, CH3-indole), 4. 03 (t, *J*= 6.5 Hz, 2H, O-CH_2-), 3.74 (s, 3H, N-CH_3), 3.67 (s, 2H, N-CH_2), 3.52 (s, 2H, CH_2-Ph), 3.31 (d, 2H, *J*= 2.3 Hz, CH_2-C≡CH), 2.91 (d, *J*= 11.6 Hz, 2H), 2.34 (s, 3H, N-CH_3), 2.29 (t, *J*= 2.3 Hz, C≡CH), 2.0 (t, *J*= 10.8, 2H), 1.77-1.72 (m, 4H), 1.41-1.31 (m, 2H), 1.62-1.52 (m, CH); ^{13}C NMR (100 MHz, $CDCl_3$) δ 153.5 (C5-indole), 138.4 (C-Ph), 133.6 (C-indole), 137.2 (C-indole), 129.5 (2xCH-Ph), 128.3 (2xCH-Ph), 127.7 (C-indole), 127.2 (CH-Ph), 112.2 (CH6-indole), 109.5 (CH7-indole), 103.5 (CH4-indole), 102.0 (CH3-indole), 78.6 (-C≡), 73.6 (≡CH), 66.7 (CH_2-O), 63.6 (CH_2-Ph), 53.9 (2xCH_2), 52.0 (CH_2-indole), 44.9 (CH_2-C≡CH), 41.8 (N-CH_3), 36.2 (CH_2), 32.8 (CH_2), 32.4 (CH_2), 30.1 (N-CH_3); MS (EI) *m/z* (%): 91 (48) $[PhCH_2]^+$, 202 (100), 361 (3) $[M-NCH_3CH_2C{\equiv}CH)]^+$, 429 (4) $[M]^+$. Anal. Calcd. For $C_{28}H_{35}N_3O$: C, 78.28; H, 8.21; N, 9.78. Found: C, 77.99; H, 8.45; N, 9.79. 4.2HCl: white powder; mp 221-3 ºC; IR (KBr) ν 3424, 3195, 2928, 2561, 2506, 1619, 1486, 1471, 1210 cm^{-1}. ^1H NMR (300 MHz, D_2O) δ 7.33-7.25 (m, 6H, CH7-indole + 5H-Ph), 7.06 (d, *J* = 2.4 Hz, 1H, CH4-indole), 6.84 (dd, *J* = 9.0, 2.4 Hz, 1H, CH6-indole), 6.58 (s, 1H, CH3-indole), 4.45 (s, 2H, CH_2), 4.08 (s, 2H, CH_2), 3.96 (t, *J* = 6.2 Hz, 2H, O-CH_2-), 3.84 (d, *J* = 2.4 Hz, 2H, CH_2-C≡CH), 3.59 (s, 3H, indole-CH_3), 3.32 (d, *J* = 12.6 Hz, 2H, CH_2), 2.96 (t, *J* = 2.4 Hz, 1H, C≡CH), 2.85-2.75 (m 5H, CH_2 + N-CH_3), 1.84 (d, *J* = 13.6 Hz, 2H, CH_2), 1.75-1.63 [m, 1H, CH], 1.61-1.53 (m, 2H, CH_2-

CH_2O-), 1.32-1.18 (m, 2H, CH_2). Anal. Calcd. for $C_{28}H_{35}N_3O.2HCl.1/3(H_2O)$: C, 66.13; H, 7.47; Cl, 13.94; N, 8.26. Found: C, 66.04; H, 7.89; Cl, 13.84; N, 8.59.

***N*-{[5-(3-(1-Benzylpiperidin-4-yl)propoxy)-1-methyl-1*H*-indol-2-yl]methyl}-*N*-methylprop-2-yn-1-amine (5).** To a solution of 1-methyl-2-{[ethyl(prop-2-yn-1-yl)amino]ethyl}-1*H*-indol-5-ol **4**[52] (0.22 g, 0.963 mmol) and 1-nenzyl-4-(3-chloropropyl)piperidine **12** (0.36 g, 1.44 mmol, 1.5 equiv) in DMF (5 mL), NaH (69.4 mg, 1.73 mmol, 1.8 equiv, 60% /mineral) was added. The reaction mixture was stirred at room temperature overnight and then heated at 100 ºC for 1 h. After complete reaction (tlc analysis), the reaction was concentrated, diluted with water, and extracted with CH_2Cl_2. The organic phase was washed with brine, dried ($MgSO_4$), and evaporated at reduced pressure. The crude product was purified by flash chromatography (CH_2Cl_2/AcOEt, 10:1 to 5/1, v/v) to give compound **5** (0.268 g, 63%) as a white solid: R*f*= 0.28 (CH_2Cl_2/MeOH, 20/1); mp 90-91 ºC; IR (KBr) ν 3265, 2935, 2908, 2799, 2760, 1619, 1489, 1471, 1395, 1269, 1204, 1190, 1160, 1029 cm^{-1}; ^1H NMR (400 MHz, $CDCl_3$) δ 7.35 - 7.25 (m, 5H, Ph) , 7.19 (d, *J*= 8.8 Hz, 1H, CH7-indole), 7.05 (d, *J*= 2.14 Hz, 1H, CH4-indole), 6.85 (dd, *J*= 8.8 and 2.3 Hz, 1H, CH6-indole), 6.35 (s, 1H, CH3-indole), 3.98 (t, *J*= 6.6 Hz, 2H, O-CH_2-), 3.75 (s, 3H, indole-CH_3), 3.69 (s, 2H, indole-CH_2), 3.52 (s, 2H, CH_2-Ph), 2.33 (d, *J*= 2.2 Hz, 2H, CH_2-C≡CH), 2.91 (d, *J*= 10.8 Hz, CH_2), 2.36 (s, 3H, N-CH_3), 2.31 (t, *J*= 2.0 Hz, C≡CH), 1.97 (t, *J*= 12 Hz, 2H, CH_2), 1.83 [m, 2H, CH_2-(CH_2O)], 1.72 (d, *J*= 9.1 Hz, 2H, CH_2), 1.46-1.41 [m, 2H, CH_2-$(CH_2)_2O$], 1.29-1.31 (m, 3H, CH+CH_2); ^{13}C NMR (100 MHz, $CDCl_3$) δ 153.2 (C5-indole), 138.3 (C-Ph), 136.9 (C2-indole), 133.3 (C-indole), 129.2 (2xCH-Ph), 128.0 (2xCH-Ph), 127.4 (C-indole), 126.8 (CH-Ph), 112.0 (CH6-indole), 109.5 (CH7-indole), 103.3 (CH4-indole), 102.0 (CH3-indole), 78.3 (-C≡), 73.4 (≡CH), 69.0 (CH_2-O), 63.4 (CH_2-Ph), 53.8 (2xCH_2), 51.7 (indole-CH_2), 44.6 (CH_2-C≡), 41.5 (N-CH_3), 35.5 (CH-

piperidine), 32.8 [CH_2-$(CH_2)_2O$], 32.2 ($2CH_2$), 29.8 (indole-N-CH_3), 26.7 [CH_2-CH_2O]; MS (EI) *m/z* (%): 91 (77) $[PhCH_2]^+$, 352 (22) $[M-CH_2Ph]^+$, 374 (100) $[M-NCH_3CH_2C{\equiv}CH)]^+$, 404 (7) $[M-CH_2C{\equiv}CH)]^+$, 428 (5) $[M - CH_3]^+$, 443 (40)$[M]^+$. Anal. Calcd. for $C_{29}H_{37}N_3O$: C, 78.51; H, 8.41; N, 9.47. Found: C, 78.36; H, 8.31; N, 9.23. 5.2HCl: white powder; mp 203-5 ºC; IR (KBr) ν 3193, 2937, 2512, 1619, 1486, 1469, 1209 cm^{-1}; ^1H NMR (300 MHz, D_2O) δ 7.32-7.22 (m, 6H, CH7-indole + 5H-Ph), 7.05 (d, *J* = 2.2 Hz, 1H, CH4-indole), 6.83 (dd, *J* = 9.0, 2.3 Hz, 1H, CH6-indole), 6.58 (s, 1H, CH3-indole), 4.45 (s, 2H, CH_2), 4.07 (s, 2H, CH_2), 3.90 (t, *J* = 6.1 Hz, 2H, O-CH_2-), 3.83 (d, *J* = 2.2 Hz, 2H, CH_2-C≡CH), 3.59 (s, 3H, indole-CH_3), 3.30 (d, *J* = 12.0 Hz, 2H, CH_2), 2.97-2.94 (m, 1H, C≡CH), 2.81-2.72 (m 5H, CH_2 + N-CH_3), 1.84-1.75 (m, 2H, CH_2), 1.65-1.55 [m, 2H, CH_2], 1.49-1.36 (m, 1H, CH), 1.41-1.46 [m, 2H, CH_2-$(CH_2)_2O$], 1.29-1.09 (m, 4H). Anal. Calcd. for $C_{29}H_{37}N_3O.2HCl$: C, 67.43; H, 7.61; Cl, 13.73; N, 8.13. Found: C, 67.38; H, 7.81; Cl, 13.13; N, 8.02.

***N*-{[5-(4-(1-Benzylpiperidin-4-yl)butoxy)-1-methyl-1*H*-indol-2-yl]methyl}-*N*-methylprop-2-yn-1-amine (6).** To a solution of 1-methyl-2-{[ethyl(prop-2-yn-1-yl)amino]ethyl}-1*H*-indol-5-ol **4**[52] (0.35 g, 1.56 mmol) and 1-benzyl-4-(4-chlorobutyl)piperidine **13** (0.5 g, 1.88 mmol, 1.2 equiv) in 8 mL of DMF, NaH (0.1 g, 2.5 mol, 1.6 equiv, 60% mineral oil) was added. The reaction mixture was stirred at room temperature overnight and then heated at 70 ºC for 8 h. Then, the reaction was concentrated, diluted with water, and extracted with CH_2Cl_2. The organic phase was washed with brine, dried ($MgSO_4$), and evaporated. The crude product was purified by flash chromatography (CH_2Cl_2/MeOH, 50:1 to 30/1, v/v) to give compound **6** (0.547 g, 76%) as a white solid: R*f*= 0.28 (CH_2Cl_2/MeOH, 20/1); mp 93-4 ºC; IR (KBr) ν 3260, 2937, 2918, 1619, 1489, 1472, 1203, 1193, 1160, 1008 cm^{-1}; ^1H NMR (500 MHz, $CDCl_3$) δ 7.32-7.23 (m, 5H), 7.17 (d, *J*= 8.8 Hz, 1H, CH7-indole), 7.03 (d, *J*= 2.3 Hz,

1H, CH4-indole), 6.85 (dd, *J*= 8.8 and 2.4 Hz, 1H, CH6-indole), 6.32 (s, 1H, CH3-indole), 3.98 (t, *J*= 6.6 Hz, 2H, -CH_2O-), 3.67 (s, 2H, CH_2-N), 3.73 (s, 3H, N-CH_3), 3.49 (s, 2H, CH_2-Ph), 3.31 (d, *J*= 2.4 Hz, CH_2-C≡CH, 2H), 2.88 (d, *J*= 10.5 Hz, 2H, CH_2pip), 2.34 (s, 3H, N-CH_3), 2.28 (t, *J*= 2.4 Hz, 1H, C≡CH), 2.00-1.85 (m, 2H, CH_2pip), 1.83-1.73 (m, 2H, CH_2-CH_2O), 1.66 (br d, *J*= 9.4 Hz, CH_2pip), 1.51-1.45 [m, 2H, CH_2-$(CH_2)_2O$], 1.34-1.22 (M, 4H, CH_2pip + CH_2-$(CH_2)_3O$); ^{13}C NMR (125 MHz, $CDCl_3$) δ 153.5 (C5-indole) 138.5 (C-Ph), 137.0 (C2-indole), 133.3 (C7a-indole), 129.2 (2xCH_2Ph), 128.1 (2xCHPh), 127.5 (C3a-indole), 126.8 (CH-Ph), 112.0 (CH6-indole), 109.5 (CH7-indole), 103.4 (CH4-indole), 102.0 (CH_3-indole), 78.4 (-C≡), 73.4 (≡CH), 68.8 (CH_2-O), 63.5 (CH_2-Ph), 53.9 (2xCH_2-piperidine), 51.8 (N-CH_2-indole), 44.7 (CH_2-C≡CH), 41.7 (N-CH_3), 36.3 [CH_2-$(CH_2)_3O$], 35.6 (CH-piperidine), 32.3 (2 x CH_2-piperidine), 29.8 (N-CH_3), 29.7 (CH_2-CH_2O), 23.3 [CH_2-$(CH_2)_2O$]; MS (EI) *m/z* (%): 91 (55) $[PhCH_2]^+$, 172 (71), 228 (45), 366 (41) $[M\text{-}Bn]^+$, 388 $[M\text{-}NCH_3CH_2C{\equiv}CH)]^+$, 418 (8) $[M\text{-}CH_2C{\equiv}CH)]^+$, 457 (26) $[M]^+$. Anal. Calcd. for $C_{30}H_{39}N_3O$: C, 78.73; H, 8.59; N, 9.18. Found: C, 78.65; H, 8.71; N, 9.07. 6.2HCl: white powder; mp 197-9 ºC; IR (KBr) ν 3421, 3195, 2928, 2851, 2561, 2509, 1619, 1485, 1472, 1458, 1408, 1209 cm^{-1}; ^{1}H NMR (300 MHz, D_2O) δ 7.33-7.24 (m, 6H, CH7-ind + 5H-Ph), 7.05 (d, *J* = 2.2 Hz, 1H, CH4-ind), 6.84 (dd, *J* = 9.0, 2.4 Hz, 1H, CH6-ind), 6.59 (s, 1H, CH3-ind), 4.48 (s, 2H, CH_2), 4.05 (s, 2H, CH_2), 3.90 (t, *J* = 6.5 Hz, 2H, O-CH_2-), 3.86 (d, *J* = 2.2 Hz, 2H, CH_2-C≡CH), 3.58 (s, 3H, indole-CH_3), 3.28 (d, *J* = 12.3 Hz, 2H, CH_2), 2.98 (t, *J* = 2.3 Hz, 1H, C≡CH), 2.77-2.70 (m 5H, CH_2 + N-CH_3), 1.76 (d, *J* = 13.9 Hz, 2H, CH_2), 1.61-1.51 [m, 2H, CH_2], 1.41-1.23 (m, 3H, CH + CH_2), 1.29-1.05 (m, 4H). Anal. Calcd. for $C_{30}H_{39}N_3O.2HCl$: C, 67.91; H, 7.79; Cl, 13.36; N, 7.92. Found: C, 67.54; H, 7.45; Cl, 13.25; N, 8.10;

***N*-{[5-(2-bromoethoxy)-1-methyl-1*H*-indol-2-yl)methyl}-*N*-methylprop-2-yn-1-amine (25).** A mixture of 1-methyl-2-{[ethyl(prop-2-yn-1-yl)amino]ethyl}-1*H*-indol-5-ol **14**[52] (0.215 g, 0.942 mmol), 1,2-dibromoethane (1.77 g, 9.42 mmol) and potassium carbonate (0.65 g, 4.71 mmol) in 2-butanone (8 mL) was reacted at 85 °C for 6 h. The mixture was evaporated *in vacuo* and the residue was partitioned between dichloromethane (10 mL) and water (10 mL). The organic layer was dried (Na_2SO_4) and evaporated. The residue was purified by column chromatography, eluting with 4% methanol in dichloromethane affording compound **25** (117.3 mg, 37%): R*f*= 0.76 (CH_2Cl_2/AcOEt, 10/1); mp 75-7 ºC; IR 3274, 29712937, 2877, 2800, 1619, 1579, 1488, 1473, 1400, 1267, 1205, 1198, 1159, 1118, 1025, 889, 842, 794, 776, 690 cm^{-1}; ^1H NMR (300 MHz, $CDCl_3$) δ 7.2 (d, *J*= 8.8 Hz, 1H, CH7-indole), 7.07 (d, *J*= 2.4 Hz, 1H, CH4-indole), 6.9 (dd, *J*= 8.8, 2.5 Hz, 1H, CH6-indole), 6.36 (s, 1H, CH3-indole), 4.33 (t, *J*= 6.4 Hz, 2H, -CH_2-O-), 3.75 (s, 3H, N-CH_3), 3.69 (s, 2H, N-CH_2), 3.66 (t, *J*= 6.4 Hz, 2H, -CH_2-Br), 3.32 (d, *J*= 2.4 Hz, 2H, N-CH_2-C≡), 2.36 (s, 3H, N-CH_3), 2.31 (t, *J*= 2.4 Hz, 1H, ≡CH); ^{13}C NMR (75 MHz, $CDCl_3$) δ 152.2 (C5-indole), 137.3 (C2-indole), 133.8 (C7a-indole), 127.4 (C3a-indole), 112.2 (CH6-indole), 109.7 (CH7-indole), 104.4 (CH4-indole), 102.1 (CH3-indole), 78.3 (-C≡), 73.5 (≡CH), 69.1 (CH_2-O), 51.7 (CH_2-N), 44.7 (-CH_2-C≡), 41.5 (N-CH_3), 29.9 (N-CH_3), 29.6 (CH_2-Br); MS (EI) *m/z*(%): 131 (48), 160 (66) $[M-((Br(CH_2)_2)-NCH_3CH_2C{\equiv}CH)]^+$, 267 (100) $[M-NCH_3CH_2C{\equiv}CH)]^+$, 334 (25)$[M]^+$. Anal. Calcd. for $C_{16}H_{19}BrN_2O$: C, 57.32; H, 5.71; Br, 23.83; N, 8.36. Found: C, 57.50; H, 5.70; Br, 23.24; N, 8.54.

***N*-{[5-(2-(4-Benzylpiperidin-1-yl)ethoxy)-1-methyl-1*H*-indol-2-yl]methyl}-*N*-methylprop-2-yn-1-amine** (**7**). 4-Benzylpiperidine (36 μL, 0.2 mmol) was added to a mixture of **25** (34 mg, 0.1 mmol) and potassium carbonate (42 mg, 0.3 mmol) in *N,N*-dimethylformamide (1 mL). The reactants were heated at 80 ºC overnight under an

atmosphere of argon. The reaction mixture was poured into water (5 mL) and extracted with dichloromethane (3 x 20 mL). The organic layers were combined, dried (Na_2SO_4) and concentrated. The residue was purified by column chromatography, eluting with 3.3% methanol in dichloromethane affording compound **7** (33.5 mg, 77%): white solid; R*f*= 0.49 (CH_2Cl_2/MeOH, 10/1); ^{1}H NMR (400 MHz, $CDCl_3$) □ 7.31-7.25 (m, 2H), 7.23-7.14 (m, 4H), 7.06 (d, *J*= 2.36 Hz, 1H, CH4-indole), 6.88 (dd, *J*= 8.83 and 2.43 Hz, 1H, CH6-indole), 6.35 (s, 1H, CH3-indole), 4. 16 (t, *J*= 6.06 Hz, 2H, -CH_2-O), 3.74 (s, 3H, CH_3), 3.68 (s, 2H, N-CH_2), 3.32 (d, *J*= 2.35 Hz, 2H, CH_2), 3.034 (d, *J*= 11.7 Hz, CH_2), 2.83 (t, *J*= 6.03 Hz, CH_2), 2.56 (d, *J*= 7.016 Hz, CH_2), 2.35 (s, 3H, CH_3), 2.31 (t, *J*= 2.37 Hz, C≡CH), 2.086 (td, *J*= 11.77, 2.18 Hz, 1H, CH_2), 1.67 (d, *J*= 12.87 Hz, CH_2), 1.56 (m, CH), 1.38 (qd, *J*= 12.15, 3.79 Hz, CH_2); ^{13}C NMR (100 MHz, $CDCl_3$) δ 152.9 (C5-indole), 140.6 (C-Ph), 137.0 (C2-indole), 133.3 (C7a-indole), 129.0 (2xCH-Ph), 128.0 (2xCH-Ph), 127.4 (C3a-indole), 125.7 (CH-Ph), 111.0 (CH6-indole), 109.5 (CH7-indole), 103.4 (CH4-indole), 102.0 (CH3-indole), 78.3 (≡CH), 73.4 (-C≡), 66.6 (CH_2O), 57.6 (CH_2), 54.2 (2xCH_2), 51.7 (indole-CH_2), 44.65 (CH_2), 43.1 (CH_2), 41.5 (N-CH_3), 37.67 (CH), 32.0 (2xCH_2), 29.8 (CH_3); MS (EI) m/z (%): 188 (100), 202 (42), 429 (6)$[M]^+$. 7.2HCl: white powder; mp 218-220 ºC**;** IR (KBr) ν 3421, 3189, 2929, 2498, 1619, 1486, 1208, 1163 cm^{-1}; ^{1}H NMR (300 MHz, D_2O) δ 7.28 (d, *J*= 8.9 Hz, 1H, CH7-indole), 7.20-7.15 (m, 2H), 7.10-7.06 (m, 4H), 6.87 (dd, *J*= 9.0, 1.9 Hz, 1H, CH6-indole), 6.61 (s, 1H, CH3-indole), 4.49 (s, 2H, CH_2), 4.25 – 4.13 (m, 2H, -CH_2O), 3.87 (d, *J*= 1.8 Hz, 2H, CH_2), 3.60 (s, 3H, CH_3), 3.47 (d, *J*= 12.2 Hz, 2H, CH_2), 3.39-3.30 (m, 2H, CH_2), 2.98 (t, *J*= 1.9 Hz, 1H, C≡CH), 2.87-2.77 (m, 5H, CH_2 + N-CH_3), 2.43 (d, *J* = 6.6 Hz, 2H, CH_2), 1.75-1.71 (m, 3H, CH + CH_2), 1.41-1.28 (m, 2H, CH_2). Anal. Calcd. for $C_{28}H_{37}Cl_2N_3O$ + 2/3(H_2O): C, 65.36; H, 7.51; N, 8.17. Found: C, 65.08; H, 7.74; N, 8.40.

***N*-{[5-(3-bromopropoxy)-1-methyl-1*H*-indol-2-yl]methyl}-*N*-methylprop-2-yn-1-amine (26).** A mixture of 1-methyl-2-{[ethyl(prop-2-yn-1-yl)amino]ethyl}-1*H*-indol-5-ol **14**[52] (21 mg, 0.092 mmol), 1,3-dibromopropane (186 mg, 0.92 mmol) and potassium carbonate (64 mg, 0.46 mmol) in 2-butanone (1 mL) was reacted at 85 °C for 6 h. The mixture was evaporated, and the residue was partitioned between dichloromethane (10 mL) and water (10 mL). The organic layer was dried (Na_2SO_4) and evaporated in vacuo to give compound **26** (25.4 mg, 80%): R*f*= 0.62 (CH_2Cl_2/AcOEt, 10/1); mp 71-2 ºC; IR (KBr) ν 3275, 1488, 1468, 1206, 1026 cm^{-1}; ^1H NMR (400 MHz, $CDCl_3$) δ 7.2 (d, *J*= 8.9 Hz, 1H, CH7-indole), 7.07 (d, *J*= 2.4 Hz, 1H, CH4-indole), 6.87 (dd, *J*= 8.8 and 2.4 Hz, 1H, CH6-indole), 6.35 (s, 1H, CH3-indole), 4.14 (t, *J*= 5.8 Hz, 2H, -CH_2-OH), 3.75 (s, 3H, N-CH_3), 3.69 (s, 2H, ind-CH_2-N), 3.65 (t, *J*= 6.5 Hz, 2H, -CH_2-Br), 3.32 (d, *J*= 2.4 Hz, 2H, CH_2-C≡), 2.36 (s, 3H, N-CH_3), 2.33 [t, *J*= 5.9 Hz, CH_2-(CH_2O)], 2.30 (t, *J*= 2.4 Hz, 1H, ≡CH); ^{13}C NMR (100 MHz, $CDCl_3$) δ 152.8 (C5-indole), 137.1 (C2-indole), 133.5 (C7a-indole), 127.2 (C3a-indole), 111.9 (CH6-indole), 109.6 (CH7-indole), 103.6 (CH4-indole), 102.1 (CH3-indole), 78.3 (-C≡), 73.4 (≡CH), 66.3 (CH_2-O), 51.7 (CH_2-N), 44.6 (CH_2-C≡), 41.5 (N-CH_3), 32.6 [CH_2-(CH_2O)], 30.3 (CH_2-Br), 29.8 (N-CH_3); MS (EI) *m/z* (%): 131 (60), 160 (100) [M-(($Br(CH_2)_3$)-CH_3NCH_2C≡CH)]$^+$, 227 (7) [M-($Br(CH_2)_3$)]$^+$, 281 (96) [CH_3NCH_2C≡CH)]$^+$, 348 (21)[M]$^+$. Anal. Calcd. for $C_{17}H_{21}BrN_2O$: C, 58.46; H, 6.06; Br, 22.88; N, 8.02. Found: C, 58.49; H, 6.08; Br, 22.11; N, 8.23.

***N*-{[5-(3-(4-Benzylpiperidin-1-yl)propoxy)-1-methyl-1*H*-indol-2-yl]methyl}-*N*-methylprop-2-yn-1-amine (8)**. 4-Benzylpiperidine (0.111 mL, 0.632 mmol, 2 equiv) was added to a mixture of **26** (111 mg, 0.316 mmol, 1 equiv) and potassium carbonate (131 mg, 0.648 mmol, 3 equiv) in *N,N*-dimethylformamide (4 mL). The reaction mixture was heated at 70 ºC for 7 h under an atmosphere of argon. The reaction mixture

was poured into water (5 mL) and extracted into dichloromethane (3 x 20 mL). The organic layers were combined, dried (Na_2SO_4) and concentrated. The residue was purified by column chromatography, eluting with 4% methanol in dichloromethane affording compound **8** (89.2 mg, 64%) as white crystalline solid: R*f*= 0.43 (CH_2Cl_2/MeOH, 10/1); mp 82-3 ºC; IR (KBr) ν 3274, 2923, 1619, 1487, 1469, 1390, 1205, 1133, 1027 cm^{-1}; ^1H NMR (400 MHz, $CDCl_3$) δ 7.31-7.25 (m, 2H), 7.21-7.12 (m, 4H), 7.02 (d, *J*= 2.26 Hz, 1H, CH4-indole), 6.83 (dd, *J*= 8.83 and 2.43 Hz, 1H, CH6-indole), 6.32 (s, 1H, CH3-indole), 4. 03 (t, *J*= 6.28 Hz, 2H, -CH_2O), 3.73 (s, 3H, CH_3), 3.67 (s, 2H, CH_2-N), 3.30 (d, *J*= 2.36 Hz, 2H, CH_2≡), 3.02 (d, *J*= 11.45 Hz, CH_2), 2.59 (t, *J*= 7.37 Hz, CH_2), 2.55 (d, *J*= 6.77 Hz, CH_2), 2.34 (s, 3H, CH_3), 2.29 (t, *J*= 2.33 Hz, C≡CH), 2.08-1.92 (m, 4H, 2xCH_2), 1.66 (d, *J*= 12. 7 Hz, CH_2), 1.55 (m, CH), 1.40 (qd, *J*= 12.19, 3.24 Hz, CH_2); ^{13}C NMR (100 MHz, $CDCl_3$) δ 153.1 (C5-indole), 140.5 (C-Ph), 137.0 (C2-indole), 133.3 (C7a-indole), 129.0 (2xCH-Ph), 128.1 (2xCH-Ph), 127.4 (C3a-indole), 125.7 (CH-Ph), 111.9 (CH6-indole), 109.5 (CH7-indole), 103.4 (CH4-indole), 102.0 (CH3-indole), 78.3 (≡CH), 73.4 (-C≡), 67.2 (CH_2-O), 55.7 (CH_2), 53.8 (2xCH_2), 51.7 (CH_2), 44.7 (CH_2), 43.0 (CH_2), 41.5 (N-CH_3), 37.7 (CH), 31.7 (2xCH_2), 29.8 (CH_3), 26.7 (CH_2); MS (ES) *m/z* (%): 188 (99), 444 (100) $[M+H]^+$, 445 (40) $[M+2H]^+$, 466 (2)$[M+Na]^+$. Anal. Calcd. for $C_{29}H_{37}N_3O$: C, 78.51; H, 8.41; N, 9.47. Found: C, 78.63; H, 8.59; N, 9.44. 8.2HCl: white powder; mp 216-8 ºC**;** IR (KBr) ν 3196, 2931, 2559, 2509, 1619, 1485, 1472, 1454, 1250, 1211 cm^{-1}; ^1H NMR (300 MHz, D_2O) δ 7.27 (d, *J* = 9.1 Hz, 1H, CH7-indole), 7.20-7.15 (m, 2H), 7.10-7.06 (m, 4H), 6.84 (dd, *J* = 9.0, 1.5 Hz, 1H, CH6-indole), 6.60 (s, 1H, CH3-indole), 4.48 (s, 2H, CH_2), 3.99 (t, *J* = 5.4 Hz, 2H, -CH_2O), 3.87 (s, 2H, CH_2), 3.59 (s, 3H, CH_3), 3.41 (d, *J* = 11.8 Hz, 2H, CH_2), 3.16 – 3.05 (m, 2H), 2.99-2.97 (m,1H, C≡CH), 2.81-267 (m, 5H, CH_2 + N-CH_3), 2.43 (d, *J* = 6.1 Hz, 2H, CH_2), 2.06-1.97 (m, 2H, CH_2), 1.74-1.70 (m,

3H, CH + CH_2), 1.34-1.22 (m, 2H, CH_2). Anal. Calcd. for $C_{29}H_{37}N_3O.2HCl$ .1/2(H_2O): C, 66.27; H, 7.67; Cl, 13.49; N, 8.00; Found: C, 66.02; H, 7.62; Cl, 13.45; N, 8.25.

***N*-{[5-(3-(4-Benzylpiperazin-1-yl)propoxy)-1-methyl-1*H*-indol-2-yl]methyl}-*N*-methylprop-2-yn-1-amine** (**9**). 1-Benzylpiperazine (0.148 g, 0.845 mmol) was added to a mixture of **26** (0.147g, 0.422 mmol) and potassium carbonate (0.116 g, 0.845 mmol) in *N,N*-dimethylformamide (10 mL). The reactants were heated at 70 ºC overnight under an atmosphere of argon. The reaction mixture was poured into water (50 mL) and extracted into ethyl acetate (3 x 100 mL). The organic layers were combined, dried (Na_2SO_4) and concentrated *in vacuo*. The residue was purified by column chromatography, eluting with 2% MeOH in CH_2Cl_2 affording compound **9** (0.16 g, 85%) as a solid: R*f*= 0.43 (CH_2Cl_2/MeOH, 10/1); mp 103-4 ºC; IR (KBr) ν 3138, 2958, 2943, 2806, 2762, 1621, 1492, 1480, 1207, 1159 cm^{-1}; ^1H NMR (400 MHz, $CDCl_3$) δ 7.37-7.25 (m, 5H), 7.19 (d, *J*= 8.8 Hz, 1H, CH7-indole), 7.07 (d, *J*= 2.4 Hz, 1H, CH4-indole), 6.88 (dd, *J*= 8.8 and 2.4 Hz, 1H, CH6-indole), 6.35 (s, 1H, CH3-indole), 4.06 (t, *J* = 6.4 Hz, 2H, -CH_2O), 3.75 (s, 3H, N-CH_3), 3.69 (s, 2H, CH_2Ph), 3.54 (s, 2H, CH_2-N), 3.33 (d, *J*= 2.3 Hz, 2H, CH_2C≡), 2.53 (m, 8H, 4 x CH_2), 2.36 (s, 3H, N-CH_3), 2.32 (t, *J*= 2.3 Hz, 1H, C≡CH), 2.01 [m, 2H, $CH_2(CH_2O)$]; ^{13}C NMR (100 MHz, $CDCl_3$) δ 153.1 (C5-indole), 138.0 (C-Ph), 136.9 (C2-indole), 133.2 (C7a-indole), 129.1 (2xCH-Ph), 128.1 (2xCH-Ph), 127.4 (C3a-indole), 126.9 (CH-Ph), 111.9 (CH6-indole), 109.5 (CH7-indole), 103.2 (CH4-indole), 101.9 (CH3-indole), 78.3 (-C≡), 73.4 (≡CH), 67.1 (CH_2-O), 63.0 (CH_2-N), 55.33 (CH_2), 53.1 (CH_2), 53.0 (2xCH_2), 51.7 (CH_2), 44.6 (CH_2), 41.5 (N-CH_3), 29.8 (N-CH_3), 26.9 [$CH_2(CH_2O)$]; MS (ES) *m/z* (%): 445 (100) $[M+H]^+$, 467 (2) $[M+Na]^+$. Anal. Calcd. for $C_{28}H_{36}N_4O$: C, 75.64; H, 8.16; N, 12.60. Found: C, 75.39; H, 8.40; N, 12.52. 9.3HCl: white powder; mp 227-230 ºC; IR (KBr) ν 3195, 2953, 2561, 2516, 2442, 1620, 1485, 1472, 1442, 1211 cm^{-1}; ^1H

NMR (300 MHz, D_2O) δ, 7.36-7.31 (m, 5H), 7.27 (d, *J* = 9.1 Hz, 1H, CH7-indole), 7.05 (d, *J* = 2.4 Hz, 1H, CH4-indole), 6.84 (dd, *J* = 9.0, 2.5 Hz, 1H, CH6-indole), 6.61 (s, 1H, CH3-indole), 4.50 (s, 2H, CH_2), 4.21 (s, 2H, CH_2), 4.00 (t, *J* = 5.7 Hz, 2H, -CH_2O), 3.88 (d, *J* = 2.5 Hz, 2H, CH_2-C≡), 3.60 (s, 3H, CH_3), 3.50-3.35 (m, 4H), 3.33 – 3.22 (m, 2H), 2.98 (t, *J* = 2.5 Hz, 1H, C≡CH), 2.78 (s, 3H, N-CH_3), 2.14 – 1.98 (m, 2H, CH_2). Anal. Calcd. for $C_{28}H_{39}Cl_3N_4O$+1/2(H_2O): C, 59.73; H, 7.16; N, 9.95. Found: C, 59.59; H, 7.49; N, 10.20.

Biological evaluation

Inhibition experiments of AChE and BuChE. To assess the inhibitory activity of the compounds towards AChE (E.C.3.1.1.7) or BuChE (E.C.3.1.1.8), we followed the spectrophotometric method of Ellman[78] using purified AChE from *Electrophorus electricus* (Type V-S) or human recombinant (expressed in the HEK-293 cell line) or BuChE from equine or human serum (lyophilized powder) (Sigma-Aldrich, Madrid, Spain). The reaction took place in a final volume of 3 mL of a phosphate-buffered solution (0.1 M) at pH = 8, containing 0.035 U/mL of *Ee*AChE, 0.24 U/mL of hrAChE, or 0.05 U/mL of BuChE and 0.35 mM of 5,5'-dithiobis-2-nitrobenzoic acid (DTNB, Sigma-Aldrich, Madrid, Spain). Inhibition curves were made by pre-incubating this mixture with at least nine concentrations of each compound for 10 min. A sample with no compound was always present to determine the 100% of enzyme activity. After this pre-incubation period, acetylthiocholine iodide (0.35 mM) or butyrylthiocholine iodide (0.5 mM) (Sigma-Aldrich, Madrid, Spain) were added, allowing 15 min more of incubation, where the DTNB produces the yellow anion 5-thio-2-nitrobenzoic acid along with the enzymatic degradation of acetylthiocholine iodide or butyrylthiocholine iodide. Changes in absorbance were detected at 405 nm in a spectrophotometric plate

reader (FluoStar OPTIMA, BMG Labtech). Compounds inhibiting AChE or BuChE activity would reduce the color generation, thus IC_{50} values were calculated as the concentration of compound that produces 50% AChE activity inhibition. Data are expressed as means ± s.e.m. of at least three different experiments in quadruplicate.

Kinetic analysis of AChE inhibition. To obtain estimates of the mechanism of action of compound **5**, reciprocal plots of 1/V versus 1/[S] were constructed at different concentrations of the substrate acetylthiocholine (0.1-1 mM) by using Ellman's method.[78] Experiments were performed in a transparent 48-well plate containing each well 350 μL of the DTNB solution in PBS, 1 μL of buffer (control) or inhibitor solution to give desired final concentration. Final volume (1 mL) was reached by adding phosphate buffer solution (pH 8). Reaction was initiated by adding 45 μL of AChE at 30 ºC to give a final concentration of 0.18 U/mL. Progress curves were monitored at 412 nm over 1.33 min in a fluorescence plate-reader Fluostar Optima (BMG-technologies, Germany). Progress curves were characterized by a linear steady-state turnover of the substrate and values of a linear regression were fitted according to Lineweaver–Burk replots using Origin software. The plots were assessed by a weighted least square analysis. Determination of Michaelis constant for the substrate ATCh was done at 7 different concentrations (0.1 – 1 mM) to give a value of K_M = 0.29 ± 0.01 mM, and V_{max} = 2.82 ± 0.06 min^{-1}. Slopes of the reciprocal plots were then plotted against the concentration of **5** (range 0-10 μM) as previously described[79] to evaluate K_i data. Data analysis was performed with Origin Pro 7.5 software (Origin Lab Corp.).

Inhibition experiments of MAO-A and MAO-B. A purification of mitochondria from rat liver homogenates was prepared as previously described[80] and used as source for MAO activities. Total protein was measured by the method of Bradford using bovine-serum albumin as standard. The inhibitory activity of the compounds towards MAO-A

and MAO-B was determined following the method of Fowler and Tipton[81] using [^{14}C]-labelled substrates (Perkinelmer, USA). MAO-B activity was determined towards 20 μM [^{14}C]-phenylethylamine (PEA) (2.5 mCi/mmol) and MAO-A activity towards [^{14}C]-(5-hydroxy-triptamine) (5-HT) 100 μM (0.5 mCi/mmol). Inhibition curves were made by pre-incubating this mixture with at least nine concentrations of each compound for 30 min. A sample without compound was always present to determine the 100% of enzyme activity. The reaction was carried out at 37ºC in a final volume of 225 μl in 50 mM phosphate buffer (pH 7.2) and stopped by the addition of 100 μl 2 M citric acid. Radiolabelled aldehyde product were extracted into toluene/ethyl acetate (1:1, v/v) containing 0.6% (w/v) 2, 5-diphenyloxazole (PPO) before liquid scintillation counting (Tri-Carb 2810TR). Data are means ± SEM of at least four different experiments in triplicate.

Reversibility studies. To study the nature of the enzymatic inhibition exerted by **5**, we determined the activity of the enzyme in the presence and in the absence of the inhibitor by two different methods: after three consecutive washings with buffer and after different times of pre-incubation of the enzyme with the inhibitor. For the first method, enzyme samples were pre-incubated for 30 min at 37 ºC with 6 nM compound **5** for MAO-A and 45 nM for MAO-B. Samples were then washed and centrifuged at 25.000xg for 10 min at 4 ºC consecutively for three times. Finally, total protein was measured and MAO-A and MAO-B activities were determined as above described. For the second method, samples of enzyme and inhibitor **5** at indicated concentration were pre-incubated for 0, 5, 15 and 30 minutes before measuring MAO-A and MAO-B activities as above described.

Progress curves of substrate consumption. To clarify the behavior of **5** towards MAO-A and MAO-B, the inhibitor was pre-incubated for long periods (0 to 420 min) with MAO-A (10 nM inhibitor concentration) and MAO-B (100 nM inhibitor concentration). The concentrations of **5** used in this assay were 2 times the corresponding IC_{50} value. After the corresponding periods, substrates were added and MAO activities were determined as above described. Data are the mean ± SEM of three independent esperiments in triplicate.

Kinetic analysis of MAO-B inhibition. To obtain estimates of the mechanism of action of compound **5**, reciprocal plots of 1/V versus 1/[S] were constructed at different concentrations of the substrate β-phenylethylamine (1-200 μM) by using Fowler and Tipton's method.[81] The plots were assessed by a weighted least-squares analysis. Data analysis was performed with GraphPad Prism 3.0 software (GraphPad Software Inc.). Determination of Michaelis constants gave a value of K_M = 6.7±0.3 μM and V_{max} = 277.8±6.1 pmol/min. Slopes of the reciprocal plots were then plotted against the concentration of **5** (range 0-10 μM) as previously described[79] to evaluate K_i data.

Inhibitory capacity on $A\beta_{1-42}$ self-aggregation. The inhibition of $A\beta_{1-42}$ self-aggregation by compound **5** was studied by using the thioflavin T-based fluorometric assay previously described by Bartolini et al.[82] with little modifications. Briefly, $A\beta_{1-42}$ peptide (Bachem AG, Switzerland) was pretretated with 1,1,1,3,3,3-hexafloro-2-propanol (HFIP, Sigma Chemicals) and redissolved in 10 mM phosphate buffer (PBS, pH11.2 adjusted with NH_4OH). Final $A\beta_{1-42}$ stock solution concentration was 443 μM. To study the effect of **5** on fibril formation, experiments were performed by incubating the peptide (final Aβ concentration=40μM) with and without 10 μM compound **5** (Aβ/inhibitor = 4/1). Blanks containing only the inhibitor were also prepared. Propidium

iodide (PI, Sigma-Aldrich) was used as reference compound in the experiments at the conditions described aboved and also at equimolar ratio Aβ/PI. Samples were diluted to a final volume of 200μl with 10mM PBS (pH 7.4) and 35 μM thioflavin T in 50 mM glycine–NaOH buffer (pH 8.5) was added. Experiments were performed on a Synergy HT microplate spectrofluorometer (Bio-Tek, USA). The fluorescence intensity was carried out (λ_{exc}= 485 nm; λ_{em}= 528 nm) every 10 min for 10 h, and values at plateau (400 min) were averaged after subtracting the background fluorescence of 35 μM thioflavin T solution. The fluorescence intensities were compared and the percent inhibition due to the presence of the inhibitor was calculated by the following expression: 100-(IFi/IF_0 x 100) where IFi and IF_0 are the fluorescence intensities obtained in the presence or absence of inhibitor, respectively.

Inhibition of hAChE-induced $A\beta_{1-40}$ aggregation. Aliquots of 231μM $A\beta_{1-40}$ (Bachem AG, Switzerland) lyophilised from 1mg/ml HFIP solution were redissolved in 10 mM phosphate buffer (PBS, pH11.2 adjusted with NH_4OH). For co-incubation experiments, aliquots of human recombinant AChE (Sigma Chemicals) (0.4 μM final concentration, ratio Aβ/AChE=10/1) in the presence of 100 μM compound **5** were added. Blanks containing Aβ, AChE, Aβ plus compound **5** and AChE plus compound **5** were also prepared. To quantify the amyloid fibril formation, the Thioflavin T fluorescence method[82] was performed as above described. The fluorescence intensities were compared and the percent inhibition due to the presence of the inhibitor was calculated by the following expression: 100-(IFi/IF_0 x 100) where IFi and IF_0 are the fluorescence intensities obtained in the presence or absence of inhibitor, respectively.

Molecular modeling

Set up of the systems. All protein models were derived from X-ray crystallographic structures taken from the Protein Data Bank (PDB). AChE models were built up from the AChE-donepezil complex 1EVE.[59] The enzyme was modeled in its physiological active form with neutral His440 and deprotonated Glu327, which together with Ser200 form the catalytic triad. The standard ionization state at neutral pH was considered for the rest of ionizable residues with the exception of Asp392 and Glu443, which were neutral, and His471, which was protonated, according to previous studies.[83] Three disulfide bridges were defined between Cys residues 66-93, 254-265, 402-521, and histidine residues 398 and 440 were set up to represent the δ tautomer.[84] MAO models were build up using X-ray structures 2Z5X[67] and 2C65[85] for isoforms A and B, respectively. Structural waters were defined as those common to five different high-resolution X-ray crystallographic structures (PDB entries 2Z5X, 2Z5Y, 2V5Z, 2C70, 2VZ2).

Docking. The binding mode of compound **5** was explored by means of docking calculations carried our with rDock, which is an extension of the program RiboDock, using an empirical scoring function calibrated on the basis of protein–ligand complexes.[64,65] Docking computations were performed with a twofold purpose: (1) to explore suitable starting orientations of the inhibitor in the binding site of AChE, MAO-A and MAO-B, and (2) to examine the docking of compound **5** for the three main orientations adopted by the indole ring of Trp279 in the peripheral binding site in *Torpedo californica* AChE.[61] At this point, it is worth noting that the reliability of rDock has been assessed by docking a set of known dual binding site IAChEs taking advantage of the X-ray crystallographic structures of their complexes with AChE.[60] The docking of **5** in AChE was then explored using the three structural models of the target AChE differing in the orientations of Trp279 (PDB entries 1EVE, 1Q83 and 2CKM).

Structural water molecules that mediate relevant interactions between the benzyl piperidine moiety and the enzyme were retained in the target models. Similarly, five water molecules found in the binding site of MAO-A and MAO-B were retained in docking calculations. The docking volume was defined as the space covered by catalytic, mid-gorge and peripheral sits in AChE, and by the substrate and entrance cavities in MAO. Suitable restraints were introduced to position the benzyl piperidine moiety of **5** in AChE. Each compound was subjected to 100 docking runs. Whereas the protein was kept rigid, rDock accounts for the conformational flexibility of the ligand around rotatable bonds during docking calculations. The output docking modes were analyzed by visual inspection in conjunction with the docking scores.

The X-ray structure of the recombinant human BuChE (PDB entry 2PM8)[86] was used to explore the binding mode of **5** in this enzyme. Some graphical manipulation was required, including addition of the hydrogen atoms according to the parm99SB forcefield and modelling of poorly resolved loop between residues Leu478 and Lys486, which was modeled using the X-ray structure of the BChE-tabun complex (PDB entry 3DJY)[87]. Additionally, 3 disulfide bonds were defined between residues 94-120, 280-291 and 428-547. Residue Glu469 was modelled in the protonated state, and residue His466 was modelled as Nδ-H tautomer. Docking calculations were performed using the same protocol mentioned above.

MM-PBSA analysis. The ligand–protein poses were clusterized and re-ranked using the MM–PBSA approach in conjunction with the parmm99 force field of the Amber9 package.[88] The partial atomic charges of compound **5** were derived using the RESP protocol[89] by fitting to the molecular electrostatic potential calculated at the HF/6-31G* level with Gaussian 03.[90] Calculations were performed for 100 snapshots taken evenly during the last 5 ns of the simulations. The internal conformational energy was

determined using the standard formalism and parameters implemented in AMBER. The electrostatic contribution was computed using a dielectric constant of 78.4 for the aqueous environment, while a dielectric constant of 1 was assigned to the interior of the protein. Even though the choice of the internal dielectric constant is a subject of debate, this value is usually adopted when calculations are performed for ensembles of snapshots taken from simulations, whereas higher values are generally used for calculations of static structures [91,92]. The electrostatic potentials were calculated using a grid-spacing of 0.25 Å. Besides the standard atomic radii implemented in AMBER, calculations were also performed using a set of optimized radii developed for MM/PBSA computations with the AMBER force field.[66] The non-polar contribution was calculated using a linear dependence with the solvent-accessible surface as implemented in AMBER. Finally, entropy changes upon complexation were assumed to cancel out in the comparison of the different poses.

Molecular dynamics. The binding mode of compound **5** was explored by means of 20 ns molecular dynamics (MD) simulations performed for their complexes to AChE (using 3 different models; see above), MAO-A and MAO-B. An additional MD simulation was run for the complex with donepezil and used to calibrate the results of the simulations performed for AChE complexes. The simulation protocol was based on the computational strategy used in our previous studies,[60] which is briefly summarized here. MD simulations were run using the PMEMD module of Amber9 and the parm99SB parameters for the protein.[93] The gaff force field[94,95] was used to assign parameters to the inhibitor (and to the FAD cofactor in MAO simulations). The charge distribution of the inhibitor was further refined based on the electrostatic charges determined from a fit to the "HF/6-31G(d)" electrostatic potential obtained with Gaussian 03[90] using the RESP procedure. Na^+ cations were added to neutralize the

negative charge of the system with the XLEAP module of Amber9. The system was immersed in an octahedral box of TIP3P[96] water molecules, preserving the crystallographic waters inside the binding cavity. The final systems contained the protein–ligand complex, Na^+ cations and around 17000 water molecules, leading to simulations systems that comprise around 53000 atoms.

The geometry of the system was minimized in four steps. First, the position of hydrogen atoms was optimized using 3000 steps of steepest descent algorithm. Then, water molecules were refined through 2000 steps of steepest descent followed by 3000 steps of conjugate gradient. Next, the ligand, water molecules, and counterions were optimized with 2000 steps of steepest descent and 4000 steps of conjugate gradient, and finally the whole system was optimized with 3000 steps of steepest descent and 7000 steps of conjugate gradient. Thermalization of the system was performed in five steps of 25 ps, increasing the temperature from 100 K up to 298 K. Concomitantly, the residues that define the binding site were restrained during thermalization using a variable restraining force. Thus, a force constant of 25 kcal mol^{-1} $Å^{-2}$ was used in the first stage of the thermalization, and was subsequently decreased by increments of 5 kcal mol^{-1} $Å^{-2}$ in the next stages. Then, a series of 20 ns trajectories were run for the two compounds using a time step of 1 fs. In MAO simulations, an additional restraint force was used for the backbone of residues 487-492, which define the transmembrane segment at the C-terminus of the protein. SHAKE was used for those bonds containing hydrogen atoms, in conjunction with periodic boundary conditions at constant pressure (1 atm) and temperature (298 K), Particle-Mesh Ewald for the treatment of long-range electrostatic interactions, and a cutoff of 11 Å for nonbonded interactions.

Acknowledgements. We thank the Ministerio de Ciencia e Innovación (SAF2006-08764-C02-01; SAF2009-07271; SAF2008-05595), Comunidad de Madrid (S/SAL-0275-2006), Instituto de Salud Carlos III [Retic RENEVAS (RD06/0026/1002); Fundacion CIEN; Miguel Servet Program (CP10/00531], and COST Action D34/0003/05 (2005-2010) for financial support, and the Centro de Supercomputació de Catalunya (CESCA) for computational facilities. AS and MC thank CSIC, and Instituto de Salud Carlos III for post-doctoral I3P and "Sara Borrell" contracts, respectively. CdlR thanks MICINN for Juan de la Cierva contract (2006-2008) and Instituto de Salud Carlos III for Miguel Servet contract (2011-2016). A fellowship for JJ from Fondo de Investigaciones Sanitarias is acknowledged. JJ-J thanks Instituto de Salud Carlos III for PFIS fellowship FI10/00292. JMC thanks Prof. A. G. García (Departamento de Farmacología y Terapéutica, Facultad de Medicina, Universidad Autónoma de Madrid) for his interest and support. This work was realized in the framework of COST working group: D34/0003/05

Supporting Information available: Representation of structural models derived from docking and MD simulations, as well as energetic analysis. This material is available free of charge via the Internet at http://pubs.acs.org

References

(1) Goedert, M.; Spillantini, M. G. A century of Alzheimer's disease. *Science* **2006**, *314*, 777-781.

(2) Terry, R.D.; Gonatas, N.K; Weiss, M. Ultrastructural studies in Alzheimer's presenile dementia. *Ann J Pathol* **1964**, 44:269-297

(3) Grundke-Iqbal, I; Iqbal, K; Tung, Y.C; Quinlan, M; Wisniewski, H.M; Binder L.I.. Abnormal phosphorylation of the microtubule-associated protein τ (tau) in Alzheimer cystoskeletal pathology. *Proc. Natl. Acad. Sci* USA **1986**, 93:4913-4917

(4) Coyle, J.T; Puttfarcken, P. Oxidative stress, glutamate and neurodegenerative disorders. *Science* **1993**; 262:689-695

(5) Gella, A.; Durany, N. Oxidative stress in Alzheimer disease. *Cell. Adh. Migr.* **2009**, *3*, 88-93.

(6) Perry, E. K.; Tomlinson, B. E.; Blesseed, G.; Bergmann, K.; Gibson, P. H.; Perry, R. H. Correlation of cholinergic abnormalities with senile plaques and mental test scores in senile dementia. *British Med. J*. **1978**, *2,* 1457-1459.

(7) Talesa, V. N. Acetylcholinesterase in Alzheimer's disease, *Mech. Ageing Dev.* **2001**, *122*, 1961-1969.

(8) García-Alloza, M.; Gil-Bea, F. J.; Díez-Ariza, M.; Chen, C. P.; Francis, P. T.; Lasheras, B.; Ramirez, M. J. Cholinergic-serotonergic imbalance contributes to cognitive and behavioral symptoms in Alzheimer's disease. *Neurophsychologia* **2005**, *43*, 442-449.

(9) Terry, A. V.; Buccafusco, J. J.; Wilson, C. Cognitive dysfunction in neuropsychiatric disorders: Selected serotonin receptor subtypes as therapeutic targets. *Behav. Brain Res.* **2008**, *195*, 30-38.

(10) Dringenberg, HC. Alzheimer's disease: more than a "cholinergic disorder" – evidence that cholinergic-monominergic interactions contribute to EEG slowing and dementia. *Behav Brain Res* **2000**, 115, 235-249

(11) Riederer, P; Danielczyk, W; Grünblatt, E. Monoamine oxidase-B inhibition in Alzheimer's disease. *Neurotoxicology* **2004**, *25*, 271-7.

(12) Youdim, MB; Edmonson, D and Tipton, KF. The therapeutic potential of monoamine oxidase inhibitors. Nature Rev 2006, 7,

(13) Youdim, M. B. H.; Finberg, J. P. M.; Tipton, K. F. Monoamine oxidase. In U. Tredelenburg, N. Weiner, Springer-Verlag, Berlin, **1988**, 119-192.

(14) Johnston, J.P. Some observations upon a new inhibitor of monoamine oxidasein brain tissue. *Biochem Pharmacol* **1968**, 17(7), 1285-1297

(15) Grimsby, J; Lan, N.C; Neve, R; Chen, K; Shih, J.C. Tissue distribution of human monoamine oxidase A and B mRNA. *J Neurochem* **1990**, 55(4), 1166-1169

(16) Riederer P and Youdim MB. Monoamine oxidase activity and monoamine metabolism in the brains of parkinsonian patients treated with l-deprenyl. *J Neurochem* **1986**, 46,1359-1365.

(17) Kristal, BS; Conway, AD; Brown, AM; Jain, JC; Ulluci, PA; Li, SW; Burke, JW. Selective dopaminergic vulnerability: 3,4-dihydroxyphenylacetaldehyde targets mitochondria. *Free Radic Biol Med* **2001**, 30, 924-931

(18) Pizzinat, N; Copin, N; Vindis, C; Parini A and Cambon C. Reactive oxygen species production by monoamineoxidases in intact cells. *Naunyn Schmiedebergs Arch Pharmacol* **1999**, 359, 428-431.

(19) Caraci, F; Copani, A; Nicoletti, F; xxxxxxxx. Depression and Alzheimer's disease:Neurobiological links and common pharmacological targets. *Eur J Pharmacol* **2010**, 626, 64-71

(20) Birks J & Harvey R. Donepezil for dementia due to Alzheimer's disease. *Cochrane Database Syst Rev* **2006,** (1) CD001190.

(21) Loy C & Schneider L. Galantamine for Alzheimer's disease. *Cochrane Database Syst Rev* **2004***,* (4) CD001747

(22) Birks J, Grimley EJ, Iakovidou V. Rivastigmine for Alzheimer's disease. *Cochrane Database Syst Rev* **2000***,* (4) CD001191.

(23) Racchi, M.; Mazzucchelli, M.; Porrello, E.; Lanni, C.; Govoni, S. Acetylcholinesterase inhibitors: novel activities of old molecules. *Pharmacol. Res.* **2004**, *50*, 441-451.

(24) Muñoz-Torrero, D. Acetylcholinesterase Inhibitors as Disease-Modifying Therapies for Alzheimer's Disease. *Curr. Med. Chem.* **2008**, *15*, 2433–2455.

(25) Castro, A.; Martínez, A. Targeting beta-amyloid pathogenesis through acetylcholinesterase inhibitors. *Curr. Pharm. Des.* **2006**, *12*, 4377-4387.

(26) Cavalli, A.; Bolognesi, M. L.; Minarini, A.; Rosini, M.; Tumiatti, V.; Recanatini, M.; Melchiorre, C. Multi-target-directed ligands to combat neurodegenerative diseases. *J. Med. Chem.* **2008**, *51*, 347-372.

(27) Youdim, MB and Buccafusco JJ. Multifunctional drugs for various CNS targets in the treatment of neurodegenerative disorders. *Trends Pharm Sci* **2005**, 26, 27.

(28) Rodríguez-Franco, M. I.; Fernández-Bachiller, M. I.; Pérez, C.; Castro, A.; Martínez, A. Design and synthesis of N-benzylpiperidine-purine derivatives as new dual inhibitors of acetyl- and butyrylcholinesterase *Bioorg. Med. Chem.* **2005**, *13*, 6795-6802.

(29) Rosini, M.; Antonello, A.; Cavalli, A.; Bolognesi, M. L.; Minarini, A.; Marucci, G.; Poggesi, E.; Leonardi, A.; Melchiorre, C. Prazosin-related compounds. Effect of transforming the piperazinylquinazoline moiety into an

aminomethyltetrahydroacridine system on the affinity for α_1-adrenoreceptors. *J. Med. Chem.* **2003**, *46*, 4895-4903.

(30) Elsinghorst, P. W.; Cieslik, J. S.; Mohr, K.; Tränkle, C.; Gütschow, M. The first gallamine-tacrine hybrid: Design and characterization at cholinesterases and the M_2 muscarinic Receptor. *J. Med. Chem.* **2007**, *50*, 5685-5695.

(31) Fang, L.; Appenroth, D.; Decker, M.; Kiehntopf, M.; Roegler, C.; Deufel, T.; Fleck, C.; Peng, S.; Zhang, Y.; Lehmann, J. Synthesis and biological evaluation of NO-donor-tacrine hybrids as hepatoprotective anti-Alzheimer drug candidates. *J. Med. Chem.* **2008**, *51*, 713-716.

(32) Marco-Contelles, J.; León, R.; de los Ríos, C.; Guglietta, A.; Terencio, J.; López, M. G.; García, A. G.; Villarroya, M. Novel multipotent tacrine-dihydropyridine hybrids with improved acetylcholinesterase inhibitory and neuroprotective. activities as potential drugs for the treatment of Alzheimer's disease. *J. Med. Chem.* **2006**, *49*, 7607-7610.

(33) Zheng, H.; Youdim, M. B. H.; Fridkin, M. Site-activated multifunctional chelator with acetylcholinesterase and neuroprotective–neurorestorative moieties for Alzheimer's therapy. *J. Med. Chem*. **2009**, *52*, 4095-4098.

(34) Sterling, J; Herzig, Y; Goren, T; Finkelstein, N; Lerner, D; Goldenberg, W; Mikcolczi, I; Molnar, S; Rantal, F; Tamas, T; Toth, G; Zagyva, A; Zekany, A; Finberg, J; Lavian, G; Gross, A; Friedman, R; Razin, M; Huang, W; Krais, B; Chorev, M; Youdim, MB; Weinstock M. Novel dual inhibitors of AChE and MAO derived from hydroxyl aminoindan and phenethylamine as potential treatment for Alzheimer's disease. *J Med Chem* **2002,** 54, 5260-5279.

(35) Yogev-Falach, M; Bar-Am, O; Amit, T; Weinreb, O; Youdim, MB. A multifunctional, neuroprotective drug, ladostigil (TV3326), regulates holo-APP translation and processing. *FASEB J* **2006**, 20, 2177

(36) Youdim, MB and Weinstock, M. Molecular basis of neuroprotective activities of rasagiline and the anti-Alzheimer drug TV3326, [(N-propargyl-(3R)aminoindan-5-YL)-Ethyl methyl carbamate] *Cell Moll Neurobio* **2002**, 21, 555-573

(37) Youdim, MB; Amit, T; Bar-Am, O; xxxxx. Implications of co-morbidity for etiologu and treatment of neurodegenerative diseases with multifunctional, neuroprotective-neurorescue drugs; ladostigil. *Neurotoxic Res* **2006**, 10, 181-192

(38) Bar-Am, O; Amit, T; Weinreb, O; Youdim MB and Mandel S. Propargylamine-containing compounds as modulators of proteolitic cleavage of amyloid-beta protein precursor: involvement of MAPK and PKC activation. *J Alzheimer Dis* **2010**, 21, 361-371.

(39) Elsinghorst, PW; Härtig, W; Goldhammer, S; Grosche, J and Gütschow, M. A gorge-spanning, high affinity, cholinesterase inhibitor to explore beta-amyloid plaques. *Org Biomol Chem* **2009**, 7, 3940-3946

(40) Zheng, H; Youdim, MB, Fridkin, M. Site-activated chelators targeting acetylcholinesterase and monoamine oxidase for Alzheimer's therapy. *ACS Chem Biol* **2010**, 5, 603-610.

(41) Palermo, M; Bores, G; Huger, F; Kurys, B; Merriman, M; Olsen, G; Ong, H; Petko, W; O'Malley, G.. Combined AChE and Reversible MAO Inhibition as a potential therapeutic approach for Senile Dementia of the Alzheimer Type. *Abstracts of Papers*, 205th American Chemical Society National Meeting, **1993**; American Chemical Society, Washington DC, 1993; MEDI, abstract.

(42) Fink, DM; Palermo, MG; Bores, GM, Huger, F; Kurys, B; Merriman, M; Olsen, G; Ong, H; Petko, W; O'Malley, G.. Imino 1,2,3,4-Tetrahydrocyclopent[b]-indole Carbamates as dual inhibitors of Acetylcholinesterase and Monoamine Oxidase. *Bioorg Med Chem Lett* **1996,** 6, 625-630.

(43) Bruhlmann, C; Ooms, F; Carrupt, PA; Testa, B; Catto, M; Leonetti, F; Altomare, C; Carotti, A. Coumarins Derivatives as Dual Inhibitors of Acetylcholinesterase and Monoamine Oxidase. *J Med Chem* **2001**, 44, 3195-3198.

(44) Cruces, MA; Elorriaga, C; Fernandez-Alvarez, E and Nieto, O. Acetylenic and allenic derivatives of 2-(5-methoxyindolyl)methylamine synthesis and evaluation as selective inhibitors of monoamine oxidases A and B. *Eur J Med Chem* **1990**, 25, 257-265.

(45) Morón, J. A.; Campillo, M.; Pérez, V.; Unzeta, M.; Pardo, L. Molecular determinants of MAO selectivity in a series of indolylmethylamine derivatives: biological activities, 3D-QSAR/CoMFA analysis, and computational simulation of ligand recognition. *J. Med. Chem.* **2000**, *43*, 1684-1691.

(46) Pérez, V.; Marco, J. L.; Fernández-Álvarez, E.; Unzeta, M. Relevance of benzyloxy group in 2-indolyl methylamines in the selective MAO-B inhibition. *Brit. J. Pharmacol.* **1999**, *127*, 869-876.

(47) Inestrosa, N. C.; Alvarez, A.; Pérez, C. A.; Moreno, R. D.; Vicente, M.; Linker, C.; Casanueva, O. I.; Soto, C.; Garrido. J. Acetylcholinestearse accelerates assembly of amyloid-beta-peptides into Alzheimer's fibrils: Possible role of the peripheral site of the enzyme. *Neuron* **1996**, *16*, 881–891.

(48) De Ferrari, G. V.; Canales, M. A.; Shin, I.; Weiner, L. M.; Silman, I.; Inestrosa, N. C. A structural motif of acetylcholinesterase that promotes amyloid beta-peptide fibril formation. *Biochemistry* **2001**, *40*, 10447–10457.

(49) Rees, T. M.; Berson, A.; Sklan, E. H.; Younkin, L.; Younkin, S.; Brimijoin, S.; Soreq, H. Memory deficits correlating with acetylcholinesterase splice shift and amyloid burden in doubly transgenic mice. *Curr. Alzheimer Res.* **2005**, *2*, 291–300.

(50) Dinamarca, M. C.; Sagal, J. P.; Quintanilla, R. A.; Godoy, J. A.; Arrázola, M. S.; Inestrosa, N. C. Amyloid-beta-acetylcholinesterase complexes potentiate neurodegenerative changes induced by the Abeta peptide. Implications for the pathogenesis of Alzheimer's disease. *Mol. Neurodegener.* **2010**, *5*, 4.

(51) Cruces, M. A.; Elorriaga, C.; Fernández-Álvarez, E. The kinetics of monoamine oxidase inhibition by three 2-indolylmethylamine derivatives. *Biochem. Pharmacol.* **1990**, *40*, 535-543.

(52) Contreras, J. M.; Parrot, I.; Sippl, W.; Rival, Y. M.; Wermuth, C. G. Design, Synthesis, and Structure-Activity Relationships of a Series of 3-[2-(1-Benzylpiperidin-4-yl)ethylamino]pyridazine Derivatives as Acetylcholinesterase Inhibitors. *J. Med. Chem.* **2001**, *44*, 2707-2718.

(53) Hallinan, E. A.; Hagen, T. J.; Husa, R. K.; Tsymbalov, S.; Rao, S. N.; vanHoeck, J. P.; Rafferty, M. F.; Stapelfeld, A.; Savage, M.A.; Reichman, M. N. Substituted Dibenzoxazepines as Analgesic PGE2 Antagonists. *J. Med. Chem.* **1993**, *36*, 3293-3299.

(54) Yamanaka, T.; Ohkubo, M.; Kuroda, S.; Nakamura, H.; Takahashi, F.; Aoki, T; Mihara, K.; Seki, J.; Kato, M. Design, synthesis, and structure–activity relationships of potent GPIIb/IIIa antagonists: discovery of FK419. *Bioorg. Med. Chem.* **2005**, *13*, 4343–4352.

(55) Frølund, B.; Kristiansen, U.; Brehm, L.; Hansen, A B.; Krogsgaard-Larsen, P.; Falch, E. Partial GABAA receptor agonists. Synthesis and in vitro pharmacology

of a series of nonannulated analogs of 4,5,6,7-tetrahydroisoxazolo[4,5-*c*]pyridin-3-ol. *J. Med. Chem.* **1995**, *38*, 3287-3296.

(56) Kitbunnadaj, R.; Zuiderveld, O. P.; De Esch, I. J. P.; Vollinga, R. C.; Bakker, R.; Lutz, M.; Spek, A.L.; Cavoy, E.; Deltent, M. F.; Menge, W. M. P. B.; Timmerman, H.; Leurs, R. Synthesis and Structure−Activity Relationships of Conformationally Constrained Histamine H_3 Receptor Agonists. *J. Med. Chem,* **2003**, *46,* 5445-5457.

(57) Mandelli, G. R.; Maiorana, S.; Terni, P.; Lamperti, G.; Colibretti, M. L.; Imbimbo, B. P. Synthesis of New Cardioselective M_2 Muscarinic Receptor Antagonists. *Chem. Pharm. Bull.* **2000***, 48*, 1611-1622.

(58) Greig, N. H.; Utsuki, T.; Ingram, D.; Wang, K. Y.; Pepeu, G.; Scali, C.; Yu, Q. S.; Mamczarz, J.; Holloway, H. W.; Giordano, T.; Chen, D.; Furukawa, K.; Sambamurti, K.; Brossi, A.; Lahiri. D. K. Selective butyrylcholinesterase inhibition elevates brain acetylcholine, augments learning and lowers amyloid-β peptide in rodents. *Proc. Natl. Acad. Sci. USA* **2005**, *102*, 17213-17218.

(59) Kryger, G.; Silman, I.; Sussman, J. L. Structure of Acetylcholinesterase Complexed with E2020 (Aricept): Implications for the Design of New Anti-Alzheimer Drugs. *Structure* **1999**, *7*, 297–307.

(60) Camps, P.; Formosa, X.; Galdeano, C.; Muñoz-Torrero, D.; Ramírez, L.; Gómez, E.; Isambert, N.; Lavilla, R.; Badia, A.; Clos, M. V.; Bartolini, M.; Mancini, F.; Andrisano, V.; Arce, M. P.; Rodríguez-Franco, M. I.; Huertas, O.; Dafni, T.; Luque, F. J. Pyrano[3,2-c]quinoline-6-chlorotacrine hybrids as a novel family of acetylcholinesterase- and beta-amyloid-directed anti-Alzheimer compounds. *J. Med. Chem.* **2009**, *52*, 5365–5379.

(61) Galdeano, C.; Viayna, E.; Arroyo, P.; Bidon-Chanal, A.; Blas, J. R.; Muñoz-Torrero, D.; Luque, F. J. Structural determinants of the multifunctional profile of dual binding site acetylcholinesterase inhibitors as anti-Alzheimer agents. *Curr. Pharm. Design* **2010**, *16*, 2818-2836.

(62) Rydberg, E. H.; Brumshtein, B.; Greenblatt, H. M.; Wong, D. M.; Shaya, D.; Williams, L. D.; Carlier, P. R.; Pang, Y. –P.; Silman, I.; Sussman, J. L. Complexes of Alkylene-Linked Tacrine Dimers with *Torpedo californica* Acetylcholinesterase: Binding of Bis(5)-Tacrine Produces a Dramatic Rearrangement in the Active-Site Gorge. *J. Med. Chem*. **2006**, *49*, 5491–5500.

(63) Bourne, Y.; Kolb, H. C.; Radic, Z; Sharpless, K. B.; Taylor, P.; Marchot, P. Freeze-Frame Inhibitor Captures Acetylcholinesterase in a Unique Conformation. *Proc. Natl. Acad. Sci. USA* **2004** , *101*, 1449–1454.

(64) Morley, S. D.; Afshar, M. Validation of an Empirical RNA-Ligand Scoring Function for Fast Flexible Docking Using RiboDock®. *J. Comput.-Aided Mol. Des*. **2004**, *18*, 189–208.

(65) Barril, X.; Hubbard, R. E.; Morley, S. D. Virtual Screening in Structure-Based Drug Discovery. *Mini-Rev. Med. Chem.* **2004**, *4*, 779–791.

(66) Swanson, J. M. J.; Adcock, S. A.; McCammon, J. A. Optimized Radii for Poisson-Boltzmann Calculations with the AMBER Force Field. *J. Chem. Theory Comput.* **2005**, *1*, 484-493.

(67) Son, S.-Y.; Ma, J.; Kondou, Y.; Yoshimura, M.; Yamashita, E.; Tsukihara, T. Structure of Human Monoamine Oxidase A at 2.2-Å resolution: The control of opening the entry for substrates/inhibitors. *Proc. Natl. Acad. Sci. USA* **2008**, *105*, 5739-5744.

(68) De Colibus, L.; Li, M.; Binda, C.; Lustig, A.; Edmondson, D. E.; Mattevi, A. Three-Dimensional Structure of Human Monoamino Oxidase A (MAO A): Relation to the Structures of rat MAO A and human MAO B. *Proc. Natl. Acad. Sci USA* **2005**, *102*, 12684-12689.

(69) Binda, C.; Hubálek, F.; Li, M.; Herzig, Y.; Sterling, J.; Edmonson, D. E.; Mattevi, A. Crystal Structures of Monoamine Oxidase B in Complex with Four Inhibitors of the N-Propargylaminoindan Class. *J. Med. Chem*. **2004**, *47*, 1767-1774.

(70) Cavalli, A.; Bolognesi, M. L.; Capsoni, S.; Andrisano, V.; Bartolini, M.; Margotti, E.; Cattaneo, A.; Recanatini, M.; Melchiorre. C. A small molecule targeting the multifactorial nature of Alzheimer´s disease. *Angew. Chem. Int. Ed.* **2007**, *46*, 3689−3692.

(71) Muñoz-Ruiz, P.; Rubio, L.; García-Palomero, E.; Dorronsoro, I.; del Monte-Millán,M.; Valenzuela, R.; Usán, P.; de Austria, C.; Bartolini, M.; Andrisano, V.; Bidon-Chanal, A.; Orozco, M.; Luque, F. J.; Medina, M.; Martínez. A. Design, synthesis, and biological evaluation of dual binding site acetylcholinesterase inhibitors: New disease-modifying agents for Alzheimer´s disease. *J. Med. Chem.* **2005**, *48*, 7223−7233.

(72) Bolognesi, M. L.; Banzi, R.; Bartolini, M.; Cavalli, A.; Tarozzi, A.; Andrisano, V.; Minarini, A.; Rosini, M.; Tumiatti, V.; Bergamini, C.; Fato, R.; Lenaz, G.; Hrelia, P.; Cattaneo, A.; Recanatini, M.; Melchiorre. C. Novel Class of Quinone-Bearing Polyamines as Multi-Target-Directed Ligands To Combat Alzheimer's Disease. *J. Med. Chem.* **2007**, *50*, 4882–4897.

(73) Tumiatti, V.; Milelli, A.; Minarini, A.; Rosini, M.; Bolognesi, M. L.; Micco, M.; Andrisano, V.; Bartolini, M.; Mancini, F.; Recanatini, M.; Cavalli, A.; Melchiorre, C. Structure−Activity Relationships of Acetylcholinesterase Noncovalent

Inhibitors Based on a Polyamine Backbone. 4. Further Investigation on the Inner Spacer. *J. Med. Chem.* **2008**, *51*, 7308−7312.

(74) Bolognesi, M. L.; Bartolini, M.; Rosini, M.; Andrisano, V.; Melchiorre, C. Structure–activity relationships of memoquin: Influence of the chain chirality in the multi-target mechanism of action. *Bioorg. Med. Chem. Lett.* **2009**, *19*, 4312−4315.

(75) Jacob-Roetne R; Jacobsen H. Alzheimer's Disease: From Pathology to Therapeutic Approaches. *Angew. Chem Int Ed 2009*, **48**, 3030-3059.

(76) Perry, E. K.; Perry, R. H.; Blessed, G.; Tomlinson, B. E. Changes in Brain Cholinesterases in Senile Dementia of Alzheimer Type. *Neuropathol. App. Neurobiol.* **1978**, *4*, 273-277.

(77) Greig, N. H.; Utsuki, T.; Yu, Q.; Zhu, X.; Holloway, H. W.; Perry, T.; Lee, B.; Ingram, D. K.; Lahiri, K. A New Therapeutic Target in Alzheimer's Disease Treatment: Attention to Butyrylcholinesterase. *Curr. Med. Res. Op.* **2001**, *17*, 159-165.

(78) Ellman, G. L.; Courtney, K. D.; Andres, V.; Featherstone, R. M. A New and Rapid Colorimetric Determination of Acetylcholinesterase Activity *Biochem. Pharmacol.* **1961**, *7*, 88-95.

(79) Segel, I. H. *Enzyme Kinetics*. John Wiley: Toronto, 1975, pp 838.

(80) Gomez, N.; Unzeta, M.; Tipton, K. F.; Anderson, M. C.; O'Carrol, A. M. Determination of Monoamino Oxidase Concentrations in Rat Liver by Inhibitor Binding. *Biochem. Pharmacol.* **1986**, *35*, 4467-4472

(81) Fowler, C. J.; Tipton, K. F. Concentration Dependence of the Oxidation of Tyramine by the Two Forms of Rat Liver Mitochondrial Monoamine Oxidase. *Biochem. Pharmacol.* **1981**, *30*, 3329-3332.

(82) Bartolini, M.; Bertucci, C.; Cavrini, V.; Andrisano, V. Beta-Amyloid Aggregation Induced by Human Acetylcholinestrase: Inhibition Studies. *Biochem. Pharmacol,* **2003**, *65*, 407–416.

(83) Wlodek, S. T.; Antosiewicz, J.; McCammon, J. A.; Straatsma, T. P.; Gilson, M. K.; Briggs, J. M.; Humblet, C.; Sussman, J. L. Binding of Tacrine and 6-Chlorotacrine by Acetylcholinesterase. *Biopolymers* **1996**, *38*, 109-117

(84) Dvir, H.; Wong, D. M., Harel, M.; Barril, X.; Orozco, M.; Luque, F. J.; Muñoz-Torrero, D.; Camps, P.; Rosenberry, T. L.; Silman, I.; Sussman, J. L. 3D Structure of *Torpedo californica* Acetylcholinesterase Complexed with Huprine X at 2.1 Å Resolution: Kinetic and Molecular Dynamic Correlates. *Biochemistry* **2002**, *41*, 2970–2981.

(85) Binda, C.; Hubalek, F.; Li, M.; Herzig, Y.; Sterling, J.; Edmonson, D. E.; Mattevi, A. Binding of Rasagiline-Related Inhibitors to Human Monoamine Oxidases: A Kinetic and Crystallographic Analysis. *J. Med. Chem*. **2005**, *48*, 8148-8154.

(86) (Ngamelue, M.N, Homma, K ; Lockridge, O ; Asojo, OA. Crystallization and X-rau structure of full-length recombinant human butytylcholinesterase. *Acta Crystallogr.Sect.F* **2007**, 63:723-727

(87) (Carletti, E ; Li, H ; Li, B ; Ekström, F ; Nicolet, Y ; Loiodice, M ; Gillon, E ; Froment, MT, Lockridge, O ; Schopfer, LM ; Masson, P ; Nachon, F. Aging of cholinesterases phosphylated by tabun proceeds through O-dealkylation. *J.Am.Chem.Soc*. **2008**, 130(47):16011-16020

(88) Case DA, Darden TA, Cheatham TE III, Simmerling CL, Wang J, Duke RE, Luo R, Merz KM, Pearlman DA, Crowley M, Walker RC, Zhang W, Wang B, Hayik S, Roitberg A, Seabra G, Wong KF, Paesani F, Wu X, Brozell S, Tsui

V, Gohlke H, Yang L, Tan C, Mongan J, Hornak V, Cui G, Beroza P, Mathews DH, Schafmeister C, Ross WS, Kollman PA (2006) AMBER, version 9; University of California: San Francisco.

(89) Bayly, C. I.; Cieplak, P.; Cornell, W. D.; Kollman, P. A. *J. Phys. Chem.* **1993**, *97*, 10269–10280.

(90) M. J. Frisch, G. W. Trucks, H. B. Schlegel, G. E. Scuseria, M. A. Robb, J. R. Cheeseman, J. A. Montgomery Jr., T. Vreven, K. N. Kudin, J. C. Burant, J. M. Millam, S. S. Iyengar, J. Tomasi, V. Barone, B. Mennucci, M. Cossi, G. Scalmani, N. Rega, G. A. Petersson, H. Nakatsuji, M. Hada, M. Ehara, K. Toyota, R. Fukuda, J. Hasegawa, M. Ishida, T. Nakajima, Y. Honda, O. Kitao, H. Nakai, M. Klene, X. Li, J. E. Knox, H. P. Hratchian, J. B. Cross, V. Bakken, C. Adamo, J. Jaramillo, R. Gomperts, R. E. Stratmann, O. Yazyev, A. J. Austin, R. Cammi, C. Pomelli, J. W. Ochterski, P. Y. Ayala, K. Morokuma, G. A. Voth, P. Salvador, J. J. Dannenberg, V. G. Zakrzewski, S. Dapprich, A. D. Daniels, M. C. Strain, O. Farkas, D. K. Malick, A. D. Rabuck, K. Raghavachari, J. B. Foresman, J. V. Ortiz, Q. Cui, A. G. Baboul, S. Clifford, J. Cioslowski, B. B. Stefanov, G. Liu, A. Liashenko, P. Piskorz, I. Komaromi, R. L. Martin, D. J. Fox, T. Keith, M. A. Al-Laham, C. Y. Peng, A. Nanayakkara, M. Challacombe, P. M. W. Gill, B. Johnson, W. Chen, M. W. Wong, C. Gonzalez, J. A. Pople, *Gaussian 03*, revision B.04; Gaussian, Inc.: Pittsburgh, PA, 2003.

(91) Srinivasan, J.; Cheatham, T. E., III; Cieplak, P.; Kollman, P. A.; case, D. A. Continuum solvent studies of the stability of DNA, RNA and phosphoramidate-DNA helices. *J. Am. Chem. Soc.* **1998**, *120*, 9401-9409.

(92) Stoica, I.; Sadiq, S. Kashif; Coveney, P. V. Rapid and accurate prediction of binding free energies for saquinavir-bound HIV-1 proteases. *J. Am. Chem. Soc*. **2008**, *130*, 2639-2648.

(93) Homak, V.; Abel, R.; Okur, A.; Strockbine, B.; Roitberg, A.; Simmerling, C. Comparison of Multiple Amber Force Fields and Development of Improved Protein backbone Parameters. *Proteins*. **2006**, *65*, 712-725.

(94) Wang, J.; Wolf, R. M.; Caldwell, J. W.; Kollman, P. A.; Case, D. A. Development and Testing of a General AMBER Force Field. *J. Comput. Chem.* **2004**, *25*, 1157-1174.

(95) Wang, J.; Wang, W.; Kollman, P.A.; Case, D. A. Automatic Atom Type and Bond Type Perception in Molecular Mechanical Calculations. *J. Mol. Graphics Model.* **2006**, *25*, 247-260.

(96) Jorgensen, W. L.; Chandrasekhar, J.; Madura, J. D.; Impey, R. W.; Klein, M. L. Comparison of simple potential functions for simulating liquid water. *J. Chem. Phys* **1983**, *79*, 926-935.

Table of Contents graphic

A multipotent MAO+ChE inhibitor for Alzheimer's Disease

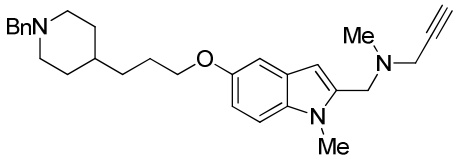

N-((5-(3-(1-benzylpiperidin-4-yl)propoxy)-1-methyl-1*H*-indol-2-yl)methyl)-*N*-methylprop-2-yn-1-amine

IC_{50} (nM) MAO-A	IC_{50} (nM) MAO-B	IC_{50} (μM) EeAChE	IC_{50} (μM) eqBuChE
5.2 ± 1.1	43.1 ± 7.9	0,35 ± 0,01	0,46 ± 0,065

1. Annex Chapter III

1.1 Supplementary Table 1.

A series of indolyl propargylamino derivatives of PF9601N were investigated as MAO (A and B) and AChE and BuChE inhibitors (Table S1). As previously found in literature, donepezil was found to be a potent AChE inhibitor although it slightly inhibited BuChE. Regarding MAO, donepezil behaved as a poor MAOI being more selective towards the B isoform. Regarding the indolyl propargylamine derivatives (FA73, FA64 and FA87), as previously reported by our group (Pérez et al., 1999), they were potent and selective MAO-B inhibitors, with FA87 being the most potent towards both isoforms, and FA65 the less selective. Surprisingly, these FA derivatives appeared to moderately and selectively inhibit BuChE, with the exception of FA65 that, surprisingly, inhibited only AChE in the high nanomolar range.

A first SAR of the replacement of the benzyloxy substituent in position 5 of the indole ring by a benzylethyloxy to give ASS50 provoked a complete loss of the inhibition towards both ChEs and dramatically decreased the inhibition towards MAO. By contrast, the introduction of a carbamate to produce ASS62 produced a significant increase in the potency towards MAO inhibition and surprisingly caused a slight change in the selectivity. No effect was found regarding ChEs inhibition.

As already reported in this Chapter, the introduction of the benzylpiperidine moiety present in donepezil into the indolyl propargylamino moiety of the FA derivatives to yield the 1-benzylpiperidine-4-yl derivatives (ASS200 to ASS251) gave an interesting SAR study. Thus, we found that the length of the tether that connects both substructures had no effect on the potency towards AChE, which was found in the submicromolar range. These derivatives also showed similar potencies against BuChE, leading to a slight selectivity towards AChE. Interestingly, compared to the parent compound donepezil, these derivatives were found to be 7-16-fold more potent for BuChE inhibition, although 39-52-fold less potent for AChE inhibition. Regarding MAO inhibition, the 1-benzylpiperidine-4-yl derivatives appeared as potent and selective MAO-AIs with the exception of ASS234 that also potently inhibited MAO-B. In this case, the length of the tether appeared to be a crucial factor for the inhibitory potency.

Compared to the 1-benzylpiperidine-4-yl derivatives, the reversion of the piperidine ring in ASS86 and ASS77 had a dramatic effect on the inhibitory potency against AChE. A drastic reduction in activity was also found upon replacement of the piperidine unit by a piperazine one (giving ASS94). These chemical modifications, although having less effect on the BuChE potency, had a significant effect on the inhibition of MAO.

Table S1. Inhibitory activities towards monoamine oxidases A (MAO-A) and B (MAO-B), and acetylcholinesterase (AChE) and butyrylcholinesterase (BuChE), by a new series of indolyl propargylamine derivative compounds. Activities of the reference compounds (donepezil, PF9601N, FA65 and FA87) are also shown. Data are the mean ± SEM of three independent experiments in triplicate.

		IC_{50} (nM)		Selectivity	IC_{50} (μM)		Selectivity
Compound	**Structure**	**MAO-A**	**MAO-B**	**MAO-B/ MAO-A**	**AChE**	**BuChE**	**BuChE/ AChE**
Donepezil	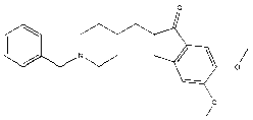	854800 ± 13300	15400 ± 2200	0.02	0.0067± 0.0004	7.4 ± 0.1	1104
PF9601N (FA73)		1250 ± 15	22 ± 1	0.017	>100	43 ± 3	>0.43
FA87		0.79 ± 0.3	0.025 ± 0.009	0.032	>100	29 ± 3	>0.29
FA65		100 ± 7	63 ± 2.4	0.63	0.25 ± 0.1	>100	>400
ASS50		1383 ± 99	1001 ± 205	0.72	>100	>100	>1
ASS62		3.2 ± 0.7	5.2 ± 1.8	1.63	>100	>100	>1
ASS86 (n=2)		143 ± 44.3	1457 ± 499	10.2	>100	0.8 ± 0.1	>0.008
ASS77 (n=3)		65.4 ± 17.4	11320 ± 2380	173.1	18.1 ± 0.4	2.2 ± 0.4	0.12
ASS94 (n=3)		30.5 ± 13.5	1640 ± 707	53.8	>100	7.6 ± 0.4	>0.08
ASS200 (n=1)		82.2 ± 3.2	745.4 ± 19.9	9.1	0.31 ± 0.04	1.1 ± 0.2	3.5
ASS188 (n=2)		6.7 ± 1.8	129.6 ± 41.4	19.3	0.42 ± 0.04	2.1 ± 0.2	5.0
ASS234 (n=3)		5.2 ± 1.1	43.1 ± 7.9	8.3	0.35 ± 0.01	0.46 ± 0.06	1.3
ASS251 (n=4)		10.5 ± 4.4	2774 ± 116	264.2	0.26 ± 0.07	0.99 ± 0.08	3.8

CHAPTER IV

ASS234, a novel multitarget compound, reduces Aβ fibrillogenesis and protects neuronal cells from Aβ and hydrogen peroxide toxicity.

Irene Bolea, Alejandro Gella and Mercedes Unzeta

Manuscript in preparation

ASS234, a novel multitarget compound, reduces Aβ fibrillogenesis and protects neuronal cells from Aβ and hydrogen peroxide toxicity

Irene Bolea[±] Alejandro Gella[#], and Mercedes Unzeta[±]

[±]Departament de Bioquímica i Biología Molecular, Facultat de Medicina, Universitat Autònoma de Barcelona, 08193 Bellaterra, Barcelona, Spain. [#] Facultat de Medicina i Ciències de la Salut. Universitat Internacional de Catalunya. C/ Josep Trueta s/n, Sant Cugat del Vallès, 08195 Barcelona, Spain.

*To whom correspondence should be addressed: Phone: +34-93-5811624; Fax: +34-93-5811573;
E-mail: Mercedes.unzeta@uab.cat

[±]Departament de Bioquímica i Biología Molecular, Facultat de Medicina, Universitat Autònoma de Barcelona

Abbreviations: AD, Alzheimer's disease; Aβ, β-amyloid peptide; fibrillogenesis; monomer; oligomer; hAChE, human acetylcholinesterase; caspases; apoptosis; necrosis

Introduction

Alzheimer's disease (AD) appears as the fourth leading cause of death and the most common cause of dementia in the elderly population. The predominant clinical manifestations are a progressive memory deterioration, disordered behaviour and impairment in language and comprehension (Tsolaki et al., 2001), which are the result of the neuronal loss in the hipoccampus and cortex of patients. These features are accompanied by the neurofibrillary tangles (NFT), intracellular fibrillar deposits mainly composed by tau protein (Goedert et al., 1988) and the senile plaques (SP), formed by the deposition of aggregated amyloid-β-peptide (Glenner & Murphy, 1989). Although the pathogenesis of AD is not yet fully understood the scientific consensus is quite firm in describring it as a multifactorial disease caused by genetic, environmental and endogenous factors, which include excessive protein misfolding and aggregation (Terry et al., 1964; Grundke-Iqbal et al., 1986) oxidative stress and free radical formation (Coyle & Puttfarcken, 1993; Perry, 2000; Gella et al., 2009), metal dyshomeostasis (Huang et al, 2004) and excitotoxic and neuroinflammatory processes (Mishizen-Eberz et al., 2004).

Currently, the available anti-AD medications are mainly based in the cholinergic hypothesis of AD (Davies & Maloney, 1976), and thus principally include acetylcholinesterase inhibitors (AChEIs), although a N-methyl-D-aspartate (NMDA) receptor antagonists has also been approved by the Food and Drug Administration (FDA) (Birks et al., 2000; Birks & Harvey, 2006; Loy & Schneider, 2004; Areosa et al., 2005). Nevertheless, these drugs are efficient to produce only modest symptomatic improvements in some of the patients, but not to cure or stop the disease progression. Thus, a new therapeutic approach based on the "one molecule, multiple targets" paradigm has recently appeared (Buccafusco & Terry, 2000; Youdim & Buccafusco, 2005). This strategy is based on the evidence that a single drug that acts on a single specific target to produce the desired clinical effects might not be suitable for the complex nature of AD. Then, the multi-target-directed ligand (MTDL) approach (Cavalli et al., 2008) has been the subject of increasing attention by many research groups, which have developed a wide variety of compounds acting on very diverse targets (Rodriguez-Franco et al., 2005; Rosini et al., 2003; Elsingorst et al., Fang et al., 2008; Zheng et al., 2009). In this context, we have recently synthesized a serie of bifunctional hybrid compounds containing the 1-benzylpiperidine moiety present in

donepezil and the 1-methyl-1*H*-indol-2-yl)methyl]-*N*-methylprop-2-yn-1-amine moiety of the monoamine oxidase B (MAO-B) inhibitor PF9601N (Bolea et al., 2011 Submitted to the Journal of Medicinal Chemistry). Among the synthesised compounds, ASS234, *N*-[5-(3-(1-benzylpiperidin-4-yl)propoxy)-1-methyl-1*H*-indol-2-yl]methyl]-N-methylprop-2-yn-1-amine, behaved as a potent monoamine oxidase A and B inhibitor and a moderately potent AChE, being also active for BuChE. Moreover, ASS234 demonstrated to bind to the peripheric anionic site (PAS) of AChE since it was able to significantly prevent the AChE-induced Aβ aggregation. These promising results led us to study in depht the behaviour of this compound against Aβ peptide aggregation. Thus, the present study describes in more detail the action of the multifunctional compound, ASS234, in terms of inhibition of self-induced and huAChE-dependent Aβ aggregation. Besides, it also shows the neuroprotective and antioxidant properties exerted by ASS234 against Aβ and H_2O_2 toxicity, in human neuroblastoma SH-SY5Y cells and PC12 cells. Finally, the possible anti-inflammatory effect of ASS234 has also been assessed in Bv2 microglial cells.

Materials and Methods

Inhibition of Aβ self-aggregation.

The inhibition of Aβ (1-40 and 1-42) self-aggregation by ASS234 was studied by using the thioflavin T-based fluorometric assay previously described by Bartolini, et al (2003) with little modifications. Briefly, Aβ peptides (Bachem AG, Switzerland) were pretretated with 1,1,1,3,3,3-hexafloro-2-propanol (HFIP, Sigma Chemicals) and redissolved in 10 mM phosphate buffer (PBS, pH11.2 adjusted with NH_4OH). Final $A\beta_{1-40}$ and $A\beta_{1-42}$ stock solutions concentration were 231μM and 443 μM, respectively. To study the effect of ASS234 on fibril formation, experiments were performed by incubating the peptides (final Aβ concentration=40μM) with and without different concentrations of ASS234 (10μM-200μM) in a microplate. Blanks containing only the inhibitor were also prepared. Samples were diluted to a final volume of 200μl with 10mM PBS (pH 7.4) and 35 μM thioflavin T in 50 mM glycine–NaOH buffer (pH 8.5) was added. Experiments were performed on a Synergy HT microplate spectrofluorometer (Bio-Tek, USA). The fluorescence intensity was carried out (λ_{exc}= 485 nm; λ_{em}= 528 nm) at 37ºC every 10 min for 8 h, and values at plateau (400 min) were averaged after subtracting the background fluorescence of 35 μM thioflavin

T. The fluorescence intensities were compared and the percent inhibition due to the presence of the inhibitor was calculated by the following expression: 100-(IFi/IF_0 x 100) where IFi and IF_0 are the fluorescence intensities obtained in the presence or absence of inhibitor, respectively.

Inhibition of huAChE-induced Aβ aggregation.

Aliquots of 231μM $A\beta_{1-40}$ or 443μM $A\beta_{1-42}$ (Bachem AG, Switzerland) lyophilised from 1mg/ml HFIP solution were redissolved in 10 mM phosphate buffer (PBS, pH11.2 adjusted with NH_4OH). Final concentration of Aβ peptides was always 40 μM. For co-incubation experiments, aliquots of human recombinant AChE (Sigma Chemicals) (0.4 μM final concentration, ratio Aβ/huAChE=100/1) in the presence of 100 μM ASS234 were added. Blanks containing Aβ, huAChE, Aβ plus ASS234 and huAChE plus ASS234 were also prepared. To quantify the amyloid fibril formation, the Thioflavin T fluorescence method (Bartolini et al., 2003) was performed at 37ºC as above described. The fluorescence intensities were compared and the percent inhibition due to the presence of the inhibitor was calculated by the following expression: 100-(IFi/IF_0 x 100) where IFi and IF_0 are the fluorescence intensities obtained in the presence or absence of inhibitor, respectively.

Negative stain electron microscopy (EM)

Ten microliters of samples were took from the microplate at the end of the ThT aggregation method and placed for ten minutes on a copper grid with a carbon surface and then dried with Whatman paper. Samples were then stained with 2% (w/v) Uranyl acetate for 1 min and dried. Transmission electron micrographs were obtained using an Hitachi H-7000 (75 kV) microscope.

Cell culture and treatments

SH-SY5Y cells

SH-SY5Y human neuroblastoma cells were obtained from the European Collection of Cell Cultures (ECACC). Cells were grown in Dulbecco's modified Eagle medium/Ham's F-12 medium (DMEM/F-12, Sigma-Aldrich;St Louis, MO; USA) with 15% fetal bovine serum (FBS), l-glutamine (PAN Biotech, Aidenbach, Germany), penicillin/streptomycin (PAN Biotech) and non-essential aminoacids (Sigma-Aldrich)

and maintained at 37ºC with 5% CO_2. Cells were seeded at 125 000 cells/well onto Collagen Type I (BD Biosciences, Bedford, MA, USA)-coated plates and starved with serum-free media overnight before treatments. ASS234 (5-10 μM) was added to the medium 60 min prior to Aβ (40 μM) treatment. All incubations and pre-incubations were at 37ºC. 24-well plates were used for cell viability assay and immunocytochemistry whereas 6-well plates were used for western blot experiments.

PC12 ***cells***

PC12 cells were obtained from the European Collection of Cell Cultures (ECACC). Cells were grown in Dulbecco's modified Eagle medium/Ham's F-12 medium (DMEM/F-12, Sigma-Aldrich;St Louis, MO; USA) with high glucose (4.5 g/L), 10% fetal bovine serum (FBS), l-glutamine (PAN Biotech, Aidenbach, Germany), and penicillin/streptomycin (PAN Biotech) and maintained at 37ºC with 5% CO_2. Cells were seeded in 48-well plates at 100 000 cells/well onto Collagen Type I (BD Biosciences, Bedford, MA, USA)-coated plates and starved with 1% FBS medium overnight before treatments. ASS234 (0.01-10 μM) was added to the medium 24 h prior to H_2O_2 (200 μM) treatment. All incubations and pre-incubations were at 37ºC.

Bv2 cells

Bv2 cells were obtained from the European Collection of Cell Cultures (ECACC). Cells were grown in Dulbecco's modified Eagle medium/Ham's F-12 medium (DMEM/F-12, Sigma-Aldrich;St Louis, MO; USA) with 10% fetal bovine serum (FBS), penicillin/streptomycin (PAN Biotech) and amphotericine and maintained at 37ºC with 5% CO_2. Cells were seeded in 48-well plates at 100 000 cells/well onto Collagen Type I (BD Biosciences, Bedford, MA, USA)-coated plates and medium was changed weekly. After 21 days culture cells were pretretaed with ASS234 (0.01-1 μM) for 60 min and then treated with 100 ng/ml *Escherichia coli* LPS plus 0.5 ng/ml INF-γ (Sigma, St. Louis, MO). Mixed cultures were 75% microglia and 25% astrocytes.

Cell viability assay

MTT [(3-(4,5-Dimethylthiazol-2-yl)-(2,5-diphenyltetrazolium bromide] assays were performed as previously described (Mosmann T, 1983) with minor modifications. After treatments, cells were incubated with 0.5 mg/ml of MTT (Sigma-Aldrich) at 37 ºC in a

CO_2 incubator for 45 min. Then, the medium with MTT was removed and the resulting formazan dye was solubilised with dimethylsulfoxide (Sigma-Aldrich). Absorbance was measured using a spectrophotometer (Sinergy HT, Biotek) at a test wavelength of 560 nm and reference wavelength of 620 nm.

Nitrite assay

Nitrite content was measured in the culture medium the Bv2 cells as an indicator of NO production. The Griess Method was used following manufacturer's instructions (Molecular Probes). Briefly, after 48 h treatment, 75 µl-aliquots of cultured supernatant were mixed with an equal volume of Griess reagent and the absorbance was determined at 570 nm using a microplate reader. Sodium nitrite, at concentrations of 0 to 100 mM, was used as a standard.

LDH activity

LDH enzymatic activity in the culture medium was used to evaluate the extent of cellular damage produced by Aβ in SH-SY5Y cells and to study the effect of ASS234. The culture medium was collected after the 24h incubation of cells with Aβ peptide with and without ASS234 pretreatment and LDH activity was determined using LDH IFCC kit (Biosystems) according to the manufacturer's instructions. The activity was expressed as the relative percentage of neuronal death using respective values for vehicle-treated cells as 100%.

Western Blot analysis

For determination of caspase-3 cleavage, caspase-9 and PARP, cells were lysed with SDS sample buffer (62.5 mM Tris-HCl, pH6.8, 2%SDS, 10%glycerol, all from Sigma-Aldrich) without dithiothreitol (DTT) and bromophenol blue, to avoid interference with protein quantification. Protein concentration was determined using BCA protein assay. Samples were sonicated to shear genomic DNA and reduce the viscosity of the lysates and then 50mM DTT and 0.1% bromophenol blue were added. Lysates were heated at 99ºC for 3 min, run on SDS-PAGE and then transferred onto nitrocellulose (Whatman-Schleicher & Schuell, Dassel, Germany) membranes. Transferred membranes were blocked with 5% (w/v) non-fat dry milk in Tris-buffered saline (TBS) containing 0.1% Tween-20 for 1h and then incubated with anti-cleaved caspase 3 antibody (1:1000),

anti-caspase 9 (1:1000), anti-PARP (1:1000) or anti-β-tubulin antibody (Sigma, 1: 100 000) overnight at 4ºC. Unless otherwise stated, these antibodies were from Cell Signaling Technology, Danvers, MA, USA. After washings, bolts were exposed to horseradish peroxidase-conjugated goat anti-rabbit (1:2000, BD Biosciences) or rabbit anti-mouse secondary antibodies (1:2000, DAKO, Glostrup, Denmark). Membranes were developed using an enhanced chemiluminiscence (ECL) detection system (Amersham Biosciences).

Nuclear fragmentation assay

After treatments, cells were washed with PBS and fixed with 4% paraformaldehyde (Sigma-Aldrich, St.Louis, MO, USA) in PBS for 10 min at RT. After two further washings, cells were stained with 0.5 μg/ml of Hoechst 33258 (Sigma-Aldrich, St.Louis, MO, USA) for 30 min at RT to evidence nuclear fragmentation and chromatin condensation. Stained nuclei were visualized under an inverted microscope (Nikon Eclipse TE2000-E, Nikon; Tokio, Japan).

Statistical analyses

Data are shown as the mean ± SEM. All statistical analyses were completed using the GraphPad Prism program (Prism 3.0, GraphPad Software Inc; San Diego, CA, USA). Differences between treatments were stablished by one-way ANOVA followed by the Bonferroni post-test. In the figures a single symbol will always mean $p<0.05$, two $p<0.01$ and three $p<0.001$.

Results

ASS234 inhibits Aβ self-induced aggregation

ASS234 slightly inhibited $A\beta_{1-40}$ self-aggregation (Fig 1A and Table 1) being a concentration-independent process and producing an average value 9.1 ± 2.4% inhibition of aggregation at the concentrations tested (10-200μM). Negative stain transmission EM (Fig 1C) was performed on samples from the microplate once finished the aggregation process in the ThT method. Micrographs showed an untreated $A\beta_{1-40}$ where numerous fibrillar structures are present whereas the appearance of fibrils when $A\beta_{1-40}$ was co-incubated with 100 μM ASS234 appeared shorter, less concentrated, and

disordered. Although at this concentration ASS234 only partially inhibited aggregation (as shown by ThT method in Fig 1A) and so fibrils are still present, electron micrographs indicate a higher presence of protofibrils than mature fibrils.

On the other hand, ASS234 potently inhibited $A\beta_{1-42}$ self-aggregation (Fig 1B) in a concentration-independent process (10-200μM) (see also Table 1). The average value is 49.8 ± 4.9 %. We used propidium iodide (PI) as reference compound and we obtained a reduction of Aβ self-induced aggregation of 33.3±2.1%, being this value significantly lower than that found for ASS234 (data not shown). When PI was tested at equimolar concentrations (Aβ/PI=1/1), similarly to that previously reported by other groups, we found a reduction of Aβ aggregation of 78.6 ± 3.8%. The electron micrographs (Fig 1D) showed an untreated $A\beta_{1-42}$ where typical amyloid fibrils are clearly detected. However, when peptide was co-incubated with 100 μM ASS234, fibrils were significantly less numerous, clearly shorter and less entangled. Moreover, it is worth noting that in ASS234 treated samples fibrils were detected together with circular bodies which diameter is between 6 and 8 nm. According to previous EM works (Lambert et al., 1998; Lashuel et al., 2002; Ono et al., 2009) such structures would be consistent with Aβ species from trimers to tetramers.

Control experiments were also conducted using a range of similarly sized molecules that demonstrate no inhibitory activity towards both $A\beta_{1-40}$ and $A\beta_{1-42}$ aggregation across the time scales and peptide concentration used in the above assay (data not shown).

ASS234 inhibits huAChE-dependent Aβ aggregation

Consistent with previous works, Aβ aggregation was significantly increased when huAChE (ratio Aβ/huAChE, 100/1) was added to the microplate (Fig 2A-C) demonstrating the capacity of huAChE to promote Aβ fibrillogenesis which is known to be exerted through its PAS (Terry, 1994; Inestrosa, 1996). In contrast, when 100 μM ASS234 was co-incubated with either $A\beta_{1-40}$ (Figure 2A) or $A\beta_{1-42}$ (Figure 2C) plus huAChE, the aggregation process was blocked in a 32.4 ± 7.0% and a 39.6 ± 13.0%, respectively (see also 2E). Electron micrographs (Figure 2B-D) clearly show that, huAChE promotes the presence of a higher amount of fibrils, but when ASS234 was co-incubated with the peptide and the enzyme, fibers are seen in less numbers and shorter, which indicates that ASS234 is also able to prevent the aggregation of Aβ peptide

induced by huAChE and, thus, demonstrating that the inhibitor is able to bind to the PAS of the enzyme.

ASS234 exerts antioxidant properties in PC12 cells

We assessed the possible antioxidant effect of ASS234 against H_2O_2 damage by using MTT method. PC12 cells treated with 200 μM H_2O_2 for 2h showed a significant decrease in cell viability of 60% (Figure 3). However, when a 24h pre-treatment was performed with ASS234 (0.01-1 μM), cell toxicity was significantly prevented in a dose-independent manner to the same extent that Trolox, a vitamin E derivative and a well known antioxidant. When cells were pretreated with 10μM ASS234, no effect was observed.

ASS234 does not protect glial cells against inflammation

We studied the possible anti-inflammatory effect of ASS234 against LPS+INF-γ damage by using the Griess method which quantifies the nitrite content in the supernatant of cultured cells. Bv2 cells treated with 100ng/ml LPS plus 0.5 ng/ml INF-γ for 48 h showed a significant increase in the amount of NO released to the medium (Figure 4). 60 min pre-treatment with ASS234 did not prevent NO release at any concentration tested (0.1-10 μM), as it did Ibuprofen, a well-known antioxidant.

ASS234 pretreatment prevents cellular toxicity

In order to investigate the direct toxic effect of $A\beta_{1-42}$ on neuronal viability, we examined the degree of cell death by using the MTT cell viability assay and measuring the LDH release in SH-SY5Y cells. As shown in Figure 5A, MTT assay revealed that $A\beta_{1-42}$ treatment provokes a reduction of cell viability of the 50%, which was significantly prevented by ASS234 pre-treatment (60 min, 5-10 μM) in a dose-independent manner. Accordingly, LDH assay showed that LDH released into the medium of cells treated with $A\beta_{1-42}$ was significantly above control levels, indicating that cell death had occurred (Figure 5B). Nevertheless, when ASS234 was added to the medium prior to treatment a significant and reduction of LDH activity was observed, which was dependent on the concentration of the compound and being 10 μM ASS234 the most effective concentration. Figure 5C shows the changes observed in the

morphology of cells after treatment with $A\beta_{1-42}$ which was found retracted and less numerous. Pre-treatment with ASS234 prevented the appearance of this morphology.

ASS234 prevents nuclear fragmentation

Hoechst 33258 nuclear staining revealed the presence of condensed nuclei and apoptotic bodies after 24h of $A\beta_{1-42}$ (40μM) treatment (Fig 6). In contrast, when ASS234 (5μM and 10 μM) was added to the culture medium prior to $A\beta_{1-42}$ exposure, the number of condensed or fragmented nuclei was considerably reduced conferring the highest reduction at 10 μM ASS234, as confirmed by the quantification.

ASS234 prevents $A\beta_{1-42}$-induced features of apoptotic cell death

As we observed the presence of condensed nuclei, we next assessed whether caspase-3, one of the main executioner caspases in apoptotic processes, was activated under our experimental conditions. Proteolytic processing of this protease results in two cleavage products, p19 and p17, which are the active forms. Then, western blot analyses of active caspase-3 were performed. Western blot of total lysates revealed the presence of p19 and p17 fragments of active caspase-3 after 24 h of $A\beta_{1-42}$ (40μM) treatment. Pretreatment with ASS234 (5 and 10 μM) before cell death induction, resulted in a significant reduction in the activation of this caspase. Caspase-3 activation was also confirmed assessing the proteolysis of PARP, one of its endogenous substrates. Western blot analysis showed proteolysis of PARP in $A\beta_{1-42}$-treated cells, as evidenced by the appearance of the 85 kDa proteolysed form. In ASS234-treated cells, $A\beta_{1-42}$-induced PARP cleavage was significantly prevented, confirming the capability of ASS234 in reducing caspase-3 activity. Caspase 9 is reported to play a prominent role as initiator caspase in Aβ-induced cell death. Therefore, we next explored whether ASS234 might prevent the activation of this protease in our experimental conditions. Proteolytic processing of this protease results in two cleavage products, p37 and p35, which are the active forms. Western blot revealed the presence of p37 and p35 fragments of active caspase-9 after treatment. ASS234 (5 and 10 μM) added prior to cell death induction, resulted in a significant reduction in the activation of this caspase. These results suggest that ASS234 prevents the apoptosis induced by $A\beta_{1-42}$.

Discussion

Screening molecules to prevent or reverse the oligomerization and fibrillization process of Aβ have been reported to be of therapeutic value in the treatment of AD (Necula M, 2007. Ono K, 2004). Among anti-Aβ aggregation compounds, several type of drugs have been specially synthesised to this purpose but also natural substances such us polyphenols (Ono K, 2004; Ono K, 2005; Riviere C, 2007; Riviere C, 2008) have been reported.

Our results show that ASS234 is able to inhibit both the Aβ-self induced and huAChE-dependent aggregation as shown in ThT studies. These results are similar to that observed for other similar compounds and also for a phenolic compound, EA (Feng Y, 2009) which reduced $A\beta_{1-42}$ cytotoxicity in the same cellular model in a dose-independent manner. Moreover, EM images demonstrates that ASS234 blocks the formation of fibrillar structures by promoting globular, non-fibrillar species of about 6-8 nm which are consistent with trimeric and tetrameric forms. It has been reported that these oligomeric forms of Aβ may represent the primary toxic species in AD (Kirkitazde et al., 2002; Walsh & Selkoe, 2007) which the smallest appear to be dimeric (Shankar et al., 2008). However, maybe due to the complex and dynamic equilibrium of Aβ, a structure-toxicity correlation of oligomers is not commonly found in literature. Recently, Ono and co-workers (2009) reported their study on different pure oligomeric preparations by using diverse techniques in which they concluded that the most interesting species to be targeted in the search of disease-modifying therapies are oligomers of the lower order (n=2-4). Nevertheless, other authors have suggested that oligomers of higher magnitude with fibril-like β-sheet structure are the most pathogenic (Chimon et al., 2007). Thus, although much effort is directed to the identification of the primay toxic Aβ species in order to design and develop agents able to block their toxicity, this complex mechanism is not yet fully understood.

Nevertheless, it does not appear so important for an anti-AD drug to reduce Aβ fibrillogenesis if it cannot prevent the neurotoxicity exerted by Aβ. In this context, our results show that treatment of SH-SY5Y cells with Aβ clearly decreased cellular MTT reduction, thereby providing a direct evidence for cellular damage induced by Ab. ASS234 was able to significantly prevent this cellular toxicity. We have observed that our experimental paradigm provokes an apoptotic cell dead as estimated by nuclear fragmentation which was significantly blocked by ASS234 in a concentration-dependent manner. This apoptosis is accompanied by a necrotic cell death as evidenced

by the extent of LDH released to the medium of cells which was as well significantly prevented with ASS234 pretreatment. Both apoptotic and necrotic processes have been reported to be related to neuronal degeneration in AD. Thus, antiapoptotic strategies that may prevent this neuronal degeneration are a matter of interest.

Caspase-3 is one of the main executionare caspases which cleavage and activation leads to the cleavage of several nuclear substrates such as PARP. ASS234 significantly reduced the cleavage and activation of both caspase-3 and PARP showing that it is able to reduce these apoptotic features in our experimental conditions. Several caspases have been suggested to play a role in the initiation of apoptotic processes. Caspase-9 has extensively been reported as an initiator caspase in mitochondria-mediated apoptosis. (Desagher & Martinou, 2000; Spierings et al., 2005). Additionally, caspase-8 has also been reported (Baliga et al., 2004) which is involved in the extrinsic pathway, activated by extracellular death ligands binding to their receptors in the cellular surface (Thorburn, 2004; Ashkenazi & Dixit, 1998). Caspase-12 has been proposed to be the initiator caspase under endoplasmic reticulum (ER) stress situations (Nakagawa et al., 2000). In our experimental conditions, caspase-9 cleavage and activation is increased following Aβ-induced toxicity which is significantly prevented by ASS234 pretreatment. Nevertheless, the extent of the blockade of caspase-9 activation by ASS234 does not explain the effect in the downstream caspase-3 activation, suggesting that other caspases may be involved in the activation of the executionare caspase-3 and the subsequent cleavage of PARP. It has been reported that Aβ bind to death receptors activating the extracellular pathway of apoptosis, thus, caspase-8 activation might be involved in our experimental paradigm.

As pretended with the design and synthesis of ASS234, it preserves the neuroprotective activity observed for the parent compound, PF9601N (Sanz et al., 2009), and other propargylamin-containing molecules (Jenner et al., 2004). The actions of ASS234 over caspases are not new, but among the mechanisms involved in the neuroprotection exerted by porpargylamines are the stabilization of mitochondria membrane permeability, induction of anti-apoptotic Bcl-2 and neurotrophic factors and regulation of antioxidant enzymes (Naoi M and Maruyama W, 2009). Thus, propargylamine-containing drugs have shown to prevent the following apoptotic processes: mPT-induced $\Delta\psi m$ reduction, mitochondrial swelling and citocrome C release, caspase activation, condensation and fragmentation of nuclear DNA and nuclear

translocation of glyceraldehydes-3-phosphate dehydrogenase (Naoi M and Maruyama W, 2009; Mandel S, 2005). Although the mechanisms by which these drugs act are not completely understood, alterations in signalling pathways, such us protein kinase C (PKC) and mitogen-activated protein kinase (MAPK)/extracellular signal-regulated kinase (ERK) seems crucial to their protective activity (Mandel S, 2005). Accordingly, our compound, may be acting through the same pathways.

The mechanisms involved in the neuroprotective properties of the multifunctional compound ASS234 against Aβ toxicity remain to be determined. Nevertheless, the multiple beneficial properties of ASS234 make it a useful candidate to be considered for the treatment of the multifactorial nature AD.

Acknowledgements

This work was realized in the framework of COST: COST Action D34/003/05 (2005-2010)

References

Areosa SA, Sheriff F, Mc Shane R. (2005). Memantine for dementia. *Cochrane Database Syst Rev* (2) CD003154 .

Ashkenazi A and Dixit VM (1998) Death receptors: signalling and modulation. Science 281(5381):1305-1308

Baliga BC, Read SH, Kumar S (2004) The biochemical mechanism of caspase-2 activation. Cell Death Differ (11):1234-1241

Birks J and Harvey R. (2006). Donepezil for dementia due to Alzheimer's disease. *Cochrane Database Syst Rev* (1) CD001190.

Birks J, Grimley EJ, Iakovidou V et al. (2000). Rivastigmine for Alzheimer's disease. *Cochrane Database Syst Rev* (4) CD001191.

Buccafusco JJ and Terry AV Jr (2000) Multiple central nervous system targets for eliciting beneficial effects on memory and cognition. J Pharmacol Exp Ther 295(2):438-446

Cavalli, A.; Bolognesi, M. L.; Minarini, A.; Rosini, M.; Tumiatti, V.; Recanatini, M.; Melchiorre, C. Multi-target-directed ligands to combat neurodegenerative diseases. *J. Med. Chem.* **2008**, *51*, 347-372.

Chimon S, Shaibat MA, Jones CR et al (2007) Evidence of fibril-like beta-sheet structures in a neurotoxic amyloid intermediate of Alzheimer's beta-amyloid. Nat Struct Mol Biol Dec 2 [Epub ahead of print]

Coyle, J.T; Puttfarcken, P. Oxidative stress, glutamate and neurodegenerative disorders. *Science* **1993**; 262:689-695

Davies P and Maloney AJ (1976). Selective loss of central cholinergic neurons in Alzheimer's disease. *Lancet* 2: 1403

Desagher S and Martinou JC (2000) Mitochondria as the central control point of apoptosis. Trends Cell Biol 10(9):369-377Review

Elsinghorst, P. W.; Cieslik, J. S.; Mohr, K.; Tränkle, C.; Gütschow, M. The first gallamine-tacrine hybrid: Design and characterization at cholinesterases and the M_2 muscarinic Receptor. *J. Med. Chem.* **2007**, *50*, 5685-5695.

Fang, L.; Appenroth, D.; Decker, M.; Kiehntopf, M.; Roegler, C.; Deufel, T.; Fleck, C.; Peng, S.; Zhang, Y.; Lehmann, J. Synthesis and biological evaluation of NO-donor-tacrine hybrids as hepatoprotective anti-Alzheimer drug candidates. *J. Med. Chem.* **2008**, *51*, 713-716.

Gella, A.; Durany, N. Oxidative stress in Alzheimer disease. *Cell. Adh. Migr.* **2009**, *3*, 88-93.

Glenner GG and Murphy MA (1989) Amyloidosis of the nervous system. *J Neurol Sci* 94(1-3):1-28

Goedert M, Wischik CM, Crowder RA et al (1988) Cloning and sequencing of the cDNA encoding a core protein of the paired helical filament of Alzheimer disease: identification as the microtubule-associated protein tau. *Proc Natl Acad Sci USA* 85(11):4051-4055

Greig, N. H.; Utsuki, T.; Ingram, D.; Wang, K. Y.; Pepeu, G.; Scali, C.; Yu, Q. S.; Mamczarz, J.; Holloway, H. W.; Giordano, T.; Chen, D.; Furukawa, K.; Sambamurti, K.; Brossi, A.; Lahiri. D. K. Selective butyrylcholinesterase inhibition elevates brain acetylcholine, augments learning and lowers amyloid-b peptide in rodents. *Proc. Natl. Acad. Sci. USA* **2005**, *102*, 17213-17218.

Grundke-Iqbal, I; Iqbal, K; Tung, Y.C; Quinlan, M; Wisniewski, H.M; Binder L.I.. Abnormal phosphorylation of the microtubule-associated protein (tau) in Alzheimer cystoskeletal pathology. *Proc. Natl. Acad. Sci* USA **1986**, 93:4913-4917

Huang X, Moir RD, Tanzi RD et al (2004) Redox-active metals, oxidative stress and Alzheimer's disease pathology. *Ann Y Acad Sci* 1012:153-163

Inestrosa, N. C.; Alvarez, A.; Pérez, C. A.; Moreno, R. D.; Vicente, M.; Linker, C.; Casanueva, O. I.; Soto, C.; Garrido. J. Acetylcholinestearse accelerates assembly of amyloid-beta-peptides into Alzheimer's fibrils: Possible role of the peripheral site of the enzyme. *Neuron* **1996**, *16*, 881–891.

Kirkitadze MD, Bitan G and Teplow DB (2002) Paradigm shifts in Alzheimer's disease and other neurodegenerative disorders: the emerging role of oligomeric assemblies. J Neurosci Res 69(5):567-577 Review

Lashuel H.A, Hartley D.M, Petre B.M, Wall J.S, Simon M.N, Walz T, Lansbury Jr. P.T. Mixtures of wild-type and a pathogenic (E22G) form of Abeta40 in vitro accumulate protofibrils, including amyloid pores. J Mol Biol 332 (2003) 795-808.

Loy C and Schneider L. (2004). Galantamine for Alzheimer's disease. *Cochrane Database Syst Rev,* (4)CD001747.

Mandel S, Weinreb O, Amit T and Youdim MB. Mechanisms of neuroprotective action of the anti-Parkinson drug rasagiline and its derivatives. *Brain Res Brain Res Rev* 48 (2005) 379-387

Mishizen-Eberz AJ, Rissman RA et al (2004) Biochemical and moleculat studies of NMDA receptor subunits NR1/2A/2B in hippocampal subregions throughout progression of Alzheimer's disease pathology. *Neurobiol Dis* 15:80-92.

Nakagawa T, Zhu H, Morishima N et al (2000) Caspase-12 mediates endoplasmic-reticulum-specific apoptosis and cytotoxicity by amyloid beta. *Nature* 403, 98-103.

Naoi M and Mayurama W. Functional mechanisms of neuroprotection by inhibitors of type B monoamine oxidase in Parkinson's disease. *Expert Rev Neurother* 9 (2009) 1233-1250

Ono K, Hasegawa H, Naiki H, Yamada M. Anti-amyloidogenic activity of tannic acid and its activity to destabilize Alzheimer's beta-amyloid fibrils in vitro. Biovhim Biophis Acta 1690 (2004) 193-202.

Ono K, Hasegawa H, Naiki H, Yamada M. Preformed beta-amyloid fibrils are destabilised by coenzyme Q10 in vitro. Biochem Biophys Res Commun 330 (2005) 111-116

Perry, E. K.; Tomlinson, B. E.; Blesseed, G.; Bergmann, K.; Gibson, P. H.; Perry, R. H. Correlation of cholinergic abnormalities with senile plaques and mental test scores in senile dementia. *British Med. J.* **1978**, *2,* 1457-1459.

Riviere C, Richard T, Quentin L, Krisa S, Merillon J.M, Monti J.P. Inhibitory activity of stillbenes on Alzheimer's beta-amyloid fibrils in vitro. Bioorg Med Chem 15 (2007) 1160-1167.

Riviere C, Richard T, Vitrac X, Merillon J.M, Valls J, Monti J.P. New polyphenols active on beta-amyloid aggregation. Bioorg Med Chem Lett 18 (2008) 828-831.

Rodríguez-Franco, M. I.; Fernández-Bachiller, M. I.; Pérez, C.; Castro, A.; Martínez, A. Design and synthesis of N-benzylpiperidine-purine derivatives as new dual inhibitors of acetyl- and butyrylcholinesterase *Bioorg. Med. Chem.* **2005**, *13*, 6795-6802

Rosini, M.; Antonello, A.; Cavalli, A.; Bolognesi, M. L.; Minarini, A.; Marucci, G.; Poggesi, E.; Leonardi, A.; Melchiorre, C. Prazosin-related compounds. Effect of transforming the piperazinylquinazoline moiety into an aminomethyltetrahydroacridine system on the affinity for α_1-adrenoreceptors. *J. Med. Chem.* **2003**, *46*, 4895-4903.

Sanz E, Quintana A, Hidalgo J et al (2009) PF9601N confers MAO-B independent neuroprotection in ER-stress-induced cell death. *Mol Cell Neurosci* 41,19-31

Terry, R.D.; Gonatas, N.K; Weiss, M. Ultrastructural studies in Alzheimer's presenile dementia. *Ann J Pathol* **1964**, 44:269-297

Thornburn A (2004) Death receptor-induced cell killing. *Cell Signal* 16, 139-144

Tsolaki M, Kokarida K, Iakovidou V et al (2001). Extrapyramidal symptoms and signs in Alzheimer's disease: prevalence and correlation with the first symptom. *Am J Alzheimer Dis Other Demen* 16:268-278

Walsh DM and Selkoe DJ (2004) Oligomers on the brain: The emerging role of soluble protein aggregates in neurodegeneration. *Protein Pept Lett* 11:213-228

Youdim MHB and Buccafusco JJ (2005) CNS Targets for multi-functional drugs in the treatment of Alzheimer's and Parkinson's diseases. *J Neural Trans*m, 112(4):519-537 review

Zheng, H.; Youdim, M. B. H.; Fridkin, M. Site-activated multifunctional chelator with acetylcholinesterase and neuroprotective–neurorestorative moieties for Alzheimer's therapy. *J. Med. Chem*. **2009**, *52*, 4095-4098.

Figure Legends

Figure 1. (A-B) Representative figures of ThT fluorescence of (A) $A\beta_{1-40}$ and (B) $A\beta_{1-42}$ aggregation with and without ASS234 along time. Aβ peptides (final concentration 40μM) were incubated with and without 100μM ASS234 for the period indicated. Temperature was 37ºC. (●) Aβ; (○) Aβ and ASS234 co-incubation. (C-D) Representative electron micrographs of (C) $A\beta_{1-40}$ and (D) $A\beta_{1-42}$ samples taken from the microplate at the end of the ThT aggregation method. Experiments were performed at least in triplicate.

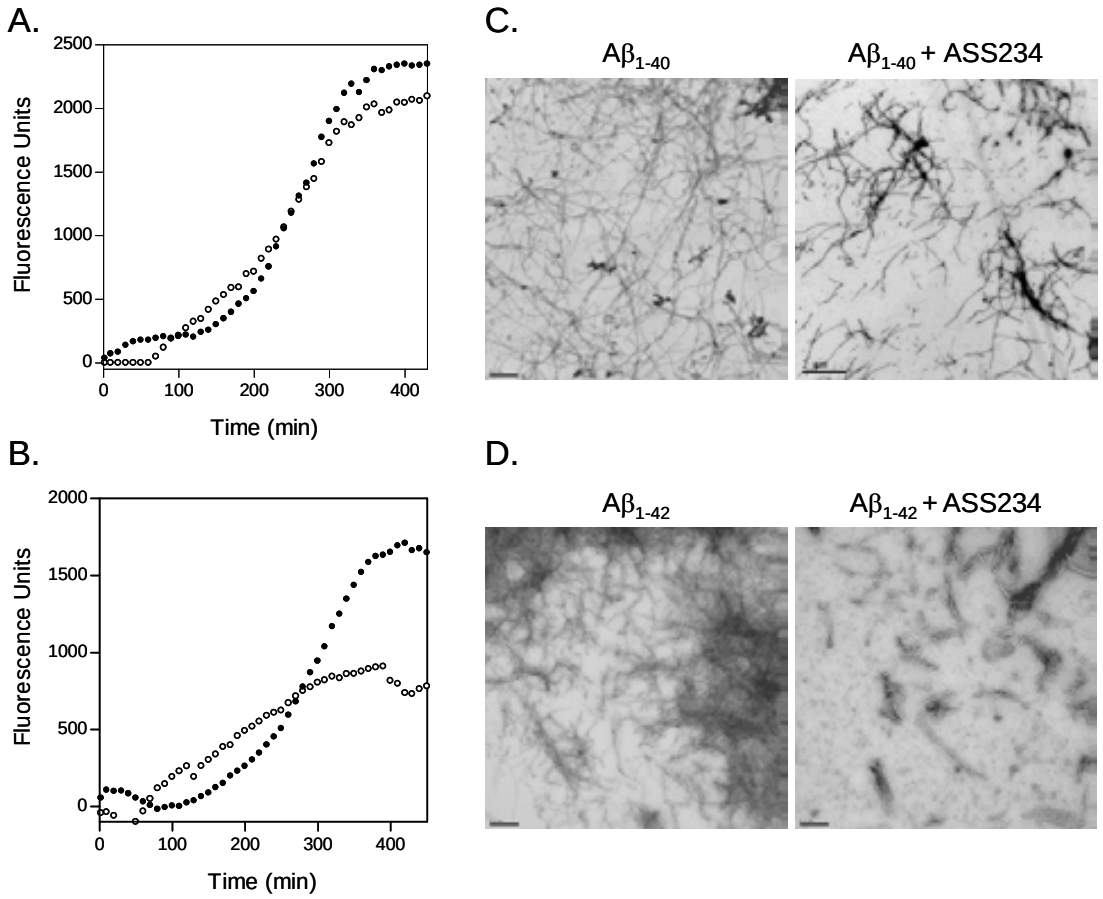

Table 1. Inhibition of $A\beta_{1-40}$ and $A\beta_{1-42}$ self-induced aggregation produced by different concentrations of ASS234.

	Inhibition of Aβ self-aggregation (%)	
Concentration (μM)	$A\beta_{1-40}$	$A\beta_{1-42}$
10	10.4 ± 3.3	47.8 ± 2.1
50	6.6 ± 1.5	60.1 ± 7.2
100	7.8 ± 1.3	50.3 ± 3.7
200	10.9 ± 4.7	41.1 ± 6.9

Aβ peptide final concentration was 40 μM. The ratio Aβ/ASS234 was equal to 4/1.

Data are the mean ± SEM of at least three independent experiments.

Figure 2. (A-C) ThT fluorescence values of (A) $A\beta_{1-40}$ and (C) $A\beta_{1-42}$ aggregation at plateau (400 min) with and without huAChE and ASS234. Aβ peptides final concentration was 40μM and ASS234 was 100μM. The ratio Aβ/AChE was equal to 100/1. Temperature was 37ºC. (B-D) Representative electron micrographs of (B) $A\beta_{1-40}$ and (C) $A\beta_{1-42}$ at plateau. (E) % of inhibition ± SEM of AChE-induced Aβ aggregation by ASS234. Experiments were performed at least in triplicate. Effect of AChE is noted with # whereas effect of ASS234 is noted with *. One symbol means $p<0.05$, and two means $p<0.01$.

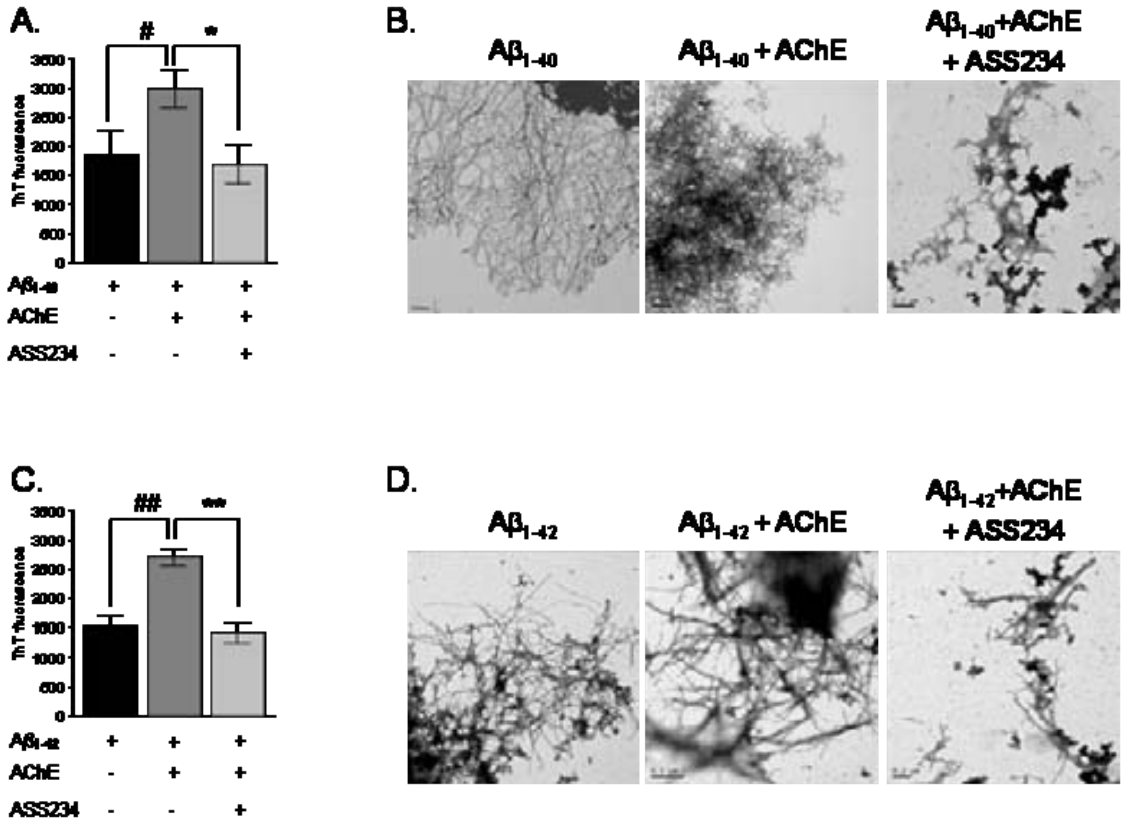

E.

ASS234 Concentration (μM)	% inhibition of AChE-induced Aβ aggregation ± SEM	
	$A\beta_{1-40}$	$A\beta_{1-42}$
100	32.4 ± 7.0	39.6 ± 13.6

The concentration of ASS234 and Aβ was 100μM and 40μM, respectively. The ratio Aβ/AChE was equal to 100/1. Data are the mean ± SEM of at least three independent experiments.

Figure 3. Antioxidant effect of ASS234 on PC12 cells. Cell viability was reduced to 40% when cells were treated with 200μM hydrogen peroxide (H_2O_2) for 2h. A significant increase in cell viability was observed when cells were pretreated with ASS234 (0.01-1 μM) whereas no effect was observed at 10 μM concentration. 100 μM Trolox was used as positive control. Data are the mean ± SEM. Experiments were performed in triplicate. Effect of H_2O_2 is noted with * whereas effect of ASS234 and trolox is noted with #. Three symbols mean $p<0.001$.

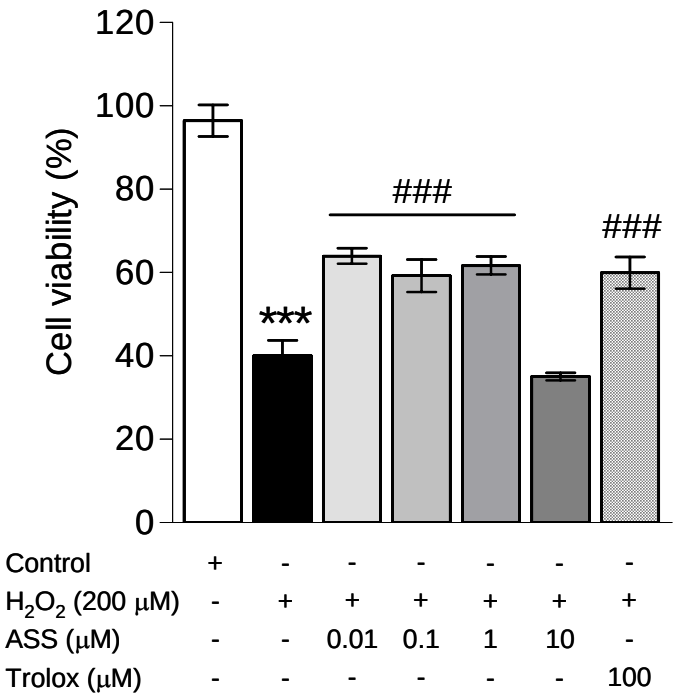

Figure 4. Nitrite concentration in the supernatant of Bv2 cells after treatment with LPS (100ng/ml) plus INF-γ (0.5 ng/ml) measured by the Griess method. A significant amount of NO was released to the medium after 48h treatment. ASS234 pre-treatment (1h prior to damage) was not able to reduce NO release as was done by ibuprofen, a well-known anti-inflammatory drug, used in this assay as positive control. Experiments were performed in triplicate. Effect of treatment is noted with * whereas effect of pre-treatment is noted with #. Three symbols mean p<0.001.

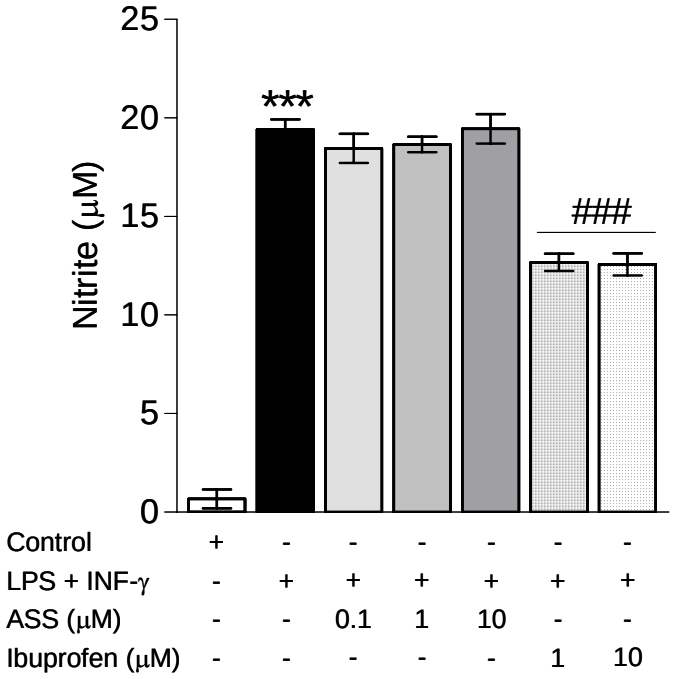

Figure 5. (A) Cell viability assay. MTT method was performed after ASS234 pre-treatment (5-10μM, 60 min) and Aβ42 treatment (40μM, 24h). Cell viability was reduced to 50% which was significantly prevented when cells were pre-treated for 60 min with 5μM or 10 μM ASS234. (B) LDH enzymatic activity was significantly increased after Aβ42 treatment. ASS234 pre-treatment was able to prevent the Aβ-induced LDH release to the culture medium in a dose-dependent manner. (C) Micrographs showing the morphological changes of SH-SY5Y cells after Aβ exposure and after ASS234 pretreatment. Experiments were performed in triplicate. Effect of treatment is noted with # whereas effect of pre-treatment is noted with *. Three symbols means p<0.001.

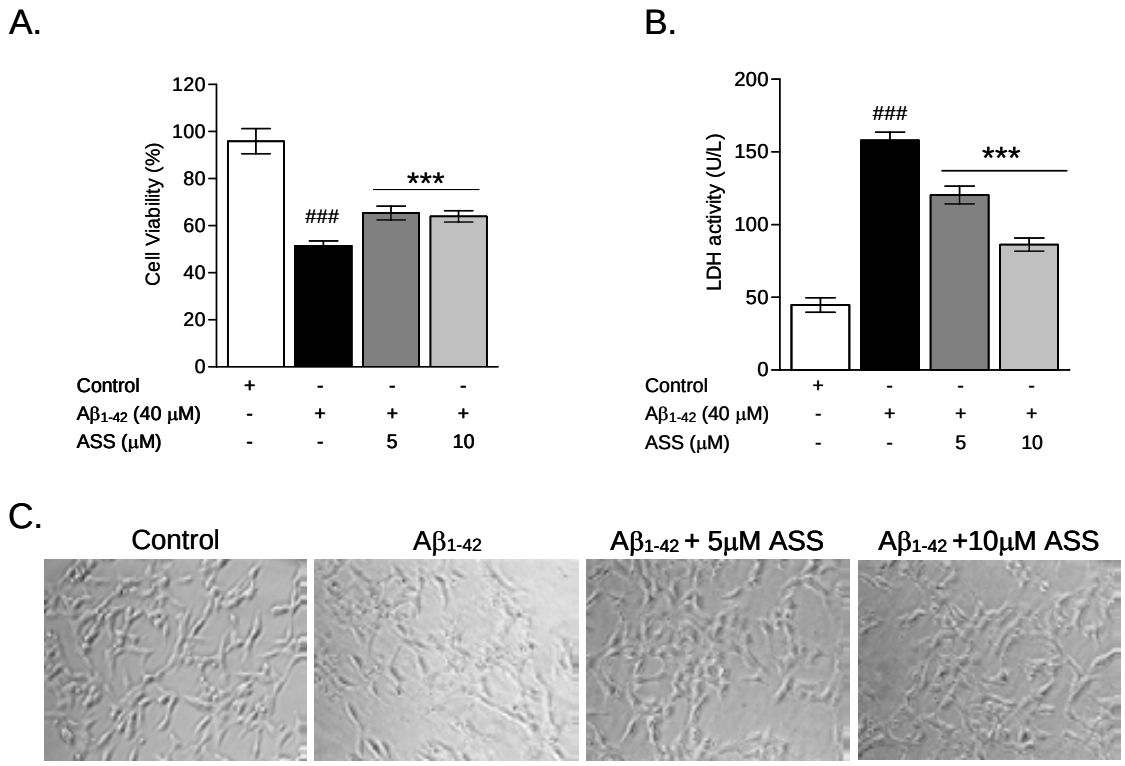

Figure 6. Nuclear fragmentation assay. Cells were treated with $A\beta_{1-42}$ (40μM) for 24h with and without ASS234 (5μM and 10μM) pre-treatment (60 min), fixed and counterstained with Hoechst 33258. Nuclei were visualized under an inverted fluorescence microscope. Results were replicated in three independent experiments. Values are the mean ± SEM. Statistical analysis were carried out using a one-way ANOVA test, followed by the Bonferroni post-test. Effect of treatment is noted with # whereas effect of pre-treatment in noted with *. One symbol means $p<0.05$, two $p<0.001$ and three $p<0.001$.

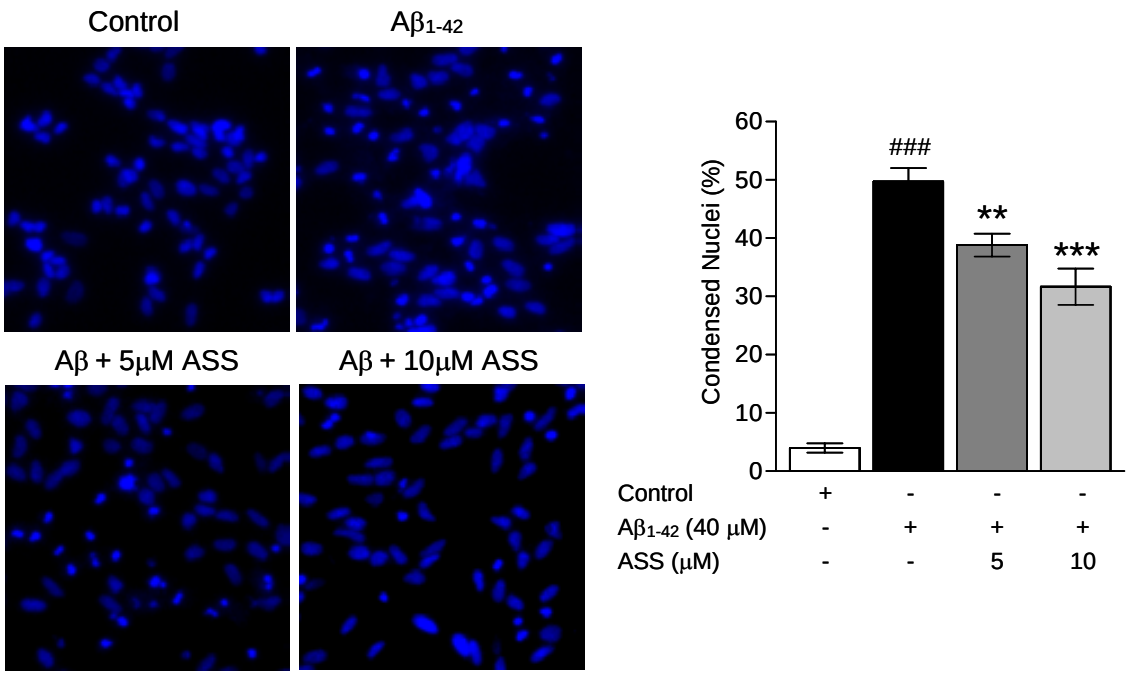

Figure 7. Immunoblot analysis of active caspase-3 levels, and PARP and caspase-9 cleavage. Cells were pre-treated with ASS234 (5 and 10 μM) before inducing apoptosis with $A\beta_{1-42}$ (40 μM). Results were replicated in three independent experiments. Values are the mean ± SEM. Statistical analysis were carried out using a one-ANOVA test, followed by Bonferroni post-test. Effect of treatment is noted with # whereas effect of pre-treatment in noted with *. One symbol means p<0.05, two p<0.001 and three p<0.001.

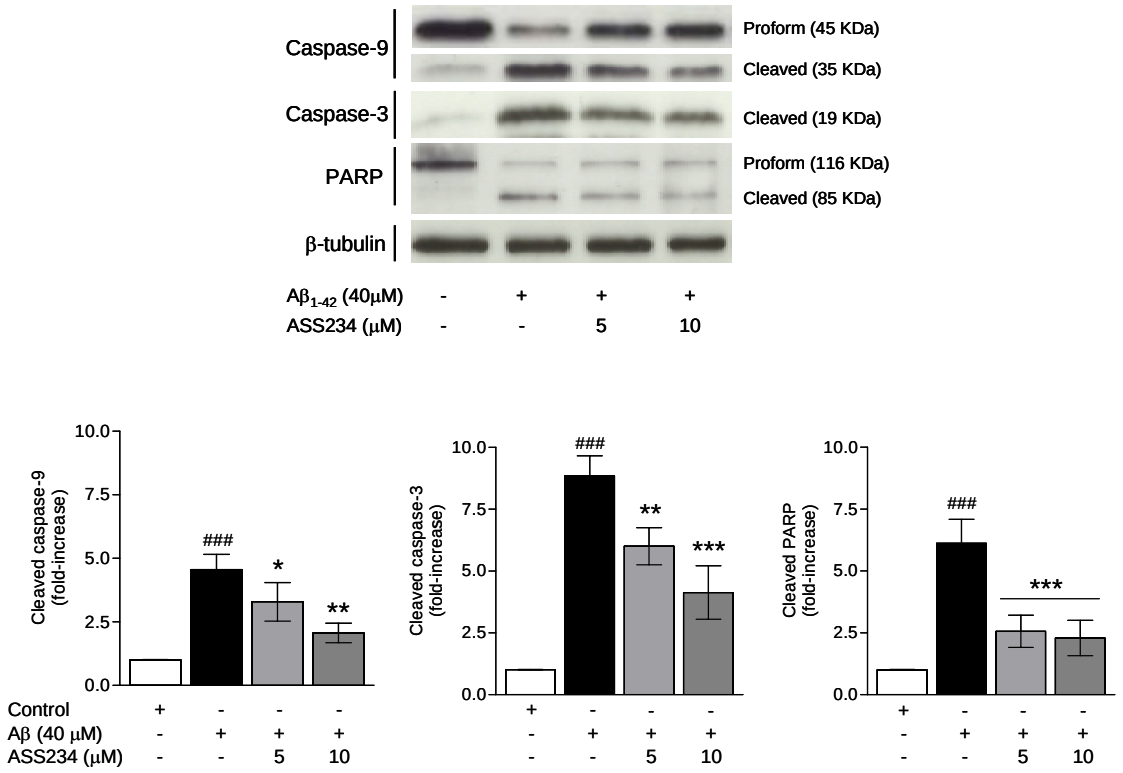

IV. DISCUSSION

Alzheimer's disease (AD) is an age-related neurodegenerative disorder characterised by progressive memory loss, decline in language skills and other cognitive impairments (Goedert & Spillantini, 2006). The etiology of AD is not yet fully understood but several factors such us amyloid β deposits (Castro et al., 2006), τ-protein aggregation (Grundke-Iqbal et al., 1986), oxidative stress and free radical formation (Coyle & Puttfarcken, 1993; Perry, 2000), mitochondrial dysfunction (Swerdlow & Khan, 2009), metal dyshomeostasis (Huang et al., 2004) and excitotoxic and neuroinflammatory processes (Mishizen-Eberz et al., 2004) are thought to play significant roles in the pathogenesis of the disease. These processes lead to a selective loss of cholinergic neurons producing a depletion of acetylcholine (ACh) levels in specific brain regions that mediate memory and learning (Talesa, 2001). Consequently, the current therapies for AD are mainly based on restoring ACh with cholinesterase inhibitors (ChEIs) such as donepezil (Birks & Harvey, 2006), rivastigmine (Birks et al., 2000) and galanthamine (Loy & Schneider, 2004), which, however, have limited therapeutic benefits. The poor effectiveness of ChEIs has been related to the multifactorial and complex nature of AD, which means that one molecule targeting only one specific feature of the disorder is maybe inadequate for the treatment. Moreover, neuronal loss has been considered to be the ultimate stage of the disease, thereby being too late to obtain a clear disease-modifying effect when acting at this stage. In this context, at present, the most innovative paradigm is the so-called multi-target-directed ligand (MTDL) approach which was pioneered by Buccafusco et al., 2000, and describes compounds the multiple biological profiles of which are rationally designed to combat a particular disease. Thus, the MTDL strategy seems to have enhanced benefits so that many research groups have developed a wide variety of compounds acting on very diverse types of targets (Rodriguez-Franco et al., 2005; Rossini et al., 2003; Elsinghorst et al., 2003; Zheng et al., 2009).

PF9601N is a propargylamine-containing irreversible monoamine oxidase B inhibitor (MAOBI) previously identified by our group in an extensive screen of potential MAOIs (Pérez et al., 1999). Besides its potent inhibitory capacity, it has been shown to exert neuroprotective properties in several *in vitro* and *in vivo* models of PD and also to prolong the effects of exogenously administered levodopa in different experimental models of PD (Perez et al., 2003; Cutillas et al., 2002; Prat et al., 2000). Nevertheless, the beneficial effects of PF9601N, which have been related to the propargylamine group present in the molecule, appear to extend beyond Parkinson's disease as they are mediated through actions in

pathways that are commonly involved in the neurodegeneration observed in other neurodegenerative disorders such as Alzheimer's disease (AD).

In this work, we demonstrate that pre-treatment with PF9601N produces a significant decrease in the KA-evoked release of the excitatory aminoacids, suggesting a protective effect of this compound against excitotoxicity. The excitotoxicity induced by a hyperactivation of ionotropic glutamatergic receptors has been reported to be involved in a number of neurodegenerative diseases, including those following stroke and head trauma as well as Huntington's disease, PD and Alzheimer's disease (Beal, 1992). The present results also show that excitotoxic damage provokes considerable astroglial reactivity, proved by a significant increase in GFAP immunoreactivity. In contrast, animals pre-treated with PF9601N showed less astrogliosis. Yu et al. (1995) have also shown that some aliphatic propargylamine does inhibit GFAP mRNA expression. Microglial cells have been reported to be the first population to react against CNS lesions. Their reactions, which appear quite homogeneous and independent from the type of lesion, include changes in their morphology, proliferation and an increase in surface molecules (Stoll et al., 1998; Stoll & Jander, 1999). The present results showed the intrastriatal administration of kainate to induce both an increase in the number of lectin-positive cells and a change in their morphology, characteristic of their activation process. It is difficult to distinguish p53 induction between microglia and macrophages, since they share intracellular and membrane markers (Flaris et al., 1993), such as lectin domains and CR3 (Stoll & Jander, 1999). However, these results suggest a possible immunomodulator effect of PF9601N, since it is able to prevent the microglial reactivity induced by kainate. This is the first time that a propargylamine-derived compound proves to reduce excitotoxicity which gives more value to this compound as a neuroprotective drug.

The excitotoxicity caused by kainate is still not fully understood, as both necrotic and apoptotic cell deaths are provoked (Portera-Cailliau et al., 1997). Its toxic effects are associated with p53 induction and collapse of the mitochondrial membrane potential (Liu et al., 2001). Since PF9601N has been reported to oppose these effects, it could prove useful in the treatment of excitotoxic origin. Its high selectivity as an inhibitor of MAO-B also confers an additional benefit, as an adjunct to the levodopa treatment of Parkinson's disease. Thus, the protective properties of PF9601N observed in this model, as well as the properties previously observed in several models of Parkinson's disease, suggest that PF9601N could be a good candidate to be used for the treatment of PD and maybe other neurodegenerative disorders that also involve excitotoxicity.

In the search for disease-modifying drugs to be used in the therapy of AD, we considered the innovative MTDL approach and developed a strategy based on the design of a single molecule with multipotent properties of ChE and MAO inhibition. This strategy is not new but has been previously analysed by other groups (Zheng et al., 2009; Sterling et al., 2002; Fink et al., 1996). What was new and original in our case was the first combination of the N-benzyl piperidine and the N-propargylamine moieties present in the AChEI donepezil (Barner & Grey, 1998) and the MAOI, PF9601N (Pérez et al., 1999) connected through an appropriate linker. The compounds obtained behaved like potent AChEI (nM range), although they did not affect BuChE, and only moderately inhibited MAOA. Despite the lack of the multipotent effect, this work allowed us to establish that the length of the spacer is a sensitive moiety to modulate AChE inhibition, which would control the dual interaction of these molecules with both the CAS and PAS sites. Thus, the length of the spacer appeared as an interesting feature to be considered for future improvement of the formulations.

The second strategy used in this work in the search for better and valuable MTDLs, gave more interesting compounds as they were able to inhibit, although moderately, both AChE and BuChE. Normally, AChE predominates in the brain, while BuChE activity levels are low. However, in AD the relative enzymatic activity is altered to such an extent that BuChE increases while AChE decreases (Perry et al., 1978; Greig et al., 2001). This is also found in glial cells which are recruited and activated around plaques and tangles, suggesting that this cell type might be a source of the enzyme (Wright et al., 1994). Then, if the therapeutic goal is to increase ACh levels in the brain, a compound able to inhibit BuChE as well as inhibiting AChE would be valuable to elicit a larger protective response. Several authors have suggested the importance of the dual inhibition to provide additional benefits in AD treatment (Darvesh et al., 2003; Giacobini, 2000; Greig et al., 2001). Consistent with these suggestions, it has been reported that inhibition of BuChE in AD is correlated with cognitive improvement (Giacobini et al., 2002). Moreover, in the SAR study reported in this thesis, the length of the spacer appeared as a sensitive moiety to modulate BuChE, although no effect was observed in AChE. Among the compounds assessed, ASS234 appeared as the most interesting one, since it non-selectively inhibited both AChE and BuChE. Furthermore, the dual binding site inhibition (CAS and PAS) on AChE gives more value to this compound. AChE has been found to be associated with senile plaques (SP) in AD brains (Geula & Mesulam, 1989) and it has been found to accelerate the

assembly of Aβ by forming a stable Aβ–AChE complex, thus enhancing its neurotoxic effects. Thus, in the search for molecules to be used in AD therapy, it becomes useful to prevent Aβ aggregation, besides restoring cholinergic neurotransmission. ASS234 not only inhibits the AChE-dependent Aβ aggregation more potently than the parent compound donepezil but also inhibits the self-induced Aβ aggregation more potently than the reference compound, propidium iodide, making this molecule a very interesting compound with a promising anti-cholinergic and anti-Aβ profile.

In addition to the ChEIs, the synthesised compounds appeared as potent MAOIs (nM range). This is of great value since besides the cholinergic deficit found in AD patients, several authors have found disturbances of other neurotransmitter systems clearly accounting for the symptoms (Perry et al., 1999; Dringerberg, 2000). Although the current hypothesis is that cholinergic dysfunction by itself may not be sufficient to produce learning and memory deficits and that a complex interplay between neurotransmitter systems would be necessary to produce the AD symptoms, the study of these neurotransmitter system abnormalities has unfortunately received less attention (Dringerberg, 2000; Hydn et al., 2004; Liu et al., 2008). The results in this thesis suggest that ASS234, the compound with the best ChEI/MAOI capacity, might be beneficial not only for modulating the cholinergic neurotransmission but also for restoring the serotoninergic neurotransmission. Besides, the potent MAO-A inhibition exerted by ASS234 enables the drug to produce an antidepressant activity like that of moclobemide, a tricyclic antidepressant primarily used to treat depression. This result is very interesting since depressive symptoms are so commonly found in AD patients that recent reports have investigated the relationship between AD and depression. These have concluded that depression is a risk factor for AD development (for review, see Caraci et al., 2010). However, as ASS234 appears as an irreversible MAO-A, one feature that remains to be investigated is the risk of inhibiting peripheric MAO-A, which may result in a drastic increase of the vasopressor effects of the diet-derived tyramine (the so called "cheese effect") that leads to severe hypertensive crisis.

The rise in the investigation of potential AD therapies at present is based upon the notion of the "amyloid cascade hypothesis" (Hardy & Higgins, 1992) which claims that the metabolism of Aβ is the main intiator of AD. In this thesis we report a more detailed investigation of the anti-Aβ profile of ASS234. Screening molecules to prevent or reverse the oligomerization and fibrillization process of Aβ have been reported to be of therapeutic

value in the treatment of AD (Necula, 2007. Ono, 2004). Among the anti-Aβ aggregation compounds, several types of drugs have been specifically designed and synthesised to this purpose but also some natural substances such us polyphenols have been used (Ono, 2004, 2005; Riviere, 2007, 2008).

Besides the ThT studies showing a decrease in fibril formation, EM images demonstrate that ASS234 blocks the formation of fibrillar structures by promoting globular, non-fibrillar species of about 6-8 nm which are consistent with trimeric and tetrameric forms (Lashuel et al., 2002; Ono et al., 2009). It has been reported that these oligomeric forms of Aβ may represent the primary toxic species in AD (Kirkitazde et al., 2002; Walsh & Selkoe, 2007). However, a structure-toxicity correlation of oligomers is not commonly found in literature, maybe due to the complex and dynamic equilibrium of Aβ. Recently, Ono and co-workers (2009) reported their study on different pure oligomeric preparations by using diverse techniques in which they concluded that the most interesting species to be targeted in the search for disease-modifying therapies are oligomers of the lower order (n=2-4). Nevertheless, other authors have suggested that oligomers of a higher magnitude with fibril-like β-sheet structures are the most pathogenic (Chimon et al., 2007). Thus, although much effort is directed to the identification of the primay toxic Aβ species this complex mechanism is not yet fully understood, highlighting the need for a better understanding of the *in vivo* polymerization process of Aβ for a better development of anti-aggregant drugs.

Nevertheless, it does not appear so important for an anti-AD drug to reduce Aβ fibrillogenesis if it cannot prevent the neurotoxicity exerted by the peptide. In this context, our results show that treatment of SH-SY5Y cells with Aβ clearly decreased cellular MTT reduction, thereby providing direct evidence of cellular damage induced by the peptide, which was significantly prevented by ASS234. We also observed that our experimental paradigm provokes an apoptotic cell death as estimated by nuclear fragmentation which was significantly blocked by ASS234 in a concentration-dependent manner. This apoptosis is accompanied by a necrotic cell death as evidenced by the extent of LDH released to the medium of cells which was also significantly prevented with ASS234 pre-treatment. Both apoptotic and necrotic processes have been reported to be related to neuronal degeneration in AD. Thus, neuroprotective strategies that may prevent this neuronal degeneration are a matter of interest.

Caspase-3 is one of the main executioner caspases the cleavage and activation of which leads to the cleavage of several nuclear substrates such as PARP. ASS234 significantly reduced the cleavage and activation of both caspase-3 and PARP showing that it is able to reduce these apoptotic features in our experimental conditions. Several caspases have been suggested to play a role in the initiation of apoptotic processes. Caspase-9 has extensively been reported as an initiator caspase in mitochondria-mediated apoptosis. (Desagher & Martinou, 2000; Spierings et al., 2005). Additionally, caspase-8, which is involved in the extrinsic pathway and activated by extracellular death ligands binding to their receptors in the cellular surface (Thorburn, 2004; Ashkenazi & Dixit, 1998) has also been reported (Baliga et al., 2004). Caspase-12 has been proposed to be the initiator caspase under endoplasmic reticulum (ER) stress situations (Nakagawa et al., 2000). In our experimental conditions, caspase-9 cleavage and activation is increased following Aβ-induced toxicity which is significantly prevented by ASS234 pretreatment. Nevertheless, the extent of the blockade of caspase-9 activation by ASS234 does not explain the effect in the downstream caspase-3 activation, suggesting that other caspases may be involved in the activation of the executioner caspase-3 and the subsequent cleavage of PARP. It has been reported that Aβ bind to death receptors activating the extracellular pathway of apoptosis, thus, caspase-8 activation might be involved.

As was attempted with the design of ASS234, it preserves the neuroprotective activity observed for the parent compound, PF9601N (Sanz et al., 2009), and other propargylamin-containing molecules (Jenner, 2004; Weinreb et al., 2006). The actions of ASS234 over caspases are not new, but among the mechanisms involved in the neuroprotection exerted by porpargylamines are the stabilisation of mitochondria membrane permeability, induction of anti-apoptotic Bcl-2 and neurotrophic factors and regulation of antioxidant enzymes (Naoi M and Maruyama W, 2009). Thus, propargylamine-containing drugs have been shown to prevent the following apoptotic processes: mPT-induced $\Delta\psi m$ reduction, mitochondrial swelling and citocrome C release, caspase activation, condensation and fragmentation of nuclear DNA and nuclear translocation of glyceraldehydes-3-phosphate dehydrogenase (Naoi M and Maruyama W, 2009; Mandel S, 2005). Although the mechanisms by which these drugs act are not completely understood, alterations in signalling pathways, such as protein kinase C (PKC) and mitogen-activated protein kinase (MAPK)/extracellular signal-regulated kinase (ERK) seem crucial to their protective activity (Mandel S, 2005). Accordingly, our compound as a propargylamine, may be acting

by means of the same pathways. Further studies in the mechanisms involved in the neuroprotective properties ASS234 against Aβ toxicity are warranted.

Regarding the bioavailability and pharmacokinetics of ASS234, although there are no studies concerning this yet, it seems that therapy with a single drug that has multiple biological functions would have significant advantages over individual target drugs or a cocktail of drugs. In addition, the risk of possible drug-drug interactions would be avoided and the therapeutic regimen greatly simplified compared to the multiple medication treatment. All of these considerations are of particular relevance, as one of the major contributions to the attrition rate in drug development continues to be the candidate drug's pharmacokinetic profiling (Kola & Landis, 2004). Therefore, it seems imperative that future trials may use multifunctional molecules, rather than single compounds, with demonstrated ability to bind to very diverse types of targets.

Overall, the results presented in this thesis allow us to suggest that ASS234 is a potential candidate to be used in AD therapy as it combines the action against the symptomatic effects, exerted by its inhibitory activity towards ChEs and MAOs, with a neuroprotective effect, which would participate in the disease-modifying effects. Additional studies to confirm the potentiality of ASS234 as an anti-AD drug are warranted.

V. CONCLUSIONS

From the present work we have obtained the following conclusions:

1. PF9601N is able to prevent the excitotoxic damage induced by KA, in a process that involves decreasing the evoked release of the excitatory amino acids and increasing the output of the inhibitory and neuroprotective taurine.
2. PF9601N significantly prevents the KA-induced activation of glial cells as well as significantly reducing the KA-induced apoptotic process.
3. The combination of the N-benzyl piperidine and the N-propargylamine moieties present in donepezil and PF9601N attached to a central pyridine or naphthyridine ring produces compounds able to potently and selectively inhibit AChE but not being capable of significantly inhibiting MAO.
4. The new series of synthesised hybrid molecules bearing the benzyl piperidine moiety of donepezil and the indolyl propargylamino moiety of PF9601N, appear as potent MAO-A and MAO-B inhibitors (nM range) as well as moderately potent AChE and BuChE inhibitors (subμM range). The length of the tether that connects the two main structural fragments in the hybrid compounds has a relevant effect on the binding to MAO whereas it seems to have little impact on the inhibitory activity against AChE and BuChE.
5. Of the hybrid compounds, ASS234 is the most potent ChEI/MAOI and also shows a good inhibitory profile of the AChE-dependent Aβ aggregation, indicating that it is able to interact with the PAS of AChE and thus behaving as a dual binding site inhibitor.
6. ASS234 significantly inhibits the Aβ self-induced aggregation by binding directly to the peptide and preventing the formation of Aβ fibres.
7. ASS234 seems to promote non-toxic Aβ species since it prevents Aβ toxicity in SH-SY5Y neuronal cells by blocking LDH release and reducing the number of condensed nuclei.
8. ASS234 reduces the Aβ-induced apoptosis by blocking the expression of caspase-9, the downstream caspase-3 and the subsequent cleavage of PARP.
9. ASS234 protects against hydrogen peroxide-induced toxicity in cultured PC12 cells but it does not exert a beneficial effect against LPS+INF-γ in Bv2 cells.
10. Overall, the present data suggest that ASS234 is a promising MTDL that may have potential disease-modifying role in the treatment of Alzheimer's disease (AD) since

it is able to interact with diverse targets involved in the pathogenesis underlying AD. Further investigations with this compound are warranted.

VI. REFERENCES

REFERENCES

Adlard PA and Bush AI (2006) Metals and Alzheimer's disease. *J Alzheimers Dis* 10:145-163

Ahlskog JE and Uitti RJ (2010) Rasagiline, Parkinson neuroprotection, and delayed-start trials, still no satisfaction? *Neurology* 74(14):1143-1148 Review

Aisen P, Gauthier S, Ferris S et al (2009) A phase III, placebo-controlled, double-blind, randomised trial of tamiprosate in the clinical management of patients with mild-to-moderate Alzheiemr's disease (the Alphase study). *61st American Academy of Neurology Annual Meeting; Seattle, WA, USA*. April 25-May 2, S32.003

Akao Y, MAyurama W, Shimizu S et al (2002) Mitochondrial permeability transition mediates apoptosis induced by N-methyl(R)salsolinol, an endogenous neurotoxin, and is inhibited by bcl-2 and rasagiline, N-propargyl-1®-aminoindan. *J Neurochem* 82(4):913-923

Akiyama H, Barger S, Barnum S et al (2000) Inflammation in Alzheimer's disease. *Neurobiol Aging* 21:383-421

Allderdice PW, Gardner HA, Galutira D et al (1991) The cloned butyrylcholinesterase (*BCHE*) maps to a single chromosome site, 3q26. *Genomics* 11:452-454

Alonso ADC, Zaidi T, Grundke-Iqbal I et al (1994) Role of abnormally phosphorylated tau in the breakdown of microtubules in Alzheimer's disease. *Proc Natl Acad Sci USA*, 91:5562-5566

Alvarez A, Alarcon R, Opazo C et al (1998) Stable complexes involving acetylcholinesterase and amyloid-beta peptide change the biochemical properties of the enzyme and increase the neurotoxicity of Alzheimer's fibrils. *J Neurosci* 18:3213-3223

Alvarez-Arcaya A, Combarros O, Llorca J et al (2000) The butyrylcholinesterase K variant is a protective factor for sporadic Alzheimer's disease in women. *Acta Neurol Scand* 102:350-353

Avila M, Balsa MD, Fernandez-Alvarez E et al (1993) The effect of side-chain substitution at position 2 and 3 of the heterocyclic ring of N-acetylenic analogues of triptamine as monoamine oxidase inhibitors. *Biochem Pharmacol* 45, 2231-2237

Alzheimer's Association. Alzheimer's disease: facts and figures. *Alzheimer's dementia* 2009, 5; 234-270

Alzheimer A, Stelzmann RA, Schnitzlein HN et al (1995). An english translation of Alzheimer's 1907 paper, "Uber eine eigenartige Erkankung der Himrinde". *Clin Anat* 8:429-431

Arendt T and Bigl V (1986) Alzheimer plaques and cortical cholinergic innervation. *Neuroscience* 17:227-279

Areosa SA, Sheriff F, Mc Shane R. (2005). Memantine for dementia. *Cochrane Database Syst Rev* (2) CD003154 .

Arpagaus M, Kott M, Vatsis KP et al (1990) Structure of the gene for human butyrylcholinesterase. Evidence for a single copy. *Biochemistry* 9:124-131

Arendt T, Bigl V, Walther F et al (1984). Decreased ratio of CFS acetylcholinesterase and butyrylcholinesterase activity in Alzheimer's disease. *Lancet* 1:173

Arendt T, Fischer S, Bigl V et al (1987). Age related changes in human nucleus basalis of Meynert in comparison to dementing disorders. In: Trojan S, Stasny F (eds) Ontogenesis of the brain, Vol 4. Universitas Carolina, Praha, pp53-55

Arendt T, Bruckner NK, Lange M et al (1992). Changes in acetylcholinesterase and butyrylcholinesterase in Alzheimer's disease resemble embryonic development – a study of molecular forms. *Neurochem Int* 21:381-396

Avramovich-Tirosh Y, Amit T, Bar-Am O et al (2007) Therapeutic targets and potential of the novel brain-permeable multifunctional iron chelator-monoamine oxidase inhibitor drug, M30, for the treatment of Alzheimer's disease. *J Neurochem* 100(2):490-502

Badia A, Banos JE, Camps P et al (1998) Synthesis and evaluation of tacrine-huperzine A hybrids as acetylcholinesterase inhibitors of potential interest for the treatment of Alzheimer's disease. *Bioorg Med Chem* 6:427-440

Baker GB and Reynolds GP (1989) Biogenic amines and their metabolites in Alzheimer's disease: noradrenaline, 5-hydroxytryptamine and 5-hydroxyindole-3-acetic acid are depleted in the hippocampus but not in substantia innominata. *Neurosci Lett* 100:335-339.

Ballard CG, Greig NH, Guillozet-Bongaarts AL et al (2005). Cholinesterases: roles in the brain during health and disease. *Curr Alzheimer Res* 2:307-318

Ballard C, Day S, Sharp S et al (2008) Neuropsychiatric symptoms in dementia: importance and treatment considerations. *Int Rev Psychiatry* 20(4):396-404. Review

Balsa D, Fernandez-Alvarez E, Tipton KF et al (1991) Monoamine oxidase inhibitory potencies and selectivities of 2[N-(2-propynyl)-aminomethyl]-1-methyl indole derivatives. *Biochem Soc Trans* 19:215-218

Balsa D, Perez V, Fernandez-Alvarez E et al (1994) Kinetic behaviour of some acetylenic incolalkylamine derivatives and their corresponding parent amines. *J Neural Transm Suppl* 41, 281-285.

Bar-Am O, Amit T, Youdim BM (2004) Contrasting neuroprotective and neurotoxic actions of respective metabolites of anti-Parkinson drugs rasagiline and selegiline. *Neurosci Lett* 355:169-172

Bar-Am O, Weinreb O, Amit T et al (2005) Regulation of Bcl-2 family proteins, neurotrophic factors, and APP processing in the neurorescue activity of propargylamine. *FASEB J* 19(13):1899-1901

Bar-Am O, Weinreb O, Amit T et al (2009) The novel cholinesterase-monoamine oxidase inhibitor and antioxidant, ladostigil, confers neuroprotection in neuroblastoma cells and aged rats. *J Mol Neurosci* 37(2):135-145

Barner EL and Gray SL (1998) Donepezil use in Alzheimer's disease. Ann Pharmacother 32:70-77

Barnham KJ, Masters CL, Bush AI (2004). Neurodegenerative diseases and oxidative stress. *Nat Rev Drug Discov*, Mar;3(3):205-14.

Bartolini M, Bertucci C, Bolognesi ML et al (2007) Insight into the kinetic of amyloid beta (1-42) peptide self-aggregation: elucidation of inhibitors' mechanism of action. *Chembiochem* 8(17):2152-2161

Bartolini M, Naldi M, Fiori J et al (2011) Kinetic characterization of amyloid-beta 1-42 aggregation with a multimethodological approach. *Anal Biochem* 414(2):215-225.

Bartus RT, Dean RL, Beer B et al (1982), The cholinergic hypotheses of geriatric memory dysfunction. *Science* 217:408-414

Bartzokis G (2007) Acetylcholinesterase inhibitors may improve myelin integrity. *Biol Psychiatry* 62(4):294-301. Epub 2006 Oct 27. Review

Basha MR, Wei W, Bakheet SA et al (2005) The fetal basis of amyloidogenesis: exposure to lead and latent overexpression of amyloid precusor protein and beta-amyloid in the aging brain. *J Neurosci* 25:823-829

Bayer TA, Cappai R, Masters CL et al (1999). It all sticks together—the APP-related family of proteins and Alzheimer's disease. *Mol Psychiatry* 4:524-528

Bayer A and Reban J (2004). Alzheimer's disease and relative conditions. pp3-330. MEDEA Press

Beal MF (1992). Does impairment of energy metabolism result in excitotoxic neuronal death in neurodegenerative illnesses? Ann Neurol. Feb;31(2):119-30

Beckman JS, Beckman TW, Chen J et al (1990) Apparent hydroxyl radical production by peroxynitrite: implications for endothelial injury from nitric oxide and superoxide. *Proc Natl Acad Sci USA* 87:1620-1624

Behl C, Davies JB, Lesley R et al (1994) Hydrogen peroxide mediates amyloid beta protein toxicity. *Cell* 77:817-827

Belluti F, Rampa A, Piazzi L et al (2005) Cholinesterase inhibitors: xhantostigime derivativesblocking the acetylcholinesterase-induced the beta-amyloid aggregation. *J Med Chem* 48:4444-4456.

Belluti F, Bartolini M, Bottegoni G et al (2011) Benzophenone-based derivatives: a novel series of potent and selective dual inhibitors of acetylcholinesterase and acetylcholinesterase-induced beta-amyloid aggregation. *Eur J Med Chem* 46(5):1682-1693

Benseny-Cases N, Cócera M and Cladera J (2007) Conversion of non-fibrillar b-sheet oligomers into amyloid fibrils in Alzheimer's disease amyloid peptide aggregation. *Biochem Biophys Res Communications* 361:916-921

Berliocchi L, Bano D and Nicotera P (2005) Ca2+ signals and death programmes in neurons. *Philos Trans R Soc Lond B Biol Sci* 360:2255-2258

Bhat RV, Budd Haeberlein SL, Avila J (2004) Glycogen synthase kinase 3: a drug target for CNS therapies. *J Neurochem* 89(6):1313-1317. Review

Bierer LM, Haroutunian V, Gabriel S et al (1995). Neurochemical correlates of dementia severity in Alzheimer's disease: relative importance of the cholinergic deficits. *J Neurochem* 64:749-760

Biesold D, Inanami O, Sato A et al (1989) Stimulation of the nucleus basalis of Meynert increases cerebral cortical blood flow in rats. *Neurosci Lett* 98:39-44

Bigl V, Arendt T and Biesold D (1990). The nucleus basalis of Meynert during aging and in dementing neuropsychyatric disorders. In: Steriade M, Biesold D (eds) Brain cholinergic systems. *Oxford University Press*, Oxford, pp364-386

Bird TD (2008). Genetic aspects of Alzheimer's disease. *Genet Med* 10:231-239

Birks J and Flicker L (2003) Selegiline for Alzheimer's disease. *Cochrane Database Syst Rev*, CD000442

Birks J and Harvey R. (2006). Donepezil for dementia due to Alzheimer's disease. *Cochrane Database Syst Rev* (1) CD001190.

Birks J, Grimley EJ, Iakovidou V et al. (2000). Rivastigmine for Alzheimer's disease. *Cochrane Database Syst Rev* (4) CD001191.

Bitan G, Kirkitadze MD, Lomakin A et al (2003) Amyloid beta-protein (Abeta) assembly: Abeta 40 and Abeta 42 oligomerize through distinct pathways. *Proc Natl Acad Sci USA* 100:330-335.

Bolognesi ML, Andrisano V, Bartolini M et al (2005) Propidium-based polyamine ligands as potent inhibitors of acetylcholinesterase and acetylcholinesterase-induced amyloid-beta aggregation. *J Med Chem* 48:24-27

Bolognesi ML, Minarini A, Tumiatti V et al (2006) Lipoic acid, a lead structure for multitarget-directed drugs for neurodegeneration. *Mini-Rev Mec Chem* 6:1269-1274

Bolognesi ML, Minarini A, Rosini M et al (2008) From dual binding site acetylcholinesterase inhibitors to multi-target-directed ligands (MTDLs): a step forward in the treatment of Alzheimer's disease. *Mini Rev Med Chem* 8(10):960-967

Bolognesi ML, Cavalli A and Melchiorre C (2009) Memoquin: a multi-target-directed-ligand as an innovative therapeutic opportunity for Alzheimer's disease. *Neurotherapeutics* 6:152-162

Bondareff W, Mountjoy CQ and Roth M (1982) Loss of neurons of origin of the adrenergic projections to the cerebral cortex (nucleus locus coeuleus) in senile dementia. *Neurology* 32:164-168

Bragin V, Chemodanova M, Dzhafarova N et al (2005) Integrated treatment approach improves cognitive function in demented and clinically depressed patients. *Am J Alzheimer's Dis Other Dementias* 20:21-26

Bruhlmann C, Marston A, Hostettmann K et al (2004) Screening of non-alkaloid natural compounds as acetylcholinesterase inhibitors. *Chem Biodiversity* 1:819-829.

Buccafusco JJ and Terry AV Jr (2000) Multiple central nervous system targets for eliciting beneficial effects on memory and cognition. J Pharmacol Exp Ther 295(2):438-446

Bullock R and Lane R (2007) Executive discontrol in dementia, with emphasis on subcortical pathology and the role of butyrylcholinesterase. *Curr Alzheimer Res* 4:227-293

Burke WJ, Li SW, Chung HD et al (2004) Neurotoxicity of MAO metabolites of catecholamine neurotransmitters: role in neurodegenerative diseases. *Neurotoxicology* 25:101-115

Bush AI (2003) The metallobiology of Alzheimer's disease. *Trends Neurosci* 26:207-214

Bush AI and Tanzi RE (2008) Therapeutics for Alzheimer's disease based on the metal hypothesis. *Neurotherapeutics* 5:421-432

Butterfield DA, Griffin S, Munch G, et al (2002). Amyloid beta-peptide and amyloid pathology are central to the oxidative stress and inflammatory cascades under which Alzheimer's disease brain exists. *J Alzheimers Dis*, Jun;4(3):193-201.

Byeon SR, Lee JH, Sohn JH et al (2007) Bis-styrylpyridine and bis-styrylbenzene derivatives as inhibitors for Ab fibril formation. *Bioorg Med Chem Lett* 17:1466-1470

Byun JH, Kim H, Kim Y et al (2008) Aminostyrylbenzofuran derivatives as potent inhibitors for A□ fibril formation. *Bioorg Med Chem Lett* 18:5591-5593.

Caraci F, Copani A, Nicoletti F et al (2010) Depression and Alzheimer's disease: Neurobiological links and common pharmacological targets. *Eur J Pharmacol* 626:64-71

Camps P, El AR, Gorbig DM et al (1999) Synthesis, in vitro pharmacology, and molecular modeling of very potent tacrine-huperzine A hybrids as acetylcholinestrase inhibitors of potential interest for the treatment of Alzheimer's disease. *J Med Chem* 42:3227-3242

Camps P, Cusack B, Mallender WD et al (2000a) Huprine X is anovel high-affinity inhibitor of acetylcholinesterase that is of interest for treatment of Alzheimer's disease. *Mol Pharmacol* 57:409-417

Camps P, El AR, Morral J et al (2000b) New tacrine-huperzine A hybrids (huprines): highly potent, tight-binding acetylcholinesterase inhibitors of interest for the treatment of Alzheimer's disease. *J Med Chem* 43:4657-4666

Camps P, Gomez E, Munoz-Torrero D et al (2001) Synthesis, in vitro pharmacology, and molecular modeling of syn-huprines as acetylcholinesterase inhibitors. *J Med Chem* 44:4733-4736

Camps P and Munoz-Torrero D (2001) Tacrine-huperzine A hybrids (huprines): a new class of highly potent and selective acetylcholinesterase inhibitors of interest for the treatment of Alzheimer's disease. *Mini Rev Med Chem* 1:163-174.

Camps P, Formosa X, Galdeano C et al (2008) Novel donepezil-based inhibitors of acetyl- and butyrylcholinesterase and acetylcholinesterase-induced beta-amyloid aggregation. *J Med Chem* 51(12):3588-3598

Camps P, Formosa X, Galdeano C et al (2009) Pyrano[3,2-c]quinoline-6-chlorotacrine hybrids as a novel family of acetylcholinesterase and beta-amyloid-directed anti-Alzheimer compounds. *J Med Ch*em 52(17):5365-5379

Carrillo MC, Minami C, Kitani K et al (2000) Enhancing effect of rasagiline on superoxide dismutase and catalase activities in the dopaminergic system in the rat. *Life Sci* 67:577-585

Carrillo MC, Kanai S, Nokubo M et al (1991) (-)deprenyl induces activities of both superoxyde dismutase and catalase but not of glutathione peroxidase in the striatum of young male rats. *Life Sci* 48:517-521

Castro A and Martinez A (2006) Targeting beta-amyloid pathogenesis through acetylcholinesterase inhibitors. *Curr Pharm Des* 12(33):4377-4387. Review

Cavalli A, Bolognesi ML, Minarini A, et al (2008). Multi-target-Directed Ligands To Combat Neurodegenerative Diseases. *J Med Chem* 51(3);347-372.

Cavalli A, Bolognesi ML, Capsoni S et al (2007) Small molecule targeting the multifactorial nature of Alzheimer's disease. *Agew Chem Int* Ed 46, 3689.3682

Chartier-Harlin MC, Crawford F and Houlden H et al (1991). Early-onset Alzheimer's disease caused by mutations at codon 717 of the beta-amyloid precursor protein gene. *Nature* 353(6347):844-846

Chatonnet A and Lockridge O (1989) Comparison of butyrylcholinesterase and acetylcholinesterase. *Biochem J* 260:625-634

Cheng Y, Feng Z, Zhang QZ et al (2006) Beneficial effects of melatonin in experimental models of Alzheimer's disease. *Acta Pharmacol Sin* 27:129-139.

Christensen H, Maltby N, Jorm AF et al (1992). Cholinergic "blockade"as a model of the cholinergic deficits in Alzheimer's disease. *Brain* 115:1681-1699

Churcher I (2006) Tau therapeutic strategies for the treatment of Alzheimer's disease. *Curr Top Med Chem* 6(6):579-595 Review

Cohen G, Pasik P, Cohen B et al (1984) Pargyline and deprenyl prevent the neurotoxicity of 1-methyl-4-phenyl-1,2,3,6-tetrahydropyrydine (MPTP) in monkeys. *Eur J Parmacol* 106:209-210

Combs CK, Carlo JC, Kao SC et al (2001) beta-amyloid stimulation of microglial and monocytes results in TNF-alpha-dependent expression on inducible nitric oxide synthase and neuronal apoptosis. *J Neurosci* 21:1179-1188

Conn PJ and Pinn JP (1997) Pharmacology and functions of metabotropic glutamate receptors. *Annu Rev Pharmacol Toxicol* 37:205-237

Corder EH, Saunders AM, Stritmater WJ et al (1993) Gene-dose of apolipoprotein E type 4 allele and the risk of Alzheimer's disease in late onset families. *Science* 261, 921-923

Corder EH, Saunders AM, Strittmatter WJ et al (1993).Gene dose of apolipoprotein E type 4 allele and the risk of Alzheimer's disease in late onset families. *Science* 261(5123):921-923

Coyle J.T and Puttfarcken P (1993) Oxidative stress, glutamate and neurodegenerative disorders. *Science* 262:689-695

Craig LA, Hong NS and Mc Donald RJ (2011) Revisiting the cholinergic hypothesis in the development of Alzheimre's disease. *Neurosci Biobehav* Reviews.

Creeley CE, Wozniak DF, Nardi A et al (2008). Donepezil markedly potentiates memantine neurotoxicity in the adult rat brain. *Neurobiol Aging*. 29(2),153-67

Cross AJ, Crow TJ, Perry EK et al (1981) Reduced dopamine-beta-hydroxylase activity in Alzheimer's disease. *Br Med J* 282:93-94

Cross AJ (1990) Serotonin in Alzheimer type dementia and other dementing illnesses. *Ann N Y Acad Sci* 600:405-415

Cummings JL, Doody R and Clark C (2007). Disease-modifying therapies for Alzheimer disease. *Neurology* 69:1622-1634

Cutillas B, Ambrosio S, Unzeta M (2002) Neuroprotective effect of the monoamine oxidase inhibitor PF9601N [*N*-(2-propynyl)-2-(5-benzyloxy-indolyl) methylamine] on rat nigral neurons after 6-hydroxydopamine-striatal lesion. *Neurosci Lett* 329:165-168

Darvesh S and Hopkins DA (2003). Differential distribution of acetylcholinesterase and butyrylcholinesterase in the human thalamus. *J Comp Neurol* 463:25-43

Darvesh S, Grantham DL and Hopkins DA (1998). Distribution of butyrylcholinesterase in the human amygdale and hippocampal formation. *J Comp Neurol* 393:374-390

Darvesh S, Hopkins DA and Geula C (2003) Neurobiology of butyrylcholinesterse. *Nat Rev Neurosci* 4:131-138

Davies P and Maloney AJ (1976). Selective loss of central cholinergic neurons in Alzheimer's disease. *Lancet* 2: 1403

Dawson GR, Seabrook GR, Zheng H et al (1999) Age-related cognitive deficits, impaired long-term potentiation and reduction in synaptic marker density in mice lacking the beta-amyloid precursor protein. *Neuroscience* 90:11-13.

Dedeoglu A, Cormier K, Payton S et al (2004) Preliminary studies of a novel bifunctional metal chelator targeting Alzheimer's amyloidogenesis. *Exp Gerontol* 39:1641-1649.

DeKosky ST, Ikonomovic MD, Styren SD et al (2002). Upregulation of choline acetyltransferase activity in hippocampus and frontal cortex of elderly subjects with mild cognitive impairment. *Ann Neurol* 51:145-155

De los Rios C, Marco JL, Carreiras MD et al (2002) Novel tacrine derivatives that block neuronal calcium channels. *Bioorg Med Chem* 10:2077-2088

Del Toro D, Coma M, Uribesalgo I et al (2005) The amyloid beta protein precursor and Alzheimer's disease – Therapeutic approaches. *Curr Med Chem* 5:271-283

Detari L, Rasmusson DD and Semba K (1999). The role of basal forebrain neurons in tonic and phasic activation of the cerebral cortex. *Prog Neurobiol* 58:249-277

Deustch JA (1971). The cholinergic synapse and the site of memory. *Science* 174:788-794

Dickson DW, Crystal HA, Bevona C et al (1995) Correlations of synaptic and pathological markers with cognition of the elderly. *Neurobiol Aging* 16(3)285-298

Dobson CM (2004) Principles of protein folding, misfolding and aggregation. *Seminars in Cell & Develop Biol* 15:3-16

Drouet B, Pincon-Raymond M, Chambaz J et al (2000) Molecular basis of Alzheimer's disease. *Cell Mol Life Sci* 57:705-715

Drubin DG and Kirschner MW (1986) Tau protein function in living cells. J Cell Biol 103:2739-2746.

Durairajan SS, Yuan Q, Xie L et al (2008) Slavianolic acid B inhibits A□ fibril formation and disaggregates preformed fibrils and protects against Ab-induced cytotoxicity. *Neurochem Int* 52:741-750.

Ebmeier KP, Hunter R, Curran SA et al (1992) effect of a single dose of acetylcholinesterase inhibitor velnacrine on recognition memory and regional derebral blood flow in Alzheimer's disease. *Psychopharmacology* 108(1-2):103-109

Edbauer D, Winkler E, Regula JT et al (2003) Reconstitution of gamma-secretase activity. *Nat Cell Biol* 5:486-488.

Ekblom J, Jossan SS, Oreland L et al (1994) Reactive gliosis and monoamine oxidase B. *J Neural Transm* Suppl 41:253-258

Eliezer D, Barre P. Kobaslija M et al (2005) Residual structure in the repeat domain of tau: echoes of microtubule binding and paired helical filament formation. *Biochemistry* 44:1026-1036

Elsinghorst, P. W.; Cieslik, J. S.; Mohr, K, et al (2007). The first gallamine-tacrine hybrid: Design and characterization at cholinesterases and the M_2 muscarinic Receptor. *J. Med. Chem*, *50*, 5685-5695.

Fang, L.; Appenroth, D.; Decker, Met al (2008). Synthesis and biological evaluation of NO-donor-tacrine hybrids as hepatoprotective anti-Alzheimer drug candidates. *J. Med. Chem*, *51*, 713-716.

Ferrer I, Gómez-Isla T, Puig B et al (2005) Current advances on different kinases involved in tau phosphorylation, and implications in Alzheimer's disease and tauopathies. *Curr Alzheimer Res* 2:3-18.

Fibiger HC (1991). Cholinergic mechanisms in learning, memory, and dementia: a review of recent evidence. *Trends Neurosci* 14:220-223

Filip V and Kolibas E (1999) Selegiline in the tretament of Alzheimer's disease: a long-term randomised placebo-controlled trial. Czech and Slovak Senile Dementia of Alzheimer type Study Group. *J Psychiatry Neurosci* 24:234-243

Finberg JP, Lamensdorf I, Commisiong JW et al (1996) Pharmacology and neuroprotective properties of rasagiline. *J Neural Transm Suppl* 48:95-101

Fink DM, Palermo MG, Bores GM et al (1996) Imino 1,2,3,4-tetrahydrocyclopent[b]indole carbamates as dual inhibitors of acetylcholinesterase and monoamine oxidase. *Bioorg Med Chem Lett* 6:625-630

Fisher A (2008) M1 muscarinic agonists target major hallmarks of Alzheimer's disease-the pivotal role of brain M1 receptors. *Neurodegener Dis* 5:237-240

Flaris NA, Densmore TL, Molleston MC, Hickey WF. (1993) Characterization of microglia and macrophages in the central nervous system of rats: definition of the differential expression of molecules using standard and novel monoclonal antibodies in normal CNS and in four models of parenchymal reaction. *Glia* Jan;7(1):34-40.

Fonnum F (1984) Glutamate: a neurotransmitter in mammalian brain. *J Neurochem* 42:1-11

Francis PT, Sims NR, Procter AW et al (1993) Cortical pyramidal neuronal loss may cause glutamatergic hypoactivity and cognitive impairment in Alzheimer's disease: investigative and therapeutic perspectives. *J Neurochem* 60:1589-1604

Francis PT, Nordberg A, Arnold SE (2005) A preclinical view of cholinesterase inhibitors in neuroprotection: do they provide more than symptomatic benefits in Alzheimer's disease? *Trends Phatmacol Sci* 26:104-111

Francis PT, Palmer AM, Snape M et al (1999) The cholinergic hypothesis of Alzheimer's disease: a review of progress *J Neurol Neurosurg Psychiatry* 66:137-147

Garai K, Sahoo B, Kaushalya SK et al (2007) Zinc lowers amyloid beta toxicity by selectively precipitating aggregation intermediates. *Biochemistry* 46:10655-10663

Geerlings MI, Shoevers RA, Beekman AT et al (2000) Depression and risk of cognitive decline and Alzheimer's disease. Results of two prospective community-based studies in The Netherlands. *Br J Psychiatry* 176:568-575

George ST and Balasubramanian AS (1981) The aryl acylamidases and their relationship to cholinesterases in human serum, erythrocyte and liver. *Eur J Biochem* 121:177-186

Getman DK, Eubanks JH, Camp S et al (1992) The human gene encoding acetylcholinesterase is located on the long arm of chromosome 7. *Am J Hum Genet* 51:170-177

Geula C and Mesulam MM (1999) in Alzheimer Disease (2nd edn) (eds. Terry R, Katzman R, Bick K & Sisodia SS) 269-292 (Lippincot Williams & Wilkins, Philadelphia, Pennsylvania)

Geula C, Greenberg BD, and Mesulam MM (1994). Cholinesterase activity in the plaques, tangles and angiopathy of Alzheimer's disease does not emanate from amyloid. *Brain Res* 644:327-330

Geula C and Mesulam MM (1995). Cholinesterases and the pathology of Alzheimer's disease. *Alzheimer Dis Assoc Disord* 9 Suppl 2:23-28

Geula C and Mesulam MM (1989) Cortical cholinergic fibers in aging and Alzheimer's disease: a morphometric study. *Neuroscience* 33 (3):469-481

Giacobini E (2003). Cholinesterases: new roles in brain function and in Alzheimer's disease. Neurochem *Res* 50:433-440

Giacobini E (2000) Cholinesterases and cholinesterase inhibitors (ed. Giacobini E) 181-226 (Martin Dunitz Ltd. London)

Giacobini E, Spiegel R, Enz A et al (2002) Inhibition of acetyl- and butyryl-cholinesterase in the cerebrospinal fluid of patients with Alzheimer's disease by rivastigmine: correlation with cognitive deficit. *J Neural Transm* 109:1053-1065.

Giacobini E (2002) Long term stabilising effect of cholinesterase inhibitors in the therapy of Alzheimer's disease. *J Neural Transm* 181-187

Gilman S, Koller M, Black RS et al (2005) Clinical effects of Abeta immunization (AN1792) in patients with AD in an interrupted trial. *Neurology* 64(9):1553-1562

Glenner GG and Murphy MA (1989) Amyloidosis of the nervous system. *J Neurol Sci* 94(1-3):1-28

Glenner GG and Wong CW (1984) Alzheimer's disease: intial report of the purification and characterization of a novel cerebrovascular amyloid protein. *Biochim Biophys Res Commun* 16;120(3):885-890

Gnerre C, Catto M, Leonetti F et al (2000) Inhibition of monoamine oxidases by functionalised coumarine derivatives: biological activities, QSARs and 3D-QSARs. *J Med Chem* 43: 4747-4758.

Goate A, Chartier-Harlin MC, Mullan M et al (1991). Segregation of a missense mutation in the amyloid precursor protein gene with familial Alzheimer's disease. *Nature* 349(6311):704-706

Goedert M, Spillantini MG, Potier MC et al (1989a) Cloning and sequencing of the cDNA encoding an isoforma of microtubule-associated protein tau containing four tandem repeats: differential expression oo tau protein mRNAs in human brain. *EMBO J* 8:393-399.

Goedert M, Spillantini MG, Jakes R et al (1989b) Multiple isoforms of human microtubule-associated protein tau: sequences and localization in neurofibrillary tangles of Alzheimer's disease. *Neuron* 3(4):519-526

Goedert M, Wischik CM, Crowder RA et al (1988) Cloning and sequencing of the cDNA encoding a core protein of the paired helical filament of Alzheimer disease: identification as the microtubule-associated protein tau. *Proc Natl Acad Sci USA* 85(11):4051-4055

Goedert M and Spillantini MG (2006) A century of Alzheimer's disease. *Science* 314(5800):777-781Review

Greenamyre JT and Young AB (1989) Excitatory amino acids in Alzheimer's disease. *Neurobiol Aging* 10:593-602

Greig NH, Utsuki T, Yu Q et al (2001) A new therapeutic target in Alzheimer's disease: attention to butyrylcholinesterase. *Curr Med Res Opin* 17:159-165

Greig NH, Utsuki T Ingram DK et al (2005) Selective butyrylcholinesterase inhibition elevates brain acetylcholine, augments learning and lowers Alzheimer beta-amyloid peptide in rodent. *Proc Natl Acad Sci USA* 102(47):17213-17218

Grillo-Bosch D, Carulla N, Cruz M (2009) Retro-enantio N-methylated peptides as beta-amyloid aggregation inhibitors. *ChemMecChem* 4(9):1488-1494

Grimsby, J; Lan, N.C; Neve, R; et al (1990). Tissue distribution of human monoamine oxidase A and B mRNA. *J Neurochem*, 55(4), 1166-1169

Grossberg GT, Edwards KR and Zhao Q (2006). Rationale for combination therapy with galantamine and memantine in Alzheimer's disease. *J Clin Pharmacol* 46(7 Suppl 1):17S-26S Review

Grundke-Iqbal I, Iqbal K, Tung Y.C, et al (1986). Abnormal phosphorylation of the microtubule-associated protein (tau) in Alzheimer cystoskeletal pathology. *Proc. Natl. Acad. Sci* USA, 93:4913-4917

Gualtiery CT and Morgan DW (2008) The frequency of cognitive impairment in patients with anxiety, depression, and bipolar disorder: an unaccounted source of variance in clinical trials. *J Clin Psychiatry* 69(7):1122-1130

Guillozet AL, Smiley JL, Mash DC et al (1997) Butyrylcholinesterase in the life cycle of amyloid plaques. *Ann Neurol* 42:909-918

Hamaguchi T, Ono K, Murase A et al (2009) Phenolic compounds prevent Alzheimer's pathology through different effects on the amyloid-b-aggregation pathway. *Am J Pathol* 175:2557-2565.

Hardy JA and Higgins GA (1992) Alzheimer's disease: the amyloid cascade hypothesis. *Science* 256, 184-185

Hardy J (1997a). Amyloid, the presenilins, and Alzheimer's disease. *Trends Neurosci* 20(4):154-159

Hardy J (1997b). The Alzheimer family of diseases: many etiologies, one pathogenesis? *Proc Natl Acad Sci USA* 94, 2095-2097

Hardy J and Selkoe DJ (2002) The amyloid hypothesis of Alzheimer's disease: progress and problems on the road to therapeutics. *Science* 297, 353-356

Harkins SW, Taylor JR, Mattay V et al (1997) Tacrine treatment in Alzheimer's diseaseenhances cerebral blood flow and mental status and decreases caregiver suffering. *Ann NY Acad Sci* 826:472-474

Harman D. (1956). Aging: a theory based on free radical and radiation chemistry. *J Gerontol*, Jul;11(3):298-300.

Harman D (1972) Free radical theory of aging:dietary implications. *Am J Clin Nutr* 25(8):839-843

Haroutunian V, Santucci AC and Davis KL (1990) Implications of multiple transmitter system lesions for cholinomimetic therapy in Alzheimer's disease. *Prog Brain Res* 84:333-346

Harper JD and Landsbury Jr PT (1997) Models of amyloid seeding in Alzheimer's disease and scrapie: mechanistic truths and physiological consequences of the time-dependent solubility of amyloid proteins. *Annu Rev Biochem* 66:385-407

Hauptmann S, Keil U, Scherping I et al (2006) Mitochondrial dysfunction in sporadic and genetic Alzheimer's disease. *Exp Gerontol* 41:668-73

Heinonen EH, Antilla MI, Lammintausta RA (1994) Pharmacokinetic aspects of l-deprenyl (selegiline) and its metabolites. *Clin Pharmacol Ther* 56:742-749

Hilt D, Gawryl M, Koening G et al (2009) EVP-6124: safety, tolerability and cognitive effects of a novel A7 nicotinic receptor agonist in Alzheimer's disease patients on stable donepezil or rivastigmine therapy. International Conference on Alzheimer's Disease, Vienna, Austria, July 11-16

Holmes C, Boche D, Wilkinson D et al (2008) Long-term effects of Abeta 42 immunisation in Alzheimer's disease: follow-up of a randomised, placebo-controlled phase I trial. *Lancet* 372:216-223

Holmes C, Ballard C, Lehmann D et al (2005) Rate of progression of cognitive decline in Alzheimer's disease: effect of butyrylcholinesterase K gene variation. *J Neurol Neurosurg Psychiatry* 76(5):640-643

Hoozemans JJ, Veerhuis R, Van Haastert ES et al (2005) The unfolded protein response is activated in Alzheimer's disease. *Acta Neuropathol* 100(2):165-172.

Huang X, Moir RD, Tanzi RD et al (2004) Redox-active metals, oxidative stress and Alzheimer's disease pathology. *Ann Y Acad Sci* 1012:153-163

Huang TH, Yang DS, Plaskos NP et al (2000) Structural studies of soluble oligomers of the Alzheimer beta-amyloid peptide. *J Mol Biol* 297:73-87

Inestrosa NC, Alvarez A, Perez CA (1996) Acetylcholinesterase accelerates assembly of amyloid beta peptides into Alzheimer's fibrils: possible role of the peripheral site of the enzyme. *Neuron* 16:881-891

Iqbal K and Grundke-Iqbal I (2008) Alzheimer neurofibrillary degeneration: significance, etiopathogenesis, therapeutics and prevention. *J Cell Mol Med* 21(1):38-55 Review

Isaacs AM, Senn DB, Yuan M et al (2006) Acceleration of amyloid-beta peptide aggregation by physiological concentrations of calcium. *J Biol Chem* 281:27916-17923

Jellinger KA (2003). General aspects of neurodegeneration. *J Neural Transm Suppl* (65)101-144.

Jenner P (2004) Preclinical evidence for neuroprotection with monoamine oxidase-B inhibitors in Parkinson's disease. *Neurology* 63, S13-S2

Jin M, Shepardson N, Yang T et al (2011) Soluble amyloid-beta protein dimmers isolated from Alzheimer cortex directly induce tau hyperphosphorilation and neuritic degeneration. *Proc Natl Acad Sci USA*. Apr 5;108(14):5819-5824

Johnston, J.P.(1968) Some observations upon a new inhibitor of monoamine oxidasein brain tissue. *Biochem Pharmacol*, 17(7), 1285-1297

Kamal A, Stokin GB, Yang Z et al (2000) Axonal transport of amyloid precursor protein is mediated by direct binding to the kinesin light chain subunit of kinsesin-I. *Neuron* 28:449-459

Kamal MA, Al-Jafari AA, Yu QS et al (2006) Kinetic analysis of the inhibition of human butyrylcholinesterase with cymserine. *Biochim Biophys Acta* 1760:200-206

Kamenetz F, Tomita T, Hsieh H (2003) APP processing and synaptinc function. *Neuron* 37:925-937

Kelly KM, Gross RA and Mac Donald RL (1991) Tetrahydroaminoacridine (THA) reduces voltage-dependent calcium currents in rat sensory neurons. *Neurosci Lett* 132: 247-250

Ki CS, Na DL, Kim JW et al (1999) No association between the genes for butyrylcholinesterase K variant and apolipoprotein E4 in late-onset Alzheimer's disease. *Am J Med Genet* 88:113-135

Klein WL, Kraft GA and Finch CD (2001) Targeting small Abeta oligomers: the solution to an lazheimer's disease conundrum. *Trends Neurosci* 24 219-224

Koffie RM, Meyer-Luehmann M, Hashimoto T et al (2009) Oligomeric amyloid-beta associates with post-synaptic densities and correlates with excitatory synapse loss near senile plaques. *Proc Natl Acad Sci USA* 106(10):4012-4017

Kogen H, Toda N, Tago K et al (2002) Design and synthesis of dual inhibitors of acetylcholinesterase and serotonin transporter targeting potential agents for Alzheimer's disease. *Org Lett* 4:3359-3362.

Knockaert M, Greengard P and Meijer L (2002) Pharmacological inhibitors of cyclin-dependent kinases. *Trends Pharmacol Sci* 23(9):417-425. Review

Kristal BS, Conway AD, Brown AM et al (2001) Selective dopaminergic vulnerability: 3,4-dihydroxyphenylacetaldehyde targets mitochondria. *Free Radic Biol Med* 30:924-931

Lahiri DK, Lewis S and Farlow MR (1994) Tacrine alters processing of beta-amyloid precursor protein in different cell lines. *J Neurosci Res* 37:777-787

Lambert MP, Barlow AK, Chromy BA et al (1998) Diffussible, nonfibrillar ligands derived from Abeta1-42 are potent central nervous system neurotoxins. *Proc Natl Acad Sci USA* 95:6448-6453.

Lamensdorf I, Eisenhofer G, Harvey-White J et al (2000) 3,4-dihydroxyphenylacetaldehyde potentiates the toxic effects of metabolic stress in PC12 cells. *Brain Res* 868:191-201

Lane RM, Potkin SG and Enz A (2006) Targeting acetylcholinesterase and butyrylcholinesterase in dementia. *Int J Neuropsychopharmacol* 9(1):101-124.

Layer PG, Weikert T and Alber R (1993) Cholinesterases regulate neurite outgrowth of chick nerve cells in vitro by means of a non-enzymatic mechanism. *Cell Tissue Res* 273(2):219-226

Le Corre S, Klafki HW, Plesnila N et al (2006) An inhibitor of tau hyperphosphorylation prevents severe motor impairments in tau transgenic mice. *Proc Natl Acad Sci USA* 103(25):9673-9678

Lee MG, Hassani OK, Alonso A et al (2005) Cholinergic basal forebrain neuron busrt with theta during walking and paradoxical sleep. *J Neurosci* 25:4365-4369

Lehman DJ, Johnston C and Smith AD (1997) Synergy between the genes for butyrylcholinesterase K variant and apolipoprotein E4 in late-onset confirmed Alzheimer's disease. *Hum Mol Genet* 6:1933-1936

Lehman DJ, Nagi Z, Litchfield S et al (2000) Association of butyrylcholinesterase K variant with cholinesterase-positive neuritic plaques in the temporal cortex in late-onset Alzheimer's disease. *Hum Genet* 106:447-452.

Leon R, Marco-Contelles J, Garcia AG et al (2005) Synthesis, acetylcholinesterase inhibition and neuroprotective activity of new tacrine analogs. *Bioorg Med Chem* 13:1167-1175.

LeVine H III (1993) Thioflavine T interaction with synthetics Alzheimer's disease beta-amyloid peptides: detection of amyloid aggregation in solution. *Protein Sci* 2:404-410

Levy-Lahad E, Wijsman E, Nemens E et al (1995b).A familial Alzheimer's disease locus on chromosome 1. *Science* 269(5226):970-973

Li Y, Liu L, Barger SW et al (2003) Interleukin-1 mediates pathological effects of microglial on tau phosphorilation and on synaptophysin synthesis in cortical neurons through a p38-MAPK pathway. *J Neurosci* 23:1605-1611

Li B, Stribley JA, Ticu A et al (2000) Abundant tissue butyrylcholinesterase and its possible function in the acetylcholinesterase knockout mouse. *J Neurochem* 75:1320-1331

Lin MT and Beal MF (2006). Mitochondrial dysfunction and oxidative stress in neurodegenerative diseases. *Nature* 443:787-795.

Lipton P (1999) Ischemic cell death in brain neurons. *Phisiol Rev* 79:1431-1568

Lleo A, Greenberg SM and Growdon JH (2006) Current pharmacotherapy for Alzheimer's disease. *Annu Rev Med* 57:513-533

Lockridge O, Bartels CF, Vaughan TA et al (1987) Complete amino acid sequence of human serum cholinesterase. *J Biol Chem* 262:549-557
Lopez OL, Becker JT, Wisniewski S et al (2002) Cholinesterase inhibitor treatment alters the natural history of Alzheimer's disease. *J Neurol Neurosurg Psychiatry* 72:310-314.

Lovell MA, Robertson JD, Teesdale WJ et al (1998) Cooper, iron and zinc in Alzheimer's disease senile plaques. *J Neurol Sci* 158:47-52

Loy C and Schneider L. (2004). Galantamine for Alzheimer's disease. *Cochrane Database Syst Rev,* (4)CD001747.

Makin OS and Sherpell LC (2005) X-ray diffraction studies of amyloid structure. *Methods Mol Biol* 299:67-80

Mandel SA, Amit T, Weinreb O et al (2008) Simultaneous manipulation of multiple brain targets by green tea catechins: a potential neuroprotective strategy for Alzheimer and Parkinson diseases. *CNS Neurosci Ther* 14(4):352-365 Review

Mandelkow EM and Mandelkow E (1998) Tau in Alzheimer's disease. *Trends Cell Biol* 8:425-427

Mangialasche F, Solomon A, Winblad B et al. (2010). Alzheimer's disease: clinical trials and drug development. *Lancet Neurol* 9:702-716.

Maragos WF, Greenamyre JT, Penney JB et al (1987) Glutamate dysfunction in Alzheimer's disease: a hypothesis. *Trends Neurosci* 10:65-68

Marchitti SA, Deitrich RA, Vasiliou V (2007) Neurotoxicity and metabolism of the catecholamine-derived 3,4-dihydroxyphenylacetaldehyde and 3,4-dihydroxyphenylglycoaldehyd: the role of aldehyde dehydrogenase. *Pharmacol Rev* 59:125-150

Marco JL, de los Rios C, Garcia AG et al (2004) Síntesis, biological evaluation and molecular modeling of diversely functionalised heterociclic derivatives as inhibitors of acetylcholinesterase/butyrylcholinesterase and modulators of Ca2+ channels and nicotinic receptors. *Bioorg Med Chem* 12:2199-2218.

Marco-Contelles, J.; León, R.; de los Ríos, C.; et al (2006a). New multipotent tetracyclic tacrines with neuroprotective activity. *Bioorg Med Chem* 14:8176-8185

Marco-Contelles, J, León, R, Lopez MG (2006b) Síntesis and biological evaluation of new 4H-pyrano[2,3b]quinoline derivatives that block acetylcholinesterase and cell calcium signals, and cause neuroprotection against calcium overload and free radicals. *Eur J Med Chem* 41:1464-1469.

Marco-Contelles, J.; León, R.; de los Ríos, C.; et al (2006c). Novel multipotent tacrine-dihydropyridine hybrids with improved acetylcholinesterase inhibitory and neuroprotective. activities as potential drugs for the treatment of Alzheimer's disease. *J. Med. Chem*, *49*, 7607-7610.

Marin DB, Bierer LM, Lawlor BA et al (1995) l-deprenyl and physostigmine for the treatment of Alzheimer's disease. *Psychiatry Res* 58:181-189.

Martinez A, Alonso M, Castro A et al (2002) First non-ATP competitive glycogen synthase kinase 3 beta (GSK-3beta) inhibitors: thiadiazolidinones (TDZD) as potential drugs for the treatment of Alzheimer's disease. *J Med Chem* 45(6):1292-1299

Martinez-Murillo R and Rodrigo J (1995) The localization of cholinergic naurons and markers in the CNS. In: Stone TW (ed) CNS neurotransmitters and neuromodulators: Acetylcholine. *CRC Press*, Boca Raton, pp1-38

Massoulié J, Pezzementi L, Bon S et al (1993). Molecular and cellular biology of cholinesterases. *Prog Neurobiol* 41:31-91

Massoulié J and Bon S (1982) The molecular forms of cholinesterase and acetylcholinesterase in vertebrates. *Annu Rev Neurosci* 5:57-106

Mattson MP (1997) Cellular actions of beta-amyloid precursor protein and its soluble and fibrillogenic derivatives. *Physiol Rev* 77:1081-1132

Maurer K, Volk S and Gerbaldo H (2000). Augusta D.: The history of Alois Alzheimer's First Case, *Concepts of Alzheimer disease: Biological, Clinical and Cultural Perspectives,* PJ Whitehouse, K. Maurer and JF Ballenger, Baltimore, Johns Hopkins University Press

Mayurama W, Akao Y, Carrillo MC et al (2002) Neuroprotection by propargylamines in Parkinson's disease: supresión of apoptosis and induction of prosurvival genes. *Neurotoxicol Teratol* 24(5):675-682

McEntee WJ and Crook TH (1991) Serotonin, memory, and the aging brain. *Psychopharmacology* 103(2):143-149

Mc Geer PL, Itagaki S, Tago H et al (1987) Reactive microglial in patients with senile dementia of the Alzheimer type are positive for the histocompatibility protein HLA-DR. *Neurosci Lett* 79:195-200

McGeer Pl and Rogers J (1992) Anti-inflammatory agents as a therapeutic approach to Alzheimer's disease. *Neurology* 42:447-449

McGeer Pl, Rogers J, McGeer EG et al (1990) Anti-inflammatory drugs and Alzheimer's disease? *Lancet* 335:1037

Meijer L, Flajolet M and Greengard P (2004) Pharmacological inhibitors of glycogen synthase kinase 3. *Trends Pharmacol Sci* 25(9):471-480 Review

Melchiorre C, Andrisano, V, Bolognesi ML et al (1998) Acetylcholinesterase non-covalent inhibitors based on polyamine backbone for potential use against Alzheimer's disease. *J Med Chem* 41:4186-4189.

Meldrum BS and Garthwaite J (1990) Excitatory amino acid neurotoxicity and neurodegenerative disease. *Trends Pharmacol Sci* 11:993-996

Meltzer CC, Smith G, Price JC et al (1996) Reduced binding of [^{18}F]altanserin to serotonin in type 2A receptors in aging: persistence of effect after partial volume correction. *Brain Res* 813:167-171

Messer WS Jr (2002) Cholinergic agonists and the treatment of Alzheimer's disease. *Curr Top Med Chem* 2(4):353-358 Review

Mesulam MM, Guillozet A, Shaw P et al (2002b) Widely spread butyrylcholinesterase can hydrolyse acetylcholine in the normal and Alzheimer brain. *Neurobiol Dis* 9:88-93

Mesulam MM, Guillozet A, Shaw P et al (2002a) Acetylcholinesterase knockouts establish central cholinergic pathways and can use butyrylcholinesterase to hydrolyse acetylcholine. *Neuroscience* 110:627-639

Mesulam MM and Geula C (1994) Butytylcholinesterase reactivity differentiates the amyloid plaques of aging from those of dementia. *Ann Neurol* 36:722-727

Miranda S, Opazo C, Larrondo LF et al (2000) The role of oxidative stress in the toxicity induced by amyloid beta-peptide in Alzheimer's disease. *Prog Neurobiol* 62:633-648

Mishizen-Eberz AJ, Rissman RA et al (2004) Biochemical and moleculat studies of NMDA receptor subunits NR1/2A/2B in hippocampal subregions throughout progression of Alzheimer's disease pathology. *Neurobiol Dis* 15:80-92.

Moszczynska A, Fitzmaurice P, Ang L et al (2004) Why is Parkinsonism not a feature of human metanphetamine users? *Brain* 127:363-370

Mount C and Downton C (2006) Alzheimer Disease:progress or profit. *Nat Med* 12:780-784

Mulan M, Crawford F, Houlden H et al (1992).A pathogenic mutation for probable Alzheimer's disease in the APP gene at the N-terminus of beta-amyloid. *Nat Genet* 1(5):345-347

Munoz FJ, Opazo C, Gil-Gomez G et al (2002) Vitamin E but not 17beta-estradiol protects against vascular toxicity induced by beta-amyloid wild type and the Dutch amyloid variant. *J Neurosci* 22:3081-3089

Munoz-Ruiz P, Rubio L, Garcia-Palomero E (2005) Desing, synthesis and biological evaluation of dual binding site acetylcholinesterase inhibitors: new disease-modifying agents for Alzheimer's disease. *J Med Chem* 48:7223-7233

Myhrer T (1998) Adverse psychological impact, glutamatergic dysfunction, and risk factors for Alzheimer's disease. *Neurosci Biobehav Rev* 23:131-139

Nakagawa T, Zhu H, Morishima N et al (2000) Caspase-12 mediates endoplasmic-reticulum-specific apoptosis and cytotoxicity by amyloid beta. *Nature* 403, 98-103.

Naoi M, Mayurama W, Yi H et al (2007) Neuroprotection by propargylamines in Parkinson's disease: intracellular mechanism underlying the anti-apoptotic function and search for clinical markers. *J Neural Transm Suppl*, 121-131

Nizri E, Hamra-Amitay Y, Sicsic C et al (2006) Anti-inflammatory properties of cholinergic up-regulation: a new role for acetylcholinesterase inhibitors. *Neuropharmacology* 50(5):540-547

Nordberg A (1992) Neuroreceptor changes in Alzheimer's disease. Cerebrovasc Brain Met Rev 4:303-328

Nunomura A, Perry G, Aliev G, et al. (2001). Oxidative damage is the earliest event in Alzheimer disease. *J Neuropathol Exp Neurol*, Aug;60(8):759-67.

Olanow CW, Rascol O, Hauser R et al (2009) A double-blind, delayed-start clinical trial of rasagiline in Parkinson's disease. *N Engl J Med* 36:1268-1278

Ono K, Yoshiike Y, Takashima A et al (2003) Potent anti-amyloidogenic and fibril-destabilizing effects of polyphenols in vitro: Implications for the prevention and therapeutics of Alzheimer's disease. *J Neurochem* 87: 172-181.

Ordentlich A, Barack D, Kronman C et al (1995) Contribution of aromatic moieties of tyrosine 133 and of the anionic subsite tryptophan 86 to catalytic efficiency and allosteric modulation of acetylcholinesterase. *J Biol Chem*. Feb 3 ;270(5):2082-2091

Ownby RL, Crocco E, Acevedo A et al (2006) Depression and risk for Alzheimer's disease: a systematic review, meta-analysis, and metaregression analysis. *Arch Gen Psychiatry* 63(5):530-538

Ozawa S, Kamiya H and Tsuzuki K (1998) Glutamate receptors in the mammalian central nervous system. *Prog Neurobiol* 54:581-618

Palmer AM, Francis PT, Bowen DM et al (1987) Presynaptic serotoninergic dysfunction in patients with Alzheimer's disease. *J Neurochem* 48(1);8-15

Pei JJ, Sjogren M, Winblad B (2008) Neurofibrillary neurodegeneration in Alzheimer's disease: from molecular mechanisms to identification of drug targets. *Curr Opin Psychiatry* 21:555-561

Perez V, Unzeta M (2003) PF9601N [*N*-(2-propynyl)-2-(5-benzyloxy-indolyl) methylamine], a new MAO-B inhibitor, attenuates MPTP-induced depletion of striatal dopamine levels in C57/BL6 mice. *Neurochem Int* 42:221-229

Perez V, Marco JL, Fernandez-Alvarez E et al (1999) Relevance of benzyloxy group in 2-indolyl methylamines in the selective MAO-B inhibition. *Br J Pharmacol* 127:869-876

Perez V, Marco JL, Fernandez-Alvarez E et al (1996) Kinetic studies of N-allenic analogues of tryptamine as monoamine oxidase inhibitors. *J Pharm Pharmacol* 48:718-722

Perry Ek, Perry RH,, Blessed G et al (1977b) Necropsy evidence of central cholinergic deficits in senile dementia. *Lancet* 1, 189

Perry G, Raina AK, Nunomura A, et al. (2000). How important is oxidative damage? Lessons from Alzheimer's disease. *Free Radic Biol Med*, Mar 1;28(5):831-4.

Perry EK, Gibson PH, Blessed G et al (1977a) Neurotransmitter enzyme abnormalities in senile dementia. Choline acetyltransferase and glutamic acid decarboxilase activities in necropsy brain tissue. *J Neurol Sci* 34:247-265

Perry E, Walker M, Grace J et al (1999) Acetylcholine in mind: a neurotransmitter correlate of consciousness ? *Trends Neurosci* 22:273-280

Petroianu G, Arafat K, Sasse BC et al (2006) Multiple enzyme inhibitions by histamine H3 receptor antagonists as potential procognitive agents. *Pharmazie* 61:179-182

Pierrot N, Ghisdal P, Caumont AS et al (2004) Intraneuronal amyloid-beta 1-42 production triggered by sustained increase of cytosolic calcium concentration induces neuronal death. *J Neurochem* 88:1140-1150

Pizzinat N, Copin N, Vindis C et al (1999) Reactive oxygen species production by monoamine oxidase in intact cells. *Naunyn Schiedebergs Arch Pharmacol* 359:428-431

Prat G, Perez V, Rubi A et al (2000) The novel type B MAO inhibitor PF9601N enhances the duration of L-DOPA-induced contralateral turning in 6-hydroxydopamine lesioned rats. *J Neural Transm* 107:409-417

Querfuth HW and LaFerla FM (2010) Alzheimer's disease. N Engl J Med 362:329-344

Racchi M, Mazzucchelli M, Porrello E et al (2004) Acetylcholinesterase inhibitors: novel activities of old molecules. *Pharmacol Res* 50:441-451

Radic Z, Pickering NA, Vellom DC et al (1993) Three distinct domains in the cholinesterase molecule confer selectivity for acetyl- and butyrylcholinesterase inhibitors. *Biochemistry*. Nov 16; 32(45):12074-12084

Rakover I, Arbel M, Solomon B (2007) Immunotherapy against APP beta-secretase cleavage site improves cognitive function and reduces neuroinflammation in Tg2576 mice without a significant effect on brain abeta levels. *Neurodegener Dis* 4:392-402

Rapoport M and Ferreira A (2009) PD98059 prevents neurite degeneration induced by fibrillar beta-amyloid in mature hippocampal neurons. *J Neurochem* 74(1):125-133

Rapp MA, Schnaider-Beeri M, Purohit DP et al (2009) Increased neurofibrillary tangles in patients with Alzheimer's disease with comorbid depression. *Am J Geriatr Psychiatry* 16(2):168-174

Ratia M, Giménez-Llort L, Camps P et al (2010) Behavioural effects and regulation of PKCα and MAPK by huprine X in middle aged mice. *Pharmacol, Biochem and Behav* 95:485-493.

Reddy PH and Beal MF (2008) Amyloid beta, mitochondrial dysfunction and synaptic damage: implications for cognitive decline in aging and Alzheimer's disease. *Trends Mol Med* 14:45-53.

Rees TM, Berson A, Sklan EH et al (2005) Memory deficits correlating with acetylcholinesterase splice shift and amyloid burden in doubly transgenic mice. *Curr Alzheimer Res* 2(3):291-300

Reiter RJ (1995) Oxidative processes and antioxidant defenses in the aging brain. *FASEB J* 9:526-533

Reynolds GP, Mason SL, Meldrum A et al (1995) 5-Hydroxytryptamine (5-HT) receptors in posmortem human brain brain tissue: distribution, pharmacology and effects of neurodegenerative diseases. *Br J Pharmacol* 114:993-998

Ricaurte GA, Seiden LS, Schuster CR (1984) Further evidence that amphetamines produce long-lasting dopamine neurochemical deficits by destroying dopamine nerve fibers. *Brain Res* 303:359-364

Riederer P, Danyelczyk W, Grunblat E (2004) Monoamine oxidase inhibition in Alzheimer's disease. *Neurotoxicology* 25:271-277

Riederer P and Youdim MB(1986) Monoamine oxidase activity and monoamine metabolism in brains of parkinsonian patients treated with l-deprenyl. *J Neurochem* 46:1359-1365

Rodríguez-Franco, M. I.; Fernández-Bachiller, M. I.; Pérez, C.; et al (2005). Design and synthesis of N-benzylpiperidine-purine derivatives as new dual inhibitors of acetyl- and butyrylcholinesterase *Bioorg. Med. Chem*, *13*, 6795-6802.

Rogaev EI, Sherrington R, Rogaev EA, et al (1995). Familial Alzhemier's disease in kindreds with missense mutation in a gene on chromosome 1 related to the Alzheimer's disease type 3 gene. *Nature* 376:775-778.

Rogers J, Webster S, Schultz J et al (1999) Complement activation by b-amyloid in Alzheimer's disease. *Proc Natl Acad Sci USA* 89:10016-10020

Roman S, Vivas NM, Badia A et al (2002) Interaction of a new potent anticholinesterasic compound (+/-) huprine X with muscarinic receptors in rat brain. *Neurosci Lett* 325(2):103-106

Roman S, BAdia A, Camps P et al (2004) Potentiation effects of (+/-) huprine X, a new acetylcholinesterase inhibitor, on nicotinic receptors in rat cortical synaptosomes. *Neuropharmacology* 46(1):95-102

Rosini, M.; Antonello, A.; Cavalli, A. et al (2003). Prazosin-related compounds. Effect of transforming the piperazinylquinazoline moiety into an aminomethyltetrahydroacridine system on the affinity for α_1-adrenoreceptors. *J. Med. Chem*, *46*, 4895-4903

Rosini M, Simoni E, Bartolini M et al (2008) Inhibition of acetylcholinesterase, beta-amyloid aggregation, and NMDA receptors in Alzheimer's disease: a promising direction for the multi-target-directed ligands gold rush. *J Med Chem* 51(15):4381-4384.

Rossor M and Iversen LL (1986) Non-cholinergic neurotransmitter abnormalities in Alzheimer's disease. *Br Med Bull* 42:70-74

Sabo SL, Ikin AF, Buxbaum JD et al (2003) The amyloid precursor protein and its regulatory protein, FE65, in growth cones and synapses in vitro and in vivo. *J Neurosci* 23:5407-5415

Sáez-Valero J, de Ceballos ML, Small DH et al (2002) Changes in molecular isoform distribution of acetylcholinesterase in rat cortex and cerebrospinal fluid after intracerebroventricular administration of Aβ-peptide. *Neurosci Lett*. Jun 14;325(3):199-202

Sagi Y, Weinstock M and Youdim (2003) Attenuation of MPTP-induced dopaminergic neurotoxicity by TV3326, a cholinesterase-monoamine oxidase inhibitor. *J Neurochem* 86(2):290-297

Sampaio C and Ferrerira JJ (2010) Parkinson disease: ADAGIO trial hints that rasagiline slows disease progression. *Nat Rev Neurol* 6, 126-128

Sando SB, Melquist S, Cannon A et al (2008). APOE epsilon 4 lowers age at onset and is a high risk factor for Alzheimer's disease: a case control study from central Norway. *BMC Neurol* 8:9
Sanz E, Romera M, Bellik L et al (2004) Indolalkilamines derivatives as antioxidant and neuroprotective agents in an experimental model of Parkinson's disease. *Med Sci Monit* 10, BR477-BR484

Sanz E, Quintana A, Hidalgo J et al (2009) PF9601N confers MAO-B independent neuroprotection in ER-stress-induced cell death. *Mol Cell Neurosci* 41,19-31

Sanz E, Quintana A, Battaglia V et al (2008) Anti-apoptotic effect of MAO-B inhibitor PF9601N is mediated by p53 pathway inhibition in MPP(+)-treated SH-SY5Y human dopaminergic cells. *J Neurochem* 105, 2404-2417

Saura J, Andres N, Andrade C et al (1997) Biphasic and region-specific MAO-B response to aging in normal human brain. *Neurobiol Aging* 18:497-507

Savaje MJ, Lin Y-G, Ciallella JR et al (2002) Activation of c-Jun N-terminal kinase and p38 in an Alzheimer's disease model is associated with amyloid deposition. *J Neurosci* 22:3376-3385

Schapira AH and Olanow CV (2004) Neuroprotection in Parkinson's disease: mysteries, myths and misconceptions. *JAMA* 291:358-364

Schnaitman C, Erwin VG, Greenawalt JW (1967) The submitochondrial localization of monoamine oxidase. An enzymatic marker for the outer membrane of rat liver mitochondria. *J Cell Biol* 32:719-735

Schwarzschild MA (2010) Rasagiline in Parkinson's disease. *N Engl J Med* 362:358-659

Selkoe DJ (2001) Alzheimer's disease results from the cerebral accumulation and cytotoxicity of amyloid beta protein. *J Alzheimer Dis* 3:75-80

Selkoe DJ (1994) Alzheimer's disease: a central role for amyloid. *J Neuropathol Exp Neurol* 53, 438-447

Serpell LC (2000) Alzheimer's amyloid fibrils: structure and assembly. *Biochim et Biophys Acta* 1502:16-30.

Schliebs R (2005) Basal forebrain cholinergic lesion by 192IgG-saporin: a tool to assess the consequences of cortical cholinergic dysfunction in Alzheimer's disease. In: Wiley RG, Lappi DA (eds) Molecular Neurosurgery with targeted toxins. *Humana Press*, Totowa, pp59-86

Schneider LS, Olin JT and Pawluczyk (1993) A double-bind crossover pilot study of l-deprenyl (selegiline) combined with cholinesterase inhibitor in Alzheimer's disease. *Am J Psychiatry* 150:321-323

Schubert D, Behl C, Lesley R et al (1995) Amyloid peptides are toxic via a common oxidative mechanism. *Proc Natl Acad Sci USA* 92(6):1989-1993

Sherrington R, Rogaev EI, Liang Y et al (1995). Cloning of a gene bearing missense mutations in early-onset familial Alzheimer's disease. *Nature* 375(6534):754-760

Shimmyo Y, Kihara T, Akaike A et al (2008) Multifunction of myricetin on Ab: Neurprotection via a conformational change of Aβ and reduction of Aβ via the interference of secretases. *J Neurosci Res* 86:368-377.

Shoffner JM (1997) Oxidative phosphorilation defects and Alzheimer's disease. *Neurogenetics* 1(1):13-19. Review

Shoulson I (1998) Experimental therapeutics of neurodegenerative disorders: unmet needs. *Science* 282(5391):1072-1074 Review

Siek GC, Katz LS, Fishman EB et al (1990) Molecular forms of acetylcholinesterase in subcortical areas of normal and Alzheimer disease brain. *Biol Psychiatry* 27(6):573-580

Silver A (1974) The Biology of Cholinesterases. *Elsevier*. Amsterdam

Singleton AB, Smith G, Gibson AM et al (1998) No association between the K variant of the butyrylcholinesterase gene and pathologically confirmed Alzheimer's disease. *Hum Mol Genet* 7:937-939

Small DH, Reed G, Whitefield B et al (1995) Cholinergic regulation of neurite outgrowth from isolated chick sympathetic neurons. *J Neurosci* 15(1 Pt 1):144-151

Snyder EM, Nong Y, Almeida CG et al (2005) Regulation of NMDA receptor trafficking by amyloid-beta. *Nat Neurosci* 8:1051-1058

Solomon B (2010) A new target for Alzheimer's disease immunotherapy. 11th International Geneva/Springfield symposium on Advances in Alzheimer therapy. *Neurobiol Aging* 31 (supll 1):S29

Soreq H and Seidman S (2001) Acetylcholinesterase-new roles for an old actor. *Nature Rev Neurosci* 2:294-302

Sterling J, Herzig Y, Goren T et al (2002) Novel dual inhibitors of AChE and MAO derived from hydroxyl aminoindan and ohenethylamine as potential treatment for Alzheimer's disease. *J Med Chem* 45:5260-5279.

Stoll G, Jander S, Schroeter M. (1998) Inflammation and glial responses in ischemic brain lesions. *Prog Neurobiol.* Oct;56(2):149-71. Review.

Stoll G, Jander S. (1999) The role of microglia and macrophages in the pathophysiology of the CNS. Prog Neurobiol. Jun; 58(3):233-47. Review.

Stoothoff WH and Johnson GV (2005) Tau phosphorylation: physiological and pathological consequences. *Biochim Biophys Acta* 1739(2-3):280-297 Review

Swerdlow RH and Khan SM (2009) The Alzheimer's disease mitochondrial cascade hypotheses: an update. *Exp neurol* 218:308-315. Review

Tabaton M & Gambetti P (2006) Soluble amyloid beta in the brain: the scarlet pimpernel. *J Alzheimer Dis* 9:127-132

Tabet N, Birks J, Grimley Evans J (2000) Vitamin E for Alzheimer's disease. Cochrane *Database Syst Rev* 4: CD002854

Talaga P (2001) Beta-amyloid aggregation inhibitors for the treatment of Alzheimer's disease: dream or reality. *Mini Rev Med Chem* 1(2):175-186 Review.

Talesa VN (2001) Acetylcholinesterase in Alzheimer's disease. *Mech Ageing Dev* 122(16):1961-1969Review

Tariot PN and Aisen PS (2009) Can lithium or valproate untie tangles in Alzheimer's disease? *J Clin Psychiatr* 70:919-921

Tariot PN, Aisen P, Cummings J et al (2009) The ADCS valproate neuroprotection trial: primary efficacy and safety results. *Alzheimers Dement* 5 (4 supll 1):P84-85

Tariot PN, Farlow MR; Grossber GT et al (2004) Memantine treatment in patients with moderate to severe Alzheimer's disease already receiving donepezil: a randomized controlled trial. *JAMA* 291:317-324.

Tatton W, Chalmers- Redman R and Tatton N (2003) Neuroprotection by deprenyl and other propargylamines: glyceraldehide-3-phosphate dehydrogenase rather than monoamine oxidase B. J Neural Transm 110,509-515

Teplow DB (1998). Structural and kinetic features of amyloid beta-protein fibrillogenesis. *Amyloid* 5(2):121-142 Review

Terry RD, Gonatas NK and Weiss M (1964) Ultrastructural studies in Alzheimer's presenile dementia. *Ann J Pathol*, 44:269-297

Thal DR, Griffin WST and Braak H (2008) Parenchymal and vascular Aβ-deposition and its effects on the degeneration of neurons and cognition in Alzheimer's disease. *J Cell Mol Med* 12(5B):1848-1862

The Parkinson Study Group (1993) Effets of tocopherol and deprenyl on the progression of disability in early Parkinson's disease. The Parkinson Study Group. *N Engl J Med* 32,176-183

The Parkinson Study Group (1996) Effects of lazabemide on the progression of disability in early Parkinson's disease. The Parkinson Study Group. *Ann Neurol* 40,99-107

The Parkinson Study Group (2004) A controlled, randomised, delayed-start study of rasagiline in early Parkinson's disease. *Arch Neurol* 61, 561-566

The Parkinson Study Group (2005) A randomised, placebo-controlled trial of rasagiline in levodopa-treated patients with Parkinson's disease and motor fluctuations: the PRESTO study. *Arch Neurol* 62,241-248

Thomas T (2000) Monoamine oxidase B inhibitors in the treatment of Alzheimer's disease. *Neurobiol Aging* 21(2):343-348 Review

Thornburn A (2004) Death receptor-induced cell killing. *Cell Signal* 16, 139-144

Tipton KF, Boyce S, O'Sullivan J et al (2004) Monoamine oxidases: certainties and uncertainties. *Curr Med Chem* 11:1965-1982

Toda N, Tago K, Marumoto S et al (2003) Desing, synthesis and structure-activity relationships of duak inhibitors of acetylcholinesterase and serotonin transporter as potential agents for Alzheimer's disease. *Bioorg Med Chem* 11:1935-1955.

Tomita T (2009) Secretase inhibitors and modulators of for Alzheimer's disease treatment. *Expert Rev Neurother* 9:661-679.

Touchon J, Bergman H, Bullock R et al (2006) Response to rivastigmine or donepezil in Alzheimer's patients with symptoms suggestive of cnoncomitant Lewy body pathology. *Curr Med Res Opin* 22,49-59

Trojanowski JQ, Schmidt ML, Shin RW et al (1993) Altered tau and neurofilament proteins in neurodegenerative diseases: diagnostic implications for Alzheimer's disease and Lewy body dementias. *Brain Pathol* 3:45-54

Tsigelny I, Shindyalov IN, Bourne PE et al (2000) Common EF-hand motifs in cholinesterases and neurologins suggest a role for Ca2+ binding in cell associations. *Protein Sci* 9:431-447

Tsolaki M, Kokarida K, Iakovidou V et al (2001). Extrapyramidal symptoms and signs in Alzheimer's disease: prevalence and correlation with the first symptom. *Am J Alzheimer Dis Other Demen* 16:268-278

Tsunekawa H, Noda Y, Mouri A et al (2008) Synergistic effects of selegiline and donepezil on cognitive impaitment induced by amyloid beta (25-35). *Behav Brain Res* 190:224-232

Tsuyoshi, T and Mihara Hisakazu (2008) Peptide and protein mimetics inhibiting amyloid b-peptide aggregation.. *Acc Chem Res* 41(10), 1310-1318.

Vajda FJE (2002) Neuoprotection and neurodegenerative diseases. *J Clin Neurosci* 9(I):4-8

Valoti M (2007) CYP-dependent metabolism of PF9601N, a new monoamine oxidase inhibitor, by C56/BL6 mouse and human liver microsomes. *J Pharm Pharm Sci* 10:473-485

Van der Schyf CJ, Gal S, Geldenhuys WJ et al., (2006) Multifunctional neuroprotective drugs targeting monoamine oxidase inhibition, iron chelation, adenosine receptors, and cholinergic and glutamatergic action for neurodegenerative disorders. *Expert Opin Investig Drugs* 15(8):873-886. Review

Van Marum RJ (2008) Current and future therapy for Alzheimer's disease. *Fundam Clin Pharmacol* 22:265-274

Vassar R, Bennett BD, Babu-Khan S et al (1999) Beta-secretase cleavage of Alzheimer's amyloid precursor protein by the transmembrane aspartic protease BACE. *Science* 286:735-741

Vellom DC, RDIC z, Li Y et al (1993) Amino acid residues controlling acetylcholinesterase and butytylcholinesterase specificity. *Biochemistry* 32:12-17

Venneri A, McGeown WJ, Shanks MF (2005) Empirical evidence of neuroprotection by dual cholinesterase inhibition in Alzheimer's disease. *Neuroreport* 16:107-110.

Venneri A and Lane R (2009). Effects of cholinesterase inhibition on brain white matter volume in Alzheimer's disease. *Neuroreport* 20(3):285-288

Vetrivel KS, Zhang YW, Xu H et al (2006) Pathological and physiological functions of presenilins. *Mol Neurodeger* 1:4

Viayna E, Gomez T, Galdeano C et al (2010) Novel huprine derivatives with inhibitory activity toward -amyloid aggregation and formation as disease-modifying anti-Alzheimer drug candidates. *ChemMedChem* 5(11):1855-1870

Waldholdz M (1993) FDA approves sale of Cognex for Alzheimer's, *WSJ*. 10 Sep, B5.

Walsh DM and Selkoe DJ (2004) Oligomers on the brain: The emerging role of soluble protein aggregates in neurodegeneration. *Protein Pept Lett* 11:213-228

Walsh DM, Hartley DM, Kusumoto Y et al (1999) Amyloid -protein fibrillogenesis. Structure and biological activity of protofibrillar intermediates. *J Biol Chem* 274 (36):25945-25952

Wang BS, Wang H, Wei ZH et al (2009) Efficacy and safety of natural acetylcholinesterase inhibitor huperzine A in the treatment of Alzheimer's disease: an up-dated meta-analysis. *J Neural Transm* 116:457-465

Weinreb O, Amit T, Bar-Am O et al (2006) Involvement of multiple survival signal transduction pathways in the neuroprotective, neurorescue and APP processing activity of rasagiline and its propargyl moiety. *J Neural Transm Suppl* 457-465

Weinreb O, Mandel S, Bar-Am O et al (2009) Multifunctional neuroprotective derivatives of rasagiline as anti-Alzheimer's disease drugs. *Neurotherapeutics* 6:163-174.

Weinstock M, Gorodetsky E, Poltyrev T et al (2003) A novel cholinesterase and brain-selective monoamine oxidase inhibitor for the treatment of dementia comorbid with depression and Parkinson's disease. *Prog Neuropsychopharmacol Biol Psychiatry* 27(4):555-561. Review

Wenk GL, Parsons CG, Danyscz W (2006) Potential role of N-methyl-D-aspartate receptors as executors of neurodegeneration resulting from diverse insults: focus on memantine. *Behav Pharmacol* 17:411-424

Wimo A, Jönsson L, Gustavsson A et al (2010) The worldwide societal costs of dementia: Estimates for 2009. *Alzheimers Dementia* 2010, 6;98-110

Winblad B, Minthon L. Floesser A et al (2009) Results of the first in-man study with the active aβ immunotherapy CAD106 in Alzheimer patients. *Alzheimers Dement* 5(4 Suppl 1):P113

Wright CI, Geula C and Mesulam MM (1993) Protease inhibitors and indoleamines selectively inhibit cholinesterases in the histopathologic structures of Alzheimer's disease. *Proc Natl Acad Sci USA* 90:683-686

Wright CI, Geula C and Mesulam MM (1993) Neuroglial cholinesterases in the normal brain and in Alzheimer's disase: relationship to plaques, tangles and patterns of selective vulnerability. *Ann Neurol* 34:373-384

Wu J, Basha MR, Zawia NH (2008) The environment, epigenetics and amyloidogenesis. *J Mol Neurosci* 34:1-7

Wu HM, Tzeng NS, Qiag L et al (2009) Novel neuroprotective mechanisms of memantine: increase in neurotrophic factor release from astroglia and antiinflammation by preventing microglial activation. *Neuropsychopharmacology* 34:2344-2357

Wu RM, Chiueh CC, Pert A et al (1993) Apparent antioxidant effect of l-deprenyl on hydroxyl radical formation and nigral injury elicited by MPP+ in vivo. *Eur J Pharmacol* 243:241-247

Yamamoto T and Hirano A (1985) Nucleus raphe dorsalis in Alzheimer's disease: neurofibrillary tangles and loss of large neurons. *Ann Neurol* 17:573-577

Yan SD, Chen X, Fu J et al (1996) RAGE and amyloid-beta peptide neurotoxicity in Alzheimer's disease. *Nature* 382:685-691
Yang HQ, Sun ZK, Zhao YX et al (2009) PMS777, a new cholinesterase inhibitor with anti-platelet activated factor activity, regulates amyloid precursor protein processing in vitro. *Neurochem Res* 34:528-535.

Yang HQ, Ba MW, Ren RJ et al (2007) Mytogen activated protein kinase and protein kinase c activation mediate promotion of sAPPalpha secretion by deprenyl. *Neurochem Int* 50:74-82

Yogev-Falach M, Amit T, Bar-Am O et al (2002) Involvement of MAP kinase in the regulation of amyloid precursor protein processing by novel cholinesterase inhibitors derived from rasagiline. *FASEB J* 16(12):1674-1676

Yogev-Falach M, Bar-Am O, Amit T et al (2006) A multifunctional, neuroprotective drug, ladostigil (TV3326), regulates holo-APP translation and processing. *FASEB J* 20(12):2177-2179

Yoshiije Y, Tanemura K, Murayama O et al (2001) New insights on how metals disrupt amyloid β aggregation and their effects on amyloid β cytotoxicity. *J Biol Chem* 276:32293-32299

Youdim, M. B. H.; Finberg, J. P. M.; Tipton, K. F. (1988) Monoamine oxidase. In U. Tredelenburg, N. Weiner, Springer-Verlag, Berlin, 119-192.

Youdim MHB and Buccafusco JJ (2005) CNS Targets for multi-functional drugs in the treatment of Alzheimer's and Parkinson's diseases. *J Neural Trans*m, 112(4):519-537 review

Youdim MB, Amit T, Bar-Am O et al (2006) Implications of co-morbidity for etiology and treatment of neurodegenerative diseases with multifunctional neuroprotective-neurorescue drugs; ladostigil. *Neurotoxic Res* 10:181-192.

Yu PH, Davis BA, Zhang X, Zuo DM, Fang J, Lai CT, Li XM, Paterson IA, Boulton AA. (1995) Neurochemical, neuroprotective and neurorescue effects of aliphatic N-methylpropargylamines; new MAO-B inhibitors without amphetamine-like properties. *Prog Brain* Res. 106:113-21. Review.

Zheng H, Youdim MB, Weiner LM et al (2005) Novel potential neuroprotective agents with both iron chelating and amino acid-based derivatives targeting central nervous system neurons. *Biochem Pharmacol* 70(11):1642-1652

Zheng, H.; Youdim, M. B. H.; Fridkin, M (2009) Site-activated multifunctional chelator with acetylcholinesterase and neuroprotective−neurorestorative moieties for Alzheimer's therapy. *J. Med. Chem*, *52*, 4095-4098.

Zheng H, Youdim MB, Fridkin M et al (2010). Site-activated chelators targeting AChE and MAO for Alzheimer's therapy. *ACS Chem Biol*, 5:603

Zimmerman GR, Lehar J et al (2007) Multi-target therapeutics: when the hole is greater than the sum of the parts. *Drug Discov Today* 12, 34-42

Zisook S (1985) A clinical overview of monoamine oxidase inhibitors. *Psychosomatics* 26(3):240-246, 251 Review

VII. APPENDIX

Appendix I

Sodium Bicarbonate Enhances Membrane-bound and Soluble Human Semicarbazide-sensitive Amine Oxidase Activity *In Vitr*o.

Mar Hernández-Guillamón, Irene Bolea, Montse Solé, Keith F. Tipton and Mercedes Unzeta.

Journal of Biochemistry, 2007 Nov;142(5):571-576

J. Biochem. **142,** 571–576 (2007)
doi:10.1093/jb/mvm165

Sodium Bicarbonate Enhances Membrane-bound and Soluble Human Semicarbazide-sensitive Amine Oxidase Activity *In Vitro*

Mar Hernandez-Guillamon[1,*], Irene Bolea[1,*], Montse Solé[1], Mercè Boada[2,3], K.F. Tipton[4] and Mercedes Unzeta[1,†]

[1]*Dept. Bioquímica i Biologia Molecular, Facultat de Medicina, Institut de Neurociències, Universitat Autònoma de Barcelona;* [2]*Servei de Neurología, Hospital Universitari de la Vall d'Hebron;* [3]*Fundació ACE. Institut Català de Neurociències Aplicades. Barcelona, Spain; and* [4]*Biochemistry Department, Trinity College, Dublin 2, Ireland*

Received June 25, 2007; accepted August 3, 2007; published online September 10, 2007

Semicarbazide-sensitive amine oxidase (SSAO) is a multifunctional enzyme with different biological roles that depend on the tissue where it is expressed. Because SSAO activity is altered in several pathological conditions, we were interested in studying the possible regulation of the human enzyme activity. It has been previously reported that SSAO activity is increased in the presence of Dulbecco's modified Eagle medium (DMEM) *in vitro*. The aim of the present work was to investigate the effects of the different constituents of DMEM on human SSAO activity. We found that sodium bicarbonate was the only component able to mimic the enhancement of both human aorta and plasma SSAO activity *in vitro*, suggesting a possible physiological role of bicarbonate as an intrinsic modulator of the human enzyme. Failure to take this activating effect into account could also result in inaccuracies in the reported tissue activities of this enzyme.

Key words: activity enhancement, dulbecco's modified eagle medium, semicarbazide-sensitive amine oxidase, sodium bicarbonate, vascular adhesion protein-1.

Abbreviations: DMEM, Dulbecco's modified Eagle medium; MAO, monoamine oxidase; SSAO, semicarbazide-sensitive amine oxidase.

The term 'semicarbazide-sensitive amine oxidase' (SSAO) is generally used to describe those enzymes classified as E.C.1.4.3.6 [amine: oxygen oxidoreductase (deaminating) (copper-containing)]. Semicarbazide inhibition allows SSAOs to be distinguished from monoamine oxidases (MAOs) [amine: oxygen oxidoreductase (deaminating) (flavin-containing); E.C.1.4.3.4 (MAO), which are sensitive to acetylenic inhibitors, such as clorgyline and L-deprenyl, but are less affected by semicarbazide. The substrate specificities of MAO and SSAO overlap to some extent but, whereas MAO catalyzes the oxidative deamination of primary, secondary and some tertiary amines, SSAO activity appears to be restricted to primary amines. Methylamine, which arises from the metabolism of adrenaline, lecithin, sarcosine and creatinine, is metabolized by SSAO from many sources. It has been proposed that methylamine and aminoacetone, which are not MAO substrates, are important physiological SSAO substrates (*1*, *2*).

SSAO is associated with cell membranes in mammalian tissues and is also present in blood plasma (*3*). Membrane-bound SSAO shows high activity in endothelial and smooth muscle cells of blood vessels (*4*, *5*). The soluble SSAO in blood plasma is believed to be derived from the membrane-bound enzyme, and it has recently been reported that soluble SSAO is shed from the adipocyte membrane by a metalloprotease activity (*6*). The physiological roles of SSAO are still far from clear, and it has been described as an enzyme with multifunctional behaviour that depends on the tissue where it is expressed (*7*). SSAO is also known as vascular adhesion protein-1 (VAP-1), which is involved in lymphocytes trafficking, and its expression in endothelial cells is induced during an inflammatory response (*8*).

SSAO activity has been shown to be altered in several pathological conditions. Plasma SSAO is increased in patients suffering from diabetes types I and II (*9*), in patients afflicted by congestive heart failure (*10*), in non-diabetic morbid obesity (*11*), in inflammatory liver diseases (*12*) and in severe Alzheimer's disease (*13*). It has also been implicated in atherosclerosis (*14*) and in the development of diabetic complications (*15*). Furthermore, it has been shown that plasma SSAO can induce apoptosis in smooth muscle cells through its catalytic action on methylamine as substrate, which might contribute to vascular cell damage (*16*) and in the development of diabetic retinopathy (*15*).

Although some factors in human plasma have been reported to modulate platelet MAO activity (*17*, *18*), little is known about the possible modulation of SSAO under physiological conditions.

We have previously described the activation of membrane-bound SSAO from human lung by a low molecular weight component present in human plasma (*19*). In addition, it has also been reported that the standard cell culture medium, Dulbecco's modified Eagle medium

*The authors wish it to be known that, in their opinion the first authors contributed equally to this work.
†To whom the correspondence should be addressed. Tel: +34 93 5811439, Fax: +34 93 5811573,
E-mail: Mercedes.Unzeta@uab.es

 © 2007 The Japanese Biochemical Society.

(DMEM), enhances the SSAO activity present in foetal calf serum *in vitro* (*20*).

The aim of the present work was to investigate the effects of the DMEM and its constituents on human SSAO activity *in vitro*. Here we report, for the first time, that sodium bicarbonate ($NaHCO_3$) is the only component of DMEM able to enhance SSAO activity. The kinetic behaviour of this modulator is reported and its possible physiological role suggested.

MATERIAL AND METHODS

Chemicals—[^{14}C]-Benzylamine was from Amersham (Amersham, UK). MDL72974A ((E)-2-(4-fluorophenethyl)-3-fluoroallylamine hydrochloride) was a kind gift from Dr P. H. Yu (University of Saskatchewan, Saskatoon, Saskatchewan, Canada). DMEM, with or without $NaHCO_3$ (3.7 mg/ml), methylamine, semicarbazide, L-deprenyl and other chemicals were from Sigma-Aldrich (St Louis, MO, USA).

Human Samples—The Ethical Committee of Universitat Autònoma de Barcelona approved the experimental protocol used for human samples in this study.

Dialyzed human plasma

Human plasma samples were obtained from Hospital Universitari de la Vall d'Hebron, Servei d'Hematologia, Barcelona, Spain, and stored at −20°C until use. Plasma was thawed at 37°C and dialyzed against fresh saline solution (1 : 500) overnight at 4°C. Dialyzed samples were stored in aliquots at −20°C.

Human aorta homogenates

Human aorta was obtained from Hospital Universitari de la Vall d'Hebron, Servei de Transplantaments, Barcelona, Spain, and stored in PBS at –80°C until use. For the homogenization process, the tissue was thawed and the tunica media was detached and saved from the rest of the tissue. The endothelial cell layer was removed by rubbing the luminal side of the vessel with a cell scraper. The final homogenate was prepared in phosphate buffer (10 ml:1 g tissue) with a polytron homogenizer. The homogenate was then stored, in aliquots, at −20°C until use.

SSAO activity determination—SSAO activity towards benzylamine as substrate was determined radiometrically at 37°C as previously described (*21*), using 100 μM [^{14}C]-benzylamine (2 mCi/mmol). Samples were pre-incubated for 30 min at 37°C with 1 μM L-deprenyl to inhibit any possible platelet MAO B contamination. The reaction was carried out at 37°C in a final volume of 225 μl in 50 mM phosphate buffer (pH 7.2) and stopped by the addition of 100 μl 2 M citric acid. Radiolabelled products were extracted into toluene/ethyl acetate (1 : 1, v/v) containing 0.6% (w/v) 2,5-diphenyloxazole before liquid scintillation counting.

SSAO activity towards methylamine 500 μM as substrate was determined by following H_2O_2 formation, using a peroxidase-coupled continuous spectrophotometric method (*22*). In this system, 4-aminoantipyrine is oxidized by the hydrogen peroxide (H_2O_2) formed during amine oxidation and then condenses with vanillic acid to give a red quinone imine dye. The absorbance at 498 nm, which was monitored using a Cary spectrophotometer, is proportional to the amount of H_2O_2 generated. SSAO activity is expressed as pmol/min mg protein. All assays were performed in the presence of L-deprenyl 1 μM to ensure the inhibition of any MAO activity. Protein was measured by the method of Bradford, using bovine-serum albumin as standard.

Kinetic studies—The effects of $NaHCO_3$ concentration (0–1 g/l) on SSAO activity towards benzylamine (25–400 μM) were determined without pre-incubation with the enzyme. The pH of $NaHCO_3$ solution was adjusted to 7.0–7.2 with HCl at the beginning of each experiment.

Reversibility studies—The reversibility of the SSAO activation by $NaHCO_3$ was determined by dialysis. Enzyme samples were pre-incubated for 30 min at 37°C with 2 g/l $NaHCO_3$. Samples were then dialyzed using a Centricon Centrifugal Filter (2 ml capacity, 3.0 Molecular Weight-Limit Membrane; Millipore, USA), following the manufacturer's instructions. Briefly, three consecutive washings were performed and samples were centrifuged at 4°C for 30 min between washings. Total protein was measured and SSAO activity was determined as described previously.

Analysis and Statistics—Results were given as means ± SEM. Statistical analysis was done by one-way ANOVA and further Newman–Keuls Multiple Comparison Test using the program Graph-Pad Prism 3.0. A P value of < 0.05 was considered to be statistically significant. K_m and V_{max} values were determined by non-linear regression, using the same program. The double-reciprocal plot is used only for illustrative purposes.

RESULTS

The ability of complete DMEM to enhance SSAO activity towards benzylamine was tested, using two different enzyme sources; circulating SSAO from human plasma and membrane-bound SSAO from human aorta. The basal SSAO activities of the aorta homogenates and plasma were 915.2 ± 95.5 and 0.73 ± 0.02 pmol/min mg protein, respectively. Pre-incubation in the presence of DMEM for 30 min increased the activity of the plasma SSAO 2.48 ± 0.10 times and that of the membrane-bound SSAO 3.43 ± 0.38 times (Fig. 1). In order to elucidate which specific component(s) of DMEM was responsible for the activation effect, each constituent, shown in Table 1, was tested alone. A concentration range of each component, including the corresponding dose present in DMEM, was incubated for 30 min with human plasma or human aorta homogenate before the SSAO activity was assayed towards benzylamine as substrate. $NaHCO_3$ was the only constituent that caused activation, and this was the same as that obtained with complete DMEM. Other inorganic salts, including those containing the sodium cation, did not show any effect on SSAO activity (data not shown). Since the pH of DMEM is 7, all compounds tested were prepared at this pH to avoid possible alterations in the activity determination caused by pH differences.

To confirm that $NaHCO_3$ was the only component responsible for the activation, the same experiments were performed using a mixture equivalent to DMEM

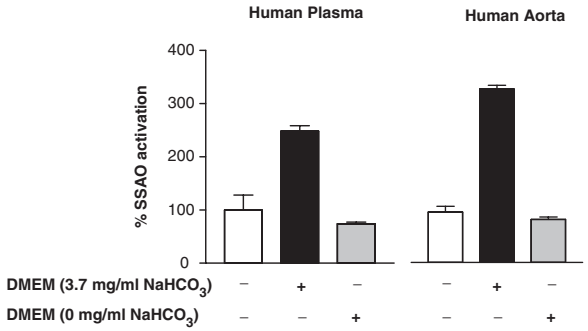

Fig. 1. **$NaHCO_3$ is the only component contained in DMEM responsible of SSAO activity enhancement.** Human aorta and human plasma were pre-incubated for 30 min with 50 μl of DMEM, with or without $NaHCO_3$. SSAO activity was determined towards 100 μM benzylamine as substrate in 50 mM phosphate buffer (pH 7.2). Data are mean ± SEM of three different experiments.

Table 1. **DMEM composition.**

Amino acid (g/l)		Vitamins (g/l)	
L-Arginine·HCl	0.084	Choline chloride	0.4
L-Cysteine·2HCl	0.0626	Folic acid	0.004
Glycine	0.03	Myo-inositol	0.0072
L-Histidine·HCl·H_2O	0.042	Niacinamide	0.004
L-Isoleucine	0.105	D-Pantothenic acid	0.004
L-Leucine	0.105	Pyridoxine·HCl	0.004
L-Lysine·HCl	0.146	Riboflavin	0.0004
L-Methionine	0.03	Thiamine·HCl	0.004
L-Phenylalanine	0.066		
L-Serine	0.042		
L-Threonine	0.095		
L-Tryptophan	0.016		
L-Tyrosine·2Na·2H_2O	0.10379		
L-Valine	0.094		
Inorganic Salts (g/l)		**Others (g/l)**	
$CaCl_2$ ·2H_2O	0.265	D-glucose	1.0
$Fe(NO_3)_3$ ·9H_2O	0.0001	Phenol Red·Na	0.015
$MgSO_4$	0.09767	Pyruvic Acid·Na	0.11
KCl	0.4		
$NaHCO_3$	3.7		
NaCl	6.4		
NaH_2PO_4	0.109		

Note: All components of DMEM were tested separately as possible SSAO modulators and $NAHCO_3$ was the only compoundable to enhance its activity.

with or without $NaHCO_3$. Figure 1 shows that the presence of $NaHCO_3$ in the medium is necessary to enhance both membrane-bound and plasma SSAO activity, suggesting this inorganic compound to be a, previously unrecognized, modulator of the SSAO activity.

Because there are significant concentrations of $NaHCO_3$ in human plasma (about 23 m Eq/l, which corresponds to 1.4 g/l), a prior dialysis process was required to study the net effect of this compound. The SSAO activity in dialyzed human plasma (0.31 ± 0.01 pmol/min mg protein) was lower than that determined without dialysis

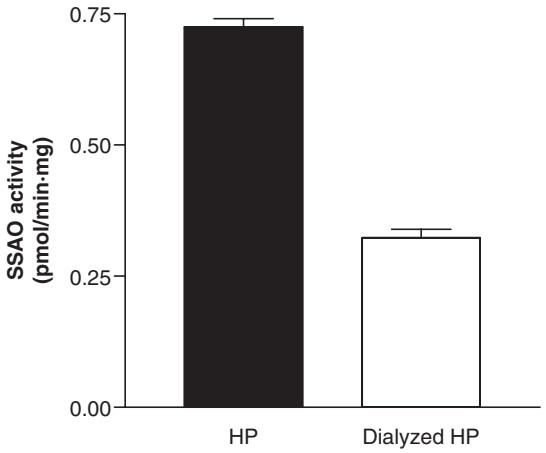

Fig. 2. **Dialysis of human plasma decreases SSAO specific activity.** Human plasma (HP) was dialyzed towards saline solution. SSAO activity present in dialyzed and non-dialyzed human plasma was assayed towards 100 μM benzylamine as substrate in 50 mM phosphate buffer (pH 7.2). Data are mean ± SEM of three different experiments.

(0.73 ± 0.02 pmol/min mg protein) (Fig. 2). These results suggest that the $NaHCO_3$ itself, as one of the components of human plasma, could be able to interact physiologically with the circulating enzyme.

Figure 3 shows the effects of varying concentrations of DMEM and $NaHCO_3$ on SSAO activity from dialyzed human plasma. The $NaHCO_3$ concentrations tested were equivalent to those contained in the different DMEM volumes used. The presence of the SSAO inhibitor, MDL 72974A, in the reaction mixtures completely destroyed the activity, confirming it to be due to SSAO. The activation of SSAO was sigmoidally dependent on the $NaHCO_3$ concentration, reaching a maximum at about 2 g/l NaHCO3 (Fig. 4). Fitting the data to the Hill equation (not shown) gave a Hill constant of 3.2 ± 0.7.

The possible time dependence of the activation was studied using high concentrations of $NaHCO_3$ (Fig. 4). The assay was initiated by the addition of the substrate to the mixture, containing the enzyme and $NaHCO_3$ that had been pre-incubated for 30 or 0 min. The enhancement of SSAO activity from dialyzed human plasma by $NaHCO_3$ was not time dependent, and, as shown in Fig. 5, this activation was completely reversible by dialysis.

The kinetic behaviour of $NaHCO_3$ towards plasma SSAO activity was determined from the initial rates in the presence of different amounts of the modulator (0–1 g/l) and increasing concentrations of the substrate, benzylamine (25–400 μM). $NaHCO_3$ behaved as a competitive activator of SSAO, as shown in the Lineweaver–Burk plot (Fig. 6A). The K_m values decreased as the amount of $NaHCO_3$ increased, whereas the V_{max} values remained constant (Fig. 6B). The decline in K_m was not a simple hyperbolic function of the $NaHCO_3$ concentration, as might be expected from the dependence shown in Figs. 3 and 4, and therefore a Ka value was not determined.

NaHCO3 also enhanced membrane-bound SSAO activity towards the physiological substrate methylamine (Fig. 7) and the presence of the classical SSAO inhibitor, semicarbazide, inhibited the enzyme activity completely.

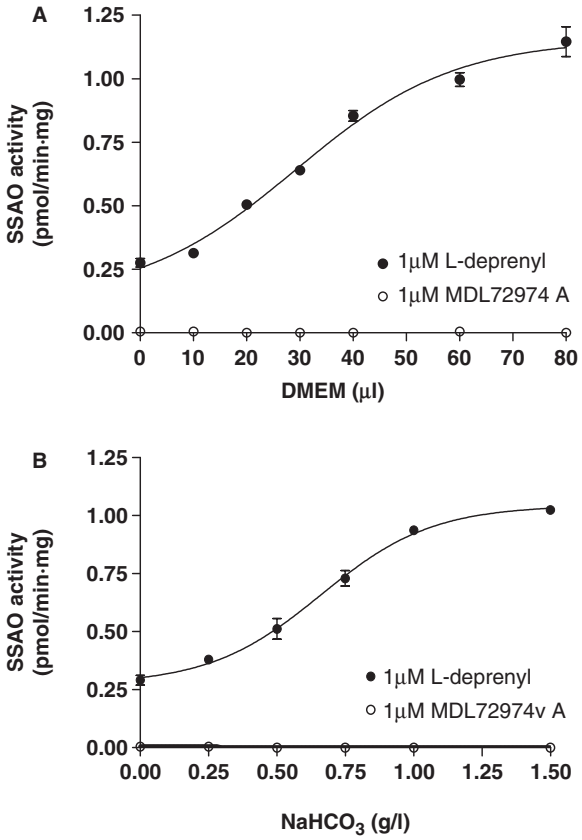

Fig. 3. **DMEM and $NaHCO_3$ enhance SSAO activity.** Dialyzed human plasma was pre-incubated with **(A)** DMEM (pH 7.0) or **(B)** $NaHCO_3$ (pH 7.2) in 50 mM phosphate buffer (pH 7.2) until a final volume of 200 μl for 30 min before adding 100 μM benzylamine as substrate. $NaHCO_3$ final concentration contained in DMEM was 3.7 g/l. Samples were previously inhibited with 1 μM L-deprenyl (black figures) or 1 μM MDL71974A (empty figures). Data are mean ± SEM of three different experiments.

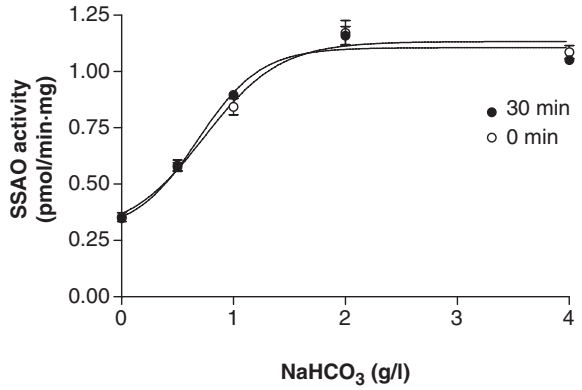

Fig. 4. **$NaHCO_3$ enhances SSAO activity in a non-time-dependent manner**. Dialyzed human plasma was pre-incubated with different $NaHCO_3$ solutions (pH 7.2) for 0 min (empty figures) or 30 min (black figures) before adding 100 μM benzylamine as substrate in 50 mM phosphate buffer (pH 7.2). Data are mean ± SEM of three different experiments.

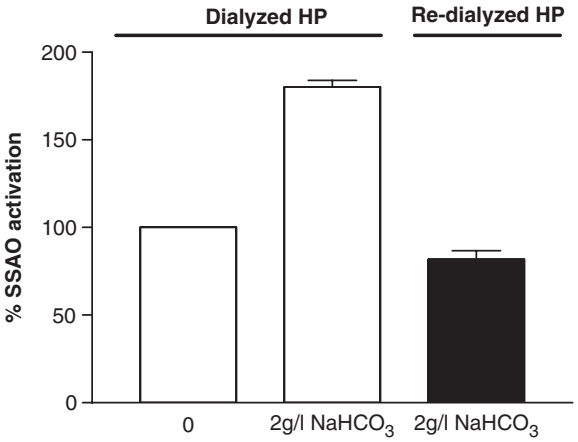

Fig. 5. **$NaHCO_3$ enhances SSAO activity in a reversible manner**. Dialyzed human plasma (Dialyzed HP) was pre-incubated for 30 min at 37°C with 2 g/l $NaHCO_3$ and then dialyzed again (see 'Materials and Methods'). Three consecutive washings were performed and samples were centrifuged at 4°C for 30 min between washings. Activity was measured by adding 100 μM benzylamine as substrate in 50 mM phosphate buffer (pH 7.2). Empty figures: dialyzed human plasma samples as control. Black figures: Samples of dialyzed human plasma that were dialyzed again after the 30 min SSAO activation process by $NaHCO_3$. Data are mean ± SEM of three different experiments.

However, the percentage of activation with methylamine was smaller than the enhancement observed using benzylamine as substrate.

DISCUSSION

SSAO activity has been reported to be altered in several pathological conditions (*7*), but little is known about the factors that may modulate its activity under physiological conditions. We have previously described the activation of human lung SSAO by a low molecular weight molecule present in human plasma, which had no effect on either MAO A or MAO B (*19*). Raimondi *et al*. (*23*) have reported bicarbonate to activate the histaminase activity of rat adipocytes at elevated pH values. Trent *et al*. (*20*) reported that culture medium was able to enhance the SSAO activity present in foetal calf serum, but they did not identify the component(s) responsible for the activation.

The present results show that DMEM enhances the activities of both the plasma and the tissue-bound forms of human SSAO and that $NaHCO_3$ is the sole component of DMEM that is responsible for this activation.

The activating effect on SSAO from dialyzed human plasma by $NaHCO_3$ was reversible and not time dependent. Kinetic studies showed the activation to be apparently competitive. Because amines can react with CO_2 to form carbamates (*24*), it is possible that these derivatives are better substrates than the free amines. Such a system is illustrated in Scheme 1A. This might account for the greater degree of activation seen with benzylamine than with methylamine because the ease of carbamate formation depends on the physico-chemical properties of the amine (*25*). However, it would be expected to give rise to complicated dependence of activity on both amine and bicarbonate concentrations (*26*). Furthermore, SSAO is

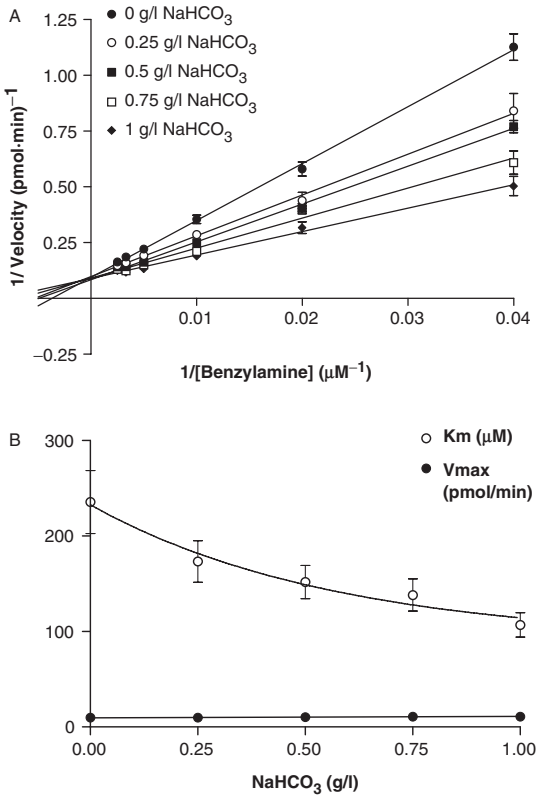

Fig. 6. **Kinetic behaviour of SSAO activation by $NaHCO_3$.** (A) Double reciprocal plots (Lineweaver–Burk transformation) of SSAO activation by $NaHCO_3$ towards benzylamine as substrate and (B) their corresponding kinetic constants towards $NaHCO_3$ concentration. Enzyme samples from dialyzed human plasma were incubated in the absence or presence of $NaHCO_3$ (0–1 g/l, pH 7.2) and, immediately, different benzylamine concentration (25–400 μM) were added to the reaction mixture in 50 mM phosphate buffer (pH 7.2). Data are mean ± SEM of six different experiments.

reported not to be active towards N-substituted amines. An alternative explanation, shown in Scheme 1B, would involve the binding of bicarbonate to the free enzyme resulting in a species (EA) with a higher affinity for substrate (S) without affecting the rate of product formation.

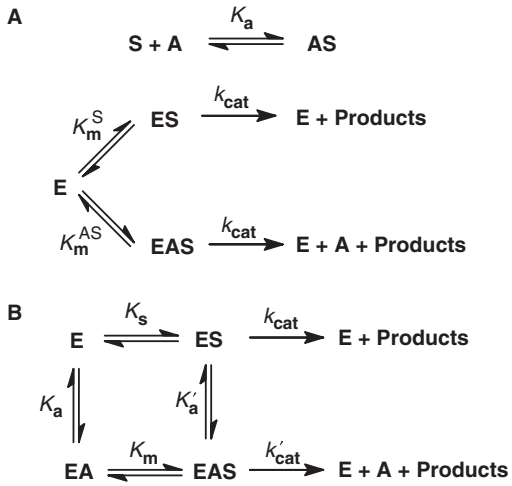

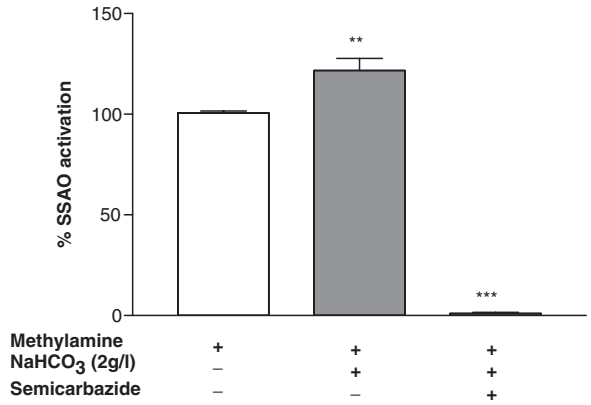

Fig. 7. **$NaHCO_3$ enhances SSAO activity towards methylamine as substrate.** Human aorta homogenate was preincubated with $NaHCO_3$ (2 g/l) in 50 mM phosphate buffer for 30 min and SSAO activity was assayed spectrophotometrically towards methylamine 500 μM as substrate. Semicarbazide (SC) 1 μM was used as SSAO inhibitor. Data are mean ± SEM of three different experiments; $^{***}P < 0.001$, $^{**}P < 0.01$ by a One-way ANOVA test and the addition of Newman–Keuls Multiple Comparison test versus control.

Under rapid-equilibrium conditions, this mechanism would result in competitive activation if $K_s > K_m$ and $k_{cat} = k'_{cat}$. Steady-state treatment of the above mechanism would, however, yield a complex equation containing squared reactant concentration terms. This might account for the apparently sigmoid dependence of activation on the concentration (Figs. 3 and 4). Interaction of more than one bicarbonate molecule with the enzyme might also contribute.

It has been reported that aminopeptidase A (PepA) from *Escherichia coli* is activated 10-fold by bicarbonate when L-leucine *p*-nitroanilide is used as substrate (*27*). In this case, the authors proposed that an exogenous bicarbonate anion as a catalytic group in an enzyme mechanism. Although our results would also seem to be consistent with such a process, more detailed protein structure studies would be necessary to investigate this hypothesis. It is also possible that activation might result from carbamoylation of lysine side chains in the enzyme itself, as a carbamoylated lysine has been shown to be essential for the activity of some class-D β-lactamases (*28*).

The report that bicarbonate increases the rate of oxidative deamination of histamine by SSAO from rat adipocyte [*24*] suggests that this activation may be a general phenomenon. It would be interesting to test such effect using different SSAO substrates.

Under physiological conditions, $NaHCO_3$ is an important buffering molecule in human plasma. The extent to which variations in the blood concentrations of bicarbonate might modulate the activity of the enzyme, enhancing the metabolism of circulating amines in respiring peripheral tissues, merits further investigation. This phenomenon could also result in inaccuracies in the SSAO activities previously reported because of the effects of dissolution of varying amounts of atmospheric CO_2 in the assay medium.

This work has been supported by grant from FIS (Ministerio de Sanidad, Instituto de Salud Carlos III, 03/0243).

REFERENCES

1. Precious, E., Gunn, C.E., and Lyles, G.A. (1988) Deamination of methylamine by semicarbazide-sensitive amine oxidase in human umbilical artery and rat aorta. *Biochem. Pharmacol.* **37**, 707–713
2. Lizcano, J.M., Fernandez de Arriba, A., Lyles, G.A., and Unzeta, M. (1994) Several aspects on the amine oxidation by semicarbazide-sensitive amine oxidase (SSAO) from bovine lung. *J. Neural Transm. (Suppl.)* **41**, 415–420
3. Lyles, G.A. (1996) Mammalian plasma and tissue-bound semicarbazide-sensitive amine oxidases. *Int. J. Cell. Biol.* **28**, 259–274
4. Castillo, V., Lizcano, J.M., and Unzeta, M. (1998) Semicarbazide-sensitive amine oxidase (SSAO) from human and bovine cerebrovascular tissues: biochemical and immunohistological characterization. *Neurochem. Int.* **33**(5), 415–423
5. Lewinsohn, R. (1984) Mammalian monoamine oxidizing enzymes with special reference to benzylamine oxidase in human tissues. *Braz. J. Med. Biol. Res.* **17**, 223–256
6. Abella, A., Garcia-Vicente, S., Viguerie, N., Ros-Baro, A., Camps, M., Palacin, M., Zorzano, A., and Marti, L. (2004) Adipocytes release a soluble form of VAP-1/SSAO by a metalloprotease-dependent process and in a regulated manner. *Diabetologia* **47**, 429–438
7. O'Sullivan, J., Unzeta, M., Healy, J., O'Sullivan, M.I., Davey, G., and Tipton, K.F. (2004) Semicarbazide-sensitive amine oxidases: enzymes with quite a lot to do. *Neurotoxicology* **25**, 303–315
8. Smith, D.J., Salmi, M., Bono, P.J., Leu, T., and Jalkanen, S. (1998) Cloning of vascular adhesion protein 1 reveals a novel multifunctional adhesion molecule. *J. Exp. Med* **188**, 17–27
9. Boomsma, F., van den Meiracker, A.H., Winkel, S., Aanstoot, H.J., Batstra, M.R., Man in't Veld, A.J., and Bruining, G.J. (1992) Circulating semicarbazide-sensitive amine oxidase is raised both in type I (insulin-dependent), in type II (non-insulin-dependent) diabetes mellitus and even in childhood type I diabetes at first clinical diagnosis. *Diabetologia* **42**, 233–237
10. Boomsma, F., van Veldhuisen, D.J., de Kam, P.J., Man in't Veld, A.J., Mosterd, A., Lie, K.I., and Schalekamp, M.A. (1997) Plasma semicarbazide-sensitive amine oxidase is elevated in patients with congestive heart failure. *Cardiovasc. Res.* **33**, 387–391
11. Weiss, H.G., Klocker, J., Labeck, B., Nehoda, H., Aigner, F., Klinger, A., Ebenbichler, C., Foger, B., Lechleitner, M., Patsch, J.R., and Schwelberger, H.G. (2003) Plasma amine oxidase: a postulated cardiovascular risk factor in nondiabetic obese patients. *Metabolism* **52**, 688–692
12. Kurkijarvi, R., Adams, D.H., Leino, R., Mottonen, T., Jalkanen, S., and Salmi, M. (1998) Circulating form of human vascular adhesion protein-1 (VAP-1): increased serum levels in inflammatory liver diseases. *J. Immunol.* **161**, 1549–1557
13. Del Mar Hernandez, M., Esteban, M., Szabo, P., Boada, M., and Unzeta, M. (2005) Human plasma semicarbazide sensitive amine oxidase (SSAO), beta-amyloid protein and aging. *Neurosci. Lett.* **384**, 183–187
14. Yu, P.H. and Deng, Y.L. (1998) Endogenous formaldehyde as a potential factor of vulnerability of atherosclerosis: involvement of SSAO-mediated methylamine turnover. *Atherosclerosis* **140**, 357–363
15. Gronvall-Nordquist, J.L., Backlund, L.B., Garpenstrand, H., Ekblom, J., and Landin, B. (2001) Follow-up of plasma semicarbazidesensitive amine oxidase activity and retinopathy in type 2 diabetes mellitus. *J. Diabet. Complic.* **15**, 250–256
16. Hernandez, M., Sole, M., Boada, M., and Unzeta, M. (2006) Soluble semicarbazide sensitive amine oxidase (SSAO) catalysis induces apoptosis on vascular smooth muscle cells. *Biochim. Biophys. Acta* **1763**, 164–173
17. Berrettini, W.H. and Vogel, W.H. (1978) Evidence for an endogenous inhibition of platelet MAO in chronic schizophrenia. *Amer. J. Psychiat* **135**, 605–607
18. Yu, P.H. and Boulton, A.A. (1979) Activation of platelet monoamine oxidase by plasma in the human. *Life Sci* **25**, 31–36
19. Dalfo, E., Hernandez, M., Lizcano, J.M., Tipton, K.F., and Unzeta, M. (2003) Activation of human lung semicarbazide sensitive amine oxidase by a low molecular weight component present in human plasma. *Biochim. Biophys. Acta* **1638**, 278–286
20. Trent, M.B., Conklin, D.J., and Boor, P.J. (2002) Culture medium enhances semicarbazide-sensitive amine oxidase activity. *In Vitro Cell. Dev. Biol. Anim* **38**, 523–528
21. Fowler, C.J. and Tipton, K.F. (1981) Concentration dependence of the oxidation of tyramine by the two forms of rat liver mitochondrial monoamine oxidase. *Biochem. Pharmacol* **30**, 3329–3332
22. Holt, A., Sharman, D.F., Baker, G.B., and Palcic, M.M. (1997) A continuous spectrophotometric assay for monoamine oxidase and related enzymes in tissue homogenates. *Anal. Biochem* **244**, 384–392
23. Raimondi, L., Banchelli, G., Ignesti, G., Pirisino, R., and Conforti, L. (1997) The histaminase activity of rat white adipocytes. *Inflamm. Res* **46**, 125–131
24. Donaldson, T.L. and Nguyen, Y.N. (1980) Carbon dioxide reaction kinetics and transport in aqueous amine membranes. *Ind. Eng. Chem. Fundam* **19**, 260–266
25. Demaison, J., Császár, A.G., Kleiner, I., and Møllenda, H. (2007) Equilibrium vs ground-state planarity of the CONH linkage. *J. Phys. Chem. A* **111**, 2574–2586
26. McDonald, A.G. and Tipton, K.F. (2003) Kinetics of catalyzed reactions: biological. In *Encyclopedia of Catalysis* (Horváth, I.T., ed.) Vol. 4, pp. 395–471, John Wiley & Sons, Inc., New York
27. Sträter, N., Sun, L., Kantrowitz, E.R., and Lipscomb, W.N. (1999) A bicarbonate ion as a general base in the mechanism of peptide hydrolysis by dizinc leucine aminopeptidase. *Proc. Natl Acad. Sci. USA* **96**, 11151–11155
28. Golemi, D., Maveyraud, L., Vakulenko, S., Samama, J.P., and Mobashery, S. (2001) Critical involvement of a carbamylated lysine in catalytic function of class D beta-lactamases. *Proc. Natl Acad. Sci. USA* **98**, 14280–14285

Appendix II

A Diet Enriched in Polyphenols and Polyunsaturated Fatty Acids, LMN Diet, Induces Neurogenesis in the Subventricular Zone and Hippocampus of Adult Mouse Brain.

Tony Valente, Juan Hidalgo, Irene Bolea, Bartolomé Ramírez, Neus Anglès, Jordi Reguant, José Ramón Morelló, Cristina Gutiérrez, Mercè Boada and Mercedes Unzeta.

Journal of Alzheimer's Disease, 2009;18(4):849-865

Journal of Alzheimer's Disease 18 (2009) 849–865
DOI 10.3233/JAD-2009-1188
IOS Press

A Diet Enriched in Polyphenols and Polyunsaturated Fatty Acids, LMN Diet, Induces Neurogenesis in the Subventricular Zone and Hippocampus of Adult Mouse Brain

Tony Valente[a,*], Juan Hidalgo[b], Irene Bolea[a], Bartolomé Ramirez[c], Neus Anglés[c], Jordi Reguant[c], José Ramón Morelló[c], Cristina Gutiérrez[a], Mercè Boada[d] and Mercedes Unzeta[a]
[a]*Departament de Bioquimica i Biologia Molecular, Institut de Neurociències, Facultat de Medicina, Torre M2, Universitat Autònoma de Barcelona, Bellaterra, Barcelona, Spain*
[b]*Institut de Neurociències, and Departamento de Biología Celular, Fisiologia, e Inmunología, Facultat de Biociències, Universitat Autònoma de Barcelona, Bellaterra, Barcelona, Spain*
[c]*La Morella Nuts SA, Reus, Tarragona, Spain*
[d]*Fundació ACE, Institut Català de Neurociències Aplicades, Barcelona, Spain*

Accepted 13 May 2009

Abstract. At present it is widely accepted that there are at least two neurogenic sites in the adult mammalian brain: the subventricular zone (SVZ) of lateral ventricles and the subgranular zone (SGZ) of the hippocampus dentate gyrus. The adult proliferation rate declines with aging and is altered in several neurodegenerative pathologies including Alzheimer's disease. The aim of this work was to study whether a natural diet rich in polyphenols and polyunsaturated fatty acids (LMN diet) can modulate neurogenesis in adult mice and give insight into putative mechanisms. Results with BrdU and PCNA demonstrated that the LMN fed mice had more newly generated cells in the SVZ and SGZ, and those with DCX (undifferentiated neurons) and tyrosine hydroxylase, calretinin, and calbindin (differentiated neurons) immunostainings and western blots demonstrated a significant effect on neuronal populations, strongly supporting a positive role of the LMN diet on adult neurogenesis. In primary rat neuron cultures, the LMN cream dramatically protected against damage caused by both hydrogen peroxide and Aβ_{1-42}, demonstrating a potent antioxidant effect that could play a major role in the normal adult neurogenesis and, moreover, the LMN diet could have a significant effect combating the cognitive function decline during both aging and neurodegenerative diseases such as Alzheimer's disease.

Keywords: 129S1/SvImJ mice, adult neurogenesis, diet, hippocampus, olfactory bulb, polyphenols, polyunsaturated fatty acids

INTRODUCTION

It is now well known that neurogenesis occurs in at least two regions of the adult mammalian brain: the subventricular zone of the lateral ventricles (SVZ) and the subgranular layer (SGZ) of the dentate gyrus (DG) [1–5]. The new cells generated in the SVZ migrate through the rostral migratory stream (RMS) to the olfactory bulb (OB), where they can differentiate into several types of interneurons and glial cells [6–8]. These new neurons reach functional maturation and present properties similar to those of the oldest granular cells [9]. In the hippocampus, the newly generated cells in SGZ differentiate into granular neurons [10,

*Address for correspondence: Tony Valente, Departament de Bioquimica i Biologia Molecular, Institut de Neurociències, Facultat de Medicina, Torre M2, Universitat Autònoma de Barcelona, 08193 Bellaterra, Barcelona, Spain. Tel.: +34 93 581 1624; Fax: +34 93 581 3861; E-mail: tonyvalente@gmail.com.

ISSN 1387-2877/09/$17.00 © 2009 – IOS Press and the authors. All rights reserved

11], which develop efficiently and have all the characteristics of mature neurons [12].

The rate of neurogenesis decreases with aging [13, 14], probably resulting in the decline of mental and motor function. Also, under certain neurodegenerative pathologies (Alzheimer's disease, Parkinson's disease, multiple sclerosis, etc.), the neuronal loss induces substantial physical and cognitive impairments. Several cellular therapies, including the use of stem cells, are being studied in an attempt to generate new neurons in affected brain areas.

Adult progenitor cells are regulated by the specific microenvironments in which these cells reside [5]. As such, neural factors (Notch, BMPs, Ephrins, Noggin, and Shh), growth factors (FGF, EGF, IGF, etc.), and proneural genes play an important role in regulating proliferation and differentiation of adult neurogenic niches [5,15,16].

Exogenous factors such as physical activity, enriched environments, caloric restriction, vitamin E, and modulators of neural activity can act as regulators of neurogenesis [17–22]. These factors could be valuable therapeutic tools for delaying the development of neurodegenerative disorders. However, many other still unknown factors may regulate adult neurogenic niches.

The anti-inflammatory and antioxidant properties of polyphenols can play an important role during aging and in neurodegenerative and cardiovascular diseases [23–25]. Moreover, they have anti-tumorigenic properties in several cancer cells [26–29]. On the other hand, curcumin, blueberry, and polyunsaturated fatty acids such as omega 3 and docosahexaenoic acid (DHA) can induce neurogenesis in adult brain [30–33]. In this context, the aim of this work was to study the effect of the natural LMN diet (Patent submitted, ref WO2007063158) on neurogenesis in 129S1/SvImJ adult mice; experiments in primary rat neurons were also carried out to analyze the effects of the LMN cream against oxidative stress and Aβ_{1-42} neurotoxicity. The LMN diet contains nuts, cocoa, vegetable oils rich in unsaponifiable fatty acids, and flours rich in soluble fibers.

MATERIALS AND METHODS

Animals and diets

We used 129S1/SvImJ adult male mice that were 12–14 weeks old. The animals were kept under controlled temperature, humidity, and light conditions and were treated according to European Community Council Directive 86/609/EEC.

Two groups of animals were fed for 40 days with either a control diet (Harlan global diet 2014, Mucedola SRL, Milano, Italy) ($n = 8$) or the LMN diet (Harlan global diet 2014 with 9.27% LMN, Mucedola SRL, Milano, Italy) ($n = 10$). The mice received three sequential intraperitoneal injections (the first at 6 days before sacrifice, the second at 3 days before sacrifice, and the last at 12 h before sacrifice) of 50 mg/kg 5-bromo-2'-deoxyuridine (BrdU, thymidine analog which is incorporated in the DNA during the synthesis phase and is therefore an exogenous proliferation marker). Twelve hours after the last BrdU injection, the animals were sacrificed by beheading, and the brains were quickly removed. One brain hemisphere was processed for immunohistological techniques. Briefly, the hemisphere was fixed in 4% paraformaldehyde overnight at 4 °C, cryoprotected in a 30% sucrose/PBS solution for 48 h at 4°C, frozen in dry ice and 5 series of 20 μm sections were obtained in a Leica cryostat. The sections obtained were preserved in free-floating solution (30% ethylenglycol, 30% glycerol in PBS) at -20 °C. The other brain hemisphere was dissected into the olfactory bulb, cortex, hippocampus, and cerebellum and immediately frozen for use in Western blot techniques.

Immunohistochemistry

Free-floating sections were processed for immunohistochemistry as previously described [34]. Briefly, the sections were washed in PBS (phosphate buffered saline), and the endogenous peroxidase or alkaline phosphatase activity was inactivated with 2% H_2O_2 in PBS or with levamisole (0.48g levamisole/L of PBS), respectively. Then, the sections were permeabilized with a 2N HCl solution and neutralized with sodium borate solution. After extensive washes in PBS-0.5% triton, the sections were incubated in blocking solution (0.2 M glycine, lysine 0.2 M, 10% fetal bovine serum (FBS), 0.2% gelatin, 0.3% triton on PBS). Subsequently, the sections were incubated with the primary antibody (see below) in an incubating solution (0.2 M glycine, lysine 0.2 M, 5% FBS, 0.2% gelatin, 0.3% triton on PBS) for at least 12 h at 4 °C with gentle agitation. The slides were again rinsed extensively in PBS-0.5% triton, and the sections were incubated with the appropriate secondary antibody coupled to biotin. After rinsing, the slides were incubated with the corresponding ABC complex solution (coupled with peroxidase, HRP, or alkaline phosphatase, AP). Peroxidase

was developed with 0.05% diaminobenzidine in 0.1 M PB and 0.01% H_2O_2, while the alkaline phosphatase was developed with NBT/BCIP solution. All the sections were mounted on gelatinized slides and covered with Mowiol medium. Alternatively, some slides were counterstained with methyl green solution. The primary antibodies used were: mouse anti-BrdU (1:100, Millipore); mouse anti-Proliferating cell nuclear antigen, PCNA (1:500 for IHC and 1:1000 for WB, Millipore); mouse anti-Microtubule associated protein 2, MAP2a&b (1:1000 for IHC and 1:2000, Millipore); mouse anti-Neuronal nuclei protein, NeuN (1:1000 for IHC and 1:2500 for WB, Millipore); rabbit anti-glial fibrillary acidic protein, GFAP (1:500 for IHC and 1:20000 for WB, Dako); rabbit anti-doublecortin, DCX (1:1000 for IHC and 1:1000 for WB, Abcam); rabbit anti-tyrosine hydroxylase, TH (1:500 for IHC and 1:1000 for WB, Abcam); rabbit anti-calretinin, Calr (1:2000 for IHC and 1:20000 for WB, Swant); rabbit anti-calbindin, Calb (1:2000 for IHC and 1:10000 for WB, Swant); rabbit anti-parvalbumin, Parv (1:1000 for IHC and 1:2000 for WB, Swant); rabbit anti-neuron-glia antigen 2, Ng2 (1:2000 for IHC and 1:5000 for WB, a kind gift from Dr. W.B. Stallcup).

For double immunohistochemistry, BrdU staining was carried out with diaminobenzidine plus 0.05% cobalt chloride and 0.05% nickel ammonium sulfate. A dark blue color was observed in the BrdU-positive cells. The second immunohistochemistry (for GFAP, Ng2, NeuN, Calb, Calr or TH) was carried out with diaminobenzidine, as described above, and the color obtained was brown.

Sections were photographed in an NIKON Eclipse 901 microscope/Nikon digital sight camera, using a 10 $\times$ and 20 $\times$ objective lens. Brain anatomy was defined and termed according to a mouse brain atlas [35].

Preparation of brain lysates and Western blotting

Hippocampus, olfactory bulb, cortex, and cerebellum samples from LMN- and control-fed mice were homogenized in RIPA buffer at 4°C to obtain a total cellular fraction, in the presence of protease and phosphatase inhibitors. Total extracts (30 μg) were resolved on 10% SDS-PAGE gels (using the Bio-Rad Mini-PROTEAN 3 system) and transferred to nitrocellulose membranes for immunoblotting. The membranes were incubated with the antibodies shown above. The bands were visualized using the ECL chemiluminescence system (Amersham Pharmacia Biotech). Optical density measurements were made using Adobe Photoshop. The reproducibility of each Western blot was confirmed by multiple repeated trials with all control ($n = 8$) and LMN-fed mice ($n = 10$) homogenates and the westerns shown in figures represent typical results.

Cell counts

To estimate the number of BrdU-positive cells in the SVZ and SGZ, ten sequential sagittal of 5 section series for each animal ($n = 7$) were counted at high magnification using an optical microscope equipped with an ocular eye-piece graticule. All positive cells in the layers of the olfactory bulb or the sections of the dentate gyrus were counted. Slices were sampled from the respective coordinates according to a mouse brain atlas [35]. Thus, for the SVZ, the complete structure per slice was counted, between the 0.60–1.68 mm lateral coordinates, and for the DG, between the 1.20–2.28 mm lateral coordinates. Similar cell counts were made for the double immunohistochemistry between BrdU-positive cells and NeuN, Ng2, GFAP, Calretinin, calbindin, or tyrosine hydroxylase.

Cell culture

Mixed neuron-glial cell cultures were prepared from the cerebral cortices and hippocampal of rat brains on embryonic day 17. Briefly, Sprague Dawley rats were anesthetized with CO_2 and decapitated in order to extract the fetuses. Fetal brains were removed, the meninges were eliminated and the cortex and hippocampus were dissected. Cells were enzimatically dissociated in Krebs Ringer Buffer (KRB) containing 2.5 mg/ml trypsin (Sigma) at 37°C for 10 minutes. After that, the cells were mechanically dissociated by gentle pipetting using a fire-polished glass Pasteur pippete with KRB solution containing 0.08 mg/ml DNase I (Sigma) and 0.6 mg/ml trypsin inhibitor (Invitrogen). Cells were centrifuged, resuspended, counted, and diluted in DMEM (Sigma) supplemented with 10% FBS (Sigma) and penicillin/streptomycin (100 U/ml and 100 μg/ml, respectively, Invitrogen). The cells were plated onto poly-D-lysine-coated 12-well plates at a cell density of $0.20–0.25.10^6$ cells/ml for hippocampal cells and $1.8.10^6$ cells/ml for cortical cells. Cells were grown in a humidified atmosphere of 5% CO_2 at 37°C. Four hours after plating, the medium was entirely replaced by serum-free Neurobasal medium (Gibco) supplemented with 2% B27 (Gibco), 2 mM L-glutamine and penicillin/streptomycin (100 U/ml and 100 μg/ml, respectively). One-half of the medium was removed

every 3 or 4 days and replaced with an equal volume of fresh medium. Hippocampal mixed cell cultures were treated at 11–12 days *in vitro* (DIV) whereas cortical mixed cell cultures were treated at 13–14 days *in vitro* (DIV). More than 50% of the cultured cells were identified as neurons by immunocytochemical analysis using a monoclonal antibody against microtubule-associated protein 2 on day 7 of culture.

LMN cream treatment

Cells were treated with several concentrations of LMN cream (0.05, 0.10, 0.20, 0.30, 0.40, 0.50, 0.60, 0.70, 0.80, and 1.00 mg/ml) dissolved in a PBS sterile solution, during 24 h at 37 °C, 5%, CO_2. Cell viability was measured by MTT (3-(4,5-dimethylthiazol-2-yl)-2,5-diphenyltetrazolium bromide) reduction assay [36]. Thus, MTT (0.5 mg/ml) was added during 2 h at 37 °C, 5% CO_2. After this time, the precipitate formed (formazan blue) was dissolved in DMSO and the plates were quantified spectrophotometrically at 560 nm in a fluorimetric Sinergy reader. Some plaques were fixed in 2% paraformaldehyde during 15 minutes, washed in PBS and stored at 4°C for immunocytofluorescence.

H_2O_2 treatment

Cells were pretreated with several concentrations of LMN cream (0.10–1.00 mg/ml) during 24 h at 37 °C, 5% CO_2. After this time, the medium was removed and replaced with an equal volume from non-treated primary neural cell culture (conditioned medium). Then, the cells were treated with 50 μM of H_2O_2 during 24 h at 37°C, 5% CO_2. For cell viability assay, MTT (0.5 mg/ml) was added during 2 h at 37 °C, 5% CO_2, the precipitate formed was dissolved in DMSO and the plates were analyzed in a fluorimetric Sinergy. Some plaques were fixed in 2% paraformaldehyde during 15 minutes, washed in PBS and stored at 4°C for inmunocytochemistry.

$A\beta_{1-42}$ treatment

Cells were pretreated with several concentrations of LMN cream (0.10-1.00 mg/ml) during 24 h at 37 °C, 5% CO_2. After this time, the cells were treated directly with 5 μM of the $A\beta_{1-42}$ during 48 h at 37°C, 5% CO_2. Alternatively, some plaques were pretreated with several concentrations of LMN cream and before the treatment with $A\beta_{1-42}$ (48 h at 37°C, 5% CO_2), the medium was removed and replaced with an equal volume of cell cultured conditioned medium. In all cases, the cell viability was measured by the MTT assay described previously. On the other hand, some plaques were fixed in 2% paraformaldehyde during 15 minutes, washed in PBS, and stored at 4°C for inmunocytochemistry. For Caspase 3 western blots, after 24 h of $A\beta_{1-42}$ treatment, the cell cultures were washed in PBS, and the cells were scraped in a lysis buffer with 2% SDS, 10% Glycerol in 62.5 mM Tris-HCl pH = 6.8, and 50 μg of total protein were resolved on 12% SDS-PAGE gels as described above. The reproducibility of each Western blot was confirmed by multiple repeated trials.

Immunocytofluorescence

For immunocytofluorescence, the cells were fixed in 4% paraformaldehyde during 15 minutes, washed in PBS and then blocked with 0.2% gelatin-10% FBS-0.1% Tween in PBS for 1 h. The incubation with primary antibody (anti-MAP2a&b, anti-GFAP) was made overnight at 4°C. After several washes in PBS the cells were incubated with the appropriated secondary antibody (goat anti-mouse or goat anti-rabbit Alexa 488 or 594). All plates were analyzed and photographed in a Nikon microscope.

Statistical analysis

All data are presented as the means ± SEM, and a statistical difference between several animal groups was tested by ANOVA and the Student-Newman-Keuls multiple comparison test using the GraphPad Prism program version 4.0 (San Diego, USA). Statistical significance was set at $p < 0.05$.

RESULTS

Neural proliferation and differentiation in SVZ

As expected, all animals showed many newly generated cells in the SVZ, as revealed by both BrdU and PCNA staining (Fig. 1, A-H). However, the LMN-fed mice showed a dramatic increase in neurogenesis that was evident not only in the new cells that emerged from the SVZ (Fig. 1, F, H) but also throughout the RMS (Fig. 1, E) and the OB (Fig. 1, D).

An increase in cell proliferation markers (BrdU and PCNA) cannot be directly correlated with an increase in the differentiated neuronal populations of the OB. For instance, many neural progenitors do not become

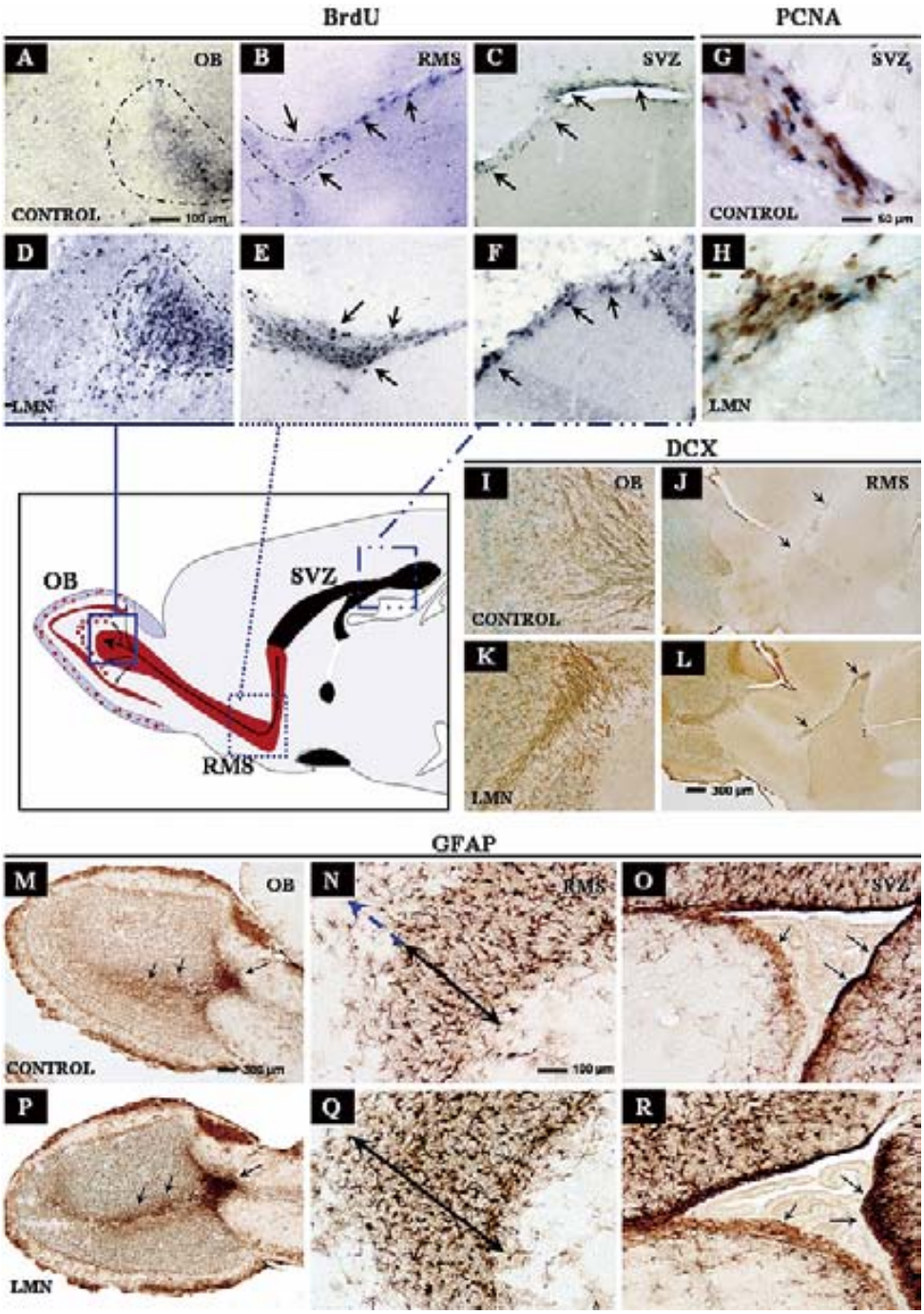

Fig. 1. Increased neurogenesis and gliogenesis in adult LMN-fed mice. (A-F) The number of BrdU-positive cells increased noticeably in the SVZ-RMS-OB system of the LMN-fed mice (D-F) compared to the control mice (A-C). This increase was higher in the OB (arrows in D) and RMS (arrows in E) than in the SVZ (arrows in F) of the LMN-fed mice. (G-H) The number of PCNA-positive cells was greater in the SVZ of the LMN fed mice (H) than in the control mice (G). (I-L) The undifferentiating neuronal marker, DCX protein, was assessed in control (I-J) and LMN-fed mice (K-L). A noticeable increase in DCX expression was found in the OB (K) and RMS (arrows in L) of the LMN-fed mice. (M-R) The undifferentiated glial cells were detected with GFAP marker in both control and LMN-fed mice. The number of these cells was increased in the OB (P), RMS (Q), and SVZ (R) of the LMN-fed mice. A more dense astrocyte layer was observed in the RMS of the LMN-fed mice (arrow in Q) when compared with control mice (amplified arrow in N). OB, olfactory bulb; RMS, rostral migratory stream; SVZ, subventricular zone.

Table 1
Percentage of cell phenotype of BrdU-positive cells in the neurogenic niches#

Brain area	Layer	% NeuN/BrdU cells		% GFAP/BrdU cells		% Ng2/BrdU cells	
		LMN	Control	LMN	Control	LMN	Control
Olfactory Bulb	Periglomerular	19.8 ± 2.3	9.3 ± 2.6	2.4 ± 0.9	1.71 ± 0.8	8.9 ± 2.7	5.9 ± 2.1
	External Granular	15.4 ± 3.7	7.7 ± 2.1	4.3 ± 1.2	1.93 ± 0.7	5.8 ± 2.9	4.7 ± 1.9
	Internal Granular	5.9 ± 1.2	4.9 ± 1.7	16.5 ± 3.4	11.2 ± 3.0	4.6 ± 0.9	4.9 ± 1.2
Dentate Gyrus	Subgranular	11.8 ± 2.3	9.8 ± 2.5	18.8 ± 4.9	15.1 ± 3.9	0	0
	Granular	35.1 ± 8.8	23.9 ± 7.0	0	0	0	0
	Molecular	0	0	2.5 ± 0.9	2.1 ± 0.9	6.1 ± 0.9	4.3 ± 0.9

The cell counting analysis of immunohistochemistry was obtained from 5 independent experiments in which were used 6 sequential sections of 5 series of control mice ($n = 8$) and LMN-fed mice ($n = 10$).

fully differentiated and die by apoptosis. In order to evaluate cell survival, apostain immunohistochemistry was performed and no differences were observed in the number of apoptotic cells of the SVZ-RMS-OB of the LMN-fed mice compared to control mice (data not shown). On the other hand, progenitor cells can be differentiated into neurons and glial cells, so not all newly generated cells give rise to neurons. To determine whether the newly generated neural cells do differentiate into neurons and to which degree, we first analyzed the expression of the DCX protein, a marker of undifferentiated neurons. As expected, in the control mice many DCX-positive cells were present throughout the RMS, and these neuronal progenitors reached the OB (Fig. 1, I-J). The mice fed with the LMN diet showed a marked increase in DCX immunostaining in the undifferentiated regions of RMS and OB (Fig. 1, K-L). Thus, in general, the results strongly suggest that many of the cells newly produced (BrdU, PCNA positive) in the SVZ do differentiate into neurons. Importantly, about 41% of BrdU-positive cells co-localized with NeuN in the OB layers (Fig. 2, E; Table 1) whereas only 22% were obtained in control fed mice (Table 1).

On the other hand, many new progenitors generated in the SVZ can follow the glial fate along the RMS and differentiate into both astrocytes and oligodendrocytes of the OB. The GFAP protein is known to be a marker of immature and mature astrocytes, as well as of progenitor cells in the adult brain, and therefore we observed many GFAP-positive cells in the SVZ, RMS, and OB of all mice. In line with the previous results, more GFAP-positive cells were observed in those brain areas in the LMN diet-fed mice (Fig. 1, P-R) than in the control diet-fed mice (Fig. 1, M-O), again strongly suggesting that many of the cells newly produced in the SVZ follow a normal pattern of differentiation, in this case into glial cells. In accordance, many BrdU-positive cells co-expressed either GFAP, a marker of astrocytes, or Ng2, a marker of oligodendrocyte progenitors (Fig. 2, A, C). Cell counts showed that in LMN fed mice around 23% and 19% of the BrdU-positive cells were positively labeled for GFAP and Ng2, respectively, whereas in control fed mice were 15% for GFAP and 16% for Ng2 cells (Table 1). Importantly, Western blot analyses of the OB for PCNA, DCX, and GFAP fully confirmed the IHC results, namely, a more active proliferative and differentiating process in the LMN-fed mice (Fig. 5, A-B).

It is important to realize that while increased proliferation and differentiation of neurons and glial cells were obvious, no change was observed in the size of the SVZ, RMS, or OB. Rather, the new cells tended to be more compacted in the deeper layers of RMS (Fig. 1, N, Q).

Neuronal subpopulations in the olfactory bulb

Co-localizations studies showed that many of the new cells generated in the SVZ were differentiated into neurons (NeuN-positive cells) in several OB layers (Fig. 2, E; Table 1). The new cells generated in the adult SVZ have been described to differentiate exclusively into calretinin, calbindin, and TH interneurons [4,5]. Accordingly, we observed many neurons positive for all three markers in the glomerular layer of the OB (Fig. 3); calretinin immunostaining was also found in the mitral and external plexiform cell layers of all mice. The results clearly demonstrate that the LMN diet-fed mice showed increased immunostaining for these three specific neuronal subpopulations markers (Fig. 3, B, D, F) compared to those of control diet-fed mice (Fig. 3, A, C, E) in the various OB layers. Cell counts carried out in the glomerular layer showed that the LMN diet had a statistically significant effect for calretinin- and TH-positive cells, and a clear tendency for calbindin-positive cells (Fig. 3, I). These results were fully confirmed by the Western blots analyses carried out (Fig. 5, A, B). Finally, double staining with BrdU and these three markers showed the BrdU-Calretinin-positive cells in the glomerular lay-

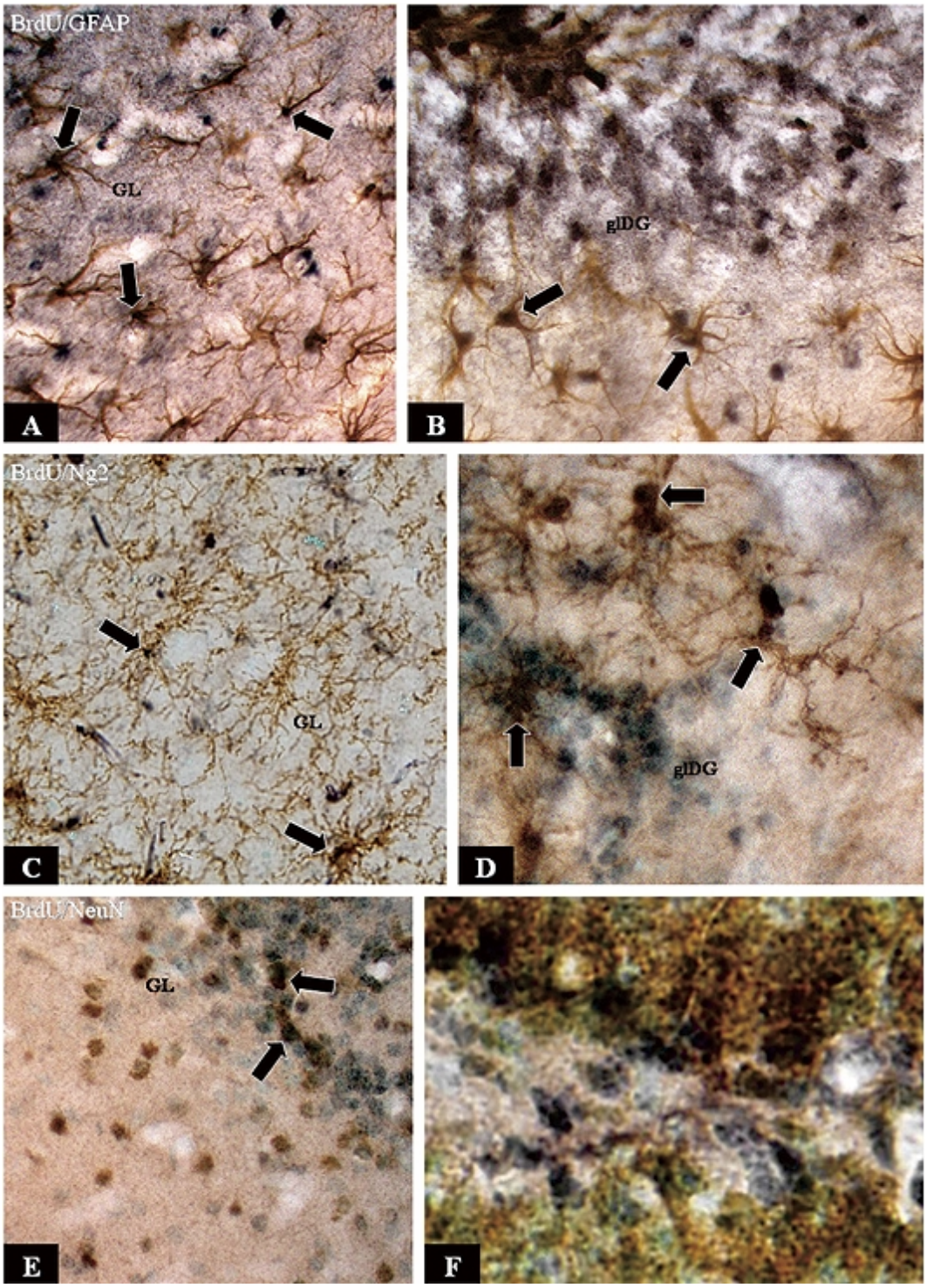

Fig. 2. Double immunohistochemistry of the BrdU-positive cells in LMN fed mice. (A-B) Some BrdU-positive cells were GFAP stained in the glomerular layer of OB (A) and the molecular layer of DG (B). (C-D) A few BrdU-positive cells were co-localized with Ng2 in the glomerular layer of OB (C) and the molecular layer of DG (D).(E-F) Many BrdU-positive cells were immunolabelled for NeuN in the glomerular layer of OB (E) and the molecular layer of DG (F). BrdU-positive cells are stained in black whereas GFAP or Ng2 or NeuN-positive cells are stained in brown. Double-labeled cells were in black arrows.

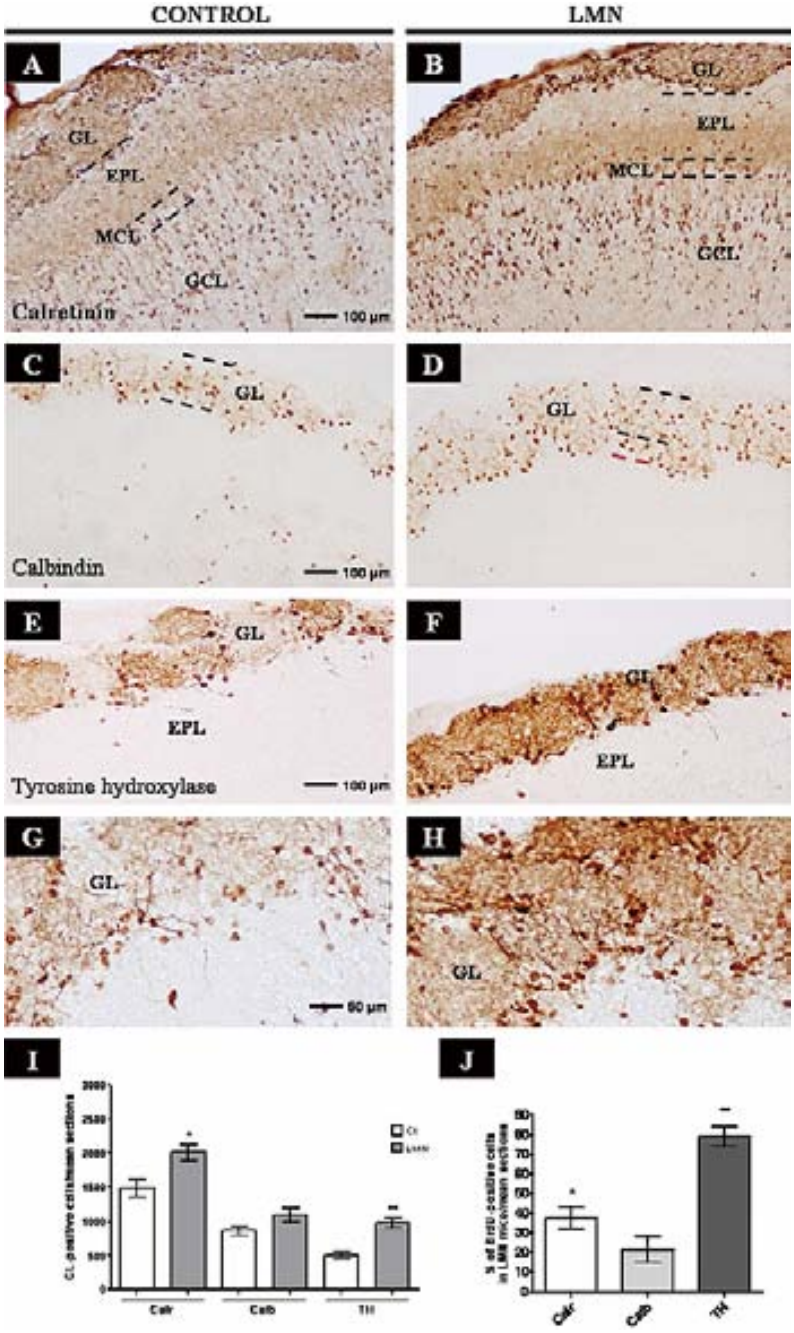

Fig. 3. Immunohistochemistry of the neuronal subpopulations in the olfactory bulb. (A-B) The number of calretinin-positive cells was higher in the GL, MCL, and GCL of the LMN-fed mice (B) than in control mice (A). An increase in the calretinin protein expression of the neuronal projections in the GL and EPL of the LMN-fed mice was also observed (B). (C-D) The number of calbindin-positive cells was greater in the GL of LMN-fed mice (D) than in controls (C), and the layer was thicker (red broken line in D). (E-H) Tyrosine hydroxylase neuronal subpopulations were found in the GL of control mice (E,G). The number of tyrosine hydroxylases increased noticeably in the LMN-fed mice, and the tyrosine hydroxylase protein in the neuronal projections of this olfactory layer was also overexpressed (F,H). (I) The number of calretinin, calbindin, and TH-positive cells increased in LMN-fed mice, but the differences were only statistically significant for calretinin and TH (**$p < 0.01$; *$p < 0.05$). (J) The LMN-fed mice showed an increase in the BrdU-positive cells that co-expressed calretinin, calbindin, or TH, in comparison with the control mice. Data are mean $\pm$ S.E.M. values of five separate experiments performed in control mice ($n = 8$) and LMN-fed mice ($n = 10$). GL, glomerular layer; EPL, external plexiform layer; MCL, mitral cell layer; GCL, granular cell layer.

er of LMN-fed mice increased by ∼38% in comparison with the control mice, ∼22% for calbindin, and ∼79% for TH (Fig. 3, J). Interestingly, the LMN diet also induced an increase in the tyrosine hydroxylase immunostainings in the glomerular layer projections (Fig. 3, G, H).

Neural proliferation and differentiation in hippocampus

Other progenitor cell niches have been described in the DG of the hippocampus in adult brain, where the new neurons migrate into the granular layer (Fig. 4, C'). In agreement with the previous results in the SVZ, the LMN diet-fed mice also showed more BrdU-positive cells in the SGZ (Fig. 4, B) than the control mice (Fig. 4, A), and cell counts carried out in all animals demonstrated a statistically significant effect (Fig. 4, C). These findings were confirmed by the Western-blot analysis for PCNA (Fig. 5, C-D).

As for the SVZ, proliferating cells in the DG can eventually differentiate into neurons and glial cells, so we carried a similar analysis here to determine if the normal program is under way in the DG. In line with the SVZ results, more neuronal progenitors were induced in the LMN-fed mice (Fig. 4, G) than in control-fed mice (Fig. 4, F) as suggested by DCX immunostaining. Moreover, Western blot analysis showed that DCX levels increased significantly in the hippocampus of LMN-fed mice (Fig. 5, C-D). The neuronal fate of many of these newly produced cells was confirmed by the co-localization of BrdU-positive cells with NeuN in many of the neurons of the granular layer (35%) of LMN fed mice when compared with control fed mice (24%) (Table 1). These data strongly suggest that the LMN diet induced proliferation of cells in the DG, many of which differentiated into neurons that could eventually integrate into the granular layer. In this regard, NeuN immunostaining suggests that the granular density in the DG was in fact higher in LMN-fed mice (Fig. 4, I) than in control mice (Fig. 4, H).

The results were complemented with immunohistochemistry against calbindin (Fig. 4, J-K). Calbindin-positive cells are the cell phenotype that is formed from neural progenitors in the subgranular zone. An increase in the number of calbindin-positive cells was observed in LMN-fed mice (Fig. 4, K, M) compared with control mice (Fig. 4, J, L). This effect was not as prominent as in the SVZ, and indeed the western blots did show a tendency of the LMN diet that was not statistically significant (Fig. 5, C, D).

Regarding the differentiation of the proliferating cells into glial cells, the results are not as clear-cut as for the SVZ. Thus, the increase in the proliferation rate of the LMN fed mice was accompanied by only a slight increase in the GFAP-positive progenitors of the SGZ (Fig. 4, E) compared with those of control animals (Fig. 4, D); western blot analysis confirmed the immunohistochemistry results (Fig. 5, C, D). Some BrdU-positive cells were co-immunostained with GFAP in the subgranular layer (19%) and in the molecular layer (2%) of the DG (Table 1 and Fig. 2, B). On the other hand, in the LMN-fed mice, 6% of BrdU-positive cells were co-localized with Ng2 marker in the molecular layer of DG (Table 1).

Effect of LMN on rat primary cell cultures

Rat primary cell cultures treated 24 h with several LMN cream concentrations showed no loss of cell viability. Cortical cell cultures showed a significant increase in cell viability at a concentration of 1.0 mg/ml of LMN (Fig. 6, A), whereas in hippocampal cell cultures this effect was observed at a concentration of 0.70 mg/ml (Fig. 6, B).

Antioxidant effect of LMN on rat primary cell cultures

LMN cream showed a noticeable antioxidant effect (approximately 80%) in rat cortical cell cultures incubated with 50 μM of H_2O_2 (Fig. 6, C). Moreover, this antioxidant effect was dependent of the LMN concentration (0.20-0.70 mg/ml). In the hippocampal cell cultures similar results were obtained (Fig. 6, D). However, in these cell cultures the antioxidant LMN range concentration was restricted to 0.50 and 0.60 mg/ml and its antioxidant capacity was approximately 100%.

Neuroprotective effect of LMN on rat primary cell cultures

LMN had a noticeable neuroprotective effect in rat cortical mixed cell cultures treated with 53 μM of Aβ_{1-42} (Fig. 7, A). This neuroprotection was dose-dependent in the cell cultures when we replaced the culture medium by conditioned medium before treatment with Aβ_{1-42} (Fig. 7, B). In the hippocampal mixed cell cultures the neuroprotection of LMN against Aβ_{1-42} toxicity was noticeable (Fig. 7, C). Moreover, this neuroprotection was independent of the LMN concentration even when we replaced the cell culture medium by conditioned medium before treatment with Aβ_{1-42}

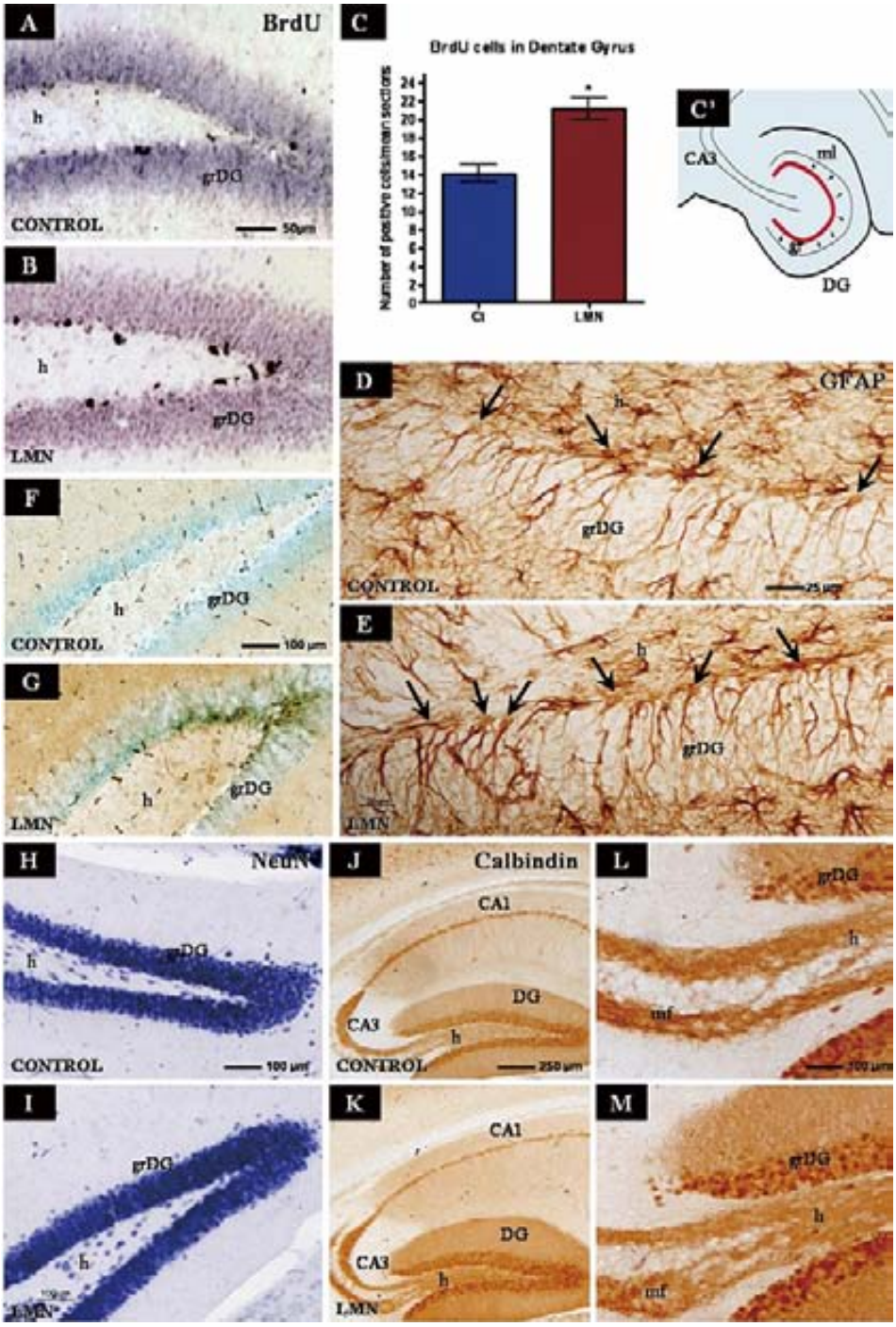

Fig. 4. Immunohistochemistry of neural markers in the hippocampus. (A-C) The number of BrdU-positive cells was observed in the subgranular zone of DG (A-B) and clearly increased in the LMN-fed mice (B). Quantification of BrdU-positive cells showed a significant increase in the LMN-fed mice (C). (D-E) GFAP immunohistochemistry showed an increase in the number of astrocyte progenitors (D-E) in the LMN-fed mice (arrows). (F-G) DCX-positive cells increased in the subgranular and granular layers of the DG of LMN-fed mice (G) in comparison with control mice (F). (H-I) NeuN immunohistochemistry showed an increase in the granular neurons of the LMN-fed mice (I). (J-M) The number of calbindin-positive cells was higher in the granular layer of the DG of LMN-fed mice (K, M) than in control mice (J, L). Data are mean $\pm$ S.E.M. values of five separate experiments performed in control mice ($n = 7$) and LMN-fed mice ($n = 7$). h, hilus; grDG, granular layer of DG; CA1, hippocampal region; CA3, hippocampal region; DG, dentate gyrus.

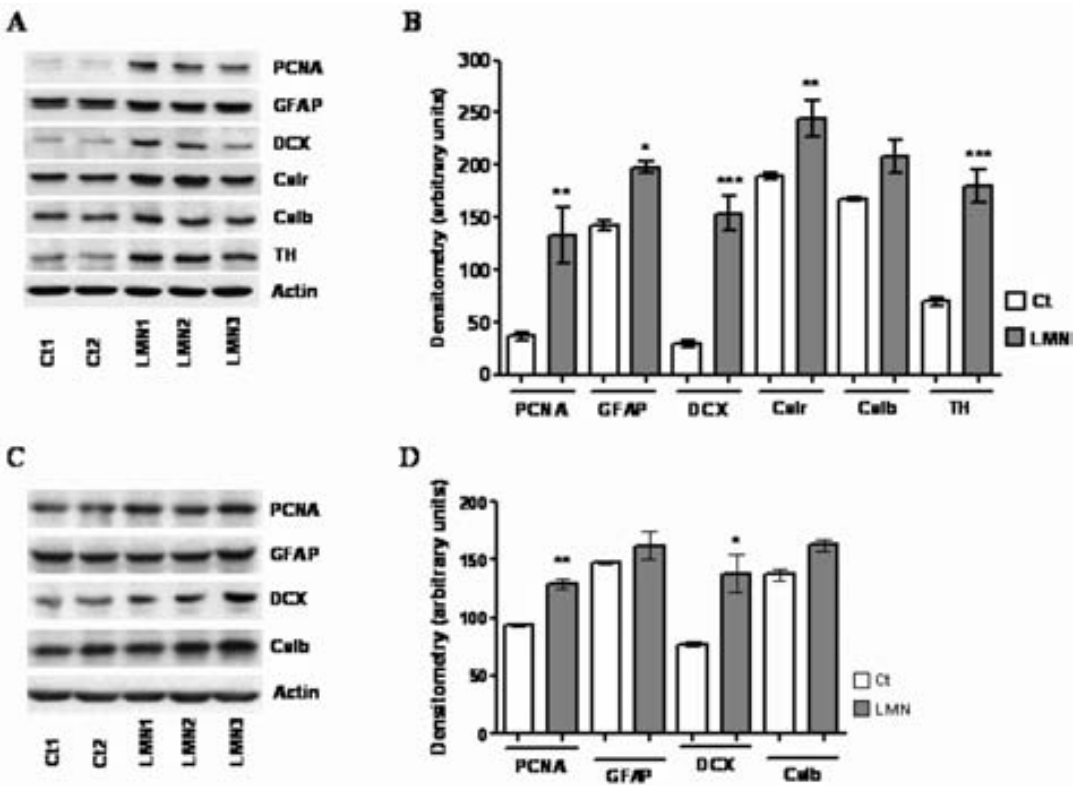

Fig. 5. Immunoblots for neural markers in OB and DG. (A) PCNA, GFAP, DCX, calretinin, calbindin, and TH were overexpressed in the olfactory bulb homogenates of three LMN-fed mice. (B) The up-expression of PCNA, GFAP, DCX, calretinin, and TH proteins in the LMN-fed mice was statistically significant with respect to control mice (*** vs Ct, $p < 0.001$; ** vs Ct, $p < 0.01$; * vs Ct, $p < 0.05$). (C) Up-expression of PCNA and DCX protein was observed in the hippocampus of LMN-fed mice by immunoblot. (D) Quantification of PCNA and DCX showed a significant increase in the LMN-fed mice (*** vs Ct, $p < 0.001$; ** vs Ct, $p < 0.01$). The immunoblot quantification of calbindin and GFAP proteins showed an increase in LMN-fed mice but this was not significant. Data are mean ± S.E.M. values. The quantification analysis of immunoblots was obtained from 3 independent experiments in which were used all the mice from each group: control mice ($n = 8$) and LMN-fed mice ($n = 10$).

(Fig. 7, D). Hippocampal western blots of Caspase 3 showed that the apoptotic cell death induced by Aβ_{1-42} was strongly blocked by 24 h pre-treatment with LMN (Fig. 7, E). Immunocytofluorescence revealed an activation of GFAP in astroglial cells and a neuronal loss in hippocampal mixed cell cultures treated with 5 μM of Aβ_{1-42} (Fig. 7, J-K) when compared with control cell cultures (Fig. 7, F-G). However, when the hippocampal mixed cell cultures were pre-treated previously with LMN, the neuronal loss was noticeable reduced (Fig. 7, H-I). Similar results were obtained in cortical mixed cell cultures by immunocytofluorescence and western blot (data not shown).

DISCUSSION

The present results show an increase in the number of newly generated cells in the neurogenic adult brain sites of LMN-fed mice. This increase was higher in the SVZ-RMS than in the SGZ. In rats, approximately 80,000 new neurons are incorporated daily into the OB [37] while 250,000 new neurons are incorporated monthly into the DG [38]. Therefore, in adults neurogenesis is much higher in the SVZ than in the hippocampus. The LMN results in adult mice are in agreement with these data.

In LMN-fed mice, the number of neuronal (DCX) and glial (GFAP) precursors also increase along the RMS and in the granular layer of the DG. At the same time, there are no changes in apoptotic cell death in these areas when compared with control-fed mice. These findings suggest that LMN induces the proliferation of the transit-amplifying cells and that these newly generated cells began their differentiation process normally following their corresponding migratory route. We characterized the neuronal phenotype of these new

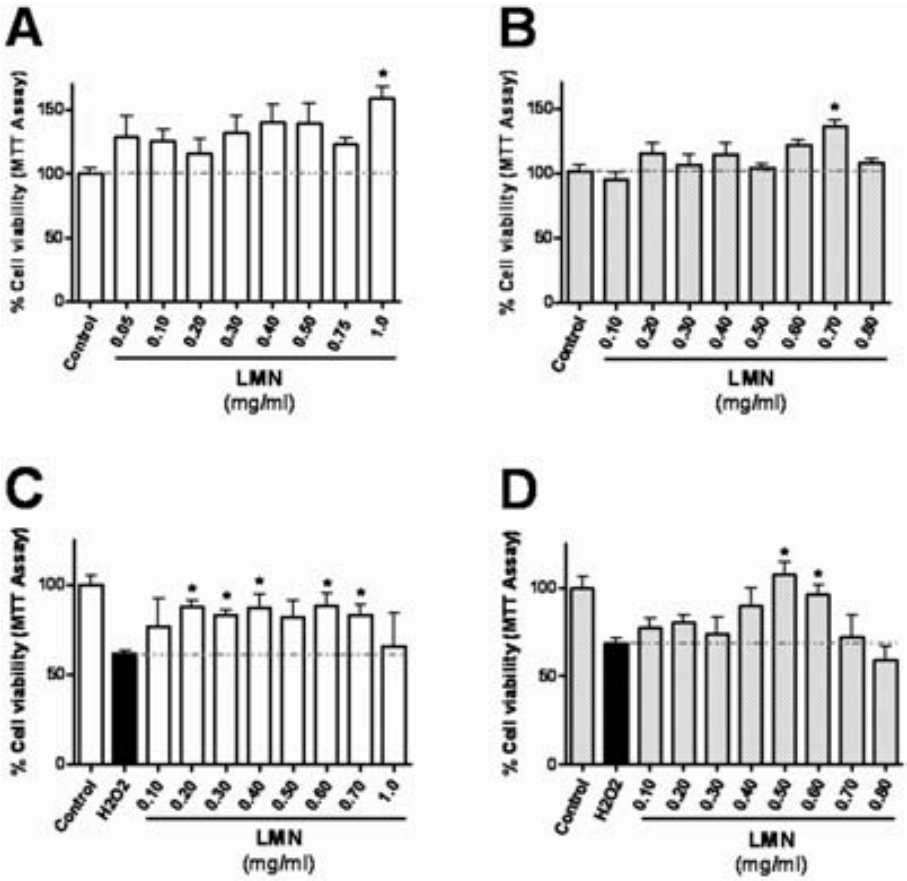

Fig. 6. LMN presents a trophic (A-B) and antioxidant (C-D) effect in cortical (A, C) and hippocampal (B, D) mixed cell cultures. The cell viability of primary cell cultures were expressed as MTT reduction percentages obtained from the incubation with different concentrations of LMN (A-D) and in the presence of 50 μM H_2O_2 (C-D). Data are mean $\pm$ S.E.M. values of three separate experiments performed in triplicate; * vs control, $p < 0.05$.

cells in OB and determined that calretinin and TH neuronal subpopulations are noticeably increased in the glomerular layer of LMN-fed mice. On the other hand, in the hippocampus an increase in BrdU-positive cells and calbindin neurons are observed in DG of LMN-fed mice. Moreover, in rat hippocampal primary cell cultures treated with LMN cream, an increase in the number of neurons (MAP2-positive cells) was found. All together these results confirm that the LMN diet also promotes neuronal proliferation in the hippocampus and SVZ.

The proportion of each neuronal subpopulation in the OB of the adult mouse may depend on the strain and age. Some studies have analyzed the phenotype of the new glomerular generated cells in other strains and ages [39–41], but to our knowledge this is the first study of neurogenesis and specific diets in 129S1/SvImJ mice. In the present study, we tested the effect of a combined diet which contains such natural compounds as nuts, cocoa, vegetable oils rich in unsaponifiable fatty acids, and flours rich in soluble fibers. A few recent studies show the positive effects of polyphenolic compounds, curcumin or blueberry [30, 33], and polyunsaturated fatty acids, DHA [32] on adult mouse hippocampal neurogenesis but not in SVZ. The neurogenesis rate is regulated by a balance between mitotic activity, cell cycle arrest, cell differentiation, and apoptosis. It has been reported that a curcumin diet regulates apoptosis *in vivo* [26] and activates the cellular signal transduction pathway involved in survival response [33]. A blueberry diet induces hippocampal plasticity factors (IGF-1 and IGF-1R), which may modulate adult neurogenesis [30]. And finally, DHA promotes adult neurogenesis by reducing the apoptosis of newly generated cells [32]. Therefore, it seems that these natural compounds modulate apoptosis and cell

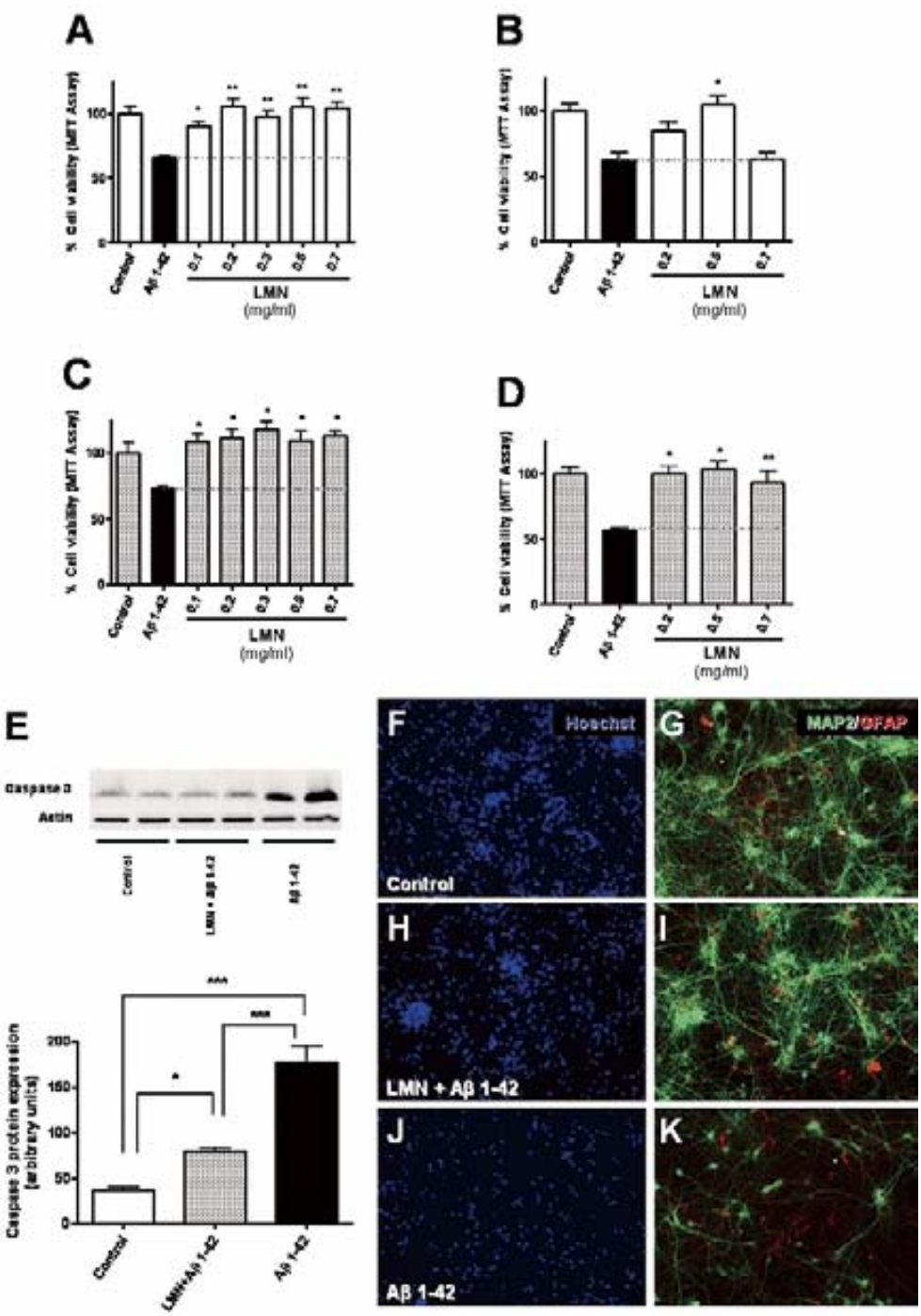

Fig. 7. LMN prevents neurotoxicity of Aβ_{1-42} in cortical (A, B) and hippocampal (C-K) mixed cell cultures. (A-B) The cell viability of primary cell cultures was expressed as MTT reduction percentages obtained from the incubation with different concentrations of LMN (A-D) and in the presence of 5 μM Aβ_{1-42}(**C-D**). The neuroprotector effect of LMN was reduced in cortical cell cultures (B) and was maintained in hippocampal cell cultures (D) when the cell medium was replaced by conditioned medium before treatment with Aβ_{1-42}. (E) The up-expression of caspase 3 induced by A$\beta_{1-42}$was noticeable recovered in the hippocampal cell cultures pre-treated with LMN (Data are mean $\pm$ S.E.M. values of three separate experiments performed in triplicate; * vs control, $p < 0.05$). (F-K) Immunocytofluorescence of MAP2a&b and GFAP in hippocampal cell cultures (F-G) showed a clear neuronal protection in the cell cultures pre-treated previously with LMN (H-I) when compared with cell cultures treated only with Aβ_{1-42} (J-K).

survival and can therefore act on the proliferation rate (unlike LMN, which has no effect on apoptosis). Their role in the proliferation rate appears to be related to the induction of the proliferation and differentiation of neural progenitors. Therefore, a combination of polyphenolic compounds and polyunsaturated fatty acids can directly regulate neural proliferation/differentiation in the SVZ-RMS and SGZ of the adult mouse brain. Further studies are necessary to elucidate the role of the LMN diet in the selective induction of neuronal subpopulations in the olfactory bulb and hippocampus.

Environmental enrichment, spatial learning, and physical activity regulate hippocampal neurogenesis and modulate cognitive ability [17,19,42–46]. Hippocampal formation has been widely linked to memory storage and processing [47–49]. In several neuropathologies, the memory regions of the brain are strongly affected [50–52]. Thus, in epilepsy [53–55], Alzheimer's disease [56,57], Parkinson's disease [58, 59], Huntington disease [60–62], and ischemia [63–65], neurogenesis is induced in the SVZ and hippocampus in response to neuronal death in the pathological areas [66–68]. Moreover, some neuronal precursors reach these degenerative areas and, in some cases, replace dead neurons [69–71]. Thus, the induction of neurogenesis in adult brain may be a good tool against neurodegeneration diseases.

The accumulation of Aβ peptide is one hallmark of Alzheimer's disease [72]. Aβ induces a cascade of oxidative damage to neurons that can eventually result in neuronal death [73]. In previous studies it was reported that Aβ_{1-42}aggregation cause the breakdown of neural circuits, neuronal death, and consequently dementia [73–75]. In addition, Aβ_{1-42} has been shown to induce oxidative stress (such as 8OHdG, a measure of oxidized DNA, 4 hydroxynonenal as a result of lipid peroxidation, and protein carbonyl and 3-nitrotyrosine as markers of protein oxidation) and neurotoxicity *in vitro* and in *vivo* [73–75]. On the other hand, Aβ is able to generate free radicals trough a peptide domain linked to Cu^{2+} [76]. The β-peptide reduces Cu^{2+} to Cu^{1+} and this complex induces the hydrogen peroxide generation contributing to the oxidative stress [77]. It has been reported that Aβ induces the H_2O_2 formation in PC12 cells and that catalase protected these cells from the Aβ toxicity [78].

Our findings show that LMN cream has a very high antioxidant capacity in rat cortical and hippocampal primary cell cultures lesioned with H_2O_2, a potent oxidative stress inductor. In addition, LMN cream protects neurons from cell damage caused by Aβ_{1-42}, probably the main cause of pathological consequences in Alzheimer's disease. In this context, the antioxidant effect of LMN diet observed, when primary cell cultures were treated with H_2O_2, together with the protective effect herein reported on hippocampal cells lesioned with Aβ, could both be explained by the strong antioxidant properties of LMN diet.

Several lines of evidence indicates that in experimental conditions, damage signals like oxidative stress, hypoxia, etc., can promote neuronal degeneration [79] and the resulting inflammatory cytokines induced can play a dual role in either promoting neurodegeneration or neuroprotection [80]. It is now widely accepted that inflammation and oxidative stress are hallmarks of Alzheimer's disease; there is convincing evidence that neuroinflammation can inhibit neurogenesis, and that this can be blocked with indomethacin, a common nonsteroidal anti-inflammatory drug [81]. In this regard, further studies are warranted on the possible antiinflammatory effect of the LMN diet in addition to its antioxidant roles to elucidate whether they are underlying its effects on neurogenesis *in vivo*.

Taken into account that the LMN diet can induce neurogenesis in the SVZ and SGZ of adult mice in normal conditions and that the LMN cream can protect cortical and hippocampal neurons against oxidative stress and Aβ_{1-42} toxicity, these results allow us to conclude that in pathological conditions, LMN diet supplementation, rich in polyphenols and polyunsaturated fatty acids (nuts, cocoa, vegetable oils rich in unsaponifiable fatty acids, and flours rich in soluble fibers) could protect against cognitive decline during aging and maintain neuronal homeostasis in neurodegenerative disorders such as Alzheimer's disease.

ACKNOWLEDGMENTS

We wish to thank John Bates and Christian Brassington for assistance with the English. We also thank Lorena Ramirez for her technical contribution. This work was supported by a grant from the Spanish Ministry of Industry, Program INGENIO 2010, Project CENIT ref: MET-DEV-FUN2006-2009.

Authors' disclosures available online (http://www.j-alz.com/disclosures/view.php?id = 76).

REFERENCES

[1] Altman J (1962) Are new neurons formed in the brains of adult mammals? *Science* **135**, 1127-1128.

[2] Eriksson PS, Perfilieva E, Björk-Eriksson T, Alborn AM, Nordborg C, Peterson DA, Gage FH (1998) Neurogenesis in the adult human hippocampus. *Nat Med* **4**, 1313-1317.
[3] Gross CG (2000) Neurogenesis in the adult brain: death of a dogma. *Nat Rev Neurosci* **1**, 67-73.
[4] Taupin P, Gage FH (2002) Adult neurogenesis and neural stem cells of the central nervous system in mammals. *J Neurosci Res* **69**, 745-749.
[5] Alvarez-Buylla A, Lim DA (2004) For the long run: maintaining germinal niches in the adult brain. *Neuron* **41**, 683-686.
[6] Corotto FS, Henegar JA, Maruniak JÁ (1993) Neurogenesis persists in the subependymal layer of the adult mouse brain. *Neurosci Lett* **149**, 111-114.
[7] Luskin MB (1993) Restricted proliferation and migration of postnatally generated neurons derived from the forebrain subventricular zone. *Neuron* **11**, 173-189.
[8] Lois C, Alvarez-Buylla A (1994) Long-distance neuronal migration in the adult mammalian brain. *Science* **264**, 1145-1148.
[9] Carleton A, Petreanu LT, Lansford R, Alvarez-Buylla A, Lledo PM (2003) Becoming a new neuron in the adult olfactory bulb. *Nat Neurosci* **6**, 507-518.
[10] Eckenhoff MF, Rakic P (1988) Nature and fate of proliferative cells in the hippocampal dentate gyrus during the life span of the rhesus monkey. *J Neurosci* **8**, 2729-2747.
[11] Stanfield BB, Trice JE (1988) Evidence that granule cells generated in the dentate gyrus of adult rats extend axonal projections. *Exp Brain Res* **72**, 399-406.
[12] Song HJ, Stevens CF, Gage FH (2002) Neural stem cells from adult hippocampus develop essential properties of functional CNS neurons. *Nat Neurosci* **5**, 438-445.
[13] Kuhn HG, Dickinson-Anson H, Gage FH (1996) Neurogenesis in the dentate gyrus of the adult rat: age-related decrease of neuronal progenitor proliferation. *J Neurosci* **16**, 2027-2033.
[14] Bizon JL, Gallagher M (2003) Production of new cells in the rat dentate gyrus over the lifespan: relation to cognitive decline. *Eur J Neurosci* **18**, 215-219.
[15] Pencea V, Bingaman KD, Wiegand SJ, Luskin MB (2001) Infusion of brain-derived neurotrophic factor into the lateral ventricle of the adult rat leads to new neurons in the parenchyma of the striatum, septum, thalamus, and hypothalamus. *J Neurosci* **21**, 6706-6717.
[16] Kuhn HG, Winkler J, Kempermann G, Thal LJ, Gage FH (1997) Epidermal growth factor and fibroblast growth factor-2 have different effects on neural progenitors in the adult rat brain. *J Neurosci* **17**, 5820-5829.
[17] Fabel K, Kempermann G (2008) Physical activity and the regulation of neurogenesis in the adult and aging brain. Neuromolecular Med **10**, 59-66.
[18] Kitamura T, Sugiyama H (2006) Running wheel exercises accelerate neuronal turnover in mouse dentate gyrus. *Neurosci Res* **56**, 45-52.
[19] Huang FL, Huang KP, Wu J, Boucheron C (2006) Environmental enrichment enhances neurogranin expression and hippocampal learning and memory but fails to rescue the impairments of neurogranin null mutant mice. *J Neurosci* **26**, 6230-6237.
[20] Matsumori Y, Hong SM, Fan Y, Kayama T, Hsu CY, Weinstein PR, Liu J (2006) Enriched environment and spatial learning enhance hippocampal neurogenesis and salvages ischemic penumbra after focal cerebral ischemia. *Neurobiol Dis* **22**, 187-198.
[21] Levenson CW, Rich NJ (2007) Eat less, live longer? New insights into the role of caloric restriction in the brain. *Nutr Rev* **65**, 412-415.
[22] Ciaroni S, Cuppini R, Cecchini T, Ferri P, Ambrogini P, Cuppini C, Del Grande P (1999) Neurogenesis in the adult rat dentate gyrus is enhanced by vitamin E deficiency. *J Comp Neurol* **411**, 495-502.
[23] Ramassamy C (2006) Emerging role of polyphenolic compounds in the treatment of neurodegenerative diseases: a review of their intracellular targets. *Eur J Pharmacol* **545**, 51-64.
[24] Joseph JA, Shukitt-Hale B, Casadesus G (2005) Reversing the deleterious effects of aging on neuronal communication and behavior: beneficial properties of fruit polyphenolic compounds. *Am J Clin Nutr* **81**, 313S-316S.
[25] Inoue H, Jiang XF, Katayama T, Osada S, Umesono K, Namura S (2003) Brain protection by resveratrol and fenofibrate against stroke requires peroxisome proliferator-activated receptor alpha in mice. *Neurosci Lett* **352**, 203-206.
[26] Freudlsperger C, Greten J, Schumacher U (2008) Curcumin induces apoptosis in human neuroblastoma cells via inhibition of NFkappaB. *Anticancer Res* **28**, 209-214.
[27] Adhami VM, Mukhtar H (2007) Anti-oxidants from green tea and pomegranate for chemoprevention of prostate cancer. *Mol Biotechnol* **37**, 52-57.
[28] Siddiqui IA, Malik A, Adhami VM, Asim M, Hafeez BB, Sarfaraz S, Mukhtar H (2008) Green tea polyphenol EGCG sensitizes human prostate carcinoma LNCaP cells to TRAIL-mediated apoptosis and synergistically inhibits biomarkers associated with angiogenesis and metastasis. *Oncogene* **27**, 2055-2063.
[29] Corona G, Deiana M, Incani A, Vauzour D, DessìMA, Spencer JP (2007) Inhibition of p38/CREB phosphorylation and COX-2 expression by olive oil polyphenols underlies their anti-proliferative effects. *Biochem Biophys Res Commun* **362**, 606-611.
[30] Casadesus G, Shukitt-Hale B, Stellwagen HM, Zhu X, Lee HG, Smith MA, Joseph JA (2004) Modulation of hippocampal plasticity and cognitive behavior by short-term blueberry supplementation in aged rats. *Nutr Neurosci* **7**, 309-316.
[31] Beltz BS, Tlusty MF, Benton JL, Sandeman DC (2007) Omega-3 fatty acids upregulate adult neurogenesis. *Neurosci Lett* **415**, 154-158.
[32] Kawakita E, Hashimoto M, Shido O (2006) Docosahexaenoic acid promotes neurogenesis *in vitro* and *in vivo*. *Neuroscience* **139**, 991-997.
[33] Kim SJ, Son TG, Park HR, Park M, Kim MS, Kim HS, Chung HY, Mattson MP, Lee J (2008) Curcumin stimulates proliferation of embryonic neural progenitor cells and neurogenesis in the adult hippocampus. *J Biol Chem* **283**, 14497-14505.
[34] Valente T, Junyent F, Auladell C (2005) Zac1 is expressed in progenitor/stem cells of the neuroectoderm and mesoderm during embryogenesis: differential phenotype of the Zac1-expressing cells during development. *Dev Dyn* **233**, 667-679.
[35] Paxinos G, Franklin KBJ (2001) *The mouse brain in stereotaxic coordinates*. Second edition. Academic Press, San Diego, USA
[36] Denizot F, Lang R (1986) Rapid colorimetric assay for cell growth and survival, modifications to the tetrazolium dye procedure giving improved sensitivity and reliability. *J Immunol Meth* **89**, 271-277.
[37] Kaplan MS, McNelly NA, Hinds JW (1985) Population dynamics of adult-formed granule neurons of the rat olfactory bulb. *J Comp Neurol* **239**, 117-125.
[38] Cameron HA, McKay RD (2001) Adult neurogenesis produces a large pool of new granule cells in the dentate gyrus. *J Comp Neurol* **435**, 406-417.

[39] Bagley J, LaRocca G, Jimenez DA, Urban NN (2007) Adult neurogenesis and specific replacement of interneuron subtypes in the mouse main olfactory bulb. *BMC Neurosci* **8**, 92.
[40] Whitman MC, Greer CA (2007) Adult-generated neurons exhibit diverse developmental fates. *Dev Neurobiol* **67**, 1079-1093.
[41] Batista-Brito R, Close J, Machold R, Fishell G (2008) The distinct temporal origins of olfactory bulb interneuron subtypes. *J Neurosci* **28**, 3966-3975.
[42] Tanapat P, Hastings NB, Gould E (2005) Ovarian steroids influence cell proliferation in the dentate gyrus of the adult female rat in a dose- and time-dependent manner. *J Comp Neurol* **481**, 252-265.
[43] Mirescu C, Peters JD, Gould E (2004) Early life experience alters response of adult neurogenesis to stress. *Nat Neurosci* **7**, 841-846.
[44] Kempermann G, Kuhn HG, Gage FH (1997) More hippocampal neurons in adult mice living in an enriched environment. *Nature* **386**, 493-495.
[45] Gould E, Cameron HA, Daniels DC, Woolley CS, McEwen BS (1992) Adrenal hormones suppress cell division in the adult rat dentate gyrus. *J Neurosci* **12**, 3642-3650.
[46] Gould E, Cameron HA, McEwen BS (1994) Blockade of NMDA receptors increases cell death and birth in the developing rat dentate gyrus. *J Comp Neurol* **340**, 551-565.
[47] Bird CM, Burgess N (2008) The hippocampus and memory: insights from spatial processing. *Nat Rev Neurosci* **9**, 182-194.
[48] Neves G, Cooke SF, Bliss TV (2008) Synaptic plasticity, memory and the hippocampus: a neural network approach to causality. *Nat Rev Neurosci* **9**, 65-75.
[49] Martin SJ, Clark RE (2007) The rodent hippocampus and spatial memory: from synapses to systems. *Cell Mol Life Sci* **64**, 401-431.
[50] Sluimer JD, Vrenken H, Blankenstein MA, Fox NC, Scheltens P, Barkhof F, van der Flier WM (2008) Whole-brain atrophy rate in Alzheimer disease: identifying fast progressors. *Neurology* **70**, 1836-1841.
[51] Libon DJ, Bogdanoff B, Leopold N, Hurka R, Bonavita J, Skalina S, Swenson R, Gitlin HL, Ball SK. (2001) Neuropsychological profiles associated with subcortical white matter alterations and Parkinson's disease: implications for the diagnosis of dementia. *Arch Clin Neuropsychol* **16**, 19-32.
[52] Bigel MG, Smith ML (2001) The impact of different neuropathologies on pre- and postsurgical neuropsychological functioning in children with temporal lobe epilepsy. *Brain Cogn* **46**, 46-49.
[53] González-Martínez JA, Bingaman WE, Toms SA, Najm IM (2007) Neurogenesis in the postnatal human epileptic brain. *J Neurosurg* **107**, 628-635.
[54] Scharfman HE, Hen R (2007) Neuroscience. Is more neurogenesis always better? *Science* **315**, 336-338.
[55] Scharfman HE (2004) Functional implications of seizure-induced neurogenesis. *Adv Exp Med Biol* **548**, 192-212.
[56] Waldau B, Shetty AK (2008) Behavior of neural stem cells in the Alzheimer brain. *Cell Mol Life Sci* **65**, 2372-2384.
[57] Li B, Yamamori H, Tatebayashi Y, Shafit-Zagardo B, Tanimukai H, Chen S, Iqbal K, Grundke-Iqbal I (2008) Failure of neuronal maturation in Alzheimer disease dentate gyrus. *J Neuropathol Exp Neurol* **67**, 78-84.
[58] Arias-Carrión O, Freundlieb N, Oertel WH, Höglinger GU (2007) Adult neurogenesis and Parkinson's disease. *CNS Neurol Disord Drug Targets* **6**, 326-335.
[59] Shan X, Chi L, Bishop M, Luo C, Lien L, Zhang Z, Liu R (2006) Enhanced de novo neurogenesis and dopaminergic neurogenesis in the substantia nigra of 1-methyl-4-phenyl-1,2,3,6-tetrahydropyridine-induced Parkinson's disease-like mice. *Stem Cells* **24**, 1280-1287.
[60] La Spada AR (2005) Huntington's disease and neurogenesis: FGF-2 to the rescue? *Proc Natl Acad Sci U S A* **102**, 17889-17890.
[61] Curtis MA, Penney EB, Pearson J, Dragunow M, Connor B, Faull RL (2005) The distribution of progenitor cells in the subependymal layer of the lateral ventricle in the normal and Huntington's disease human brain. *Neuroscience* **132**, 777-788.
[62] Curtis MA, Eriksson PS, Faull RL (2007) Progenitor cells and adult neurogenesis in neurodegenerative diseases and injuries of the basal ganglia. *Clin Exp Pharmacol Physiol* **34**, 528-532.
[63] Tang H, Wang Y, Xie L, Mao X, Won SJ, Galvan V, Jin K (2007) Effect of neural precursor proliferation level on neurogenesis in rat brain during aging and after focal ischemia. *Neurobiol Aging* **30**, 299-308.
[64] Ishibashi S, Kuroiwa T, Sakaguchi M, Sun L, Kadoya T, Okano H, Mizusawa H (2007) Galectin-1 regulates neurogenesis in the subventricular zone and promotes functional recovery after stroke. *Exp Neurol* **207**, 302-313.
[65] Salazar-Colocho P, Lanciego JL, Del Rio J, Frechilla D (2008) Ischemia induces cell proliferation and neurogenesis in the gerbil hippocampus in response to neuronal death. *Neurosci Res* **61**, 27-37.
[66] Tonchev AB, Yamashima T, Sawamoto K, Okano H (2005) Enhanced proliferation of progenitor cells in the subventricular zone and limited neuronal production in the striatum and neocortex of adult macaque monkeys after global cerebral ischemia. *J Neurosci Res* **81**, 776-788.
[67] Tonchev AB, Yamashima T, Guo J, Chaldakov GN, Takakura N (2007) Expression of angiogenic and neurotrophic factors in the progenitor cell niche of adult monkey subventricular zone. *Neuroscience* **144**, 1425-1435.
[68] Parent JM (2002) The role of seizure-induced neurogenesis in epileptogenesis and brain repair. *Epilepsy Res* **50**, 179-189.
[69] Taupin P (2006) Therapeutic potential of adult neural stem cells. *Recent Patents CNS Drug Discov* **1**, 299-303.
[70] Sugaya K (2003) Neuroreplacement therapy and stem cell biology under disease conditions. *Cell Mol Life Sci* **60**, 1891-1902.
[71] Sugaya K (2005) Possible use of autologous stem cell therapies for Alzheimer's disease. *Curr Alzheimer Res* **2**, 367-376.
[72] Butterfield DA, Boyd-Kimball D (2005) The critical role of methionine 35 in Alzheimer's amyloid beta-peptide (1-42)-induced oxidative stress and neurotoxicity. *Biochim Biophys Acta* **1703**, 149-156.
[73] Irie K, Murakami K, Masuda Y, Morimoto A, Ohigashi H, Hara H, Ohashi R, Takegoshi K, Fukuda H, Nagao M, Shimizu T, Shirasawa T (2007) The toxic conformation of the 42-residue amyloid beta peptide and its relevance to oxidative stress in Alzheimer's disease. *Mini Rev Med Chem* **7**, 1001-1008.
[74] Butterfield DA, Boyd-Kimball D (2004) Amyloid beta-peptide(1-42) contributes to the oxidative stress and neurodegeneration found in Alzheimer disease brain. *Brain Pathol* **14**, 426-432.
[75] Sultana R, Perluigi M, Butterfield DA (2006) Redox proteomics identification of oxidatively modified proteins in Alzheimer's disease brain and *in vivo* and *in vitro* models of AD centered around Abeta(1-42). *J Chromatogr B Analyt Technol Biomed Life Sci* **833**, 3-11.
[76] Atwood CS, Moir RD, Huang X, Scarpa RC, Bacarra NM,

Romano DM, Hartshorn MA, Tanzi RE, Bush AI (1998) Dramatic aggregation of Alzheimer abeta by Cu(II) is induced by conditions representing physiological acidosis. *J Biol Chem* **273**, 12817-12826.

[77] Huang X, Atwood CS, Hartshorn MA, Multhaup G, Goldstein LE, Scarpa RC, Cuajungco MP, Gray DN, Lim J, Moir RD, Tanzi RE, Bush AI (1999) The A beta peptide of Alzheimer's disease directly produces hydrogen peroxide through metal ion reduction. *Biochemistry* **38**, 7609-7616.

[78] Behl C, Davis JB, Lesley R, Schubert D (1994) Hydrogen peroxide mediates amyloid beta protein toxicity. *Cell* **77**, 817-827.

[79] Rojo L, Sjöberg MK, Hernández P, Zambrano C, Maccioni RB (2006) Roles of cholesterol and lipids in the etiopathogenesis of Alzheimer's disease. *J Biomed Biotechnol* **3**, 73976.

[80] Rojo LE, Fernández JA, Maccioni AA, Jimenez JM, Maccioni RB (2008) Neuroinflammation: implications for the pathogenesis and molecular diagnosis of Alzheimer's disease. *Arch Med Res* **39**, 1-16.

[81] Monje ML, Toda H, Palmer TD (2003) Inflammatory blockade restores adult hippocampal neurogenesis. *Science* **302**, 1760-1765.

Appendix III

Oxidative Stress in Alzheimer's Disease: Pathogenesis, Biomarkers & Therapy

Alejandro Gella & Irene Bolea

Alzheimer's Disease / Book 2, ISBN 979-953-307-022-2

In press

Chapter Number

Oxidative Stress in Alzheimer's Disease: Pathogenesis, Biomarkers and Therapy

Alejandro Gella and Irene Bolea
Universitat Internacional de Catalunya
Universitat Autònoma de Barcelona
Spain

1. Introduction

Alzheimer's disease (AD) is the most common cause of dementia in the elderly with profound medical and social consequences. The pathogenesis of AD is a complex and heterogeneous process which classical neuropathological hallmarks found in the brain are extracellular deposits of beta-amyloid (Aβ)-containing plaques and intracellular neurofibrillary tangles (NFTs) composed of hyperphosphorylated tau protein. Mutation of *presenilin-1* (PS-1), *presenilin-2* (PS-2), and altered *amyloid precursor protein* (APP) genes has been reported to cause inherited AD. In addition, other genes such as apolipoprotein E-4 (APOE), endothelial nitric oxide synthase-3, and alpha-2-macroglubulin have also been associated with AD. A further number of hypothesis have been proposed for AD mechanism, which include: the amyloid cascade, vascular damage, excitotoxicity, deficiency of neurotrophic factors, mitochondrial dysfunction, trace element neurotoxicity, inflammation and oxidative stress hypothesis.

The oxidative stress (OS) hypothesis of aging postulated by Dr. Denham Harman in 1956 proposed that brain aging is associated to a progressive imbalance between the anti-oxidant defenses and the pro-oxidant species that can occur as a result of either an increase in free radical production or a decrease in antioxidant defence. The fact that age is the main risk factor for AD development provides considerable support to the OS hypothesis since the effects produced by reactive oxygen species (ROS) can accumulate over the years (Nunomura et al., 2001). The link between AD and OS is additionally supported by the finding of decreased levels of antioxidant enzymes, increased protein, lipid and DNA oxidation and advanced glycation end products (AGEs) and ROS formation in neurons of AD patients (Perry et al., 2000; Barnham et al., 2004). It has been reported that the accumulation of the oligomeric form of Aβ, the most toxic form of the peptide, induces OS in neurons (Butterfield, 2002), supporting the hypothesis and suggesting that OS plays a causative role in the development of AD. Then, a large amount of literature has demonstrated that OS is an important feature in AD pathogenesis that deserves to be deeply studied (Perry et al, 2002: Markesbery et al, 1999). In this Chapter, we address the main factors involved in the generation of oxidative stress and provide an overview of the oxidative stress biomarkers status in Alzheimer's disease. The Chapter concludes with a revision of the controversial efficacy of antioxidants as potential treatment in AD therapy as well as an update of the main antioxidant compounds found to have a beneficial effect in AD.

2. Mitochondria as a source of reactive oxygen species

Several years after the postulation of the OS hypothesis, Dr. Harman proposed that life span is determined by the rate of ROS damage to the mitochondria (Harman, 1972) giving for the first time an important role to this organelle in the ageing process and establishing the basis for "mitochondrial theory of ageing". It is important to note that the central nervous system (CNS) is especially vulnerable to oxidative damage as a result of the high oxygen consumption rate (20% of the total oxygen consumption), the abundant content of easily peroxidizable fatty acids, and the relative paucity of antioxidant enzymes compared to other tissues. In aerobic organisms, mitochondria produce semireduced oxygen species during respiration. The initial step of the respiratory chain reaction yields the superoxide radical ($^{\bullet}O_2^-$), which produces hydrogen peroxide (H_2O_2) by addition of an electron. The reduction of H_2O_2 through the Fenton reaction produces the highly reactive hydroxyl radical ($OH^{\bullet}$), which is the chief instigator of oxidative stress damage and reacts indiscriminately with all biomacromolecules (Figure 1). Under normal conditions, damage by ROS is prevented by an efficient antioxidant cascade, including both enzymatic and non-enzymatic entities. The enzymes responsible of the detoxification machinery are the cytosolic copper-zinc superoxide dismutase (CuZnSOD) and the mitochondrial manganese superoxide dismutase (MnSOD), which convert superoxide to O_2 and H_2O_2. Moreover, monoamine oxidases (MAOs) and L-amino acid oxidase can also produce H_2O_2 during its metabolism which is effectively removed by catalase (CAT) and peroxidases (e.g. glutathione peroxidase, GPx). Since CAT is compartmentalized into peroxisomes the detoxification of cytosolic and mitochondrial peroxides depends predominantly on GPx.

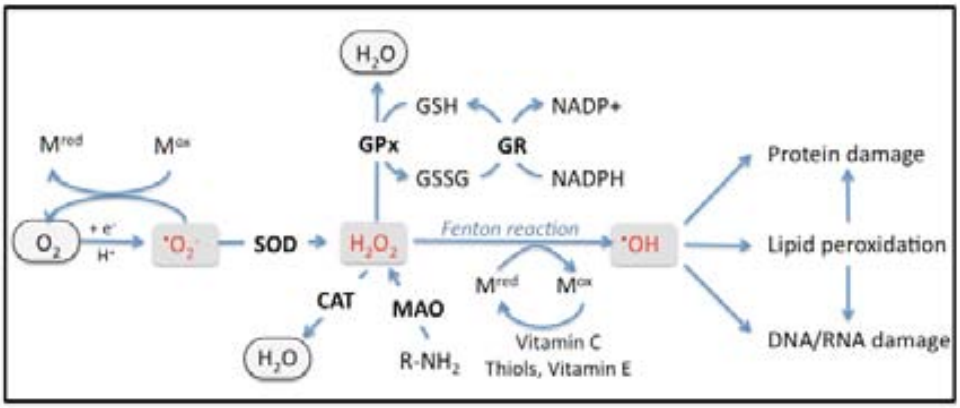

Fig. 1. Schematic illustration of the mechanism involved in reactive oxygen species (ROS) formation and elimination. Glutathione peroxidase (GPx), glutathione reductase (GR), superoxide dismutase (SOD), catalase (CAT), monoamine oxidase (MAO), glutathione (GSH), glutathione disulfide (GSSG).

The non-enzymatic antioxidant defenses include the reduction of the resulting oxidized transition metal ions (usually Fe^{3+} and Cu^{2+}) by cellular reductants such as vitamin C, thiols and perhaps even vitamin E. In this context, SOD can also serve as the reductant of oxidized metal ions for the production of hydroxyl radical from H_2O_2, which coupled with the Fenton reaction, is known as the Haber-Weiss reaction. In AD, this situation is further exacerbated by the fact that redox active transition metals are aberrantly accumulated in cytoplasm of

neurons. Moreover, Aβ peptide is considered a strong redox active agent capable of reducing transition metals and allowing for conversion of O_2 to H_2O_2 (Bondy et al, 1998).

3. Biomarkers of oxidative stress in Alzheimer's disease

Biomarkers, as indicators of signalling events in biological systems or samples, can be used as intermediate endpoints or early-outcome predictors of disease development for preventive purposes. Most effort is nowadays focused on the search of reliable and robust biomarkers which would be useful for an earlier AD diagnosis. The emphasis is being placed on the incorporation of oxidative stress biomarkers to study the increased oxidative damage (Lovell & Markesbery, 2007a). It has recently been a significant improvement in assay methods and measurement accuracy for oxidative biomarkers. Nevertheless, it appears imperative that biomarkers of oxidative damage must be validated (Dalle-Donne et al., 2006a) in order to incorporate them into epidemiological studies and provide a better understanding regarding the role of ROS in the pathogenesis and progression of AD, as well as to assess the possible effectiveness of an antioxidant therapy (Griffiths et al., 2002). Strong evidence show that oxidative markers are more prevalent in initial rather than in later stages of the disease, and thus suggesting that targeting the earlier events of the disease may be more successful that targeting the later events (e.g. beta-amyloid (Aβ) plaque deposition and/or intracellular neurofibrillary tangles formation). On the other hand, many studies provided evidence for the deleterious consequences of oxidative stress products on certain cellular targets in AD. Therefore, most highly reactive oxidants react with virtually all biomolecules, including, lipids, DNA/RNA, carbohydrates and proteins. Table 1 summarizes the main OS biomarker candidates for MCI and AD diagnosis.

Biomarker	Specimen	Diagnosis	Reference
Lipid Peroxidation			
4-HNE	Plasma	AD	Mc Grath et al., 2001
	Ventricular fluid	AD	Lovell et al., 1997
F2-Isoprostanes	Urine	AD	Kim et al., 2004
	CSF	AD	Montine et al., 2011
	CSF, plasma and urine	MCI	Pratico et al., 2002
DNA oxidation			
8-OHdG	Peripheral lymphocytes	MCI	Migliore et al., 2005
		AD	Mecocci et al., 2002
AGEs			
CML	CSF	AD	Ahmed et al., 2005
Oxidized Protein			
α-1-antitrypsin	CSF	AD	Puchades et al., 2003
Ig λ light chain	CSF	MCI	Korolainen et al., 2007
α-1-antitrypsin	Plasma	AD	Yu et al., 2003; Choi et al., 2002

Table 1. Potential OS biomarkers under validation for Alzheimer's disease. MCI, mild cognitive impairment; AD, Alzheimer's disease; CSF, cerebrospinal fluid; Ig, immunoglobulin; 4-HNE, 4-hydroxy-2-nonenal; 8-OHdG, 8-oxo-7,8-dihydro-2'-deoxyguanosine; AGEs, Advanced Glycation end products; CML, N-carboxymethyl-lysine.

3.1 Biomarkers of lipid peroxidation

Lipid oxidation (also called lipid peroxidation) has drammatic consequences in ageing and age-related disorders. Phospholipids present in brain membranes are mainly polyunsaturated fatty acids (PUFAs: arachidonic acid, linoleic acid, linolenic acid, docosahexaenoic acid, etc…), which are especially vulnerable to a free radical attack since their double bonds allow an easy removal of hydrogen ions. Oxidation of PUFAs produces a variety of reactive α,β-unsaturated aldehydes such as, acrolein, 4-hydroxy-2-nonenal (4-HNE), 4-oxo-2-nonenal (4-ONE), 4-hydroxy-2-hexanal (4-HHE), 2-hexenal, crotonaldehyde as well as the dialdehydes glyoxal and malondialdehyde (MDA). These species are highly reactive cytotoxic substances than can form stable covalent adducts with free amino groups of proteins (Lys, His and Cys residues) through Michael addition (Calingasan et al., 1999; Carini et al., 2004; Esterbauer et al., 1991; Montine et al., 1997) whick are known as advanced lipoxidation end products (ALEs). 4-HNE is a major and toxic aldehyde generated by free radical attack on PUFAs and is considered a second toxic messenger of oxygen free radicals. Therefore, it has a high biological activity and exhibits numerous cytotoxic, mutagenic, genotoxic, and signalling effects in neurons (Eckl et al., 1993; Williams et al., 2006). In addition, 4-HNE may be an important mediator of OS-induced apoptosis, cellular proliferation and signalling pathways (Uchida, 2003). HNE is permanently formed at basal concentrations under physiologic conditions, but its production is greatly enhanced in the AD brain where increased lipid peroxidation occurs (Butterfield et al., 2010; McGrath et al., 2001). Increased concentrations of 4-HNE, 4-HHE and acrolein have been found in cerebrospinal fluid (CSF) and in multiple brain regions from individuals with mild cognitive impairment and early AD compared with age-matched controls (Bradley et al., 2010a and 2010b; Lovell et al., 1997; Williams et al, 2006). In addition, a positive feedback in the pathogenesis of AD is provoked by HNE that increases Aβ production (Tamagno et al., 2008) which, in turns, induces lipid peroxidation (Butterfield et al., 2002). Furthermore, HNE-adducts have been identified in amyloid plaques and neurofibrillary tangles, the two hallmarks of AD pathogenesis (Sayre et al., 1997; Ando et al., 1998; Wataya et al., 2002).

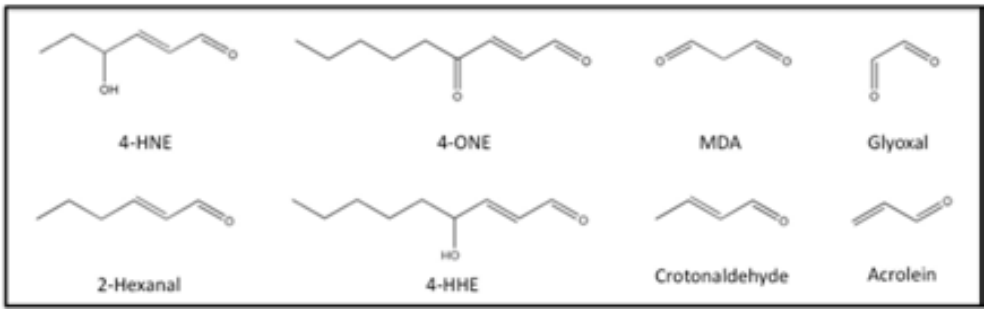

Fig. 2. Lipid peroxidation products. ROS stimulate peroxidation of polyunsaturated fatty acids (PUFA) to generate α-β-unsaturated aldehydes and dialdehydes.

F2-Isoprostanes (F2-IsoPs), which contain an F-type prostane ring, are a group of bioactive prostaglandin-like compounds generated via a non-enzymatic mechanism involving the free radical-initiated peroxidation of esterified arachidonic acid (AA). Then, they are cleaved and released into the circulation by phospholipases before excretion in the urine as free

isoprostanes (Basu, 1998). The most studied class of isoprostanes, due to their urine stability, is 8-iso-Prostaglandin F_{2a} (8-iso-PGF_{2a}; Figure 3). Urinary F2-IsoPs determination has been proposed as specific, reliable, and non-invasive marker to assess lipid peroxidation in vivo (Cracowski et al., 2002; Montushchi et al., 2004) since an increase in 8-iso-PGF_{2a} levels in CSF and urine have been found in subjects with AD (Montine et al., 1998 and 2011; Kim et al., 2004). On the other hand, oxidation of docosahexanoic acid (DHA) produces F4-neuroprostanes (F4-NeuroPs; Figure 3) (Morrow et al., 1999; Roberts et al., 1998) which levels are elevated in postmortem ventricular CSF of AD patients and are more abundant in the brain that F2-isoprostanes. Nevertheless, plasma F2-IsoPs and F4-NeuroPs do not accurately reflect central nervous system levels and are not reproducibly elevated in body fluids outside of central nervous system in Alzheimer's disease patients (Montine et al., 2002).

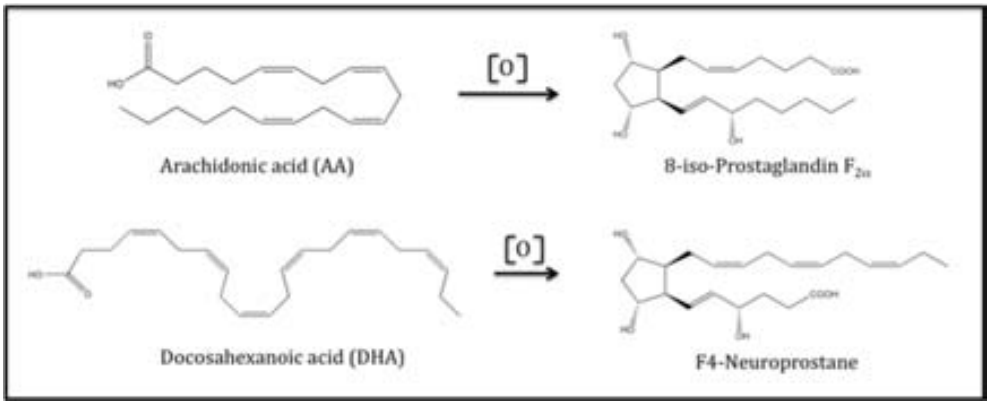

Fig. 3. Chemical structures of F4-neuroprostane and 8-iso-Prostaglandin F_{2a} arising from direct oxidation of docosahexanoic and arachidonic acids, respectively.

3.2 Biomarkers of oxidative DNA damage

Among over 30 nucleobase modifications that have been described, the most extensively studied that reflect oxidative DNA damage is 8-oxo-7,8-dihydro-2′-deoxyguanosine (8-oxodG; also known as 8-OHdG), a product of oxidatively modified DNA base guanine (Figure 4). The detection of this oxidation is important not only due to its abundance but also to its mutagenic potential through GC-to-TA transversion mutations upon replication of DNA (Cheng et al., 1992). Nevertheless, oxidatively damaged DNA can be repaired and released into the bloodstream and consequently appear without further metabolism in the urine (Fraga et al., 1990; Shigenaga et al., 1989). In addition, urinary levels of 8-OHdG have been found to be independent of dietary influence in humans. The modified base 8-oxo-7,8-dihydroguanine (8-oxoGua; Figure 4) and modified nucleoside (8-oxodG; Figure 4), which are found in urine, represent the major repair products of oxidatively damaged DNA in vivo and have been considered to reflect the whole-body oxidative DNA damage (Hamilton et al., 2001; Olinnski et al., 2007). There is considerable evidence supporting that oxidative stress occurs in AD, and increased 8-oxodG levels have been found in DNA isolated from brain tissues, leukocytes and ventricular CSF of AD patients. In contrast, free 8-OHdG was found dramatically decreased in AD samples as compared to the controls (Lovell & Markesbery, 2001; Markesbery & Carney, 1999; Mecocci et al., 2002; Migliore et al., 2005).

Taken together, these data indicate a double insult in AD patients by increasing oxidative damage and decreasing DNA repair mechanisms efficiency. More recent studies showed an elevated 8-OHdG in both nuclear and mitochondrial DNA (mtDNA) isolated from vulnerable brain regions in amnestic mild cognitive impairment (MCI), the earliest clinical manifestation of AD, and thus suggesting that oxidative DNA damage is an early event in AD and is not merely a secondary phenomenon (Lovell & Markesbery, 2007b).

Many methods such as HPLC-ECD, GC-MS, LC-MS, and immunoassay have been established to measure 8-OHdG in biological specimens. In this concern, the European Standards Committee of Urinary (DNA) Lesions Analysis (ESCULA) was formed in 2006 in order to validate the measurement methods of oxidatively damaged DNA and to establish reference urine values (Cooke et al., 2008; Evans et al., 2010). Finally, it is important to mention that DNA can also be modified by products of lipid peroxidation (ALEs). These α-β-unsaturated aldehydes can react with deoxyguanosine through an initial Michael addition of the exocyclic amino group followed by ring closure of N-1 onto the aldehydic group to generate a bulky exocyclic 1-N^2-propanodeoxyguanosine adduct (Liu et al., 2006; Kozekov et al., 2003) and therefore participate in the propagation of the oxidative DNA damage.

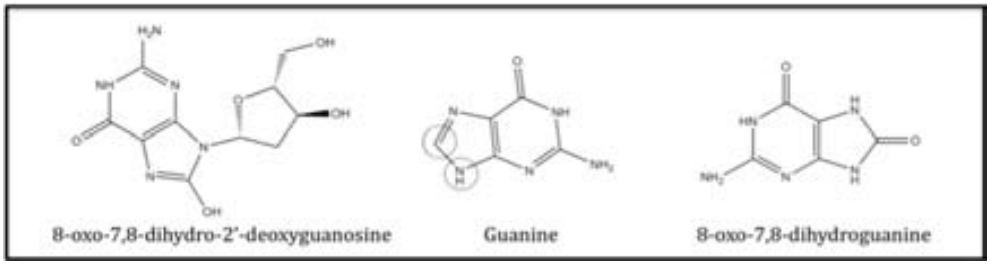

Fig. 4. Chemical structure of 8-oxo-7, 8-dihydro-2′-deoxyguanosine (8-oxodG; 8-OHdG), guanine and 8-oxo-7, 8-dihydroguanine (8-oxoGua).

3.3 Advanced glycation end products

Advanced glycation end products (AGEs), formed by a non-enzymatic reaction of sugars with amino groups in long-lived proteins, lipids, and nucleic acids, are also potent neurotoxins and proinflammatory molecules. Glycation of proteins starts as a non-enzymatic process with the spontaneous condensation of ketone or aldehyde groups of sugars with a free aminoacid group of proteins to form a labile Schiff base, consistent with the classical reaction described by Louis Camille Maillard in 1912 (Figure 5).

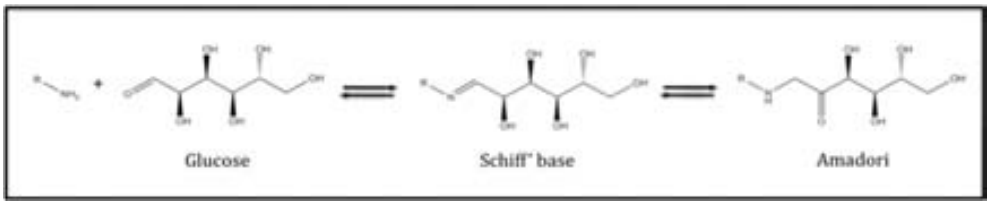

Fig. 5. Non-enzymatic reaction of the carbonyl groups of reducing sugars with primary amino groups produce corresponding Schiff bases, which undergo Amadori rearrangement to give ketoamines.

Glycation is the first step in the cascade of a complex series of very slow reactions in the body known as Amadori reactions, Schiff base reactions and Maillard reactions, all leading to the formation of irreversibly cross-linked heterogeneous aggregates. AGEs are continuously formed in the human body and progressively accumulate with age in plasma and tissues. In diabetes mellitus and AD the rate of AGEs formation is accelerated and consequently, they have been considered potentially useful biomarkers for monitoring the treatment of these disorders. Chemical structures of representative markers of AGEs are summarized in Figure 6. Supporting the argument that AGEs are involved in the pathogenesis of AD, some studies have shown the presence of AGEs in association with two major proteins of AD, Aβ and MAP-tau (Smith et al., 1995; Vitek et al., 1994; Yan et al., 1994). Extracellular AGEs accumulation has been demonstrated in senile plaques in different cortical areas. Intracellular proteins deposits including NFTs, Lewy bodies of patients with Parkinson's disease and Hirano bodies are also crosslinked by AGEs, which may explain their insolubility in detergents and resistance to proteases (Loske et al., 2000). The major component of the NFTs, the microtubuli-associated protein tau (MAP-tau) has been shown to be subject to intracellular AGEs formation. MAP-tau

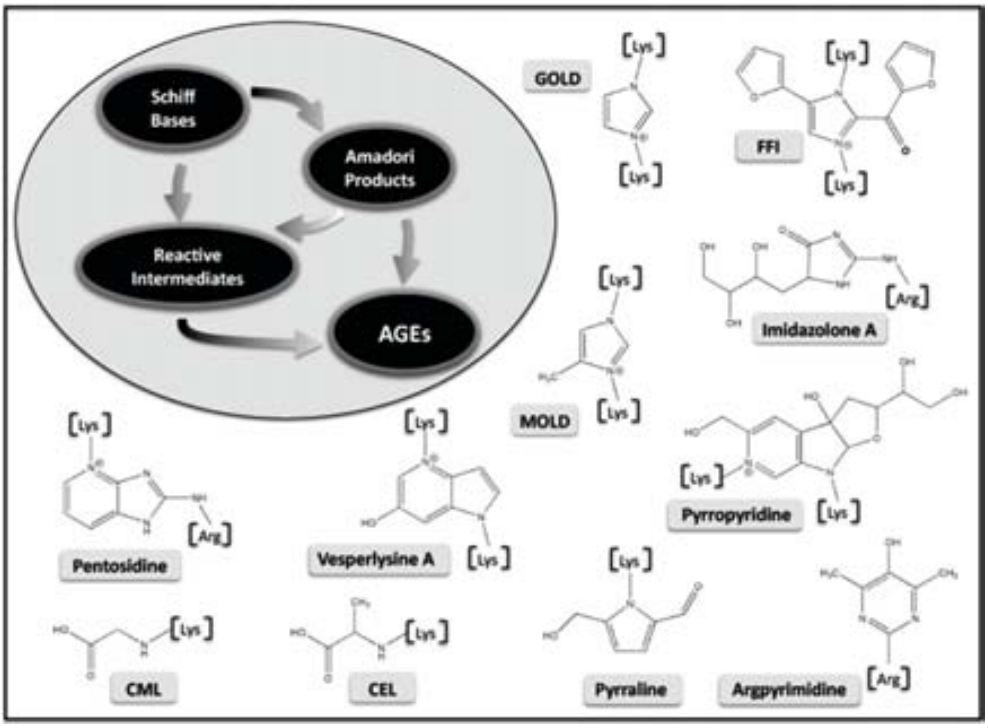

Fig. 6. A variety of highly reactive carbonyl intermediates such as 3-deoxy-glucosone, glyoxal and methyl-glyoxal can be formed by glucose or Schiff's base or Amadori product auto-oxidation which, in turn, can react with free amino groups to form AGE products. N-carboxymethyl-lysine (CML), N- carboxyethyl-lysine (CEL), glyoxal-derived lysine dimer (GOLD), methylglyoxal-derived lysine dimer (MOLD), furoyl-furanyl-imidazole (FFI), Lysine (Lys) and arginine (Arg).

can be glycated in vitro, inhibiting its ability to bind to microtubules. In addition, MAP-tau isolated from brains of AD patients is glycated in the tubulin-binding region, giving rise to the formation of β-sheet fibrils (Ledesma et al., 1998). AGEs accumulate in the human brain during aging (Kimura et al., 1996) and are present in neurofibrillary tangles and senile plaques in patients with AD (Castellani et al., 2001). Furthermore; AGE-modified Aβ peptides accelerate aggregation of soluble nonfibrillar Aβ peptides. In older adults with cerebrovascular disease, elevated N-carboxymethyl-lysine (CML) has been found in cortical neurons and cerebral vessels and has been related to the severity of cognitive impairment (Southern et al., 2007). Brain tissue AGEs can therefore be considered tissue biomarkers for AD, and increased brain AGEs concentrations are reflected in CSF (Ahmed et al., 2005) but no necessarily in plasma (Thome et al., 1996).

A positive feedback loop in the pathogenesis of AD is provoked by AGEs which increase OS and inflammation through binding with AGEs receptor (RAGE). The RAGE signalling pathway, found upregulated in AD brains, can be initiated by a diverse repertoire of pro-inflammatory ligands that include AGEs, S100/calgranulins, amphoterin, and amyloid-β peptide. Ligand binding with RAGE triggers the induction of increased reactive oxygen species, activates NADH oxidase, increases the expression of adhesion molecules, and up-regulates inflammation through NF-kB and other signalling pathways.

3.4 Biomarkers of oxidative protein damage

Carbonylation of proteins is an irreversible oxidative process, often leading to a loss of protein function, which is considered a widespread indicator of severe oxidative damage and disease-derived protein dysfunction (Dalle-Donne et al., 2006). Protein carbonyl groups are introduced to proteins by direct oxidation of several amino acid residues into ketone or aldehyde derivates (particularly lysine, arginine, threonine and proline; Figure 7) or by secondary reaction with the primary oxidation products of sugars (forming AGEs) and lipids (forming ALEs) (Berlett & Stadtman, 1997). Several studies have proved that proteins are major initial cell targets of ROS, leading to earlier formation of the protein carbonyls in biological systems. Detection of increased levels of protein carbonyls in AD has been proposed as a sign of disease-associated dysfunction, suggesting the potentiality as biomarkers for early AD diagnosis.

Recent studies show an increase in protein carbonyls together with NFTs in multiple brain regions of AD subjects (Sultana & Butterfield, 2011). Oxidative modifications of proteins can cause cross-linking of covalent bonds of proteins leading to fibril formation and insolubility. NFTs are characterized by the aggregation and hyperphosphorilation of tau proteins which is linked to oxidation through the microtubule-associated protein kinase pathway and through the activation of the transcription factor NF-kB. A wide number of studies have reported differences in specific carbonated proteins in brain, plasma and CSF of AD patients compared with control group by using 2-dimensional gel electrophoresis in combination with mass spectroscopy techniques (Castegna et al., 2002a, 2002b; Davidsson et al., 2001; Puchades et al., 2003). Some of these studies reveal the presence of specific targets of protein oxidation in AD brain: creatine kinase BB, glutamine synthase, ubiquitin carboxy-terminal hydrolase L-1, dihydropyrimidinase-related protein 2, alpha-enolase and heat shock cognate 71. Glutamine synthase and creatine kinase, both markedly decreased in AD brains, are especially sensitive to oxidative modifications since they may cause alteration of glutamate concentrations (glutamine sinthase), and therefore enhance excitotoxicity, and decrease

energy metabolism (creatine kinase). Recently, several oxidized carbonylated proteins have been characterized in frontal cortex (Korolainen et al., 2006), plasma (Yu et al., 2003; Choi et al., 2002) and CSF (Korolainen et al., 2007) of patients suffering from AD by two-dimensional oxyblotting technique.

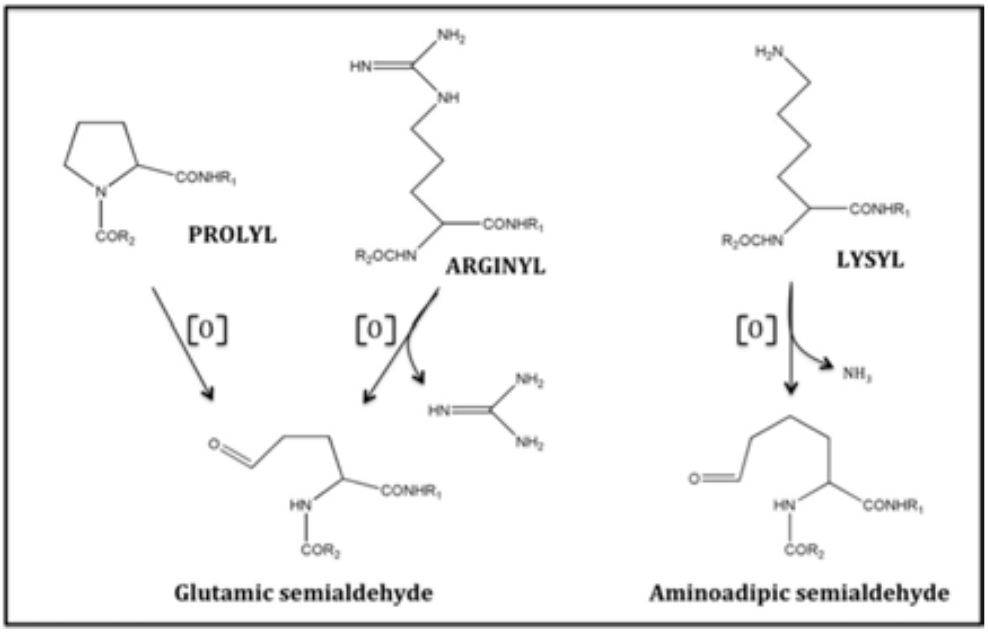

Fig. 7. Chemical structures of protein carbonyls arising from direct oxidation of aminoacid side chains. Glutamic semialdehyde (resulting from direct oxidation of arginyl and prolyl residues) and aminoadipic semialdehyde (resulting from direct oxidation of lysyl residue).

4. Antioxidant therapies in Alzheimer's disease

Currently, the only Food and Drug Administration (FDA) approved treatment for AD is the administration of the cholinesterase inhibitors (AChEI) donepezil, galantamine and rivastigmine and the N-methyl-D-aspartate (NMDA) receptor antagonist, memantine (Birks et al., 2000, 2006; Loy et al., 2004; Areosa et al., 2005). Nevertheless, to date, these drugs have demonstrated to produce only modest symptomatic improvements in some of the patients, but not to cure or stop the disease progression. Moreover, AChEI are expensive and may have side effects resulting from activation of peripheral cholinergic systems (Green et al., 2005). Then, effective treatments are greatly needed. The current therapeutic strategies being investigated for AD include targeting neurotransmission with multifunctional compounds, anti-amyloid and anti-tau therapies, drugs targeting mitochondrial dysfunction, neurotrophins, statins and also other approaches such us PUFAs and antioxidants (for review see Mangialasche et al., 2010). Among them, antioxidant therapies and PUFAs are particularly attractive due to their low toxicity, low cost and their ability to target earlier changes of the disease (e.g oxidative stress) which are linked to cognitive and functional decline. However, there is still much skepticism regarding the likelihood of success with an

antioxidant therapy since to date these compounds tested in randomised controlled trials (RCTs) have given controversial results.

4.1 Vitamins

A large amount of literature exists in relation to the potential benefits of vitamins, which act as natural free radical scavengers, in the prevention of AD (Figure 8). Vitamin A has been traditionally considered as antioxidant and it seems essential for learning, memory and cognition. Retinoic acid, a metabolic product of vitamin A, is known to slow cell death and protect from Aβ (Sahin et al., 2005). Thus, since levels of vitamin A decline with age and are found lower in AD individuals (Goodman et al., 2006) vitamin A supplementation might be useful for the treatment of some features in the ageing process. B-vitamins (B_6, B_{12} and folic acid) are lipid soluble antioxidants involved in the methylation of homocysteine (Hcy) which is highly cytotoxic. Cellular catabolism and cellular export mechanisms are the responsible for keeping low intracellular Hcy concentration. AD patients tipically present high levels of Hcy (McIlroy et al., 2002) and low levels of vitamin B_{12} and folate which appear to be associated with an increased rate of cognitive decline (Tucker et al., 2006; Morris et al., 2007). Nevertheless, in a recent study, a combination of vitamins B_{12}, B_6 and folate in mild to moderate AD individuals, although lowering Hcy, did not produce any effect on cognition compared to controls. Vitamin C (ascorbic acid), found in many fruits and vegetables, is the major water-soluble antioxidant and acts as first defence against free radicals in blood and plasma. Bagi et al, 2003, have shown that chronic vitamin C treatment is able to decrease high levels of isoprostanes in animal models. In contrast, other studies

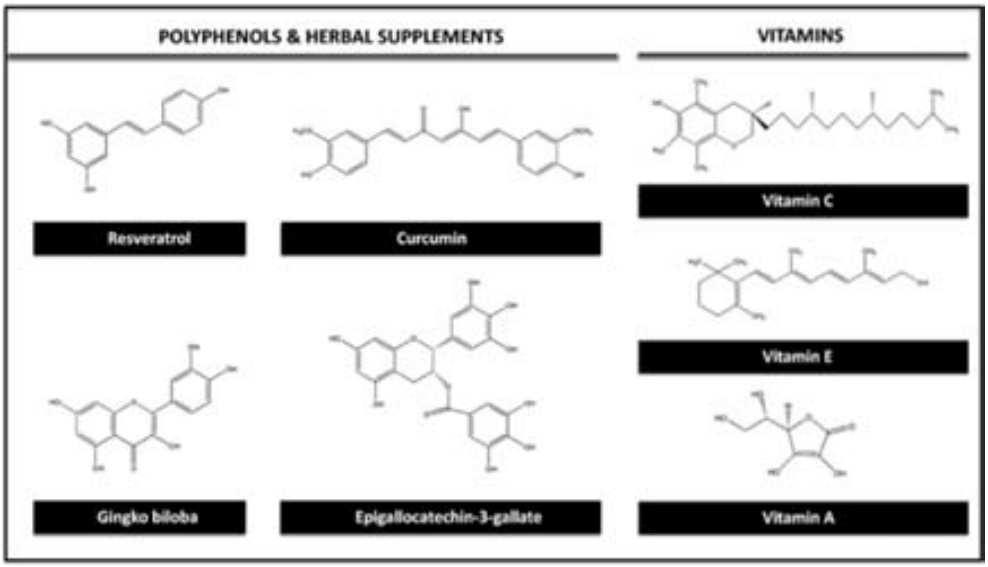

Fig. 8. Chemical structures of the principal polyphenols, herbal suplements and vitamins investigated as promising agents for the treatment of AD.

have shown that it can also act as pro-oxidant inducing neuronal oxidative stress via its interaction with metal ions (White et al., 2004). Vitamin E (α-tocopherol), present in whole grains, cereals and vegetable oils, is a lipid-soluble vitamin found in cell membranes and circulating lipoproteins. Its antioxidant capacity acts directly to a variety of ROS. It is found low in AD patients (Jiménez-Jiménez et al., 1997) and although in vitro and animal studies have been encouraging, human trials have produced conflicting results (Berman et al., 2004). A Cochrane study shows that tocopherol is not effective in a prevention trial in mild cognitive impairment (MCI) to reduce progression to AD nor clearly effective in AD patients (Tabet et al., 2000; Luchsinger et al., 2003). Besides, a harmfull effect of tocopherol at high doses has also been suggested (Tucker et al., 2005). However, several studies correlate a reduced risk to AD in elderly persons treated with vitamin E and C alone or in combination (Grundman et al., 2004; Morris et al., 1998; 2002; 2005). On the other hand, brain bioavailability of vitamin E in humans is very low and, as suggested elsewhere may not be enough to quickly inhibit AD neuropathology unless administered as a prophylactic at very early ages. The large amount of contradictory data found in literature about the use of vitamins as antioxidants indicates intricate physiological and pharmacological features of AD and remain questionable its use in human.

4.2 Polyphenols and herbal supplements

Polyphenols are a group of plant-derived chemical substances which protect plants from the stress induced by physical damage, disease, radiation and pests (Figure 8). It has been suggested that curcumin, the yellow pigment extracted from the plant *curcuma longa* (turmeric), may be a promising therapy for AD due to its extended neuroprotective actions (Mishra et al., 2008; Cole et al., 2007), including antioxidant, anti-inflammatory, inhibition of Aβ formation and removal of existing Aβ, as well as cooper and iron chelation. Epigallocathechin-3-gallate (EGCg) is found in green tea and it has been described that prevents Aβ aggregation by directly binding to the unfolded peptide. It also modulates signal transduction pathways, expression of genes regulating cell survival and apoptosis and its actions in mitochondrial function make it a potent antioxidant (Mandel et al., 2008). Resveratrol is present in red wine, peanuts and other plants and it has been found that it reduces OS, inflammation and Aβ deposition, decreases cell death and protects DNA (Mishra et al., 2008; Karuppagounder et al., 2009). A recent study suggests that moderate consumption of red wine reduces the risk of developing AD. Nevertheless, the translation to humans is still somewhat problematic and has some caveats since although polyphenols easily penetrate blood-brain barrier, they show bioavailabity problems such us low absorption, rapid metabolism and quick elimination. Efforts to increase bioavailability have been reviewed (Anand et al., 2007) and the adjuvant use widely extended (Shoba et al., 1998). Indeed, there is currently a clinical trial underway addressing curcumin bioavailability (http://clinicaltrials.gov/NCT01001637). Furthermore, the anti-AD effects of polyphenols may not be mediated solely through their direct antioxidant action but rather indirectly through any other functions. Then, it is still to be clarified whether polyphenols are able to slow the progression of AD. Herbal supplements such us *gingko biloba* have been suggested to possess beneficial properties against AD (Luo et al, 2002). Numerous animal and in vitro studies report that *gingko biloba* extract EGb761 possess neuroprotective benefits (Defeudis et al., 2002) including antioxidant, anti-inflammatory, and regulator of Aβ processing. It has also been described that *gingko* improves cognitive function in mild to

moderate AD patients (Oken et al., 1998; Le Bars et al., 2003) and reduces deterioration in subjects with more severe dementia via inhibition of the Aβ induced free radical generation (Napryeyenko et al., 2009; Yao et al., 2001). Nevertheless, a double-blind placebo controlled study found no beneficial effect of *gingko* on dementia in AD patients (Schneider et al, 2005) and DeKosky et al, 2008 showed that gingko was not better than placebo at preventing the onset of dementia. Additionally, there are two more studies finding no correlation between cognitive decline and the use of *gingko biloba* (Snitz et al., 2009; Dodge et al., 2008). Although data is controversial, it then appears that *gingko* may be useful delaying cognition impairment but not preventing the onset of AD. The ongoing clinical trial will help to elucidate this question (http://clinicaltrials.gov/NCT00814346).

4.3 Mitochondrial-related antioxidants

Since mitochondria are the major sources of ROS in the central nervous system, therapeutic strategies have largely focused in targeting mitochondria and mitochondrial-related pathways. There are several compounds showing an in vitro and in vivo antioxidant and neuroprotective action but only a few have been tested in human clinical trials with mixed results.

4.3.1 Quinone family

Ubiquinone (Coenzyme Q, CoQ) and idebenone, a synthetic analog of CoQ, (Figure 9) are the major mitochondrial targets used as therapeutics against ROS-mediated damage. They have demonstrated antioxidant properties in vitro and in animal models (Wadsworth et al., 2008). CoQ has not been yet tested in humans but idebenone has been investigated in clinical trials for its capacity to inhibit lipid peroxidation. Several studies report a significant effect in memory and attention improvements (Gutzmann et al., 2002; Senin et al., 1992; Weyer et al., 1997) but a larger study reported no effect in slowing the disease progression (Thal et al., 2003).

4.3.2 Other mitochondrial antioxidants

Alpha-lipoic acid (LA) is an organosulfur compound derived from octanoic acid and primarily a cofactor in aerobic metabolism for pyruvate dehydrogenase complex. Its reduced bioactive form produced into cells provides its antioxidant properties (Haenen et al., 1991). Acetyl L-carnitine (ALCAR) is formed within mitochondria by carnitine-*O*-acetyltransferase. Both LA and ALCAR (Figure 9) are good candidates for being used therapeutically as mitochondrial antioxidants since it was found that a combination of both decreased mitochondrial dysfunction and its consequent ROS-mediated damage in aged rats, improving cognitive functions (Aliev et al., 2009). Additional neuroprotective functions, including binding to targets involved in Aβ production have been reported (Epis et al., 2008). However, several clinical trials with ALCAR have been conducted with contradictory results: one showed no effectiveness in early onset AD (Thal et al., 2000) whereas another showed a slower deterioration in cognition (Pettergrew et al., 1995). A recent meta-analysis of ALCAR treatment trials showed an improvement in clinical scales in patients with MCI and AD (Montgomery et al., 2003). Dimebon (Figure 9), a non selective antihistamine, possesses several mechanisms of action including the inhibition of Aβ toxicity and the prevention of ROS-mediated damage (Doody et al., 2009; Okun et al., 2010). Several clinical trials have been performed in AD patients with contradictory

results: in a phase 2 clinical trial, dimebon improved cognition and behaviour, overall function in MCI and AD (Doody et al., 2008) whereas more recently, a phase 3 CONNECTION trial with AD patients showed no improvement in any parameter (http://clinicaltrials.gov/NCT00675623).

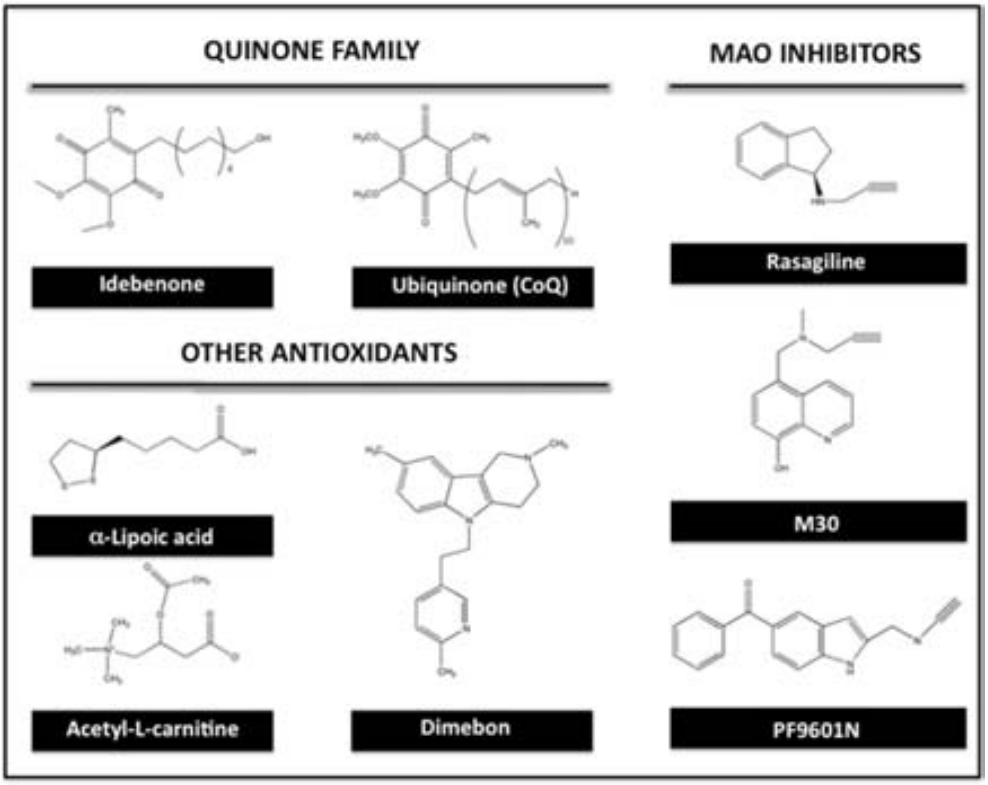

Fig. 9. Chemical structures of mitochondrial-related antioxidants investigated as promising agents for the treatment of AD.

4.3.3 Monoamine oxidase inhibitors

The therapeutic potential of monoamine oxidase inhibitors (MAOIs) for the treatment of AD has been largely reported (Thomas, 2000; Riederer et al., 2004; Youdim et al., 2005) due to their capacity to reduce the formation of toxic metabolites or oxygen radicals by blocking the catalytic activity of monoamine oxidase (MAO), enzyme located in the mitochondrial membrane and responsible of amine metabolism. It has been extensively reported that MAO-B activity besides increasing with age is found in high levels in AD patients. Selegiline, the classic MAO-B inhibitor, and also other propargylamines (Figure 9) possess potent antioxidant properties (Kitani et al., 2000; Sanz et al., 2004). Moreover, it has also been described that propargylamine-derived MAOIs exert neuroprotective effects by acting in very diverse type of targets, including metal chelation (e.g M30), reduction of Aβ aggregation and toxicity (Bar-Am et al., 2009; Youdim et al., 2005) as well as direct

actions on diverse mitochondrial-related components. Among this direct functions, propargylamines increase the expression of anti-apoptotic proteins (Akao et al., 2002), prevent citocrom c release and preserve the mitochondrial membrane potential (Mayurama et al., 2000). The great amount of beneficial functions found for MAOIs make them promising molecules for the treatment of AD. Indeed, current pharmacological challenges in AD involve the design and development of multifunctional compounds able to bind to a very diverse type of targets and among them MAO inhibition is strongly recommended.

4.4 PUFAs

The beneficial effects of omega-3 polyunsaturated fatty acids (PUFAs) have been widely reported which make them good candidates for AD therapy (Cole et al., 2005) since they act directly on intracellular pathways and regulate oxidative stress mechanisms. DHA is the major omega-3 fatty acid in the brain. A recent study although showing no effect of DHA on subjects with mild-to-moderate AD it found a slower rate of cognitive decline among those patients without de APO ε4 allele (Quinn et al., 2009). As reviewed by Mangialasche et al, 2010, some studies have reported a beneficial effect of DHA on cognitive function in patients with AD (Yurko-Mauro et al., 2009; Chiu et al., 2008) whereas others did not found a correlation (Quinn et al., 2009). In effect, a recent study showed that treatment of patients with PUFAs did not modify the neuropathology of this disorder in CSF or plasma, nor the biomarkers of inflammation (Freund-Levi et al., 2009) and a randomised control trial in patients with mild to moderate AD did not delay the rate of cognitive decline (Freund-Levi et al., 2006). Some authors suggest that benefits of omega-3 fatty acids are limited to those with very mild cognitive impairment. A phase 2 randomised clinical trial is currently ongoing (http://clinicaltrials.gov/NCT01058941).

4.5 Multiple nutrients

Dietary supplementation with a plethora of nutrients such us apple juice concentrate, red wine, caffeine, fish oil or green tea as well as calorie restriction diets have been conducted. Diverse human studies have shown that multiple formulations improve all measures of cognition, although some authors reported that the increase in memory was not found significant (Chan et al., 2008). A recent study correlates frequent consumption of fruits and vegetables, fish, and omega-3 rich oils with a decreased risk of dementia in AD (Barberger-Gateau et al., 2007). In contrast, interventional trials with antioxidants, B-vitamines and DHA did not give the promising expectations from the epidemiological data. As reported by Von Arnim et al., 2010, although some trials are encouraging, larger randomised clinical trials with combined supplements are needed to draw any conclusion. Supplement composition is still a matter of debate, because high doses of a single antioxidant have been associated with no beneficial effects for AD patients and even with an increase in mortality risk (e.g vitamin E). Many interventional studies are started very late in the disease state, when AD pathology is already at a fulminant level which severely reduces therapeutic effectiveness of tested agents. The multifactorial nature of AD and the necessity to target the earlier production of OS makes important the combination of multiple supplements. Therefore, studies combining nutrients are of particular interest and at present in progress (e.g. T-diet, NKO™, and Memory XL; http://clinicaltrials.gov/NCT01192529, NCT00867828, NCT00903695).

Exposure	Assessment	Design	Case source	Major findings	Reference
EGb 761 (intravenous)	NA	RCT	AD VaD	ADL improvement. Clinical impression of change	Haase et al, 1996
EGb 761 (oral)	NA	RCT	AD VaD	Cognitive improvement	Le Bars et al, 2000
PUFAs	Plasma assay	Cross-sectional	Normal, CI, dementia	Low n-3 and high n-6 associated with CI and AD	Conquer et al, 2000
PUFAs	Plasma assay	Cross-sectional	Normal, CI, dementia	High n-3 associated with CI and AD. Strengthened in ApoEe4 non-carriers	Laurin et al, 2003
PUFAs	Plasma assay	Prospective	Normal	No association between PUFAs and reduced risk of dementia	Kroger et al, 2009
Fish intake	FFQ	Prospective	Normal	Reduced risk of incident dementia	Barberger-Gateau et al, 2002
DHA	Serum assay	Case-control	Normal AD	MMSE and CDR improvement	Tully et al, 2003
Fish oil	FFQ	Prospective	Elderly	Slow rate of decline but not on overall cognitive status	Morris et al, 2005
PUFA	FFQ	Prospective	Elderly	Reduced MMSE decline over 5 years	Van Gelder et al, 2007
β-carotene	NA	Prospective	Elderly	Less cognitive decline only in ApoE4 carriers	Hu et al, 2006
Vitamin E	NA	RCT	MCI	No significant differences compared to placebo or donepezil	Petersen, 2005
α-tocopherol and/or selegiline	NA	RCT	Moderate AD	Longer time to institutionalization in all cases	Sano et al, 1997

Table 2. Studies on antioxidants. EGb 761, Gingko biloba special extract 761; NA, not applicable; VaD, Vascular Disease; ADL, Activities of Daily Living; RCT, Randomised Controlled Trial; ApoE, apolipoprotein E; n-3, omega-3 fatty acids; n-6, omega-6 fatty acids; FFQ, food frequency questionnaire; AD, Alzheimer's Disease; CI, cognitive impairment; MCI, Mild cognitive impairment; DHA, docohexanoic acid; PUFAs, polyunsaturated fatty acids; MMSE, Folstein Mini- Mental State examination; CDR, Clinical Dementia Rating Scale.

5. Conclusions

Oxidative stress increases with ageing and seems to be a consequence of an imbalance between ROS production and antioxidant defences. The accumulation of endogenous oxygen radicals generated in mitochondria and the consequent oxidative modifications of biological molecules have been indicated as responsible for the ageing process. There is therefore an urgent need to identify biomarkers that would help to diagnose and monitor the early AD or "preclinical AD". Indeed, a few CSF proteins (e.g. amyloid-β_{1-42}, total tau and phospho-tau) have already shown promise as diagnostic biomarkers for AD. Nevertheless, these biomarkers are not yet optimal diagnostic tools to identify those MCI patients at higher risk of conversion to AD. Thus, a key objective in the research of OS biomarkers is to identify prodromal stages of the disorder, prior to cognitive decline, for gauging the long-term therapeutic effects of drugs. The contradictory results obtained with diverse antioxidants in clinical trials may be explained by other related differences in health problems as well as due to the fact that most studies are very short and conducted with very few subjects. Methodological problems and poorly matched epidemiological studies have also been pointed as reasons for mixed findings. In fact, very few trials are adequately addressing the effect of antioxidants in AD. Although at this time there is no rationale for recommending antioxidant use for prevention or treatment of AD, the current epidemiologic evidence points toward an important role of nutrition in this pathology. The optimal time for prevention seems to be important and still to be determined. Nevertheless, it seems clear that therapies acting in the beginning of the pathological cascade may be more effective than treatments that act after the fact (e.g., removal of amyloid plaques). Then, therapy should begin as early as possible while reversal of cellular pathologies is still achievable. In conclusion, properly addressed studies with antioxidants are greatly needed to obtain convincing data about its beneficial effects as anti-AD. There is also an urgent need for better formulations with increased bioavailability. Due to the multifactorial nature of AD, it seems imperative that future trials may use drug combinations or even multifunctional molecules, rather than a single compound, able to bind to a very diverse type of target and that an antioxidant capacity may be contemplated.

6. Acknowledgment

The authors gratefully acknowledge Professors Nuria Durany (Universitat Internacional de Catalunya) and Peter Riederer (University of Würzburg).

7. References

Ahmed N, Ahmed U, Thornalley PJ, Hager K, Fleischer G, Münch G. (2005). Protein glycation, oxidation and nitration adduct residues and free adducts of cerebrospinal fluid in Alzheimer's disease and link to cognitive impairment. *J Neurochem,* 92:255-63.

Aliev G, Liu J, Schenk JC et al. (2009). Neuronal mitochondrial amelioration of alpha-lipoic acid and acetyl-L-carnitine. *J Cell Mol Med,* 13:320-333.

Akao I. (2002). Mitochondrial permeability transition mediates apoptosis induced by N-methyl(R)salsolinol, an endogenous neurotoxin, and is inhibited by Bcl-s and rasagiline. *J Neurochem,* 82:913-923.

Anand P, Kunnumakkara AB, Newman RA et al. (2007). Bioavailability of curcumin: problems and promises. *Mol Pharm,* 4:807-818.

Ando Y, Brännström T, Uchida K, Nyhlin N, Näsman B, Suhr O, Yamashita T, Olsson T, El Salhy M, Uchino M, Ando M. (1998). Histochemical detection of 4-hydroxynonenal protein in Alzheimer amyloid. *J Neurol Sci,* Apr 1;156(2):172-6.

Areosa SA, Sheriff F, Mc Shane R. (2005). Memantine for dementia. *Cochrane Database Syst Rev* (2) CD003154 .

Bagi Z, CSeko C, Toth E et al. (2003). Oxidative stress-induced dysregulation of arteriosal wall shear stress and blood pressure in hyperhomocysteinemia is prevented by chronic vitamin C treatment. *Am J Physiol Heart Circ Physiol,* 285:H2277-H2283.

Bar-Am O, Weinreb O, Amit T et al. (2009). The novel cholinesterase-monoamine oxidase inhibitor and antioxidant, ladostigil, confers neuroprotection in neuroblastoma cells and aged rats. *J Mol Neurosci,* 37:135-145.

Barberger-Gateau P, Letenneur L, Deschamps V et al. (2002). Fish, meat, and risk of dementia: cohort study. *BMJ,* 325(7370):932-933.

Barberger-Gateau P, Raffaitin C, Letenneur L et al. (2007). Dietary patterns and risk of dementia : The Three-city chort study. *Neurology,* 69(20):1921-1930.

Barnham KJ, Masters CL, Bush AI. (2004). Neurodegenerative diseases and oxidative stress. *Nat Rev Drug Discov*, Mar;3(3):205-14.

Basu S. Metabolism of 8-iso-prostaglandin F2alpha. (1998). *FEBS Lett*. May 22;428(1-2):32-6.

Berman K & Brodaty H. (2004). Tocopherol (vitamin E) in Alzheimer's disease and other neurodegenerative disorders. *Drugs,* 18:807-825.

Berlett BS, Stadtman ER. (1997). Protein oxidation in aging, disease, and oxidative stress. *J Biol Chem*. Aug 15;272(33):20313-6.

Birks J & Harvey R. (2006). Donepezil for dementia due to Alzheimer's disease. *Cochrane Database Syst Rev* (1) CD001190.

Birks J, Grimley EJ, Iakovidou V et al. (2000). Rivastigmine for Alzheimer's disease. *Cochrane Database Syst Rev* (4) CD001191.

Bondy SC, Guo-Ross SX, Truong AT. (1998). Promotion of transition metal-induced reactive oxygen species formation by beta-amyloid. *Brain Res*, 799:91-96.

Bradley MA, Markesbery WR, Lovell MA. (2010a). Increased levels of 4-hydroxynonenal and acrolein in the brain in preclinical Alzheimer disease. *Free Radic Biol Med*, Jun 15;48(12):1570-6.

Bradley MA, Xiong-Fister S, Markesbery WR, Lovell MA. (2010b). Elevated 4-hydroxyhexenal in Alzheimer's disease (AD) progression. *Neurobiol Aging*, Oct 19.

Butterfield DA, Bader Lange ML, Sultana R. (2010). Involvements of the lipid peroxidation product, HNE, in the pathogenesis and progression of Alzheimer's disease. *Biochim Biophys Acta*, Aug;1801(8):924-9.

Butterfield DA, Castegna A, Lauderback CM, Drake J. (2002). Evidence that amyloid beta-peptide-induced lipid peroxidation and its sequelae in Alzheimer's disease brain contribute to neuronal death. *Neurobiol Aging*, Sep-Oct;23(5):655-64.

Butterfield DA, Griffin S, Munch G, Pasinetti GM. (2002). Amyloid beta-peptide and amyloid pathology are central to the oxidative stress and inflammatory cascades under which Alzheimer's disease brain exists. *J Alzheimers Dis*, Jun;4(3):193-201.

Calingasan NY, Uchida K, Gibson GE. (1999). Protein-bound acrolein: a novel marker of oxidative stress in Alzheimer's disease. *J Neurochem*, Feb;72(2):751-6.

Carini M, Aldini G, Facino RM. (2004). Mass spectrometry for detection of 4-hydroxy-trans-2-nonenal (HNE) adducts with peptides and proteins. *Mass Spectrom Rev*, Jul-Aug;23(4):281-305.

Castegna A, Aksenov M, Aksenova M, Thongboonkerd V, Klein JB, Pierce WM, Booze R, Markesbery WR, Butterfield DA. (2002a). Proteomic identification of oxidatively modified proteins in Alzheimer's disease brain. Part I: creatine kinase BB, glutamine synthase, and ubiquitin carboxy-terminal hydrolase L-1. *Free Radic Biol Med,*. Aug 15;33(4):562-71.

Castegna A, Aksenov M, Thongboonkerd V, Klein JB, Pierce WM, Booze R, Markesbery WR, Butterfield DA. (2002b). Proteomic identification of oxidatively modified proteins in Alzheimer's disease brain. Part II: dihydropyrimidinase-related protein 2, alpha-enolase and heat shock cognate 71. *J Neurochem*, 2002 Sep;82(6):1524-32.

Castellani RJ, Harris PL, Sayre LM, Fujii J, Taniguchi N, Vitek MP, Founds H, Atwood CS, Perry G, Smith MA. (2001). Active glycation in neurofibrillary pathology of Alzheimer disease: N(epsilon)-(carboxymethyl) lysine and hexitol-lysine. Free Radic Biol Med, Jul 15;31(2):175-80.

Chan A, Paskavitz J, Remington R et al. (2008). Efficacy of a vitamin/nutraceutical formulation for early stage Alzheimer's disease: a 1 year, open-label pilot study with a 16-month caregiver extension. *Am J Alzheimer Dis Other Demen,* 23:571-585.

Chen X, Walker DG, Schmidt AM, Arancio O, Lue LF, Yan SD. (2007). RAGE: a potential target for Abeta-mediated cellular perturbation in Alzheimer's disease. Curr Mol Med, Dec;7(8):735-42.

Chiu CC, Su KP, Cheng TC et al. (2008). The effects of omega-3 fatty acids monotherapy in Alzheimer's disease and mild cognitive impairment: a preliminary randomised double-blind placebo controlled study. *Prog Neuropsychopharmacol Biol Psychiatry,* 32:1538-1544.

Cheng KC, Cahill DS, Kasai H, Nishimura S, Loeb LA. (1992). 8-Hydroxyguanine, an abundant form of oxidative DNA damage, causes G----T and A----C substitutions. *J Biol Chem*, Jan 5;267(1):166-72.

Choi J, Malakowsky CA, Talent JM, Conrad CC, Gracy RW. (2002). Identification of oxidized plasma proteins in Alzheimer's disease. *Biochem Biophys Res Commun*, May 24;293(5):1566-70.

Cole GM, Teter B, Frautschy SA. (2007). Neuroprotective effects of curcumin. *Adv Exp Med Biol,* 595:197-212.

Conquer JA, Tierney MC, Zecevic J et al. (2000). Fatty acid analyisis of blood plasma of patients with Alzheimer's disease, other types of dementia, and cognitive impairment. *Lipids,* 35(12):1305-1312.

Cooke MS, Olinski R, Loft S. (2008). European Standards Committee on Urinary (DNA) Lesion Analysis. Measurement and meaning of oxidatively modified DNA lesions in urine. *Cancer Epidemiol Biomarkers Prev*, Jan;17(1):3-14.

Cracowski JL, Durand T, Bessard G. (2002). Isoprostanes as a biomarker of lipid peroxidation in humans: physiology, pharmacology and clinical implications. *Trends Pharmacol Sci*, Aug;23(8):360-6.

CTdotgovdimebon ClinicalTrials.gov study NCT00675623, a safety and efficacy study of oral dimebon in patients with mild-to-moderate Alzheimer's disease (CONNECTION)

Dalle-Donne I, Rossi R, Colombo R, Giustarini D, Milzani A. (2006a). Biomarkers of oxidative damage in human disease. Clin Chem, Apr;52(4):601-23.

Dalle-Donne I, Aldini G, Carini M, Colombo R, Rossi R, Milzani A. (2006b). Protein carbonylation, cellular dysfunction, and disease progression. J Cell Mol Med, Apr-Jun;10(2):389-406.

Davidsson P, Paulson L, Hesse C, Blennow K, Nilsson CL. (2001). Proteome studies of human cerebrospinal fluid and brain tissue using a preparative two-dimensional electrophoresis approach prior to mass spectrometry. *Proteomics*, Mar;1(3):444-52.

Defeudis FV (2002). Bilobalide and neuroprotection. *Pharmacol Res* 46: 565-568.

DeKosky ST, Williamson JD, Fitzpatrick AL et al (2008) Gingko biloba for prevention of dementia: a randomised controlled trial. *JAMA,* 300:2253-2262.

Dodge HH, Zitzelberger T, Oken BS et al. (2008). A randomised placebo-controlled trial of Gingko biloba for the prevention of cognitive decline. *Neurology,* 70:1809-1817.

Doody RS. (2009). Dimebon as a potential therapy for Alzheimer's disease. *CNS Spectrosc,* 14:14-16;discussion 16-18

Doody RS, Gavrilova SI, Sano M et al. (2008). Effect of dimebon on cognition, activities of daily living, behaviour, and global function in patients with mild-to-moderate Alzheimer's disease: a randomised, double-blind, placebo-controlled study. *Lancet* 372:207-215

Epis R, Marcello E, Gardoni F et al. (2008). Modulatory effect of acetyl-L-carnitine on amyloid precursor protein metabolism in hippocampal neurons. *Eur J Pharmacol* 597:51-56

Eckl PM, Ortner A, Esterbauer H. (1993). Genotoxic properties of 4-hydroxyalkenals and analogous aldehydes. *Mutat Res*. Dec;290(2):183-92.

Esterbauer H, Schaur RJ, Zollner H. (1991). Chemistry and biochemistry of 4-hydroxynonenal, malonaldehyde and related aldehydes. *Free Radic Biol M*ed. 11(1):81-128.

Evans MD, Olinski R, Loft S, Cooke MS. (2010). Toward consensus in the analysis of urinary 8-oxo-7,8-dihydro-2'-deoxyguanosine as a noninvasive biomarker of oxidative stress. European Standards Committee on Urinary (DNA) Lesion Analysis, *FASEB J.* Apr;24(4):1249-60.

Freund-Levi Y, Eriksdotter-Jönhagen M, Cederholm T et al. (2006). Omega-3 fatty acids treatment in 174 patients with mild to moderate Alzheimer disease: OmegAD study: a randomised, double-blind trial. *Arch Neurol,* 63(10):1402-1408.

Freund-Levi Y, Hjorth E, Lindberg C et al. (2009). Effects of omega-3 fatty acids on inflammatory markers in cerebrospinal fluid and plasma in Alzheimer's disease: the OmegAD Study. *Dement Geriatr Cogn Disord,* 27:481-490.

Fraga CG, Shigenaga MK, Park JW, Degan P, Ames BN. Oxidative damage to DNA during aging: 8-hydroxy-2'-deoxyguanosine in rat organ DNA and urine. *Proc Natl Acad Sci USA*, 1990 Jun;87(12):4533-7.

Goodman AB. (2006). Retinoid receptors, transporters, and metabolizers as therapeutic targets in late onset Alzheimer disease. *J Cell Physiol,* 209:598-60.

Green C, Picot J, Loveman E et al. (2005). Modelling the cost effectiveness of cholinesterase inhibitors in the management of mild to moderately severe Alzheimer's disease. *Pharmacoeconomics,* 23:1271-1282.

Griffiths HR, Møller L, Bartosz G, Bast A, Bertoni-Freddari C, Collins A, Cooke M, Coolen S, Haenen G, Hoberg AM, Loft S, Lunec J, Olinski R, Parry J, Pompella A, Poulsen H, Verhagen H, Astley SB. (2002). Biomarkers. *Mol Aspects Med*, Feb-Jun;23(1-3):101-208.

Grundman M, Petersen RC, Ferris SH et al. (2004). Mild cognitive impairment can be distinguished from Alzheimer disease and normal aging for clinical trials. *Arch Neurol,* 61:59-66.

Gutzmann H, Khul KP, Hadler D et al. (2002). Safety and efficacy of idebenone versus tacrine in patients with Alzheimer's disease:results of a randomised, double-blind, parallel group multicenter study. *Pharmacopsychiatry,* 35:12-18.

Haase J, Halama P and Horr R. (1996). Effectiveness of brief infusions with Gingko biloba Special Extract EGb 761 in dementia of the vascular and Alzheimer type. *Z Gerontol Geriatr*,29:302-309.

Haenen GR & Bast A. (1991). Scavenging of hypochlorus acid by lipoic acid. *Biochem Pharmacol,* 42:2244-2246.

Hamilton ML, Van Remmen H, Drake JA, Yang H, Guo ZM, Kewitt K, Walter CA, Richardson A. (2001). Does oxidative damage to DNA increase with age? *Proc Natl Acad Sci USA*, Aug 28;98(18):10469-74.

Harman D. (1956). Aging: a theory based on free radical and radiation chemistry. *J Gerontol*, Jul;11(3):298-300.

Harman D. (1972). The biologic clock: the mitochondria?. *J Am Geriatr Soc,* Apr;20(4):145-7.

Hu P, Brestky P, Crimmins EM. (2006). Association between serum beta-carotene levels and decline of cognitive function in high functioning older persons with or without apolipoprotein E 4 alleles: MacArthur studies of successful aging. *J Gerontol A Biol Sci Med Sci*, 61:616-620.

Jiménez-Jiménez FJ, de Bustos F, Molina JA et al. (1997). Cerebrospinal fluid levels of alpha-tocopherol (vitamin E) in Alzheimer's disease. *J Neural Transm,* 104:703-710.

Karuppagounder SS, Pinto JT, Xu H et al. (2009). Dietary supplementation with resveratrol reduces plaque pathology in a transgenic model of Alzheimer's disease. *Neurochem Int,* 54:111-118.

Kim KM, Jung BH, Paeng KJ, Kim I, Chung BC. (2004). Increased urinary F(2)-isoprostanes levels in the patients with Alzheimer's disease. *Brain Res Bull*, Jul 30;64(1):47-51.

Kimura T, Takamatsu J, Ikeda K, Kondo A, Miyakawa T, Horiuchi S. (1996). Accumulation of advanced glycation end products of the Maillard reaction with age in human hippocampal neurons. *Neurosci Lett*, Apr 12;208(1):53-6.

Kitani KA et al. (2000). Common properties for propargylamines of enhancing superoxide dismutase and catalase acivities in the dopaminergic system in the rat: implications for the life prolonging effect of (-)deprenyl. *J Neural Transm,* 60 (Suppl) 139-156.

Korolainen MA, Nyman TA, Nyyssönen P, Hartikainen ES, Pirttilä T. (2007). Multiplexed proteomic analysis of oxidation and concentrations of cerebrospinal fluid proteins in Alzheimer disease. *Clin Chem*, Apr;53(4):657-65.

Korolainen MA, Goldsteins G, Nyman TA, Alafuzoff I, Koistinaho J, Pirttilä T. (2006). Oxidative modification of proteins in the frontal cortex of Alzheimer's disease brain. *Neurobiol Aging*, Jan;27(1):42-53.

Kozekov ID, Nechev LV, Moseley MS, Harris CM, Rizzo CJ, Stone MP, Harris TM. (2003). DNA interchain cross-links formed by acrolein and crotonaldehyde. *J Am Chem Soc*, Jan 8;125(1):50-61.

Kroger E, Verreault R, Carmicael PH et al. (2009). Omega-3 fatty acids and risk of dementia: the Canadian Study of Health and Aging. *Am J Clin Nutr,* 90(1):184-192.

Laurin D, Verreault R, Lindsay J et al. (2003). Omega-3 fatty acids and risk of cognitive impairment and dementia. *J Alzheimers Dis* 5(4):315-322.

Ledesma MD, Pérez M, Colaco C et al (1998) Tau glycation is involved in aggregation of the protein but not in the formation of filaments. *Cell Moll Biol* Nov 44(7):1111-1116.

Liu X, Lovell MA, Lynn BC. (2006). Detection and quantification of endogenous cyclic DNA adducts derived from trans-4-hydroxy-2-nonenal in human brain tissue by isotope dilution capillary liquid chromatography nanoelectrospray tandem mass spectrometry. *Chem Res Toxicol*, May;19(5):710-8.

Le Bars PL, Kieser M and Itil KZ. (2000). A 26-week analysis of a double-blind, placebo-controlled trial of the gingko biloba extract EGb 761 in dementia. *Dement Geriatr Cogn Disord,* 11:230-237.

Le Bars PL. (2003). Response patterns of EGb 761 in Alzhemier's disease: influence of neuropsychological profiles. *Pharmacopsychiatry,* 36 (Suppl 1) S50-S55.

Loske C, Gerdemann A, Schepl W, Wycislo M, Schinzel R, Palm D, Riederer P, Münch G. (2000). Transition metal-mediated glycoxidation accelerates cross-linking of beta-amyloid peptide. Eur J Biochem, Jul;267(13):4171-8.

Lovell MA, Ehmann WD, Mattson MP, Markesbery WR. (1997). Elevated 4-hydroxynonenal in ventricular fluid in Alzheimer's disease. *Neurobiol Aging*, Sep-Oct;18(5):457-61.

Lovell MA, Markesbery WR. (2007a). Oxidative damage in mild cognitive impairment and early Alzheimer's disease. *J Neurosci Res*, Nov 1;85(14):3036-40.

Lovell MA, Markesbery WR. (2007b). Oxidative DNA damage in mild cognitive impairment and late-stage Alzheimer's disease. *Nucleic Acids Res*, 35(22):7497-504.

Lovell MA, Markesbery WR. (2001). Ratio of 8-hydroxyguanine in intact DNA to free 8-hydroxyguanine is increased in Alzheimer disease ventricular cerebrospinal fluid. *Arch Neurol*, Mar;58(3):392-6.

Loy C & Schneider L. (2004). Galantamine for Alzheimer's disease. *Cochrane Database Syst Rev,* (4)CD001747.

Luchsinger JA, Tang MX, Shea S et al. (2003). Antioxidant vitamine intake and risk of Alzheimer disease. *Arch Neurol,* 60:203-208.

Luo Y, Smith JV, Paramasivam V et al. (2002). Inhibition of amyloid beta aggregation and caspase-3 activation by the Gingko biloba extract EGb 761. *Proc Natl Acad Sci USA*, 99-12197-12202.

Mandel SA, Amit T, Kalfon L. (2008). Cell signaling pathways and iron chelation in the neurorestorative activity of green tea polyphenols: special reference to epigallocatechin gallate (EGCG). *J Alzheimer Dis,* 17:681-697.

Mangialasche F, Solomon A, Winblad B et al. (2010). Alzheimer's disease: clinical trials and drug development. *Lancet Neurol* 9:702-716.

Markesbery WR, Lovell MA. (1998). Four-hydroxynonenal, a product of lipid peroxidation, is increased in the brain in Alzheimer's disease. *Neurobiol Aging*, Jan-Feb;19(1):33-6.

Markesbery WR, Carney JM. (1999). Oxidative alterations in Alzheimer's disease. *Brain Pathol*, Jan;9(1):133 46.

Mayurama W, Akao Y, Youdim MB et al. (2000). Transfection-enforced Bcl-2 overexpression and an anti-Parkinson drug, rasagiline, prevent nuclear accumulation of GAPDH induced by an endogenous dopaminergic neurotoxin, N-methyl(R)salsolinol. *J Neurochem,* 78:727-735.

McGrath LT, McGleenon BM, Brennan S, McColl D, McILroy S, Passmore AP. (2001). Increased oxidative stress in Alzheimer's disease as assessed with 4-hydroxynonenal but not malondialdehyde. *QJM*, Sep;94(9):485-90.

McIlroy SP, Dynan KB, Lawson JT et al. (2002). Moderately elevated plasma homocysteine, methylenetetrahydrofolate reductase genotype, and risk for stroke, vascular dementia and Alzheimer disease in Northern Ireland. *Stroke,* 33:2351-2356

Mecocci P, Polidori MC, Cherubini A, Ingegni T, Mattioli P, Catani M, Rinaldi P, Cecchetti R, Stahl W, Senin U, Beal MF. (2002). Lymphocyte oxidative DNA damage and plasma antioxidants in Alzheimer disease. *Arch Neurol*, May;59(5):794-8.

Migliore L, Fontana I, Trippi F, Colognato R, Coppedè F, Tognoni G, Nucciarone B, Siciliano G. (2005). Oxidative DNA damage in peripheral leukocytes of mild cognitive impairment and AD patients. *Neurobiol Aging*, May; 26(5):567-73.

Mishra S & Palanivelu K. (2008). The effect of curcumin (turmeric) on Alzheimer's disease: an overwiew. *Ann Indian Acad Neurol,* 11:13-19.

Montgomery SA, Thal LJ & Amrein R. (2003). Meta-analysis of double-blind randomised controlled clinical trials of acetyl-L-carnitine versus placebo in the treatment of mild conginitive impairment and mild Alzheimer's disease. *Int Clin Psychopharmacol*, 18:61-71.

Montine KS, Kim PJ, Olson SJ, Markesbery WR, Montine TJ. (1997). 4-hydroxy-2-nonenal pyrrole adducts in human neurodegenerative disease. *J Neuropathol Exp Neurol*, 56(8): 866-71.

Montine TJ, Markesbery WR, Morrow JD, Roberts LJ 2nd. (1998). Cerebrospinal fluid F2-isoprostane levels are increased in Alzheimer's disease. *Ann Neurol*, Sep;44(3):410-3.

Montine TJ, Quinn JF, Milatovic D, Silbert LC, Dang T, Sanchez S, Terry E, Roberts LJ 2nd, Kaye JA, Morrow JD. Peripheral F2-isoprostanes and F4-neuroprostanes are not increased in Alzheimer's disease. *Ann Neurol*, 2002 Aug;52(2):175-9.

Montine TJ, Peskind ER, Quinn JF, Wilson AM, Montine KS, Galasko D. Increased Cerebrospinal Fluid F(2)-Isoprostanes are Associated with Aging and Latent Alzheimer's Disease as Identified by Biomarkers. *Neuromolecular Med*, 2011 Mar;13(1):37-43.

Montuschi P, Barnes PJ, Roberts LJ 2nd. Isoprostanes: markers and mediators of oxidative stress. *FASEB J*, 2004 Dec; 18(15):1791-800.

Morris MC, Beckett LA, Scherr PA et al (1998) Vitamin E and vitamin C supplement use and risk of incident Alzheimer disease. *Alzheimer Dis assoc Disord*,12:121-126.

Morris MC, Evans DA, Bienias JL et al (2002) Dietary intake of antioxidant nutrients and the risk of incident Alzheimer disease in a biracial community study. *J Am Med Assoc,* 287:3230-3237.

Morris MC, Evans DA, Bienias JL et al (2003). Consumption of fish and n-3 fatty acids and risk of incident Alzheimer disease. *Arch Neurol*, 60(7):940-946.

Morris MC, Evans DA, Tagney CC (2005) Relation of the tocopherol forms to incident Alzheiemr disese and to cognitive change. *Am J Clin Nutr,* 81:508-514.

Morris MC, Evans DA, Tagney CC et al. (2005). Fish consumption and cognitive decline with age in a large community study. *Arch Neurol,* 62(12):1849-1853.

Morris MS, Jacques PF, Rosenberg IH et al. (2007). Folate and vitamine B12 status in relation to anemia, macrocytosis and cognitive impairment in older Americans in the age of folic acid fortification. *Am J Clin Nutr*, 85:193-200.

Morrow JD, Tapper AR, Zackert WE, Yang J, Sanchez SC, Montine TJ, Roberts LJ. (1999). Formation of novel isoprostane-like compounds from docosahexaenoic acid. *Adv Exp Med Biol*, 469:343-7.

Napryeyenko O, Sonnik G, Tartakovsky I. (2009). Efficacy and tolerability of gingko biloba extract EGb 761 by type of dementia: analyses of a randomised controlled trial. *J Neurol Sci*, 283:224-229.

Nunomura A, Perry G, Aliev G, Hirai K, Takeda A, Balraj EK, Jones PK, Ghanbari H, Wataya T, Shimohama S, Chiba S, Atwood CS, Petersen RB, Smith MA. (2001). Oxidative damage is the earliest event in Alzheimer disease. *J Neuropathol Exp Neurol*, Aug;60(8):759-67.

Oken BS, Storzbach DM, Kaye JA. (1998). The efficacy og Gingko biloba on cognitive function in Alzheimer's disease. *Arch Neurol,* 55:1409-1415.

Okun I, Tkachenko SE, Khvat A et al. (2010). From anti-allergic to anti-Alzheimer's: molecular pharmacology of dimebon. *Curr Alzheimer Res,* 7:97-112.

Olinski R, Siomek A, Rozalski R, Gackowski D, Foksinski M, Guz J, Dziaman T, Szpila A, Tudek B. (2007). Oxidative damage to DNA and antioxidant status in aging and age-related diseases. *Acta Biochim Pol*, 54(1):11-26.

Perry G, Raina AK, Nunomura A, Wataya T, Sayre LM, Smith MA. (2000). How important is oxidative damage? Lessons from Alzheimer's disease. *Free Radic Biol Med*, Mar 1;28(5):831-4.

Perry G, Nunomura A, Cash AD, Taddeo MA, Hirai K, Aliev G, Avila J, Wataya T, Shimohama S, Atwood CS, Smith MA. (2002). *Reactive oxygen: its sources and significance in Alzheimer disease. J Neural Transm Suppl,* (62):69-75.

Petersen RC, Thomas RG, Grudman N et al. (2005). Vitamin E and donepezil for the treatment of mild cognitive impairment. *N Engl J Med* 352:2379-2388,

Pettergrew JW, Klunk WE, Panchalingam K et al, (1995). Clinical and neurochemical effects of acetyl-L-carnitine in Alzheimer's disease. *Neurobiol Aging,* 16:1-4,

Praticò D, Clark CM, Liun F, Rokach J, Lee VY, Troianowski JQ. (2002). Increase of brain oxidative stress in mild cognitive impairment: a possible predictor of Alzheimer disease. *Arch Neurol*, Jun:59(6): 972-6.

Puchades M, Hansson SF, Nilsson CL, Andreasen N, Blennow K, Davidsson P. (2003). Proteomic studies of potential cerebrospinal fluid protein markers for Alzheimer's disease. *Brain Res Mol Brain Res*, Oct 21;118(1-2):140-6.

Quinn JF, Raman R, Thomas RG et al. (2009). A clinical trial of docohexanoic acid (DHA) for the treatment of Alzheimer's disease. *Alzheimers Assoc Int Conf Alzheimer Di*s; July 12.

Riederer P, Danielczyk W, Grünblatt E. (2004). Monoamine oxidase-B inhibition in Alzheimer's disease. *Neurotoxicology*, 25 (1-2):271-277.

Roberts LJ 2nd, Montine TJ, Markesbery WR, Tapper AR, Hardy P, Chemtob S, Dettbarn WD, Morrow JD. (1998). Formation of isoprostane-like compounds

(neuroprostanes) in vivo from docosahexaenoic acid. *J Biol Chem*, May 29;273(22):13605-12.

Sahin M, Karauzum SB, Perry G et al. (2005). Retinoic acid isomers protect hippocampal neurons from amyloid-beta induced neurodegeneration. *Neurotox Res,* 7:243-250.

Sano M, Ernesto C, Thomas RG et al. (1997). A controlled trial of selegiline, alpha tocopherol, or both as treatment for Alzheimer's disease. The Alzheimer's disease cooperative study. *N Engl J Med*, 336:1216-1222.

Sanz E, Romera M, Bellik L et al. (2004). Indolalkylamines derivatives as antioxidant and neuroprotective agents in an experimental model of Parkinson's disease. *Med Sci Monit,* 10(12):BR477-484.

Sayre LM, Zelasko DA, Harris PL, Perry G, Salomon RG, Smith MA. (1997). 4-Hydroxynonenal-derived advanced lipid peroxidation end products are increased in Alzheimer's disease. *J Neurochem*, May;68(5):2092-7.

Schneider LS, DeKosky ST, Farlow MR et al. (2005). A randomised, double-bind, placebo controlled trial of two doses of Gongko biloba extract in dementa of the Alzhemier's type. *Curr Alzheimer Res,* 2 541-551.

Senin U, Parnetti L, Barbagallo-Sangiorgi G et al. (1992). Idebenone in senile dementia of Alzheimer type:a multicenter study. *Arch Gerontol Geriatr,* 15:249-260.

Shigenaga MK, Gimeno CJ, Ames BN. (1989). Urinary 8-hydroxy-2'-deoxyguanosine as a biological marker of in vivo oxidative DNA damage. *Proc Natl Acad Sci USA*, Dec;86(24):9697-701.

Shoba G, Joy S, Joseph T et al. (1998). Influence of piperine on the pharmacokinetics of curcumin in animals and human volunteers. *Planta Med,* 64:353-356.

Smith MA, Sayre LM, Monnier VM, Perry G. (1995). Radical AGEing in Alzheimer's disease. Trends Neurosci, Apr;18(4):172-6.

Snitz BE, O'Meara ES, Carlsom MC et al. (2009). Gingko biloba for preventing cognitive decline in older adults: a randomised trial. *JAMA,* 302:2663-2670.

Southern L, Williams J, Esiri MM. (2007). Immunohistochemical study of N-epsilon-carboxymethyl lysine (CML) in human brain: relation to vascular dementia. *BMC Neurol*, Oct 16;7:35.

Sultana R, Butterfield DA. (2011). Identification of the oxidative stress proteome in the brain. *Free Radic Biol Med*, Feb 15;50(4):487-94. Epub 2010 Nov 25.

Tabet N, Birks J, Grimley EF. (2000). Vitamine E for Alhzheimer's disease. *Cochrane database Syst Rev* (4) CD002854.

Tamagno E, Guglielmotto M, Aragno M, Borghi R, Autelli R, Giliberto L, Muraca G, Danni O, Zhu X, Smith MA, Perry G, Jo DG, Mattson MP, Tabaton M. (2008). Oxidative stress activates a positive feedback between the gamma- and beta-secretase cleavages of the beta-amyloid precursor protein. *J Neurochem*, Feb;104(3):683-95.

Thal LJ, Grundman M, Berg J et al. (2003). Idebenone treatment fails to slow cognitive decline in Alzheimer's disease. *Neurology,* 61:1498-1502.

Thal LJ, Calvani M, Amato A et al. (2000). A 1-year controlled trial of acetyl-L-carnitine in early onset AD. *Neurology,* 55:805-810.

Thomas T. (2000). Monoamine oxidase-B inhibitors in the treatment of Alzheimer's disease. *Neurobiol Aging*, 21(2):343-348.

Thome J, Münch G, Muller R, Schinzel R, Kornhuber J, Blum-Degen D et al. (1996). Advanced glycation endproducts-associated parameters in the peripheral blood of patients with Alzheimer's disease. *Neurotox Res*, 4:191-209.

Tucker JM & Townsend DM. (2005). Alpha-tocopherol: roles in prevention and therapy of human disease. *Biomed Pharmacother,* 59 (7):380-387.

Tully AM, Roche HM, Doyle R et al. (2003). Low serum cholesteryl ester-docohexanoic acid levels in Alzheimer's disease: a case-control study. *Br J Nutr,* 89(4):483-489.

Uchida K. (2003). 4-Hydroxy-2-nonenal: a product and mediator of oxidative stress. *Prog Lipid Res*, Jul;42(4):318-43.

Van Gelder BM, Tijhuis M, Kalmijn S et al. (2007). Fish consumption, n-3 fatty acids, and subsequent 5-y cognitive decline in elderly men: the Zutphen Elderly Study. *Am J Clin Nutr,* 85(4):1142-1147.

Vitek MP, Bhattacharya K, Glendening JM, Stopa E, Vlassara H, Bucala R, Manogue K, Cerami A. (1994). Advanced glycation end products contribute to amyloidosis in Alzheimer disease. *Proc Natl Acad Sci USA*, May 24;91(11):4766-70.

Von Arnim CA, Gola U and Biesalski HK. (2010). More than the sumo f its parts? Nutrition in Alzheimer's disease. *Nutrition*, 26(7-8):694-700.

Wadsworth TL, Bishop JA, PAppu AS et al. (2008). Evaluation of Coenzyme Q as an antioxidant strategy for Alzheimer's disease. *J Alzheimer's Dis,* 14:225-234.

Wataya T, Nunomura A, Smith MA, Siedlak SL, Harris PL, Shimohama S, Szweda LI, Kaminski MA, Avila J, Price DL, Cleveland DW, Sayre LM, Perry G. (2002). High molecular weight neurofilament proteins are physiological substrates of adduction by the lipid peroxidation product hydroxynonenal. *J Biol Chem,* Feb 15;277(7):4644-8.

Weyer G, Babej.Dolle RM, Hadler D et al. (1997). A controlled study of 2 doses of idebenone in the treatment of Alzheimer's disease. *Neuropsychobiology,* 36:73-82.

White AR, Barnham KJ, Huang X et al. (2004). Iron inhibits neurotoxicity induced by trace cooper and biological reductants. *J Biol Inorg Chem,* 9:269-280.

Williams TI, Lynn BC, Markesbery WR, Lovell MA. (2006). Increased levels of 4-hydroxynonenal and acrolein, neurotoxic markers of lipid peroxidation, in the brain in Mild Cognitive Impairment and early Alzheimer's disease. *Neurobiol Aging*, Aug;27(8):1094-9.

Yao Z & Drieu V. (2001). Papadopoulos, the Gingko biloba extract Egb 761 rescues the PC12 neuronal cells from beta-amyloid-induced cell death by inhibiting the formation of beta-amyloid-derived diffusible neurotoxic ligands. *Brain Res,* 889:181-190.

Yan SD, Chen X, Schmidt AM, Brett J, Godman G, Zou YS, Scott CW, Caputo C, Frappier T, Smith MA, et al. (1994). Glycated tau protein in Alzheimer disease: a mechanism for induction of oxidant stress. Proc Natl Acad Sci USA, Aug 2;91(16):7787-91.

Youdim BM, Fridkin M and Zheng H. (2005). Bifunctional drug derivates of MAO-B inhibitor rasagiline and iron chelator VK28 as a more effective approach to treatment of brain aging and aging neurodegenerative diseases. *Mech Aging Dev*, 126: 317-326.

Yu HL, Chertkow HM, Bergman H, Schipper HM. (2003). Aberrant profiles of native and oxidized glycoproteins in Alzheimer plasma. *Proteomic*s, Nov;3(11):2240-8.

Yurko-Mauro K, McCarthy D, Bailey-Hall E et al. (2009). Results of the MIDAS trial: effects of docohexanoic acid on physiological and safety parameters in age-related cognitive decline. *Alzheimers Assoc Int Conf Alzheimer Dis*; July 12.

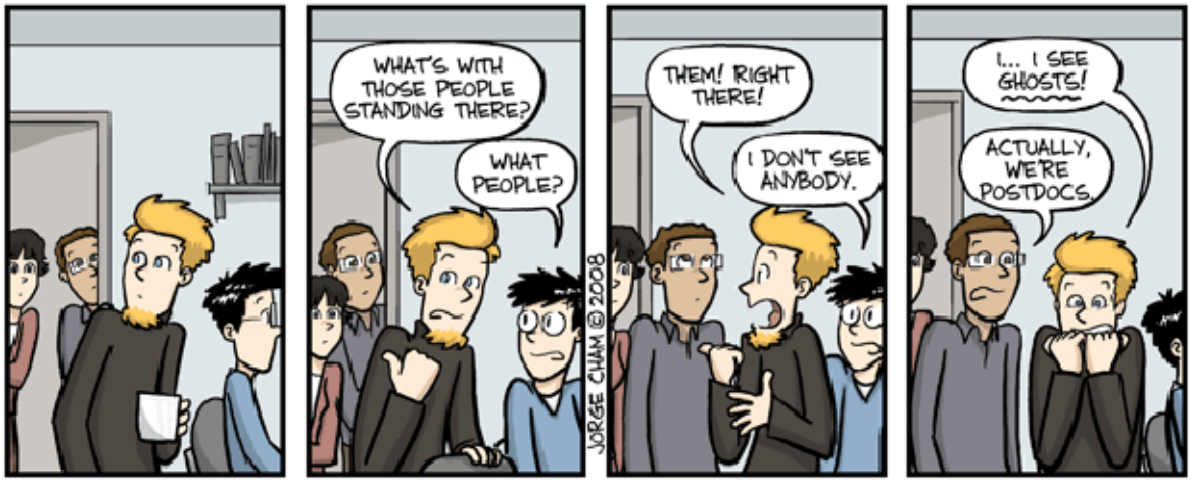
WHAT'S WITH THOSE PEOPLE STANDING THERE?
WHAT PEOPLE?
THEM! RIGHT THERE!
I DON'T SEE ANYBODY.
I... I SEE GHOSTS!
ACTUALLY, WE'RE POSTDOCS.
JORGE CHAM © 2008
WWW.PHDCOMICS.COM

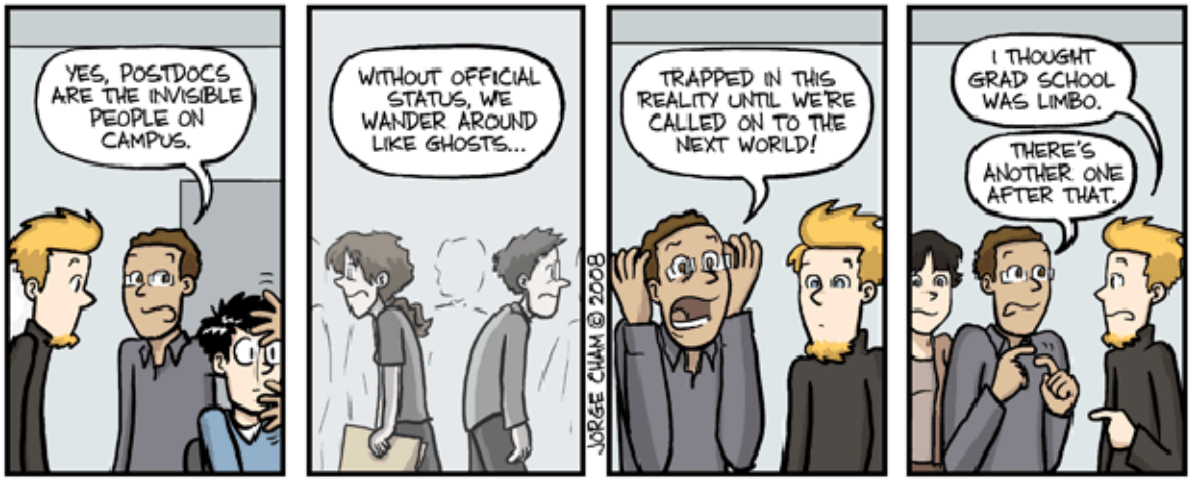
YES, POSTDOCS ARE THE INVISIBLE PEOPLE ON CAMPUS.
WITHOUT OFFICIAL STATUS, WE WANDER AROUND LIKE GHOSTS...
TRAPPED IN THIS REALITY UNTIL WE'RE CALLED ON TO THE NEXT WORLD!
I THOUGHT GRAD SCHOOL WAS LIMBO.
THERE'S ANOTHER ONE AFTER THAT.
JORGE CHAM © 2008
WWW.PHDCOMICS.COM